CIS-REGULATORY EVOLUTION OF *SALMONELLA ENTERICA*

CIS-REGUATORY EVOLUTION OF *SALMONELLA ENTERICA*

By

Suzanne E. Osborne, BSc.

A Thesis Submitted to the School of Graduate Studies
in Partial Fulfilment of the Requirements for
the Degree

Doctor of Philosophy

McMaster University Doctor of Philosophy (2012) Hamilton, Ontario

TITLE: *Cis*-regulatory Evolution of *Salmonella enterica*

AUTHOR: Suzanne E. Osborne, BSc.

SUPERVISOR: Dr. Brian K. Coombes

NUMBER OF PAGES: xviii, 266

Abstract

Originally considered the sole providence of protein coding sequences, evolutionary biology has begun to recognize the importance of non-coding DNA in dictating phenotypic adaptation. Exclusively examined in eukaryotic anatomical development, *cis*-regulatory modifications have the power to alter the spatial-temporal dynamics of gene expression without the plieotropic consequences of protein modification. Owing to the need to integrate horizontally acquired DNA into existing regulatory networks, *cis*-regulatory mutations may also significantly contribute to prokaryotic evolution. The horizontal acquisition of *Salmonella* Pathogenicity Island (SPI)-2 led to the evolutionary divergence of *Salmonella enterica* from *S. bongori*. Use of the type 3 secretion system encoded in SPI-2 allowed *S. enterica* to exploit an intracellular host niche offered by immune cells and allowed for its systemic dissemination. Here we identify ancestrally encoded *srfN* and *dalS* and demonstrate that through acquisition of a binding site for the SPI-2 regulator, SsrB, they have contributed to the pathoadaptation of *S. enterica* to the host environment. We also demonstrate that ancestral regulatory networks contribute to the establishment of an expression hierarchy for SPI-2 *in vitro* and to transcriptional priming in the host lumen prior to invasion. These findings demonstrate that *cis*-regulatory modifications have significantly contributed to the evolution of *S. enterica* as an intracellular pathogen.

Acknowledgements

First and foremost I need to acknowledge my supervisor and mentor Dr. Brian Coombes for giving me the opportunity and tools I needed to be successful. Words cannot begin to express my graditude for your unwavering faith in me over the years. I also wish to acknowledge my committee members Dr. Justin Nodwell and Dr. Murray Junop for their support and guidance throughout my graduate training.

I want to thank all the exceptional people that I have gotten to work with in the laboratory over the years for all your technical assistance, support and all the laughs in between. I especially want to acknowledge Ana and Colin who shared the emotional ride that is graduate school with me from beginning to end. You guys are my inspiration, my confidonts, my shoulders to cry on and my greatest friends. I will never forget the journey we took together.

I have been fortunate to have a remarkably encouraging family. To my parents, thank you for your love and for teaching me the value of hardwork. Thank you for expecting excellence and for giving me the freedom to define success on my own terms. I also need to extend graditude to my ‘blended’ family members for their encouragement and advice over the years. To Jeff, you are not only my brother but my best friend and are a constant source of inspiration. A big thank you to my ‘Gary’ family members: you have all always been there for me when it really mattered.

To Codi, Hera and all the horses in my life, thank you for the hours of stress-relieving entertainment and for forcing me to leave the house even when over burdened with work.

Above all, I thank my life partner Jason who was the only true witness to all the emotional highs and lows associated with completing my doctorate degree. For all the things said and things left unsaid; for all the little things that add up to a lifetime. You are my cornerstone. I would not have gotten here without you.

Table of Contents

List of Tables

List of Figures

List of Abbreviations

Cis-regulatory element (CRE)

Deoxyribonucleic acid (DNA)

Horizontal gene transfer (HGT)

Guanine (G)

Cysteine (C)

Adenine (A)

Thymine (T)

Salmonella pathogenicity island (SPI)

Type 3 secretion system (T3SS)

Enteropathogenic *Escherichia coli* (EPEC)

Enterohemorrhagic *Eschericha coli* (EHEC)

Guanine nucleotide exchange factor (GEF)

Guanosine triphosphate (GTP)

GTPase activating protein (GAP)

Intraperitoneal (i.p.)

Kilobase (kb)

Salmonella containing vacuole (SCV)

Definitive phage type 104 (DT104)

Helix-turn-helix (HTH)

Chromatin immunoprecipitation (ChIP)

Adenosine triphosphate (ATP)

Green fluorescent protein (GFP)

Inner membrane (IM)

Outer membrane (OM)

Host membrane (HM)

Evolutionary developmental biology (evo-devo)

Ribonucleic acid (RNA)

Messenger RNA (mRNA)

SsrB C-terminal domain (SsrBc)

Polymerase chain reaction (PCR)

Basepair (bp)

Million years (Myr)

Untranslated region (UTR)

Competitive index (CI)

Low phosphate, low magnesium media (LPM)

Fetal bovine serum (FBS)

Dulbecco’s modified eagle medium (DMEM)

Colony forming units (CFU)

Nucleotide (nt)

Intergenic region (IGR)

Luria broth (LB)

Bacterial artificial chromosome (BAC)

Periplasm (P)

Cytoplasm (C)

Lipopolysaccharide (LPS)

Rapid amplification of cDNA ends (RACE)

Optical density (OD)

Hemagglutinin (HA)

Splicing by overlap extention (SOE)

Open reading frame (ORF)

Sodium dodecyl sulfate (SDS)

Polyacrylamide gel electrophoresis (PAGE)

Dithiothreitol (DTT)

Horseradish peroxidise (HRP)

Hours (h)

Phosphate buffered saline (PBS)

ATP-binding cassette (ABC)

Pathogen associated molecular pattern (PAMP)

Angstrom (Å)

Histidine (HIS)

Isopropyl β-D-1thiogalactopyranoside (IPTG)

Nickel-nitriloacetic acid (Ni-NTA)

Tris buffered saline (TBS)

Relative light units (RLU)

Minutes (min)

Gravity (g)

Melting temperature (T_m)

Polar amino acids (PAA)

Fluorescence thermal shift (FTS)

Lysine, arginine, ornathine (LAO)

Wild type (Wt)

Betaine (B)

D-alanine (D-ala)

Disaccharide-tripeptide monomer (Tri)

Disaccharide-tetrapeptide monomer(Tetra)

Dimer of two tetra monomers cross-linked at the tetrapeptide side chains (Tetra-tetra)

Disaccharide-pentapeptide monomer (Penta)

Meso-diaminopimelic acid (A_2pm)

Reactive oxygen species (ROS)

Reactive nitrogen species (RNS)

Casamino acids (CAA)

Nicotinamide adenine dinucleotide phosphate (NADPH)

Revolutions per minute (rpm)

In vivo imaning system (IVIS)

Spleen (S)

Liver (L)

Cecum (C)

Small Intestine (SI)

Large Intestine (LI)

Nitric oxide (NO)

Ethylenediaminetetraacetic acid (ETDA)

Locus for enterocyte effacement (LEE)

Cytoplasmic ring (C-ring)

Yellow fluorescent protein (YFP)

Chapter One - Introduction

Chapter One - Introduction

Evolution: From Darwin to the Modern Synthesis

In ‘On the Origin of Species’, Charles Darwin argued that across populations all biological traits display variability and that, when placed in a struggle for survival, profitable variations will be preserved [1]. Modern day evolutionary theory is guided by the Modern Synthesis which combines the concept of Darwinian evolution with Mendelian and population genetics. It principally states that population variability is due to the presence of genetic mutations, that these varieties are inheritable and that beneficial varieties can become fixed within a population over time [2]. The Modern Synthesis recognizes that changes in allele frequency are driven by natural selection, genetic drift and gene flow [2]. It was proposed based on the continued advances in our understanding of evolution that the Modern Synthesis needed an update. One topic up for debate is whether *cis*-regulatory changes significantly contribute to organismal adaptation.

Cis-regulatory Evolution

Phenotype is not a straightforward end product of protein-coding sequences. It is a consequence of the amount of protein generated, as well as its temporal and spatial production dynamics. Transcriptional regulation is a critical means of controlling this expression. *Cis*-regulatory elements (CREs), the functional units of transcriptional

regulation, are segments of non-coding DNA typically located 5’ to the transcriptional start site, which comprise a collection of transcription factor binding sites [3]. Recruitment of transcription factors to the CRE in response to environmental cues allows transcriptional activity to be fine-tuned.

Early research perceived that cells did not simultaneously express their entire genetic repertoire and that induction of gene expression was influenced by mutations outside of the protein-coding sequence [4]. Closely related species often displayed greater organismal diversity then molecular diversity indicating that coding sequence alone was insufficient to account for species heterogeneity [5]. It was proposed that phenotypic complexities could arise from mutations acting on discreet transcription factor binding sites, altering the spatial, temporal, magnitude and inducibility dynamics of gene expression without the pleiotropic consequences of structural modifications [4,6,7,8]. CRE adaptation has the additional advantage that the emergence of regulatory networks allows for coordinated phenotypic responses. From these logical arguments researchers proposed that *cis*-regulatory modulation may be a driving force in phenotypic evolution.

Examples of *cis*-regulatory evolution remain limited. In contrast to protein sequences, which are precise and well-defined, CREs are flexible and their relationships to gene expression are difficult to interpret. Mutations in promoters can often be silent if they occur between transcription factor binding sites or even within these modules owing to the base tolerance allowed in many DNA recognition motifs [6]. In fact, deletion of entire transcription factor binding sites may be neutral due to the presence of multiple recognition sites [6]. The effects of mutations within promoter regions are also context-

dependent thus making it challenging to identify the corresponding phenotypic change. Despite these limitations, significant advances in elucidating the contributions of CRE adaptation to phenotypic diversity are beginning to be uncovered, particularly in the field of evolutionary developmental biology.

Seminal work in this area focused on the role of *cis*-regulatory control of organismal body plan. For example, examining the closely related *Drosophilia melanogaster* and *D. sechellia* demonstrated that hair patterning dissimilarity corresponded to *svb* transcription [9]. Similarly, loss of prominent pelvic structures in freshwater sticklebacks relative to their marine relatives correlated with differences in the spatial expression patterns of *pitx1* [10]. Loss of two binding sites for the transcription factor Engrailed accounted for differences in male wing spots observed between *D. melanogaster* and *D. biarmipes* [11]. Divergent wing pigmentation patterns between *D. elegans* and *D. gunungcola* were shown to be a consequence of only 10 nucleotide changes in the promoter of *Yellow* (*y*) [12].

Comparative analysis of human clinical isolates gave early clues that prokaryotes may also be subject to *cis*-regulatory evolution. It was recognized that HIV-1 subtypes often differ in their promoter architecture [13] and that isoniazid and ethionamide resistance in *Mycobacterium tuberculosis* could be linked to mutations in the promoters of *ahpC* [14] and *inhA* [15]. *Cis*-regulatory evolution may be even more critical to bacteria as the ability to acquire foreign DNA dictates large scale rearrangements of regulatory networks. It has been shown experimentally that synthetically reconnected transcriptional networks in bacteria are not only well tolerated but can produce fitness

advantages [16]. Regulatory networks show surprising divergence: only 30% of the PhoP regulon is conserved between *Salmonella enterica* and *Yersinia pestis* [17]. Even when components of a regulatory network are conserved between bacterial species, the wiring of the circuitry can be dissimilar. Unlike *S. enterica*, *Escherichia coli iraP* is not directly activated by PhoP due to the absence of the PhoP recognition motif in its promoter, but is instead indirectly activated by PhoP through the intermediate IraM [18,19]. The inverse orientation of the PhoP binding motif upstream of *ugtL* renders the *Salmonella* PhoP unable to activate the *Yersinia* promoter and vice versa [17]. This evidence has begun to suggest that *cis*-regulatory modifications are a critical driver of evolution and are pervasive through all kingdoms of life.

Opponents to *cis*-regulatory evolution as the major driver of phenotypic diversity argue that alternative strategies to avoid pleiotropy exist including the duplication and subsequent divergence of genes or the generation of alternative splicing sites [20]. It was recently estimated that *E. coli* and *Bacillus subtilis* have 477 and 483 gene paralogs respectively indicating that gene duplication does significantly contribute to prokaryotic adaptation [21]. Duplication of genes relaxes functional constraint and artificial duplication events have been shown to confer selective advantages in *E. coli* [22]. The proposition that altering the temporal and spatial dynamics of expression is less deleterious then a structural mutation is disputed [20]. Transcription factors themselves seem to undergo rapid evolution, a process known as *trans*-regulatory adaptation [23]. PhoP directly regulates several genes in *S. enterica* including *sseL* but the orthologous regulator in *S. bongori* is impaired in driving expression from the *sseL* promoter due to a

structural mutation in the DNA binding domain of PhoP [24]. Microarray analysis following a 20,000 generation evolution of *E. coli in vitro* demonstrated significant parallel changes in expression of 59 genes for which only 14% could be accounted for based on mutations in transcription factors [25]. Although the importance of regulatory modification to adaptation is evidenced in this work, the authors failed to examine the potential for *cis*-regulatory mutation; focusing on sequencing of protein coding sequences alone. The failure to map CRE mutations, particularly in early studies, makes it difficult to distinguish between *cis*- or *trans*-regulatory evolution. Although *trans*-regulatory variation appears to occur more often than *cis*-regulatory variation it is likely this difference is due to a larger mutational target size [26, 27]. Perhaps the greatest weakness of the *cis*-regulatory literature is that fitness consequences are often inferred but rarely empirically tested. It is clear that more evidence to support the role of *cis*-regulatory changes in evolution is needed. The wealth of available genome sequences, rapid generation time and the ease of genetic manipulations makes the use of bacteria to study evolution appealing. The use of bacterial pathogens is additionally advantageous since the use of well established animal models of infection allows researchers to quantify the fitness changes associated with specific CRE modifications.

Horizontal Gene Transfer

Phylogenetic subdivision of bacteria is complicated by a high degree of genetic fluidity caused by horizontal gene transfer (HGT); a process of genetic exchange through

transformation, conjugation or transduction of foreign DNA between members of a bacterial community [28]. Horizontally acquired genes can comprise over 20 - 30% of a bacterial genome [29]. Genomic islands are identified by atypical GC content and codon usage relative to the recipient bacteria [30,31]. Genomic islands are integrated into the bacterial genome, typically at tRNA sites [30]. When acquired sequences contain virulence genes such as endotoxins, secretion systems, invasions and antibiotic resistance genes they are referred to as pathogenicity islands [32].

Failure to regulate foreign DNA can have adverse fitness costs. Bacteria appear to employ a common strategy known as xenogenic silencing to initially down-regulate expression of acquired DNA. Global regulators such as H-NS in *E. coli* and *Salmonella*, MvaT and MvaU in *Pseudomonas* and Lsr2 in *Mycobacteria* occlude foreign DNA from transcriptional machinery by recognition of AT rich sequences [33,34]. Artificial gene transfer of a *Shigella* plasmid to *Salmonella* in the absence of the H-NS like protein Sfh was shown to cause global changes in gene expression highlighting the importance of xenogenic silencing [35]. Following this initial silencing, horizontally acquired DNA is gradually integrated into ancestral regulatory networks. Evidence exists to support regulatory integration; the RovA ancestral regulator in *Y. enterocolitica* and *Y. pestis* controls several horizontally acquired genes and the acquired regulator ToxT, which drives the expression of cholera toxin in *Vibrio cholerae*, has come under the control of the ancestral TcpP and ToxR transcription factors [36,37,38]. These systems must both promote transcription and displace the xenogenic silencers. Work on H-NS in *S. enterica* has shown that SlyA functions only to antagonize H-NS mediated silencing where PhoP

promotes transcription at the *ugtL* and *pagC* promoters [39]. The acquisition and regulatory integration of foreign DNA permits quantum leaps in bacterial evolution, granting expansion into new niches in a single step.

Evolution of Salmonella

Salmonella is a rod shaped Gram-negative bacterium from the enterobacteriaceae family that diverged from *E. coli* ~100 million years ago [40]. Microarray analysis identified 56 genes that are present in all *Salmonella* isolates but absent from the closest relatives *E. coli*, *Yersinia* and *Klebsiella*. Most of these *Salmonella*-specific genes are contained within the horizontally acquired *Salmonella* Pathogenicity Island 1 (SPI-1) [41]. SPI-1 encodes a type 3 secretion system (T3SS) required for invasion of intestinal epithelial cells. Around 40 million years ago, the *Salmonella* genus diverged into *S. enterica* and *S. bongori* species following a second major gene acquisition event: the procurement of SPI-2 in the *S. enterica* lineage (Figure 1.1) [41,42]. There are no genetic remnants of SPI-2 at the corresponding locus in *S. bongori* suggesting that SPI-2 was acquired in *S. enterica* and not lost in *S. bongori*. Similar to *S. enterica, S. bongori* contains SPI-4 and SPI-9 and incomplete fragments of SPI-3 and 5. It retains the tetrathionate respiration (*ttr*) gene cluster at the SPI-2 insertion locus [43]. *S. bongori* has a type 6 secretion system encoded at a common site of integration similar to SPI-2 in *S. enterica* and has acquired some additional genes encoding secreted substrates of the SPI-1 T3SS which display similarity to virulence proteins found in enteropathogenic *E. coli*

(EPEC), enterohaemorrhagic *E. coli* (EHEC) and *Citrobacter rodentium* [43]. *S. enterica* further subdivides into 6 subspecies; *enterica*, *salamae*, *arizonae*, *diarizonae*, *houtenae* and *indica* of which only *S. enterica* subspecies *enterica* causes disease in warm-blooded animals (Figure 1.1) [41,43]. Over 2500 distinct serovars of S. *enterica* have been identified which range in their preferred animal hosts and disease severity.

Salmonella: Disease and Treatment

S. enterica provokes a spectrum of clinical diseases in humans from self-limiting gastroenteritis (food poisoning) to a potentially fatal systemic infection known as Typhoid fever. Typically contracted from contaminated food or water, gastroenteritis clinically manifests as abdominal pain, vomiting and diarrhoea [44]. Medical intervention is rarely required for immune-competent individuals. Although infrequent in the developed world, the human-specific *S. enterica* serovar Typhi causes Typhoid fever characterized by a prolonged low grade fever, malaise and nausea. Severe cases can involve intestinal bleeding and perforation, confusion, dizziness and even death. Paratyphoid fever is similar to Typhoid fever but with reduced severity. Treatment with fluoroquinolones is typically effective, reducing fatality to less than 1% [45].

Up to 214,000 cases of non-typhoidal *S. enterica* occur annually in Canada with an associated cost of $2.24 million [46]. Similarly 1.4 million cases of food borne illness resulting from *S. enterica* occur in the United States with an average of 580 deaths annually [47,48]. Disease burden for Typhoid fever ranges globally from greater than

100/100,000 annual cases in south-central and south-east Asia to less than 10/100,000 in Europe and North America [49]. The global health and economic threat posed by *S. enterica* continues to escalate owing to the emergence of drug resistance. For example, the globally disseminated *S. enterica* serovar Typhimurium phage type DT104 carries resistance to ampicillin, chloramphenicol, streptomycin, sulphonamides and tetracycline [50].

Salmonella Pathogenicity Island 1

The onset of gastroenteritis corresponds to *S. enterica*'s capacity to penetrate the intestinal epithelium. Investigation of the genetic elements required for invasion led to the identification of the *inv* locus. Deletions at this locus attenuated invasion of cultured epithelial cells and survival following oral infection of mice [51]. The *hil* locus was subsequently discovered when screening for hyperinvasive transposon mutants [52]. Detailed mapping showed that these loci constituted a continuous 40-kb region absent from the corresponding locus in *E. coli* with a low (45.9%) GC content relative to the core genome (52%) [53]. Being required for invasion and showing homology to the *Shigella* virulence plasmid invasion genes, this horizontally acquired region was named *Salmonella* Pathogenicity Island (SPI) – 1 [54,55]. SPI-1 is organized into three operons: the *prg/org* and *inv/sip* operons which encode a type 3 secretion system (T3SS) and the *sic/sip* operon containing secreted proteins (effectors) and their chaperones [56]. These components allow direct delivery (translocation) of effectors into the host cell cytoplasm.

Uptake of bacteria into epithelial cells by macropinocytosis requires the creation of membrane ruffles via actin cytoskeleton remodelling. Microinjection of the SPI-1 effectors SopE, SopE2 or SopB, which function as guanine nucleotide exchange factors (GEFs) for the host Rho GTPases Cdc42 and Rac-1, is sufficient to induce cytoskeleton rearrangements [57,58,59,60]. Actin remodelling is further perturbed by SipC which increases F-actin formation and SipA, which decreases the critical concentration of G-actin needed to initiate polymerization and stabilizes actin filaments [61,62]. SopE, SopE2 and SopB have additionally been implicated in mediating a pro-inflammatory response following interaction with epithelial cells [58,63,64]. SopA and SipA induce polymononuclear transepithelial migration to the site of infection [65,66]. The SPI-1 effector SipB influences host cell death through activation of caspase-1 [67]. Re-establishment of normal actin architecture and inflammatory responses following invasion is mediated by the SPI-1 secreted GTPase activating protein (GAP) SptP, AvrA and SspH1 [64,68,69,70]. The apparent antagonistic role of SptP with SopE, SopE2 and SopB is coordinated by differential rates of secretion and proteosome-dependent degradation within the host cell [71,72].

Expression of SPI-1 occurs under conditions thought to mimic the intestinal lumen including high salt concentrations and low oxygen [73]. HilA is the central regulatory node driving expression of the structural components of the T3SS at the *invF* and *prgH* promoters as well as negatively autoregulating its own expression [74,75]. InvF in complex with its chaperone SicA subsequently directs expression of effectors encoded both within and outside the confines of SPI-1 [76]. Under non-inducing conditions, *hilA*

transcription is repressed by the xenogenic silencers H-NS and Hha [77]. De-repression requires a positive feed-forward loop consisting of the SPI-1 encoded regulators HilC and HilD as well as the external regulator RtsA. HilD appears to have the strongest effect on *hilA* expression. HilC, HilD and RtsA all directly activate expression of *hilA*, each other and can additionally drive HilA-independent expression from the *invF* promoter [78,79,80,81]. The observation that expression of HilD has been integrated into ancestral regulatory networks including repression by IsrM and HilE, activation by FliZ, Fur, and the two-component regulatory systems EnvZ/OmpR and SirA/BarA is consistent with *cis*-regulatory adaptation at this locus [78,82,83,84].

Salmonella Pathogenicity Island 2

When SPI-1 mutants failed to display a virulence defect following intraperitoneal (i.p.) infection it suggested that additional virulence machinery was required for systemic dissemination. SPI-2 was subsequently discovered by signature tagged mutagenesis and examination of *S. enterica* DNA library clones [85,86]. Mutants within this 25-kb locus had a 10^4 times greater lethal dose compared to wild type following an i.p. infection [85]. SPI-2, which is exclusively present in *S. enterica*, has a GC content of 44.6% and is integrated at the $tRNA^{Val}$ locus between *ydhE* and *pykF* [87]. A tetrathionate reductase complex is also present at this site but was acquired separately [88]. SPI-2 encodes a T3SS, several secreted proteins, chaperones and its own regulatory system. The SPI-2 T3SS shows greater similarity to the T3SSs in *Yersinia* and EPEC then to SPI-1 arguing

against a duplication event [86,89]. SPI-2 is organized into 4 operons: two operons encoding structural components of the T3SS, an effector/chaperone operon and a regulatory operon. The acquisition of SPI-2 allowed *S. enterica* to exploit an intracellular niche where it replicates within a phagocytic vacuole termed the *Salmonella* containing vacuole (SCV). Intracellular replication is linked to systemic dissemination and *S. enterica* mutants unable to survive within macrophages are avirulent [89,90]. Survival within host cells presents unique challenges to *S. enterica*, whereby the bacteria must not only actively prevent phagosome maturation along the normal endosomal pathway but must also arm itself against an acidic pH, low nutrient availability and an arsenal of host immune responses [91].

The SPI-2 T3SS delivers effector proteins across the phagosomal vacuole where they function to establish the SCV, preventing fusion with lysosomes and bacterial destruction. Arguably the most essential effector, SifA colocalizes with the SCV membrane and is required for the formation of *Salmonella* induced filaments (Sifs); tubular membrane extensions of the SCV [92]. Deletion of *sifA* destroys the integrity of the SCV and is as deleterious to intracellular survival as structural perturbations to the SPI-2 T3SS [93,94]. Through interaction with the host protein SKIP, SifA additionally controls SCV positioning through regulation of the microtubular motor protein kinesin-1 [95]. The SPI-2 effectors SseJ, SseF, SseG, SopD2, SifB, PipB and PipB2 also localize to the SCV membrane [96,97,98,99,100]. The concerted effects of PipB2 and SifA on kinesin-1 drive centrifugal displacement of the SCV at late time points during infection and may allow for cell to cell transfer [101,102,103]. SseF and SseG contribute to Sif

formation and perinuclear positioning of the SCV. Deletion of SseF, SseG or SopD2, leads to production of pseudo-Sifs: Sif-like extentions that lack several key features of Sifs [99,104,105]. SopD2 contributes to SCV instability and drives the vacuolar loss observed in *sifA* mutants [106]. Modulation of host immune responses is another target of the SPI-2 T3SS. Although insufficiently characterized, several effectors including SspH2, GogB and SseL have demonstrated a capacity to target pro-inflammatory signalling cascades through their deubiquitination activity [107,108,109](Unpublished data). SseL is thought to abate the pro-inflammatory response by limiting IκBα ubiquitination, a process normally inducing NF-κB activation [110]. SseL additionally appears to play a role in lipid metabolism [111]. The role of the SPI-2 effector SpiC (SsaB) is controversial as some groups report SpiC translocation and interaction with host proteins TassC and Hook3 where other laboratories describe SpiC as a structural component of the T3SS required for secretion of SPI-2 effectors [112,113,114,115,116]. A complex of SpiC/SsaM/SsaL was shown to act as a pH sensor, triggering effector secretion in reaction to a neutral pH [117]. Additional SPI-2 secreted effectors include SseI, SseK1, SseK2, SteA, SteB, SteC, SpvB, however, their exact contributions to virulence remain undetermined. The majority of effectors are not encoded within SPI-2 and reflect subsequent horizontal gene acquisition events. Their co-regulation with and secretion by the SPI-2 T3SS emphasizes the significance of regulatory amalgamation following HGT in the evolution of bacterial pathogens.

SPI-2 gene expression is amplified following entry into the intracellular niche [118,119,120]. Expression is triggered *in vitro* by conditions presumed to reflect

environmental cues encountered in the SCV including an acidic pH, warm (37°C) temperature, low concentrations of Mg^{2+} or Ca^{2+} and phosphate starvation [118,121,122]. Expression of the T3SS and effectors is absolutely dependent on the SPI-2 encoded two-component regulatory system SsrA and SsrB [118,122]. The expression of *ssrAB* is controlled by several ancestral regulators including H-NS, Hha, YdgT, PhoPQ, EnvZ/OmpR, SlyA and Fis (Figure 1.2).

SsrAB

The SPI-2 encoded histidine kinase SsrA is activated in response to a yet unidentified signal indicative of entry into the intracellular mileu and subsequently activates the response regulator SsrB. An NMR structure of the C-terminal domain of SsrB reveals a helix-turn-helix (HTH) DNA binding domain which recognizes an 18 base-pair degenerate palindrome with tail to tail architecture [123,124]. SsrB directly activates transcription from the SPI-2 *ssrA*, *ssaB*, *sseA*, *ssaG*, *ssaM* and *ssaR* promoters and several virulence factors encoded throughout the genome [124,125,126]. Microarray analysis revealed that 133 genes are down-regulated in an *ssrB* deletion [124]. Some laboratories have alleged that expression of *ssrA* and *ssrB* is uncoupled, however we have been unable to recapitulate a hidden *ssrB* promoter [127] (Unpublished data). Extensive examination of virulence regulators *in vivo* indicated that SsrB is a terminal regulatory node and that its own expression is driven by ancestral regulatory networks [128].

H-NS

H-NS is a nucleoid-associated protein known for its role in xenogenic silencing. H-NS was first identified based on its ability to polymerize along intrinsically curved DNA and was subsequently shown to influence DNA topology [129,130]. Structural analysis of H-NS reveals a distinct N-terminal oligomerization domain which mediated formation of H-NS homodimers which then associate into polymers in a head-to-tail orientation [131,132,133]. The H-NS C-terminal domain interacts with DNA in two distinct inter-convertible formations [134]. In low concentrations of divalent cations (Mg^{2+}, Ca^{2+}) H-NS polymerizes along DNA in the "stiffening" mode [134]. In this mode, H-NS is sensitive to changes in pH and temperature. At higher cation concentrations, H-NS bridges DNA leading its compaction [134]. Microarray and chromatin immunoprecipitation (ChIP) – on – chip experiments in *S.* Typhimurium revealed a strong correlation between H-NS binding and GC content [34]. The AT rich H-NS recognition motif occurs on average every 2.5 genes within horizontally acquired loci [135]. SPI-2 exhibited SsrB-dependent up-regulation in an H-NS mutant background and SsrB was subsequently shown to displace H-NS when it is bound to DNA in the polymerization mode [34,136]. The interplay between H-NS and SsrB is not fully clear as H-NS cannot bind DNA in the polymerization mode at 37°C; the permissive temperature for SsrB-dependent activation of SPI-2 [134].

S. Typhimurium also encodes the H-NS-like proteins YdgT and Hha which repress SPI-2 gene expression and contribute to virulence *in vivo* [137,138]. Over 87% of

the pathogenicity islands in *S*. Typhimurium appear co-regulated by YdgT/Hha and H-NS [139]. Based on evidence that YdgT and Hha interact with H-NS and display structural similarity to the oligomerization domain of H-NS it was hypothesized that YdgT and Hha replace H-NS monomers within the higher order oligomers thereby influencing polymerization or bridging of DNA [140,141,142]. The exact nature of YdgT/Hha and H-NS complexes and their effect on transcriptional regulation remains poorly characterized.

SlyA

A connection between SlyA and SPI-2 regulation was insinuated by the discovery that a *slyA* deletion produces a modest virulence defect in macrophage and mouse infections [128,143,144]. Structural analysis revealed a 'swiss cheese' architecture suggesting association with small molecules and the presence of a winged-helix DNA recognition domain [143,145,146,147]. SlyA is a terminal SPI-2 regulator directly activating the *ssrAB* promoter [128,144,148,149]. SlyA has been shown to antagonize H-NS mediated silencing at the *phoPQ*, *ugtL* and *pagC* promoters but this possibility has not been examined at the *ssrAB* promoter.

Fis

Originally characterized as modulating phase shifting of flagellar antigens, loss of the factor for inversion stimulation (*fis*) correlates with virulence attenuation *in vivo*

[150,151]. Microarray and proteome analysis indicated that the defect was owing to a decrease in SPI-2 gene expression [152,153]. As a nucleoid-associated protein, Fis directs DNA topology at the SPI-2 *ssrA* and *ssaG* promoters [151]. Following entry into macrophages, the *ssrA* promoter undergoes a Fis-dependent relaxation resulting in transcriptional activation [151]. Fis recognizes a degenerate DNA binding motif of which 4 copies are upstream of *ssaG* [150,154]. Interestingly, Fis-dependent expression of *ssaG* also occurred in non-inducing conditions and it was noted that the Fis and SsrB binding sites overlapped [125,150]. These regulators may drive structural gene expression from SPI-2 under different environmental conditions.

EnvZ/OmpR

The EnvZ/OmpR two-component system is a global regulator originally characterized for its role in transcription of the outer membrane proteins *ompF* and *ompC* in response to changes in osmolarity [155]. The OmpR C-terminal winged HTH DNA binding domain recognizes a degenerate DNA binding motif that remains poorly characterized [156]. Deletion of *ompR* caused a severe virulence defect and footprinting analysis revealed that OmpR directly regulates the *ssrAB* promoter [128,157,158]. This was consistent with SPI-2 osmoregulation [157]. Questions remain regarding the role of OmpR at the *ssrAB* promoter as the OmpR and SsrB binding sites overlap suggesting that these transcription factors compete for interaction with the *ssrAB* promoter region [127].

PhoPQ

The two-component regulatory system PhoPQ controls the expression of over 200 genes [159]. The activity of the sensor kinase PhoQ is dependent on the concentration of divalent cations, pH and antimicrobial peptides. Up to three divalent cations mediate formation of a metal bridge between an acidic patch in the periplasmic sensor domain of PhoQ and the bacterial inner membrane [160]. Loss of Mg^{2+} and Ca^{2+} mediated membrane tethering causes a charge repulsion between PhoQ and the membrane. The ensuing conformational shift initiates transmembrane signalling leading to phosphorylation of the response regulator PhoP [160]. The metal-mediated inhibition of PhoQ is overcome by antimicrobial peptides and an acidic pH [161,162]. Cationic antimicrobial peptides, by nature of their enhanced affinity for the acidic region of PhoQ, displace the divalent cations resulting in release of the membrane tether and activation of PhoQ [161,163]. The activation of PhoPQ following entry into host cells, coupled with observations that *phoP* mutants are attenuated for virulence, suggested a role for PhoP in controlling SPI-2 gene expression [128,164,165,166,167]. PhoP controls the levels of SsrA post-transcriptionally and directly activates the presumably hidden *ssrB* promoter [168,169]. Several SPI-2 co-regulated genes encoded elsewhere in the genome require PhoP for expression [126].

Other SPI-2 Regulators

In addition to the key regulators discussed above, additional regulatory inputs into SPI-2 expression upstream of SsrAB continue to be characterized. This includes regulation stemming from ppGpp [170], QseC [171] and alternative sigma factors RpoS [128] and RpoE [172]. This cohort of transcriptional regulators all contribute to the dynamics of SPI-2 gene expression. This plethora of ancestral regulatory input into a horizontally acquired island emphasizes the influential role of *cis*-regulatory adaptation following gene acquisition.

SPI-1 and SPI-2 Crosstalk

The contributions of SPI-1 and SPI-2 to pathogenesis are traditionally compartmentalized into two distinct stages of infection: intestinal colonization and intracellular replication respectively. This dogmatic view has been challenged by evidence of functional and regulatory crosstalk between these two pathogenicity islands. Diverse infection models including chickens and murine and bovine ileal loops have documented a role for SPI-2 in intestinal colonization at later time points [173,174,175,176]. A limited set of SPI-2 transcriptional reporters were activated within 15 minutes after infection of a murine ileal loop at which point bacteria were found localized to the apical surface of the epithelium [177].The rationale for luminal SPI-2 activation remains unknown although it may serve to prime bacteria for entry into the

intracellular environment where they must rapidly contend with an arsenal of host defences. SPI-1 may contribute to systemic dissemination as deletions were shown to attenuate intracellular replication [178]. SPI-1 and SPI-2 T3SS effectors display a degree of cooperation; the SPI-1 effector SipA persists in the host cell and synergistically mediates SVC positioning with the SPI-2 effector SifA [179]. GogB is secreted by both T3SSs and the SPI-2 co-regulated effector PipB2 is secreted by the SPI-1 T3SS [180] (Cooper, C.A. Unpublished data). These findings suggest that the SPI-1 and SPI-2 effector repertoire partially overlap. Regulatory communication between SPI-1 and SPI-2 adds another layer of complexity as expression of both islands is controlled by H-NS and EnvZ/OmpR (Figure 1.2). Deletion of structural components of the SPI-2 T3SS has been shown to influence expression of the SPI-1 master regulator *hilA* through an unknown mechanism [181]. The SPI-1 regulator HilD directly binds to the *ssrAB* promoter and is required to counteract H-NS mediated silencing during non-inducing conditions [182]. Overall these findings attest that SPI-1 and SPI-2 are not functionally autonomous and that pathogenesis requires the concerted efforts of both loci. Given that these two islands were acquired in separate horizontal gene acquisition events, the regulatory overlap is plausibly the result of CRE modification, further highlighting the importance of *cis*-regulatory adaptation to prokaryotic evolution.

Additional Salmonella Pathogenicity Islands

S. enterica encodes a plethora of pathogenicity islands in addition to SPI-1 and SPI-2, many of which contribute to virulence or host-specificity. Conserved across all eight subspecies, SPI-3 encodes a magnesium uptake system MgtCB and several more variably distributed genes [183,184]. Secretion of the adhesion SiiE is dependent on a putative type 1 secretion system encoded in SPI-4 [185,186]. SPI-4 is co-regulated with SPI-1 and is required for efficient invasion [185,186]. SPI-5 encodes *pipABCD* and *sopB*, some of which are secreted by the SPI-1 and SPI-2 T3SSs [187]. The composition of SPI-6 is variable but commonly contains fimbrial machinery as well as the PhoPQ-regulated protein PagN [188]. SPI-7 is only found in *S.* Typhi, Paratyphi C and Dublin and encodes the Vi capsular polysaccharide *viaB* [189]. SPI-8, SPI-9 and SPI-10 are found in *S.* Typhi where SPI-10 appears to encode a P4-like phage and fimbrial islet [189]. SPI-11 and SPI-12 were identified in *S.* Choleraesuis, SPI-13 and SPI-14 in *S.* Gallinarum, and SPI-15 in *S.* Typhi [190,191,192]. Two bactoprenol-linked glucose translocases (*gtrAB*) involved in serotype conversion are present in SPI-16 [192]. SPI-17 appears to have similar phage family origins as SPI-16 [192]. The hemolysin HlyE from *S.* Typhi is found in SPI-18 [193]. Three additional islands, SPI-19, SPI-20 and SPI-21, were recently shown to encode type 6 secretion systems but are sporadically distributed among *S. enterica* serovars [194].

Type 3 Secretion Systems

The type 3 secretion system (T3SS) is a macromolecular machine employed by bacteria to pathogenically and symbiotically interact with host cells [195,196]. The T3SS constitutes a pair of rings spanning the bacterial inner and outer membranes which anchors a needle structure [195,197,198]. The needle terminates in a translocon apparatus necessary for insertion into the host cell membrane. The T3SS therefore serves as a conduit; allowing direct transfer of bacterial proteins (effectors) into the host cell cytosol in one step (Figure 1.3). Targeting of effectors to the T3SS requires a loosely-defined N-terminal signal sequence. Recent computational programs have predicted that this signal is rich in polar amino acids particularly serines, has a limited number of charged residues and is enriched in coiled domains [199,200,201,202]. Reflective of their unique host interactions, effector repertoires display a high degree of diversity. The strong structural conservation of the T3SS coupled with its essentiality for pathogenesis in microbes that utilize them, identifies the T3SS as a potential antimicrobial drug target [203]. As such, extensive research has gone into elucidating the structure, assembly and regulation of this machine.

Electron microscopy gave researchers the first glimpse of the SPI-1 T3SS; it appeared to have an outer membrane ring composed of 15 InvG monomers and two 24 subunit concentric inner membrane rings consisting of PrgH and PrgK [197,198]. Similar structures were observed in *Shigella flexneri* where the T3SS was shown to contain a central channel [204]. A secretin from the YscC family (InvG and SsaC in SPI-1 and SPI-

2 respectively) oligomerizes in the absence of other components of the T3SS into a 20 nm outer membrane ring with a central pore of 5 nm [205,206,207]. Structural analysis of the C-terminus revealed that it only forms the transmembrane ring and the N-terminal domain extends into the periplasmic space to interact with and stabilize the inner membrane ring [208].

The larger inner membrane ring is formed by 24 monomers of PrgH in SPI-1 (SsaD in SPI-2). The smaller ring is made up of lipoproteins from the highly conserved YscJ family (PrgK/SsaJ in SPI-1 and SPI-2 respectively). They are tethered to the membrane by an N-terminal lipid and C-terminal transmembrane domain [209]. Crystal structures of the inner membrane ring have been solved [197,210]. Closely associated with the inner membrane ring is a poorly characterized export apparatus (InvA, SpaPQRS in SPI-1). It has been shown that assembly of the needle complex requires the export apparatus and that it is essential for T3SS function [211,212].

At the proximal end of the T3SS lies the non-conserved, poorly characterized C-ring originally identified in flagella as FliN and FliM. The YscQ family, which includes Spa33 (*S. flexneri*) and EscQ (EPEC), shows similarity to FliNM, interacts with components of the T3SS inner membrane rings and binds the ATPases, suggesting that they facilitate interactions between the basal body and cytoplasmic components of the T3SS [213,214,215].

A hollow tube with a 25 Å central channel is anchored to the outer membrane ring forming the needle. Polymerization of approximately 140 copies of the small α helical filament subunit YscF (*Yersinia*)/ MxiH (*Shigella*)/BsaL (*Burkolderia*)/PrgI (SPI-1) is

required for formation of the needle [204,216,217,218]. The filament terminates in a translocon structure composed of three proteins; two hydrophobic proteins (SipBC/SseCD in SPI-1/SPI-2) and one hydrophilic protein (SipD/SseB in SPI-1/SPI-2) [219]. The hydrophilic protein extends the helical needle with a 5 subunit ring [216,217,220]. The hydrophobic proteins are inserted into the host cell membrane and, in the presence of the hydrophilic protein, mediate the formation of a pore [221,222,223,224]. Deletion of the SPI-2 translocons SseBCD significantly attenuates virulence [225,226,227,228].

A highly conserved ATPase displaying structural similarity to the F_1F_0 α and β subunits of the ATP synthase is docked at the cytoplasmic face of the apparatus. Interaction of the ATPase with ATP and the effector is required for secretion and deletion of the ATPase attenuates virulence [229,230] (Cooper, C.A. et al Unpublished Data). YscN from *Yersinia* was the first T3SS ATPase to be characterized and shown to contain Walker A and B nucleotide binding motifs [230]. Structural analysis of EscN (EPEC) and SsaN (SPI-2) revealed hexameric ring architecture with a negatively charged central pore [231] (Cooper, C.A. et al Unpublished Data). A study examining the SPI-1 ATPase InvC demonstrated that the ATPase binds an effector - chaperone complex and this interaction is ATP-independent [232]. ATP hydrolysis appears to drive effector unfolding and disengagement from the chaperone [232].

Effector secretion requires virulence chaperones to curtail unwanted protein interactions or folding. Despite low sequence similarity, chaperones posses similar tertiary structures as evidenced by crystal structures of InvB, SicP, SigE (SPI-1), CesT

(EPEC) and SrcA (SPI-2) [233,234,235,236]. Chaperones tend to have a low molecular weight, an acidic pI and are typically encoded in immediate proximity to their substrates. Work in the *Yersinia* YopE effector demonstrated that effectors have an N-terminal chaperone binding site that is distinct from the secretion signal sequence [237]. Chaperones additionally aid in targeting of effectors to the T3SS and in transcriptional regulation. The SPI-1 chaperone SicA was required for efficient expression of SPI-1 effector proteins [238]. Similar observations were made with the *S. flexneri* chaperone IpgC [239]. Our laboratory recently identified a potential role for the SscA chaperone in modulating SPI-2 gene expression (Cooper, C.A. Unpublished data). These findings suggest that chaperone interactions may play a pivotal role in establishing regulatory hierarchy in T3SSs.

Assembly and Secretion Hierarchy

Ordered assembly of the T3SS is initially established through transcriptional and post-transcriptional regulation. GFP transcriptional reporters for the flagellar promoters demonstrated an expression hierarchy where the *flhDC* master regulators (Class I) were expressed first, then structural components of the hook basal body (Class II) and subsequently transcription of the filament (Class III) [240]. Analogous observations were made for SPI-1 where the *hilCD* transcriptional regulators were expressed first and subsequently drove expression of the T3SS basal body and finally effectors were expressed [241]. Expression of the effector operons was shown to be regulated by an InvF

– SicA complex [76,238,242]. Prioritized expression by means of divergent regulatory input appears to be a common theme in T3SS hierarchy; in *Shigella*, VirFB drive expression of the basal body where expression of effectors is specifically induced by MxiE [239,243]. Transcriptional hierarchy has also been documented in *Burkholderia pseudomallei* where effector expression was controlled by BsaN and its chaperone BicA [244]. In *Yersinia*, the temporally coordinated expression of the T3SS occurs post-transcriptionally as transcription is exclusively controlled by LcrF (*Y. pestis* and *Y. pseudotuberculosis*)/ VirF (*Y. enterocolitica*) [245,246]. A LcrQ/LcrH/YopBD complex interacts with the 5' untranslated region of effector mRNA blocking effector translation [247,248]. Secretion of the translocons YopBD following basal body assembly released the repressive complex allowing for effector translation. No work has yet examined the existence of a regulatory hierarchy for the SPI-2 T3SS.

Recent work utilizing fluorescence labelling in *Yersinia* established that T3SS assembly commences with the outer membrane ring (YscC) and proceeds in an outside-in manner [212,249]. Completion of inner membrane rings is followed by recruitment of auxiliary factors including the cytoplasmic ATPase and sorting platforms. Completion of the basal body initiates secretion. The T3SS undergoes two distinct substrate specificity switches; the needle-translocon switch and the translocon-effector switch [See [250] for full review]. In flagella, the secretion of FliK is utilized as a feedback strategy to monitor the assembly state although the exact mechanism remains controversial. Following completion of the basal body, FliK becomes juxtaposed to the inner membrane protein FlhB triggering autocleavage of FlhB and a substrate specificity switch from hook to

filament secretion [251,252,253,254]. An analogous switch from needle to translocon secretion has been characterized in the *Yersinia* T3SS where completion of needle assembly permits YscP to induce YscU autocleavage (Figure 1.4). The discovery that uncleavable YscU variants were unable to secrete translocons but retained effector secretion suggested a separate mechanism controls effector recognition [255,256]. A 'sensory complex' appears to mediate the translocon - effector specificity switch. The sensory complex appears to generally consist of a secretable substrate, the translocon and an effector-specific regulator. The complex effectively sequesters the regulator until the translocons have been secreted. Deletion of components of the sensory complex typically causes effector hyper-secretion [248,257,258,259]. In *Shigella*, a complex of OspD1, MxiE and Spa15 blocks MxiE-dependent up-regulation of effector expression prior to assembly completion [260]. In *Yersinia*, secretion of LcrQ and the YopBD translocons de-represses effector translation allowing for their subsequent secretion [247,248] .

In *Yersinia* and *Shigella*, a regulatory plug physically blocks effector secretion but, unlike the sensory complex, does not influence effector expression or translocon secretion. Disengagement of the YopN/TyeA/SycN/YscB plug in *Yersinia* following YopN secretion relieves the block on effector secretion [261,262,263]. A SsaM/SsaB/SsaL complex may serve as a similar plug for the SPI-2 T3SS but unlike *Yersinia* and *Shigella*, deletion of plug components prevents translocator secretion [116,117,264]. The exact nature of the sensory complex and regulatory plug remain to be fully elucidated.

Recent studies have provided evidence for the existence of an effector secretion hierarchy. Using a novel FlAsH labelling technique, the SPI-1 effectors SipA and SopE2 were translocated into host cells before SptP consistent with their antagonistic functions [71]. Ordered secretion of PipB2, SteA and SteC was similarly shown using a split-GFP reporter [265]. In *E. coli* O157:H7 secretion of Tir occurs prior to other effectors [266]. Although it has been proposed that relative effector-chaperone-ATPase affinities may establish a translocation order, the exact mechanism remains unknown. This prediction was based on evidence in *Y. pestis* where it was modelled that the SycH chaperone has preferential binding affinity for the effector LcrQ over YopH and that either complex displays a greater affinity for the ATPase then that of the YopE-SycE (effector-chaperone) complex [267]. A more thorough biochemical analysis of chaperone-effector affinities and quantitative analysis of the T3SS secretome will be necessary before the mechanism of secretion hierarchy can be fully elucidated.

Overall, T3SS expression, assembly and secretion are tightly coordinated processes which have been almost exclusively studied in *Yersinia*. Although some work has been done in *Shigella* and SPI-1, there is a clear knowledge gap in our understanding of SPI-2 hierarchy.

Purpose and Aims of the Current Study

The purpose of this study was to investigate the contribution of regulatory adaptation to the evolution of *S. enterica* as an intracellular pathogen. Prior to the

initiation of this work, no singular example of *cis*-regulatory modification directly contributing to fitness in prokaryotes existed, highlighting a clear knowledge gap in our understanding of phenotypic adaptation. Given the contribution of horizontal gene acquisition to bacterial evolution, and the necessity for integration of acquired DNA into existing regulatory networks, a thorough understanding of *cis*-regulatory modification is essential. Acquisition of SPI-2 conferred upon *S. enterica* the ability to exploit an intracellular replicative niche. When microarray analysis in an *ssrB* mutant background revealed that several genes ancestral to *Salmonella* were co-regulated with SPI-2, it insinuated that *cis*-regulatory integration into the SsrB regulon had occurred [124].

Coordinated assembly of the T3SS in SPI-1 and *Yersinia* is initially established through a transcriptional or post-transcriptional regulatory hierarchy respectively. Exploration into the existence of a regulatory hierarchy for the SPI-2 T3SS is lacking, highlighting a gap in our understanding of SPI-2 gene expression. Given findings that SPI-2 expression is not limited to the intracellular stage of infection and that it possesses significant regulatory overlap with SPI-1 gives credence to the need to fully examine the temporal regulation of SPI-2 during the course of infection. Although a cohort of studies have identified ancestral regulators that control expression of *ssrAB* there is a poor understanding of how these regulatory inputs coordinate the temporal and spatial expression of SPI-2. Such studies would provide a greater understanding of how *cis*-regulatory adaptation has contributed to the evolution of *S. enterica* as an intracellular pathogen.

My hypothesis was that ***cis*-regulatory modification following the horizontal gene transfer of SPI-2 has significantly contributed to the evolution of *S. enterica* as a pathogen**. The aims of this project were to; 1) Determine if ancestral genes have been integrated into the SsrB regulon and examine how this integration has contributed to pathogenesis; and 2) Examine the role of ancestral regulatory systems in the expression of SPI-2 operons and how they contribute to temporal control of gene expression.

The specific goals and findings are discussed in the following three chapters:

1. Pathogenic adaptation of intracellular bacteria by rewiring a *cis*-regulatory input function.
   - This study demonstrated that *cis*-regulatory evolution of *srfN* into the SsrB regulon has contributed to *S. enterica* fitness *in vivo*.

2. Characterization of DalS, a novel ATP-binding Cassette Transporter for D-alanine and its role in pathogenesis in *Salmonella enterica*.
   - This study characterized DalS as a periplasmic binding protein component of an ABC transporter for D-alanine that contributes to virulence in *S. enterica*.
   - Accompanying data (Appendix A) demonstrated that *dalS* has undergone *cis*-regulatory integration into the SsrB regulon. Preliminary evidence indicated DalS may be involved in peptidoglycan recycling and modulation of host nitric oxide responses.

3. Transcriptional priming of *Salmonella* Pathogenicity Island-2 precedes cellular invasion.

- This study systemically examined the contribution of ancestral regulators to the temporal and spatial expression dynamics of SPI-2, providing evidence that these regulators contribute to an *in vivo* transcriptional hierarchy.

Characterization of the ancestrally encoded *srfN* and *dalS* has provided solid evidence that *cis*-regulatory evolution in pathogenic bacteria contributes a quantifiable fitness gain in a host setting. Examination of the temporal and spatial dynamics of SPI-2 revealed the importance of ancestral regulators in moderating temporal and spatial expression of this horizontally acquired island. Overall these findings provide compelling evidence that *cis*-regulatory adaptation has significantly contributed to the pathogenic lifestyle of *S. enterica*.

Figure 1.1 – Schematic of *Salmonella* Phylogeny and Main Evolutionary Events. Horizontal gene transfer of SPI-1 led to the divergence of *Salmonella* from *Escherichia coli*. Segregation of *S. enterica* from *S. bongori* followed acquisition of SPI-2 in the *S. enterica* linage. *S. enterica* subdivides into six subspecies of which *S. enterica* subspecies enterica infects warm-blooded hosts. Over 2500 serovars of *S. enterica* exist including the human-specific *S. enterica* serovar Typhi and zoonotic *S. enterica* serovar Typhimurium.

Figure 1.1

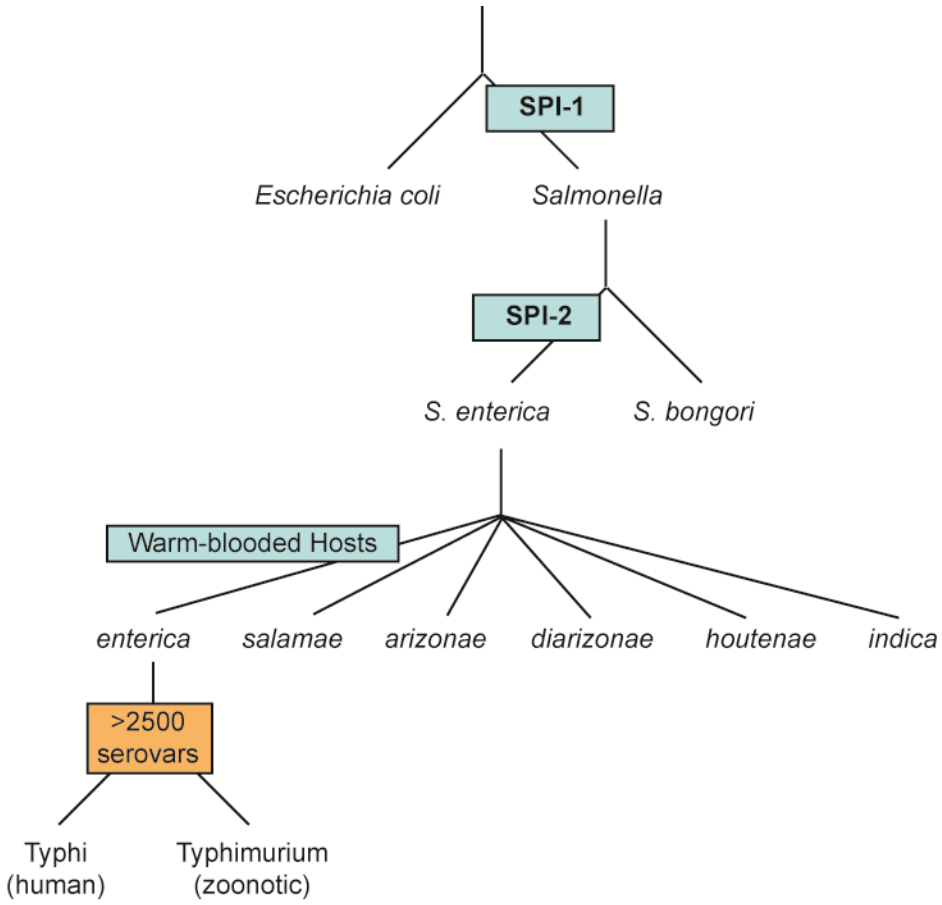
SPI-1
Escherichia coli
Salmonella
SPI-2
S. enterica
S. bongori
Warm-blooded Hosts
enterica
salamae
arizonae
diarizonae
houtenae
indica
>2500 serovars
Typhi (human)
Typhimurium (zoonotic)

Figure 1.2 – SPI-1 and SPI-2 Regulatory Inputs. SPI-1 and SPI-2 encoded genes are coloured in pink and blue respectively. Interactions leading to activation are indicated by arrowheads and repressive interactions indicated by blocked lines. A HilD, HilC and RtsA feedforward loop activates expression of the SPI-1 master regulator *hilA* and can activate the inv/spa operon independently. The effector operon is activated by an InvF/SicA complex. HilA undergoes negative autoregulation and is repressed by H-NS. HilD is activated post-transcriptionally by OmpR and is repressed by HilE. OmpR, PhoP, SlyA and Fis directly activate expression of the SPI-2 master regulator SsrB which subsequently drives expression of two structural and one effector operon in SPI-2. Expression of *ssrAB* is repressed by H-NS presumably in complex with Hha/YdgT and this repression is antagonized by SsrB. Fis additionally directly activates the *ssaG* promoter. SPI-2 is also directly activated by the SPI-1 regulator HilD

Figure 1.2

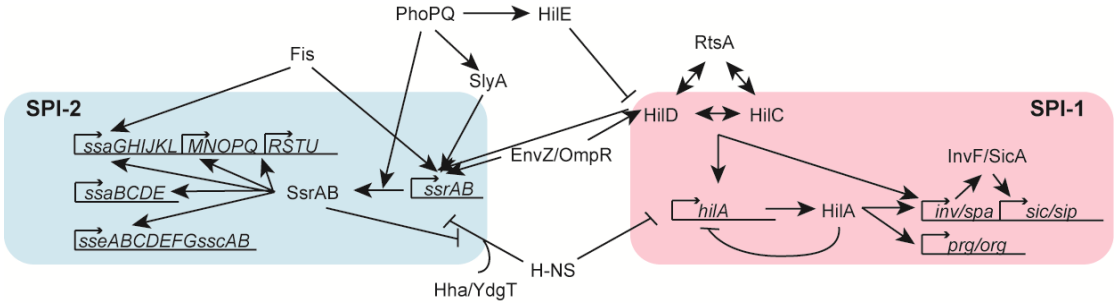
PhoPQ
HilE
Fis
SlyA
RtsA
SPI-2
HilD
HilC
SPI-1
ssaGHIJKL
MNOPQ
RSTU
EnvZ/OmpR
InvF/SicA
ssaBCDE
SsrAB
ssrAB
hilA
HilA
inv/spa
sic/sip
sseABCDEFGsscAB
prg/org
H-NS
Hha/YdgT

Figure 1.3 – Schematic of the SPI-2 type 3 secretion system. The T3SS consists of a pair of inner membrane (IM) rings formed by SsaD and SsaJ and an outer membrane (OM) ring formed by SsaC. At the cytoplasmic face of the T3SS is the ATPase SsaN, a sorting platform SsaBLM and a poorly characterized C-ring and export apparatus believed to consist of SsaKRSTU. The basal body anchors a needle filament which terminates in the translocon (SseBCD) which is required to mediate pore formation in the host membrane (HM).

Figure 1.3

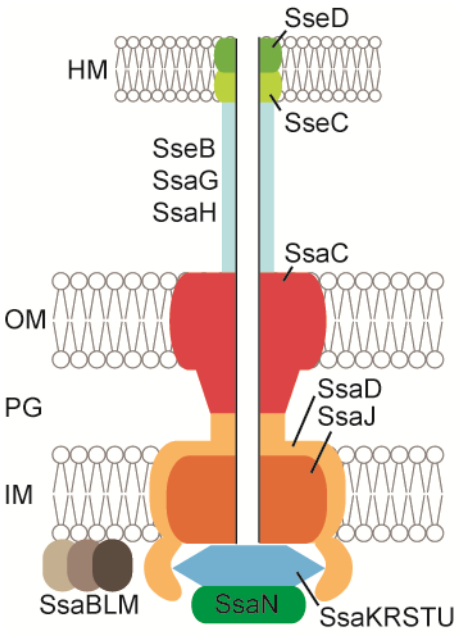
SseD
HM
SseC
SseB
SsaG
SsaH
SsaC
OM
SsaD
SsaJ
PG
IM
SsaBLM
SsaN
SsaKRSTU

Figure 1.4 - T3SS Substrate Specificity Switch. *Yersinia* nomenclature is used reflective of the majority of studies conducted. (A) Prior to needle assembly effector expression or translation is blocked by a sensory complex which broadly includes a sensor, a regulator and the translocons. Secretion of YscP is used to monitor assembly completion. (B) Completion of the needle triggers secretion of the sensor resulting in dissociation of the sensory complex. Secreted YscP becomes juxtaposed to YscU. (C) YscP triggers autocleavage of YscU enabling translocon secretion. The released regulator activates effector transcription or translation. (D) Release of the plug allows effector translocation across the host cell membrane. (Figure adapted from [250]).

Figure 1.4

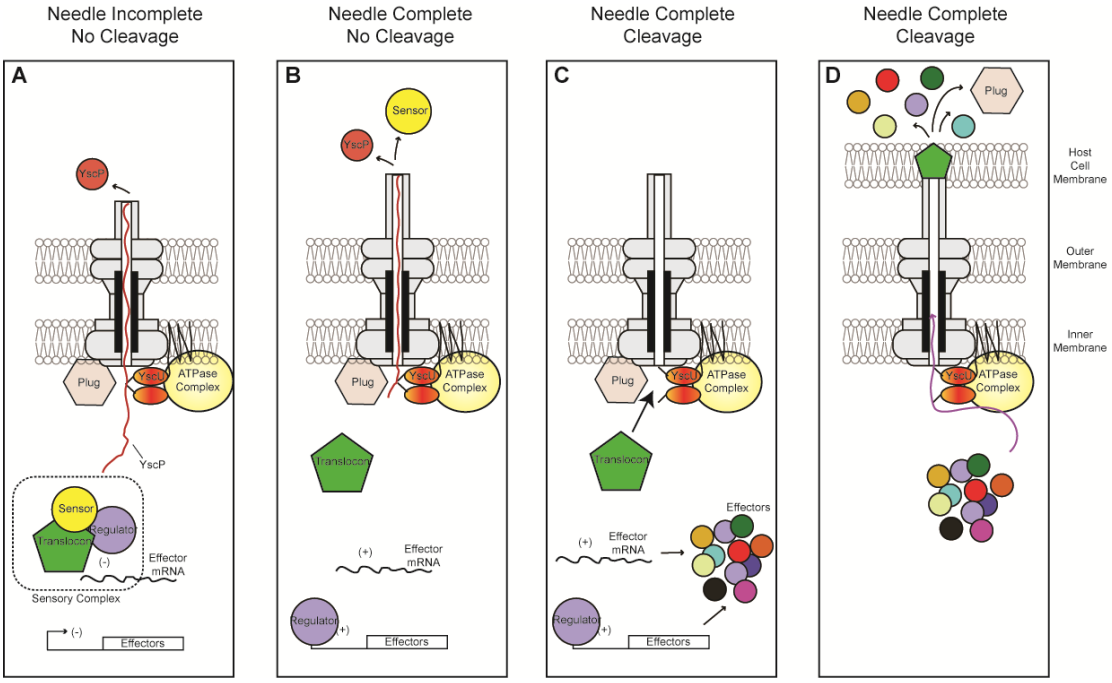
Needle Incomplete
No Cleavage
Needle Complete
No Cleavage
Needle Complete
Cleavage
Needle Complete
Cleavage
A
B
C
D
YscP
Plug
YscU
ATPase
Complex
Sensor
Regulator
Translocon
Effector
mRNA
Sensory Complex
Effectors
Host
Cell
Membrane
Outer
Membrane
Inner
Membrane

References

1. Darwin C (1859) On the Origin of Species By Means of Natural Selection; Murray J, editor. London.

2. Huxley J (1942) Evolution: The Modern Synthesis.

3. Wray GA (2007) The evolutionary significance of *cis*-regulatory mutations. Nat Rev Genet 8: 206- 216.

4. Jacob F, Monod J (1961) Genetic regulatory mechanisms in the synthesis of proteins. J Mol Biol 3: 318-356.

5. King MC, Wilson AC (1975) Evolution at two levels in humans and chimpanzees. Science 188: 107-116.

6. Wray GA, Hahn MW, Abouheif E, Balhoff JP, Pizer M, et al. (2003) The evolution of transcriptional regulation in eukaryotes. Mol Biol Evol 20: 1377-1419.

7. Jacob F (1977) Evolution and tinkering. Science 196: 1161-1166.

8. Wittkopp PJaK, G. (2012) *Cis*-regulatory elements: molecular mechanisms and evolutionary processes underlying divergence. Nature Reviews Genetics 13: 59-69.

9. Sucena E, Stern DL (2000) Divergence of larval morphology between *Drosophila sechellia* and its sibling species caused by *cis*-regulatory evolution of ovo/shaven-baby. Proc Natl Acad Sci U S A 97: 4530-4534.

10. Shapiro MD, Marks ME, Peichel CL, Blackman BK, Nereng KS, et al. (2004) Genetic and developmental basis of evolutionary pelvic reduction in threespine sticklebacks. Nature 428: 717-723.

11. Gompel N, Prud'homme B, Wittkopp PJ, Kassner VA, Carroll SB (2005) Chance caught on the wing: *cis*-regulatory evolution and the origin of pigment patterns in *Drosophila*. Nature 433: 481-487.

12. Prud'homme B, Gompel N, Rokas A, Kassner VA, Williams TM, et al. (2006) Repeated morphological evolution through *cis*-regulatory changes in a pleiotropic gene. Nature 440: 1050-1053.

13. Montano MA, Novitsky VA, Blackard JT, Cho NL, Katzenstein DA, et al. (1997) Divergent transcriptional regulation among expanding human immunodeficiency virus type 1 subtypes. J Virol 71: 8657-8665.

14. Rinder H, Thomschke A, Rusch-Gerdes S, Bretzel G, Feldmann K, et al. (1998) Significance of *ahpC* promoter mutations for the prediction of isoniazid resistance in *Mycobacterium tuberculosis*. Eur J Clin Microbiol Infect Dis 17: 508-511.

15. Lee H, Cho SN, Bang HE, Lee JH, Bai GH, et al. (2000) Exclusive mutations related to isoniazid and ethionamide resistance among *Mycobacterium tuberculosis* isolates from Korea. Int J Tuberc Lung Dis 4: 441-447.

16. Isalan M, Lemerle C, Michalodimitrakis K, Horn C, Beltrao P, et al. (2008) Evolvability and hierarchy in rewired bacterial gene networks. Nature 452: 840-845.

17. Perez JC, Groisman EA (2009) Transcription factor function and promoter architecture govern the evolution of bacterial regulons. Proc Natl Acad Sci U S A 106: 4319-4324.

18. Tu X, Latifi T, Bougdour A, Gottesman S, Groisman EA (2006) The PhoP/PhoQ two-component system stabilizes the alternative sigma factor RpoS in *Salmonella enterica*. Proc Natl Acad Sci U S A 103: 13503-13508.

19. Bougdour A, Cunning C, Baptiste PJ, Elliott T, Gottesman S (2008) Multiple pathways for regulation of *sigmaS* (RpoS) stability in *Escherichia coli* via the action of multiple anti-adaptors. Mol Microbiol 68: 298-313.

20. Hoekstra HE, Coyne JA (2007) The locus of evolution: evo devo and the genetics of adaptation. Evolution 61: 995-1016.

21. Martinez-Nunez MA, Perez-Rueda E, Gutierrez-Rios RM, Merino E New insights into the regulatory networks of paralogous genes in bacteria. Microbiology 156: 14-22.

22. Soo VW, Hanson-Manful P, Patrick WM Artificial gene amplification reveals an abundance of promiscuous resistance determinants in *Escherichia coli*. Proc Natl Acad Sci U S A 108: 1484-1489.

23. Bustamante CD, Fledel-Alon A, Williamson S, Nielsen R, Hubisz MT, et al. (2005) Natural selection on protein-coding genes in the human genome. Nature 437: 1153-1157.

24. Gal-Mor O, Elhadad D, Deng W, Rahav G, Finlay BB The *Salmonella enterica* PhoP directly activates the horizontally acquired SPI-2 gene *sseL* and is functionally different from a *S. bongori* ortholog. PLoS One 6: e20024.

25. Cooper TF, Rozen DE, Lenski RE (2003) Parallel changes in gene expression after 20,000 generations of evolution in *Escherichia coli*. Proc Natl Acad Sci U S A 100: 1072-1077.

26. Gruber JD, Vogel K, Kalay G, Wittkopp PJ Contrasting properties of gene-specific regulatory, coding, and copy number mutations in *Saccharomyces cerevisiae*: frequency, effects, and dominance. PLoS Genet 8: e1002497.

27. Landry CR, Lemos B, Rifkin SA, Dickinson WJ, Hartl DL (2007) Genetic properties influencing the evolvability of gene expression. Science 317: 118-121.

28. Boucher Y, Douady CJ, Papke RT, Walsh DA, Boudreau ME, et al. (2003) Lateral gene transfer and the origins of prokaryotic groups. Annu Rev Genet 37: 283-328.

29. Gal-Mor O, Finlay BB (2006) Pathogenicity islands: a molecular toolbox for bacterial virulence. Cell Microbiol 8: 1707-1719.

30. Hacker J, Kaper JB (2000) Pathogenicity islands and the evolution of microbes. Annu Rev Microbiol 54: 641-679.

31. Langille MG, Hsiao WW, Brinkman FS. Detecting genomic islands using bioinformatics approaches. Nat Rev Microbiol 8: 373-382.

32. Dobrindt U, Hochhut B, Hentschel U, Hacker J (2004) Genomic islands in pathogenic and environmental microorganisms. Nat Rev Microbiol 2: 414-424.

33. Ali SS, Xia B, Liu J, Navarre WW Silencing of foreign DNA in bacteria. Curr Opin Microbiol.

34. Navarre WW, Porwollik S, Wang Y, McClelland M, Rosen H, et al. (2006) Selective silencing of foreign DNA with low GC content by the H-NS protein in *Salmonella*. Science 313: 236-238.

35. Doyle M, Fookes M, Ivens A, Mangan MW, Wain J, et al. (2007) An H-NS-like stealth protein aids horizontal DNA transmission in bacteria. Science 315: 251-252.

36. Cathelyn JS, Ellison DW, Hinchliffe SJ, Wren BW, Miller VL (2007) The RovA regulons of *Yersinia enterocolitica* and *Yersinia pestis* are distinct: evidence that many RovA-regulated genes were acquired more recently than the core genome. Mol Microbiol 66: 189-205.

37. Bina J, Zhu J, Dziejman M, Faruque S, Calderwood S, et al. (2003) ToxR regulon of *Vibrio cholerae* and its expression in vibrios shed by cholera patients. Proc Natl Acad Sci U S A 100: 2801-2806.

38. Krukonis ES, DiRita VJ (2003) DNA binding and ToxR responsiveness by the wing domain of TcpP, an activator of virulence gene expression in *Vibrio cholerae*. Mol Cell 12: 157-165.

39. Perez JC, Latifi T, Groisman EA (2008) Overcoming H-NS-mediated transcriptional silencing of horizontally acquired genes by the PhoP and SlyA proteins in *Salmonella enterica*. J Biol Chem 283: 10773-10783.

40. Doolittle RF, Feng DF, Tsang S, Cho G, Little E (1996) Determining divergence times of the major kingdoms of living organisms with a protein clock. Science 271: 470-477.

41. Porwollik S, Wong RM, McClelland M (2002) Evolutionary genomics of *Salmonella*: gene acquisitions revealed by microarray analysis. Proc Natl Acad Sci U S A 99: 8956-8961.

42. Christensen H, Nordentoft S, Olsen JE (1998) Phylogenetic relationships of *Salmonella* based on rRNA sequences. Int J Syst Bacteriol 48 Pt 2: 605-610.

43. Fookes M, Schroeder GN, Langridge GC, Blondel CJ, Mammina C, et al. *Salmonella bongori* provides insights into the evolution of the *Salmonellae*. PLoS Pathog 7: e1002191.

44. Haraga A, Ohlson MB, Miller SI (2008) *Salmonellae* interplay with host cells. Nat Rev Microbiol 6: 53-66.

45. Bhan MK, Bahl R, Bhatnagar S (2005) Typhoid and paratyphoid fever. Lancet 366: 749-762.

46. Thomas K, Majowicz, S., Sockett, P., Fazil, A., Pollari, F., Dore, K., Flint, J., Edge, V.. (2006) Estimated numbers of community cases of illness due to *Salmonella, Campylobacter* and verotoxigenic *Escherichia coli*: Pathogen-specific community rates. Can J Infect Dis Med Microbiol 17: 229-234.

47. (2005) Drug Resistant *Salmonella*. Fact Sheet: World Health Organization.

48. Scharff RL Economic burden from health losses due to foodborne illness in the United States. J Food Prot 75: 123-131.

49. Crump JA, Luby SP, Mintz ED (2004) The global burden of typhoid fever. Bull World Health Organ 82: 346-353.

50. Mulvey MR, Boyd DA, Olson AB, Doublet B, Cloeckaert A (2006) The genetics of *Salmonella* genomic island 1. Microbes Infect 8: 1915-1922.

51. Galan JE, Curtiss R, 3rd (1989) Cloning and molecular characterization of genes whose products allow *Salmonella* typhimurium to penetrate tissue culture cells. Proc Natl Acad Sci U S A 86: 6383-6387.

52. Lee CA, Jones BD, Falkow S (1992) Identification of a *Salmonella* typhimurium invasion locus by selection for hyperinvasive mutants. Proc Natl Acad Sci U S A 89: 1847-1851.

53. Mills DM, Bajaj V, Lee CA (1995) A 40 kb chromosomal fragment encoding *Salmonella* typhimurium invasion genes is absent from the corresponding region of the *Escherichia coli* K-12 chromosome. Mol Microbiol 15: 749-759.

54. Groisman EA, Ochman H (1993) Cognate gene clusters govern invasion of host epithelial cells by *Salmonella* typhimurium and *Shigella flexneri*. EMBO J 12: 3779-3787.

55. Hueck CJ, Hantman MJ, Bajaj V, Johnston C, Lee CA, et al. (1995) *Salmonella* typhimurium secreted invasion determinants are homologous to *Shigella* Ipa proteins. Mol Microbiol 18: 479-490.

56. Ellermeier JR, Slauch JM (2007) Adaptation to the host environment: regulation of the SPI1 type III secretion system in *Salmonella enterica* serovar Typhimurium. Curr Opin Microbiol 10: 24-29.

57. Stender S, Friebel A, Linder S, Rohde M, Mirold S, et al. (2000) Identification of SopE2 from *Salmonella* typhimurium, a conserved guanine nucleotide exchange factor for Cdc42 of the host cell. Mol Microbiol 36: 1206-1221.

58. Hardt WD, Chen LM, Schuebel KE, Bustelo XR, Galan JE (1998) *S.* typhimurium encodes an activator of Rho GTPases that induces membrane ruffling and nuclear responses in host cells. Cell 93: 815-826.

59. Bakshi CS, Singh VP, Wood MW, Jones PW, Wallis TS, et al. (2000) Identification of SopE2, a *Salmonella* secreted protein which is highly homologous to SopE and involved in bacterial invasion of epithelial cells. J Bacteriol 182: 2341-2344.

60. Zhou D, Chen LM, Hernandez L, Shears SB, Galan JE (2001) A *Salmonella* inositol polyphosphatase acts in conjunction with other bacterial effectors to promote host cell actin cytoskeleton rearrangements and bacterial internalization. Mol Microbiol 39: 248-259.

61. Zhou D, Mooseker MS, Galan JE (1999) Role of the *S.* typhimurium actin-binding protein SipA in bacterial internalization. Science 283: 2092-2095.

62. Hayward RD, Koronakis V (1999) Direct nucleation and bundling of actin by the SipC protein of invasive Salmonella. EMBO J 18: 4926-4934.

63. Hobbie S, Chen LM, Davis RJ, Galan JE (1997) Involvement of mitogen-activated protein kinase pathways in the nuclear responses and cytokine production induced by *Salmonella* typhimurium in cultured intestinal epithelial cells. J Immunol 159: 5550-5559.

64. Murli S, Watson RO, Galan JE (2001) Role of tyrosine kinases and the tyrosine phosphatase SptP in the interaction of *Salmonella* with host cells. Cell Microbiol 3: 795-810.

65. Zhang Y, Higashide WM, McCormick BA, Chen J, Zhou D (2006) The inflammation-associated *Salmonella* SopA is a HECT-like E3 ubiquitin ligase. Mol Microbiol 62: 786-793.

66. Boyle EC, Brown NF, Finlay BB (2006) *Salmonella enterica* serovar Typhimurium effectors SopB, SopE, SopE2 and SipA disrupt tight junction structure and function. Cell Microbiol 8: 1946-1957.

67. Hersh D, Monack DM, Smith MR, Ghori N, Falkow S, et al. (1999) The *Salmonella* invasin SipB induces macrophage apoptosis by binding to caspase-1. Proc Natl Acad Sci U S A 96: 2396-2401.

68. Fu Y, Galan JE (1999) A *Salmonella* protein antagonizes Rac-1 and Cdc42 to mediate host-cell recovery after bacterial invasion. Nature 401: 293-297.

69. Collier-Hyams LS, Zeng H, Sun J, Tomlinson AD, Bao ZQ, et al. (2002) Cutting edge: *Salmonella* AvrA effector inhibits the key proinflammatory, anti-apoptotic NF-kappa B pathway. J Immunol 169: 2846-2850.

70. Haraga A, Miller SI (2003) A *Salmonella enterica* serovar typhimurium translocated leucine-rich repeat effector protein inhibits NF-kappa B-dependent gene expression. Infect Immun 71: 4052-4058.

71. Van Engelenburg SB, Palmer AE (2008) Quantification of real-time *Salmonella* effector type III secretion kinetics reveals differential secretion rates for SopE2 and SptP. Chem Biol 15: 619-628.

72. Kubori T, Galan JE (2003) Temporal regulation of *Salmonella* virulence effector function by proteasome-dependent protein degradation. Cell 115: 333-342.

73. Bajaj V, Lucas RL, Hwang C, Lee CA (1996) Co-ordinate regulation of *Salmonella* typhimurium invasion genes by environmental and regulatory factors is mediated by control of hilA expression. Mol Microbiol 22: 703-714.

74. De Keersmaecker SC, Marchal K, Verhoeven TL, Engelen K, Vanderleyden J, et al. (2005) Microarray analysis and motif detection reveal new targets of the *Salmonella enterica* serovar Typhimurium HilA regulatory protein, including *hilA* itself. J Bacteriol 187: 4381-4391.

75. Lostroh CP, Bajaj V, Lee CA (2000) The *cis* requirements for transcriptional activation by HilA, a virulence determinant encoded on SPI-1. Mol Microbiol 37: 300-315.

76. Eichelberg K, Galan JE (1999) Differential regulation of *Salmonella* typhimurium type III secreted proteins by pathogenicity island 1 (SPI-1)-encoded transcriptional activators InvF and hilA. Infect Immun 67: 4099-4105.

77. Olekhnovich IN, Kadner RJ (2007) Role of nucleoid-associated proteins Hha and H-NS in expression of *Salmonella enterica* activators HilD, HilC, and RtsA required for cell invasion. J Bacteriol 189: 6882-6890.

78. Ellermeier CD, Ellermeier JR, Slauch JM (2005) HilD, HilC and RtsA constitute a feed forward loop that controls expression of the SPI1 type three secretion system regulator *hilA* in *Salmonella enterica* serovar Typhimurium. Mol Microbiol 57: 691-705.

79. Schechter LM, Lee CA (2001) AraC/XylS family members, HilC and HilD, directly bind and derepress the *Salmonella* typhimurium *hilA* promoter. Mol Microbiol 40: 1289-1299.

80. Ellermeier CD, Slauch JM (2003) RtsA and RtsB coordinately regulate expression of the invasion and flagellar genes in *Salmonella enterica* serovar Typhimurium. J Bacteriol 185: 5096-5108.

81. Akbar S, Schechter LM, Lostroh CP, Lee CA (2003) AraC/XylS family members, HilD and HilC, directly activate virulence gene expression independently of HilA in *Salmonella* typhimurium. Mol Microbiol 47: 715-728.

82. Baxter MA, Fahlen TF, Wilson RL, Jones BD (2003) HilE interacts with HilD and negatively regulates *hilA* transcription and expression of the *Salmonella enterica* serovar Typhimurium invasive phenotype. Infect Immun 71: 1295-1305.

83. Chubiz JE, Golubeva YA, Lin D, Miller LD, Slauch JM FliZ regulates expression of the *Salmonella* pathogenicity island 1 invasion locus by controlling HilD protein activity in *Salmonella enterica* serovar typhimurium. J Bacteriol 192: 6261-6270.

84. Ellermeier JR, Slauch JM (2008) Fur regulates expression of the *Salmonella* pathogenicity island 1 type III secretion system through HilD. J Bacteriol 190: 476-486.

85. Ochman H, Soncini FC, Solomon F, Groisman EA (1996) Identification of a pathogenicity island required for *Salmonella* survival in host cells. Proc Natl Acad Sci U S A 93: 7800-7804.

86. Shea JE, Hensel M, Gleeson C, Holden DW (1996) Identification of a virulence locus encoding a second type III secretion system in *Salmonella* typhimurium. Proc Natl Acad Sci U S A 93: 2593-2597.

87. Hensel M, Shea JE, Baumler AJ, Gleeson C, Blattner F, et al. (1997) Analysis of the boundaries of *Salmonella* pathogenicity island 2 and the corresponding chromosomal region of *Escherichia coli* K-12. J Bacteriol 179: 1105-1111.

88. Hensel M, Nikolaus T, Egelseer C (1999) Molecular and functional analysis indicates a mosaic structure of *Salmonella* pathogenicity island 2. Mol Microbiol 31: 489-498.

89. Hensel M (2000) *Salmonella* pathogenicity island 2. Mol Microbiol 36: 1015-1023.

90. Fields PI, Swanson RV, Haidaris CG, Heffron F (1986) Mutants of *Salmonella* typhimurium that cannot survive within the macrophage are avirulent. Proc Natl Acad Sci U S A 83: 5189-5193.

91. Hansen-Wester I, Hensel M (2001) *Salmonella* pathogenicity islands encoding type III secretion systems. Microbes Infect 3: 549-559.

92. Brumell JH, Goosney DL, Finlay BB (2002) SifA, a type III secreted effector of *Salmonella* typhimurium, directs *Salmonella*-induced filament (Sif) formation along microtubules. Traffic 3: 407-415.

93. Brumell JH, Rosenberger CM, Gotto GT, Marcus SL, Finlay BB (2001) SifA permits survival and replication of *Salmonella* typhimurium in murine macrophages. Cell Microbiol 3: 75-84.

94. Beuzon CR, Meresse S, Unsworth KE, Ruiz-Albert J, Garvis S, et al. (2000) *Salmonella* maintains the integrity of its intracellular vacuole through the action of SifA. EMBO J 19: 3235-3249.

95. Boucrot E, Henry T, Borg JP, Gorvel JP, Meresse S (2005) The intracellular fate of *Salmonella* depends on the recruitment of kinesin. Science 308: 1174-1178.

96. Knodler LA, Vallance BA, Hensel M, Jackel D, Finlay BB, et al. (2003) *Salmonella* type III effectors PipB and PipB2 are targeted to detergent-resistant microdomains on internal host cell membranes. Mol Microbiol 49: 685-704.

97. Freeman JA, Ohl ME, Miller SI (2003) The *Salmonella enterica* serovar typhimurium translocated effectors SseJ and SifB are targeted to the *Salmonella*-containing vacuole. Infect Immun 71: 418-427.

98. Brumell JH, Kujat-Choy S, Brown NF, Vallance BA, Knodler LA, et al. (2003) SopD2 is a novel type III secreted effector of *Salmonella* typhimurium that targets late endocytic compartments upon delivery into host cells. Traffic 4: 36-48.

99. Kuhle V, Hensel M (2002) SseF and SseG are translocated effectors of the type III secretion system of *Salmonella* pathogenicity island 2 that modulate aggregation of endosomal compartments. Cell Microbiol 4: 813-824.

100. Ruiz-Albert J, Yu XJ, Beuzon CR, Blakey AN, Galyov EE, et al. (2002) Complementary activities of SseJ and SifA regulate dynamics of the *Salmonella* typhimurium vacuolar membrane. Mol Microbiol 44: 645-661.

101. Knodler LA, Steele-Mortimer O (2005) The *Salmonella* effector PipB2 affects late endosome/lysosome distribution to mediate Sif extension. Mol Biol Cell 16: 4108-4123.

102. Szeto J, Namolovan A, Osborne SE, Coombes BK, Brumell JH (2009) *Salmonella*-containing vacuoles display centrifugal movement associated with cell-to-cell transfer in epithelial cells. Infect Immun 77: 996-1007.

103. Henry T, Couillault C, Rockenfeller P, Boucrot E, Dumont A, et al. (2006) The *Salmonella* effector protein PipB2 is a linker for kinesin-1. Proc Natl Acad Sci U S A 103: 13497-13502.

104. Salcedo SP, Holden DW (2003) SseG, a virulence protein that targets *Salmonella* to the Golgi network. EMBO J 22: 5003-5014.

105. Jiang X, Rossanese OW, Brown NF, Kujat-Choy S, Galan JE, et al. (2004) The related effector proteins SopD and SopD2 from *Salmonella enterica* serovar Typhimurium contribute to virulence during systemic infection of mice. Mol Microbiol 54: 1186-1198.

106. Schroeder N, Henry T, de Chastellier C, Zhao W, Guilhon AA, et al. The virulence protein SopD2 regulates membrane dynamics of *Salmonella*-containing vacuoles. PLoS Pathog 6: e1001002.

107. Quezada CM, Hicks SW, Galan JE, Stebbins CE (2009) A family of *Salmonella* virulence factors functions as a distinct class of autoregulated E3 ubiquitin ligases. Proc Natl Acad Sci U S A 106: 4864-4869.

108. Levin I, Eakin C, Blanc MP, Klevit RE, Miller SI, et al. Identification of an unconventional E3 binding surface on the UbcH5 ~ Ub conjugate recognized by a pathogenic bacterial E3 ligase. Proc Natl Acad Sci U S A 107: 2848-2853.

109. Rytkonen A, Poh J, Garmendia J, Boyle C, Thompson A, et al. (2007) SseL, a *Salmonella* deubiquitinase required for macrophage killing and virulence. Proc Natl Acad Sci U S A 104: 3502-3507.

110. Le Negrate G, Faustin B, Welsh K, Loeffler M, Krajewska M, et al. (2008) *Salmonella* secreted factor L deubiquitinase of *Salmonella* typhimurium inhibits NF-kappaB, suppresses IkappaBalpha ubiquitination and modulates innate immune responses. J Immunol 180: 5045-5056.

111. Arena ET, Auweter SD, Antunes LC, Vogl AW, Han J, et al. The deubiquitinase activity of the *Salmonella* pathogenicity island 2 effector, SseL, prevents accumulation of cellular lipid droplets. Infect Immun 79: 4392-4400.

112. Uchiya K, Barbieri MA, Funato K, Shah AH, Stahl PD, et al. (1999) A *Salmonella* virulence protein that inhibits cellular trafficking. EMBO J 18: 3924-3933.

113. Lee AH, Zareei MP, Daefler S (2002) Identification of a NIPSNAP homologue as host cell target for *Salmonella* virulence protein SpiC. Cell Microbiol 4: 739-750.

114. Shotland Y, Kramer H, Groisman EA (2003) The *Salmonella* SpiC protein targets the mammalian Hook3 protein function to alter cellular trafficking. Mol Microbiol 49: 1565-1576.

115. Yu XJ, Ruiz-Albert J, Unsworth KE, Garvis S, Liu M, et al. (2002) SpiC is required for secretion of *Salmonella* Pathogenicity Island 2 type III secretion system proteins. Cell Microbiol 4: 531-540.

116. Yu XJ, Liu M, Holden DW (2004) SsaM and SpiC interact and regulate secretion of *Salmonella* pathogenicity island 2 type III secretion system effectors and translocators. Mol Microbiol 54: 604-619.

117. Yu XJ, McGourty K, Liu M, Unsworth KE, Holden DW pH sensing by intracellular *Salmonella* induces effector translocation. Science 328: 1040-1043.

118. Cirillo DM, Valdivia RH, Monack DM, Falkow S (1998) Macrophage-dependent induction of the *Salmonella* pathogenicity island 2 type III secretion system and its role in intracellular survival. Mol Microbiol 30: 175-188.

119. Valdivia RH, Falkow S (1997) Fluorescence-based isolation of bacterial genes expressed within host cells. Science 277: 2007-2011.

120. Pfeifer CG, Marcus SL, Steele-Mortimer O, Knodler LA, Finlay BB (1999) *Salmonella* typhimurium virulence genes are induced upon bacterial invasion into phagocytic and nonphagocytic cells. Infect Immun 67: 5690-5698.

121. Duong N, Osborne S, Bustamante VH, Tomljenovic AM, Puente JL, et al. (2007) Thermosensing coordinates a *cis*-regulatory module for transcriptional activation of the intracellular virulence system in *Salmonella enterica* serovar Typhimurium. J Biol Chem 282: 34077-34084.

122. Deiwick J, Nikolaus T, Erdogan S, Hensel M (1999) Environmental regulation of *Salmonella* pathogenicity island 2 gene expression. Mol Microbiol 31: 1759-1773.

123. Carroll RK, Liao X, Morgan LK, Cicirelli EM, Li Y, et al. (2009) Structural and functional analysis of the C-terminal DNA binding domain of the *Salmonella* typhimurium SPI-2 response regulator SsrB. J Biol Chem 284: 12008-12019.

124. Tomljenovic-Berube AM, Mulder DT, Whiteside MD, Brinkman FS, Coombes BK Identification of the regulatory logic controlling *Salmonella* pathoadaptation by the SsrA-SsrB two-component system. PLoS Genet 6: e1000875.

125. Walthers D, Carroll RK, Navarre WW, Libby SJ, Fang FC, et al. (2007) The response regulator SsrB activates expression of diverse *Salmonella* pathogenicity island 2 promoters and counters silencing by the nucleoid-associated protein H-NS. Mol Microbiol 65: 477-493.

126. Worley MJ, Ching KH, Heffron F (2000) *Salmonella* SsrB activates a global regulon of horizontally acquired genes. Mol Microbiol 36: 749-761.

127. Feng X, Walthers D, Oropeza R, Kenney LJ (2004) The response regulator SsrB activates transcription and binds to a region overlapping OmpR binding sites at *Salmonella* pathogenicity island 2. Mol Microbiol 54: 823-835.

128. Yoon H, McDermott JE, Porwollik S, McClelland M, Heffron F (2009) Coordinated regulation of virulence during systemic infection of *Salmonella enterica* serovar Typhimurium. PLoS Pathog 5: e1000306.

129. Yamada H, Muramatsu S, Mizuno T (1990) An *Escherichia coli* protein that preferentially binds to sharply curved DNA. J Biochem 108: 420-425.

130. Tupper AE, Owen-Hughes TA, Ussery DW, Santos DS, Ferguson DJ, et al. (1994) The chromatin-associated protein H-NS alters DNA topology in vitro. EMBO J 13: 258-268.

131. Esposito D, Petrovic A, Harris R, Ono S, Eccleston JF, et al. (2002) H-NS oligomerization domain structure reveals the mechanism for high order self-association of the intact protein. J Mol Biol 324: 841-850.

132. Shindo H, Iwaki T, Ieda R, Kurumizaka H, Ueguchi C, et al. (1995) Solution structure of the DNA binding domain of a nucleoid-associated protein, H-NS, from *Escherichia coli*. FEBS Lett 360: 125-131.

133. Ueguchi C, Suzuki T, Yoshida T, Tanaka K, Mizuno T (1996) Systematic mutational analysis revealing the functional domain organization of *Escherichia coli* nucleoid protein H-NS. J Mol Biol 263: 149-162.

134. Liu Y, Chen H, Kenney LJ, Yan J A divalent switch drives H-NS/DNA-binding conformations between stiffening and bridging modes. Genes Dev 24: 339-344.

135. Lang B, Blot N, Bouffartigues E, Buckle M, Geertz M, et al. (2007) High-affinity DNA binding sites for H-NS provide a molecular basis for selective silencing within proteobacterial genomes. Nucleic Acids Res 35: 6330-6337.

136. Walthers D, Li Y, Liu Y, Anand G, Yan J, et al. *Salmonella enterica* response regulator SsrB relieves H-NS silencing by displacing H-NS bound in polymerization mode and directly activates transcription. J Biol Chem 286: 1895-1902.

137. Coombes BK, Wickham ME, Lowden MJ, Brown NF, Finlay BB (2005) Negative regulation of *Salmonella* pathogenicity island 2 is required for contextual control of virulence during typhoid. Proc Natl Acad Sci U S A 102: 17460-17465.

138. Silphaduang U, Mascarenhas M, Karmali M, Coombes BK (2007) Repression of intracellular virulence factors in *Salmonella* by the Hha and YdgT nucleoid-associated proteins. J Bacteriol 189: 3669-3673.

139. Vivero A, Banos RC, Mariscotti JF, Oliveros JC, Garcia-del Portillo F, et al. (2008) Modulation of horizontally acquired genes by the Hha-YdgT proteins in *Salmonella enterica* serovar Typhimurium. J Bacteriol 190: 1152-1156.

140. Paytubi S, Madrid C, Forns N, Nieto JM, Balsalobre C, et al. (2004) YdgT, the Hha paralogue in *Escherichia coli*, forms heteromeric complexes with H-NS and StpA. Mol Microbiol 54: 251-263.

141. Nieto JM, Madrid C, Miquelay E, Parra JL, Rodriguez S, et al. (2002) Evidence for direct protein-protein interaction between members of the enterobacterial Hha/YmoA and H-NS families of proteins. J Bacteriol 184: 629-635.

142. McFeeters RL, Altieri AS, Cherry S, Tropea JE, Waugh DS, et al. (2007) The high-precision solution structure of *Yersinia* modulating protein YmoA provides insight into interaction with H-NS. Biochemistry 46: 13975-13982.

143. Stapleton MR, Norte VA, Read RC, Green J (2002) Interaction of the *Salmonella* typhimurium transcription and virulence factor SlyA with target DNA and identification of members of the SlyA regulon. J Biol Chem 277: 17630-17637.

144. Linehan SA, Rytkonen A, Yu XJ, Liu M, Holden DW (2005) SlyA regulates function of *Salmonella* pathogenicity island 2 (SPI-2) and expression of SPI-2-associated genes. Infect Immun 73: 4354-4362.

145. Haider F, Lithgow JK, Stapleton MR, Norte VA, Roberts RE, et al. (2008) DNA recognition by the *Salmonella enterica* serovar Typhimurium transcription factor SlyA. Int Microbiol 11: 245-250.

146. Dolan KT, Duguid EM, He C Crystal structures of SlyA protein, a master virulence regulator of *Salmonella*, in free and DNA-bound states. J Biol Chem 286: 22178-22185.

147. Wu RY, Zhang RG, Zagnitko O, Dementieva I, Maltzev N, et al. (2003) Crystal structure of *Enterococcus faecalis* SlyA-like transcriptional factor. J Biol Chem 278: 20240-20244.

148. Okada N, Oi Y, Takeda-Shitaka M, Kanou K, Umeyama H, et al. (2007) Identification of amino acid residues of *Salmonella* SlyA that are critical for transcriptional regulation. Microbiology 153: 548-560.

149. Navarre WW, Halsey TA, Walthers D, Frye J, McClelland M, et al. (2005) Co-regulation of *Salmonella enterica* genes required for virulence and resistance to antimicrobial peptides by SlyA and PhoP/PhoQ. Mol Microbiol 56: 492-508.

150. Lim S, Kim B, Choi HS, Lee Y, Ryu S (2006) Fis is required for proper regulation of *ssaG* expression in *Salmonella enterica* serovar Typhimurium. Microb Pathog 41: 33-42.

151. Croinin OT, Carroll RK, Kelly A, Dorman CJ (2006) Roles for DNA supercoiling and the Fis protein in modulating expression of virulence genes during intracellular growth of *Salmonella enterica* serovar Typhimurium. Mol Microbiol 62: 869-882.

152. Kelly A, Goldberg MD, Carroll RK, Danino V, Hinton JC, et al. (2004) A global role for Fis in the transcriptional control of metabolism and type III secretion in *Salmonella enterica* serovar Typhimurium. Microbiology 150: 2037-2053.

153. Yoon H, Lim S, Heu S, Choi S, Ryu S (2003) Proteome analysis of *Salmonella enterica* serovar Typhimurium *fis* mutant. FEMS Microbiol Lett 226: 391-396.

154. Hengen PN, Bartram SL, Stewart LE, Schneider TD (1997) Information analysis of Fis binding sites. Nucleic Acids Res 25: 4994-5002.

155. Jo YL, Nara F, Ichihara S, Mizuno T, Mizushima S (1986) Purification and characterization of the OmpR protein, a positive regulator involved in osmoregulatory expression of the *ompF* and *ompC* genes in *Escherichia coli*. J Biol Chem 261: 15252-15256.

156. Martinez-Hackert E, Stock AM (1997) The DNA-binding domain of OmpR: crystal structures of a winged helix transcription factor. Structure 5: 109-124.

157. Lee AK, Detweiler CS, Falkow S (2000) OmpR regulates the two-component system SsrA-ssrB in *Salmonella* pathogenicity island 2. J Bacteriol 182: 771-781.

158. Lindgren SW, Stojiljkovic I, Heffron F (1996) Macrophage killing is an essential virulence mechanism of *Salmonella* typhimurium. Proc Natl Acad Sci U S A 93: 4197-4201.

159. Monsieurs P, De Keersmaecker S, Navarre WW, Bader MW, De Smet F, et al. (2005) Comparison of the PhoPQ regulon in *Escherichia coli* and *Salmonella* typhimurium. J Mol Evol 60: 462-474.

160. Cho US, Bader MW, Amaya MF, Daley ME, Klevit RE, et al. (2006) Metal bridges between the PhoQ sensor domain and the membrane regulate transmembrane signaling. J Mol Biol 356: 1193-1206.

161. Bader MW, Sanowar S, Daley ME, Schneider AR, Cho U, et al. (2005) Recognition of antimicrobial peptides by a bacterial sensor kinase. Cell 122: 461-472.

162. Prost LR, Daley ME, Le Sage V, Bader MW, Le Moual H, et al. (2007) Activation of the bacterial sensor kinase PhoQ by acidic pH. Mol Cell 26: 165-174.

163. Bader MW, Navarre WW, Shiau W, Nikaido H, Frye JG, et al. (2003) Regulation of *Salmonella* typhimurium virulence gene expression by cationic antimicrobial peptides. Mol Microbiol 50: 219-230.

164. Alpuche Aranda CM, Swanson JA, Loomis WP, Miller SI (1992) *Salmonella* typhimurium activates virulence gene transcription within acidified macrophage phagosomes. Proc Natl Acad Sci U S A 89: 10079-10083.

165. Miller SI, Kukral AM, Mekalanos JJ (1989) A two-component regulatory system (phoP phoQ) controls *Salmonella* typhimurium virulence. Proc Natl Acad Sci U S A 86: 5054-5058.

166. Miller SI, Mekalanos JJ (1990) Constitutive expression of the *phoP* regulon attenuates *Salmonella* virulence and survival within macrophages. J Bacteriol 172: 2485-2490.

167. Merighi M, Ellermeier CD, Slauch JM, Gunn JS (2005) Resolvase-*in vivo* expression technology analysis of the *Salmonella enterica* serovar Typhimurium PhoP and PmrA regulons in BALB/c mice. J Bacteriol 187: 7407-7416.

168. Bijlsma JJ, Groisman EA (2005) The PhoP/PhoQ system controls the intramacrophage type three secretion system of *Salmonella enterica*. Mol Microbiol 57: 85-96.

169. Kim CC, Falkow S (2004) Delineation of upstream signaling events in the *Salmonella* pathogenicity island 2 transcriptional activation pathway. J Bacteriol 186: 4694-4704.

170. Song M, Kim HJ, Ryu S, Yoon H, Yun J, et al. ppGpp-mediated stationary phase induction of the genes encoded by horizontally acquired pathogenicity islands and *cob/pdu* locus in *Salmonella enterica* serovar Typhimurium. J Microbiol 48: 89-95.

171. Moreira CG, Weinshenker D, Sperandio V QseC mediates *Salmonella enterica* serovar typhimurium virulence *in vitro* and *in vivo*. Infect Immun 78: 914-926.

172. Osborne SE, Coombes BK (2009) RpoE fine tunes expression of a subset of SsrB-regulated virulence factors in *Salmonella enterica* serovar Typhimurium. BMC Microbiol 9: 45.

173. Coombes BK, Coburn BA, Potter AA, Gomis S, Mirakhur K, et al. (2005) Analysis of the contribution of *Salmonella* pathogenicity islands 1 and 2 to enteric disease progression using a novel bovine ileal loop model and a murine model of infectious enterocolitis. Infect Immun 73: 7161-7169.

174. Coburn B, Li Y, Owen D, Vallance BA, Finlay BB (2005) *Salmonella enterica* serovar Typhimurium pathogenicity island 2 is necessary for complete virulence in a mouse model of infectious enterocolitis. Infect Immun 73: 3219-3227.

175. Bispham J, Tripathi BN, Watson PR, Wallis TS (2001) *Salmonella* pathogenicity island 2 influences both systemic salmonellosis and *Salmonella*-induced enteritis in calves. Infect Immun 69: 367-377.

176. Desin TS, Lam PK, Koch B, Mickael C, Berberov E, et al. (2009) *Salmonella enterica* serovar enteritidis pathogenicity island 1 is not essential for but facilitates rapid systemic spread in chickens. Infect Immun 77: 2866-2875.

177. Brown NF, Vallance BA, Coombes BK, Valdez Y, Coburn BA, et al. (2005) *Salmonella* pathogenicity island 2 is expressed prior to penetrating the intestine. PLoS Pathog 1: e32.

178. Steele-Mortimer O, Brumell JH, Knodler LA, Meresse S, Lopez A, et al. (2002) The invasion-associated type III secretion system of *Salmonella enterica* serovar Typhimurium is necessary for intracellular proliferation and vacuole biogenesis in epithelial cells. Cell Microbiol 4: 43-54.

179. Brawn LC, Hayward RD, Koronakis V (2007) *Salmonella* SPI1 effector SipA persists after entry and cooperates with a SPI2 effector to regulate phagosome maturation and intracellular replication. Cell Host Microbe 1: 63-75.

180. Coombes BK, Wickham ME, Brown NF, Lemire S, Bossi L, et al. (2005) Genetic and molecular analysis of GogB, a phage-encoded type III-secreted substrate in *Salmonella enterica* serovar typhimurium with autonomous expression from its associated phage. J Mol Biol 348: 817-830.

181. Deiwick J, Nikolaus T, Shea JE, Gleeson C, Holden DW, et al. (1998) Mutations in *Salmonella* pathogenicity island 2 (SPI2) genes affecting transcription of SPI1 genes and resistance to antimicrobial agents. J Bacteriol 180: 4775-4780.

182. Bustamante VH, Martinez LC, Santana FJ, Knodler LA, Steele-Mortimer O, et al. (2008) HilD-mediated transcriptional cross-talk between SPI-1 and SPI-2. Proc Natl Acad Sci U S A 105: 14591-14596.

183. Blanc-Potard AB, Solomon F, Kayser J, Groisman EA (1999) The SPI-3 pathogenicity island of *Salmonella enterica*. J Bacteriol 181: 998-1004.

184. Smith RL, Kaczmarek MT, Kucharski LM, Maguire ME (1998) Magnesium transport in *Salmonella* typhimurium: regulation of *mgtA* and *mgtCB* during invasion of epithelial and macrophage cells. Microbiology 144 (Pt 7): 1835-1843.

185. Gerlach RG, Claudio N, Rohde M, Jackel D, Wagner C, et al. (2008) Cooperation of *Salmonella* pathogenicity islands 1 and 4 is required to breach epithelial barriers. Cell Microbiol 10: 2364-2376.

186. Gerlach RG, Jackel D, Geymeier N, Hensel M (2007) *Salmonella* pathogenicity island 4-mediated adhesion is coregulated with invasion genes in *Salmonella enterica*. Infect Immun 75: 4697-4709.

187. Wood MW, Jones MA, Watson PR, Hedges S, Wallis TS, et al. (1998) Identification of a pathogenicity island required for *Salmonella* enteropathogenicity. Mol Microbiol 29: 883-891.

188. Gunn JS, Belden WJ, Miller SI (1998) Identification of PhoP-PhoQ activated genes within a duplicated region of the *Salmonella* typhimurium chromosome. Microb Pathog 25: 77-90.

189. Pickard D, Wain J, Baker S, Line A, Chohan S, et al. (2003) Composition, acquisition, and distribution of the Vi exopolysaccharide-encoding *Salmonella enterica* pathogenicity island SPI-7. J Bacteriol 185: 5055-5065.

190. Shah DH, Lee MJ, Park JH, Lee JH, Eo SK, et al. (2005) Identification of *Salmonella* gallinarum virulence genes in a chicken infection model using PCR-based signature-tagged mutagenesis. Microbiology 151: 3957-3968.

191. Chiu CH, Tang P, Chu C, Hu S, Bao Q, et al. (2005) The genome sequence of *Salmonella enterica* serovar Choleraesuis, a highly invasive and resistant zoonotic pathogen. Nucleic Acids Res 33: 1690-1698.

192. Vernikos GS, Parkhill J (2006) Interpolated variable order motifs for identification of horizontally acquired DNA: revisiting the *Salmonella* pathogenicity islands. Bioinformatics 22: 2196-2203.

193. Fuentes JA, Villagra N, Castillo-Ruiz M, Mora GC (2008) The *Salmonella* Typhi hlyE gene plays a role in invasion of cultured epithelial cells and its functional transfer to *S.* Typhimurium promotes deep organ infection in mice. Res Microbiol 159: 279-287.

194. Blondel CJ, Jimenez JC, Contreras I, Santiviago CA (2009) Comparative genomic analysis uncovers 3 novel loci encoding type six secretion systems differentially distributed in *Salmonella* serotypes. BMC Genomics 10: 354.

195. Cornelis GR (2006) The type III secretion injectisome. Nat Rev Microbiol 4: 811-825.

196. Coombes BK (2009) Type III secretion systems in symbiotic adaptation of pathogenic and non-pathogenic bacteria. Trends Microbiology 17: 89-94.

197. Schraidt O, Marlovits TC Three-dimensional model of *Salmonella*'s needle complex at subnanometer resolution. Science 331: 1192-1195.

198. Kubori T, Matsushima Y, Nakamura D, Uralil J, Lara-Tejero M, et al. (1998) Supramolecular structure of the *Salmonella* typhimurium type III protein secretion system. Science 280: 602-605.

199. McDermott JE, Corrigan A, Peterson E, Oehmen C, Niemann G, et al. Computational prediction of type III and IV secreted effectors in gram-negative bacteria. Infect Immun 79: 23-32.

200. Samudrala R, Heffron F, McDermott JE (2009) Accurate prediction of secreted substrates and identification of a conserved putative secretion signal for type III secretion systems. PLoS Pathog 5: e1000375.

201. Arnold R, Brandmaier S, Kleine F, Tischler P, Heinz E, et al. (2009) Sequence-based prediction of type III secreted proteins. PLoS Pathog 5: e1000376.

202. Munera D, Crepin VF, Marches O, Frankel G N-terminal type III secretion signal of enteropathogenic *Escherichia coli* translocator proteins. J Bacteriol 192: 3534-3539.

203. Baron C, Coombes B (2007) Targeting bacterial secretion systems: benefits of disarmament in the microcosm. Infect Disord Drug Targets 7: 19-27.

204. Blocker A, Jouihri N, Larquet E, Gounon P, Ebel F, et al. (2001) Structure and composition of the Shigella flexneri "needle complex", a part of its type III secreton. Mol Microbiol 39: 652-663.

205. Burghout P, van Boxtel R, Van Gelder P, Ringler P, Muller SA, et al. (2004) Structure and electrophysiological properties of the YscC secretin from the type III secretion system of *Yersinia enterocolitica*. J Bacteriol 186: 4645-4654.

206. Koster M, Bitter W, de Cock H, Allaoui A, Cornelis GR, et al. (1997) The outer membrane component, YscC, of the Yop secretion machinery of *Yersinia enterocolitica* forms a ring-shaped multimeric complex. Mol Microbiol 26: 789-797.

207. Crago AM, Koronakis V (1998) *Salmonella* InvG forms a ring-like multimer that requires the InvH lipoprotein for outer membrane localization. Mol Microbiol 30: 47-56.

208. Spreter T, Yip CK, Sanowar S, Andre I, Kimbrough TG, et al. (2009) A conserved structural motif mediates formation of the periplasmic rings in the type III secretion system. Nat Struct Mol Biol 16: 468-476.

209. Silva-Herzog E, Ferracci F, Jackson MW, Joseph SS, Plano GV (2008) Membrane localization and topology of the *Yersinia pestis* YscJ lipoprotein. Microbiology 154: 593-607.

210. Yip CK, Kimbrough TG, Felise HB, Vuckovic M, Thomas NA, et al. (2005) Structural characterization of the molecular platform for type III secretion system assembly. Nature 435: 702-707.

211. Wagner S, Konigsmaier L, Lara-Tejero M, Lefebre M, Marlovits TC, et al. Organization and coordinated assembly of the type III secretion export apparatus. Proc Natl Acad Sci U S A 107: 17745-17750.

212. Diepold A, Wiesand U, Cornelis GR The assembly of the export apparatus (YscR,S,T,U,V) of the *Yersinia* type III secretion apparatus occurs independently of other structural components and involves the formation of an YscV oligomer. Mol Microbiol 82: 502-514.

213. Morita-Ishihara T, Ogawa M, Sagara H, Yoshida M, Katayama E, et al. (2006) *Shigella* Spa33 is an essential C-ring component of type III secretion machinery. J Biol Chem 281: 599-607.

214. Schuch R, Maurelli AT (2001) Spa33, a cell surface-associated subunit of the Mxi-Spa type III secretory pathway of *Shigella flexneri*, regulates Ipa protein traffic. Infect Immun 69: 2180-2189.

215. Biemans-Oldehinkel E, Sal-Man N, Deng W, Foster LJ, Finlay BB Quantitative proteomic analysis reveals formation of an EscL-EscQ-EscN type III complex in enteropathogenic *Escherichia coli*. J Bacteriol 193: 5514-5519.

216. Broz P, Mueller CA, Muller SA, Philippsen A, Sorg I, et al. (2007) Function and molecular architecture of the *Yersinia* injectisome tip complex. Mol Microbiol 65: 1311-1320.

217. Deane JE, Roversi P, Cordes FS, Johnson S, Kenjale R, et al. (2006) Molecular model of a type III secretion system needle: Implications for host-cell sensing. Proc Natl Acad Sci U S A 103: 12529-12533.

218. Zhang L, Wang Y, Picking WL, Picking WD, De Guzman RN (2006) Solution structure of monomeric BsaL, the type III secretion needle protein of *Burkholderia pseudomallei*. J Mol Biol 359: 322-330.

219. Mueller CA, Broz P, Cornelis GR (2008) The type III secretion system tip complex and translocon. Mol Microbiol 68: 1085-1095.

220. Derewenda U, Mateja A, Devedjiev Y, Routzahn KM, Evdokimov AG, et al. (2004) The structure of *Yersinia pestis* V-antigen, an essential virulence factor and mediator of immunity against plague. Structure 12: 301-306.

221. Picking WL, Nishioka H, Hearn PD, Baxter MA, Harrington AT, et al. (2005) IpaD of *Shigella flexneri* is independently required for regulation of Ipa protein secretion and efficient insertion of IpaB and IpaC into host membranes. Infect Immun 73: 1432-1440.

222. Schoehn G, Di Guilmi AM, Lemaire D, Attree I, Weissenhorn W, et al. (2003) Oligomerization of type III secretion proteins PopB and PopD precedes pore formation in *Pseudomonas*. EMBO J 22: 4957-4967.

223. Faudry E, Vernier G, Neumann E, Forge V, Attree I (2006) Synergistic pore formation by type III toxin translocators of *Pseudomonas aeruginosa*. Biochemistry 45: 8117-8123.

224. Goure J, Pastor A, Faudry E, Chabert J, Dessen A, et al. (2004) The V antigen of *Pseudomonas aeruginosa* is required for assembly of the functional PopB/PopD translocation pore in host cell membranes. Infect Immun 72: 4741-4750.

225. Zurawski DV, Stein MA (2003) SseA acts as the chaperone for the SseB component of the *Salmonella* Pathogenicity Island 2 translocon. Mol Microbiol 47: 1341-1351.

226. Coombes BK, Brown NF, Kujat-Choy S, Vallance BA, Finlay BB (2003) SseA is required for translocation of *Salmonella* pathogenicity island-2 effectors into host cells. Microbes Infect 5: 561-570.

227. Klein JR, Jones BD (2001) *Salmonella* pathogenicity island 2-encoded proteins SseC and SseD are essential for virulence and are substrates of the type III secretion system. Infect Immun 69: 737-743.

228. Ruiz-Albert J, Mundy R, Yu XJ, Beuzon CR, Holden DW (2003) SseA is a chaperone for the SseB and SseD translocon components of the *Salmonella* pathogenicity-island-2-encoded type III secretion system. Microbiology 149: 1103-1111.

229. Sorg JA, Blaylock B, Schneewind O (2006) Secretion signal recognition by YscN, the *Yersinia* type III secretion ATPase. Proc Natl Acad Sci U S A 103: 16490-16495.

230. Woestyn S, Allaoui A, Wattiau P, Cornelis GR (1994) YscN, the putative energizer of the *Yersinia* Yop secretion machinery. J Bacteriol 176: 1561-1569.

231. Zarivach R, Vuckovic M, Deng W, Finlay BB, Strynadka NC (2007) Structural analysis of a prototypical ATPase from the type III secretion system. Nat Struct Mol Biol 14: 131-137.

232. Akeda Y, Galan JE (2005) Chaperone release and unfolding of substrates in type III secretion. Nature 437: 911-915.

233. Cooper CA, Zhang K, Andres SN, Fang Y, Kaniuk NA, et al. Structural and biochemical characterization of SrcA, a multi-cargo type III secretion chaperone in *Salmonella* required for pathogenic association with a host. PLoS Pathog 6: e1000751.

234. Lilic M, Vujanac M, Stebbins CE (2006) A common structural motif in the binding of virulence factors to bacterial secretion chaperones. Mol Cell 21: 653-664.

235. Stebbins CE, Galan JE (2001) Maintenance of an unfolded polypeptide by a cognate chaperone in bacterial type III secretion. Nature 414: 77-81.

236. Luo Y, Bertero MG, Frey EA, Pfuetzner RA, Wenk MR, et al. (2001) Structural and biochemical characterization of the type III secretion chaperones CesT and SigE. Nat Struct Biol 8: 1031-1036.

237. Cheng LW, Anderson DM, Schneewind O (1997) Two independent type III secretion mechanisms for YopE in *Yersinia enterocolitica*. Mol Microbiol 24: 757-765.

238. Darwin KH, Miller VL (2000) The putative invasion protein chaperone SicA acts together with InvF to activate the expression of *Salmonella* typhimurium virulence genes. Mol Microbiol 35: 949-960.

239. Mavris M, Page AL, Tournebize R, Demers B, Sansonetti P, et al. (2002) Regulation of transcription by the activity of the *Shigella flexneri* type III secretion apparatus. Mol Microbiol 43: 1543-1553.

240. Kalir S, McClure J, Pabbaraju K, Southward C, Ronen M, et al. (2001) Ordering genes in a flagella pathway by analysis of expression kinetics from living bacteria. Science 292: 2080-2083.

241. Temme K, Salis H, Tullman-Ercek D, Levskaya A, Hong SH, et al. (2008) Induction and relaxation dynamics of the regulatory network controlling the type III secretion system encoded within *Salmonella* pathogenicity island 1. J Mol Biol 377: 47-61.

242. Darwin KH, Miller VL (1999) InvF is required for expression of genes encoding proteins secreted by the SPI1 type III secretion apparatus in *Salmonella* typhimurium. J Bacteriol 181: 4949-4954.

243. Demers B, Sansonetti PJ, Parsot C (1998) Induction of type III secretion in *Shigella flexneri* is associated with differential control of transcription of genes encoding secreted proteins. EMBO J 17: 2894-2903.

244. Sun GW, Chen Y, Liu Y, Tan GY, Ong C, et al. Identification of a regulatory cascade controlling Type III Secretion System 3 gene expression in *Burkholderia pseudomallei*. Mol Microbiol 76: 677-689.

245. Yother J, Chamness TW, Goguen JD (1986) Temperature-controlled plasmid regulon associated with low calcium response in *Yersinia pestis*. J Bacteriol 165: 443-447.

246. Cornelis GR, Biot T, Lambert de Rouvroit C, Michiels T, Mulder B, et al. (1989) The *Yersinia* yop regulon. Mol Microbiol 3: 1455-1459.

247. Cambronne ED, Schneewind O (2002) *Yersinia enterocolitica* type III secretion: *yscM1* and *yscM2* regulate *yop* gene expression by a posttranscriptional mechanism that targets the 5' untranslated region of *yop* mRNA. J Bacteriol 184: 5880-5893.

248. Anderson DM, Ramamurthi KS, Tam C, Schneewind O (2002) YopD and LcrH regulate expression of *Yersinia enterocolitica* YopQ by a posttranscriptional mechanism and bind to *yopQ* RNA. J Bacteriol 184: 1287-1295.

249. Diepold A, Amstutz M, Abel S, Sorg I, Jenal U, et al. Deciphering the assembly of the *Yersinia* type III secretion injectisome. EMBO J 29: 1928-1940.

250. Osborne SE, Coombes BK Expression and secretion hierarchy in the nonflagellar type III secretion system. Future Microbiol 6: 193-202.

251. Chevance FF, Hughes KT (2008) Coordinating assembly of a bacterial macromolecular machine. Nat Rev Microbiol 6: 455-465.

252. Deane JE, Abrusci P, Johnson S, Lea SM (2010) Timing is everything: the regulation of type III secretion. Cell Mol Life Sci 67: 1065-1075.

253. Fraser GM, Hirano T, Ferris HU, Devgan LL, Kihara M, et al. (2003) Substrate specificity of type III flagellar protein export in *Salmonella* is controlled by subdomain interactions in FlhB. Mol Microbiol 48: 1043-1057.

254. Makishima S, Komoriya K, Yamaguchi S, Aizawa SI (2001) Length of the flagellar hook and the capacity of the type III export apparatus. Science 291: 2411-2413.

255. Sorg I, Wagner S, Amstutz M, Muller SA, Broz P, et al. (2007) YscU recognizes translocators as export substrates of the *Yersinia* injectisome. EMBO J 26: 3015-3024.

256. Edqvist PJ, Olsson J, Lavander M, Sundberg L, Forsberg A, et al. (2003) YscP and YscU regulate substrate specificity of the *Yersinia* type III secretion system. J Bacteriol 185: 2259-2266.

257. Williams AW, Straley SC (1998) YopD of Yersinia pestis plays a role in negative regulation of the low-calcium response in addition to its role in translocation of Yops. J Bacteriol 180: 350-358.

258. Pettersson J, Nordfelth R, Dubinina E, Bergman T, Gustafsson M, et al. (1996) Modulation of virulence factor expression by pathogen target cell contact. Science 273: 1231-1233.

259. Rimpilainen M, Forsberg A, Wolf-Watz H (1992) A novel protein, LcrQ, involved in the low-calcium response of *Yersinia pseudotuberculosis* shows extensive homology to YopH. J Bacteriol 174: 3355-3363.

260. Parsot C, Ageron E, Penno C, Mavris M, Jamoussi K, et al. (2005) A secreted anti-activator, OspD1, and its chaperone, Spa15, are involved in the control of transcription by the type III secretion apparatus activity in *Shigella flexneri*. Mol Microbiol 56: 1627-1635.

261. Ferracci F, Schubot FD, Waugh DS, Plano GV (2005) Selection and characterization of *Yersinia pestis* YopN mutants that constitutively block Yop secretion. Mol Microbiol 57: 970-987.

262. Joseph SS, Plano GV (2007) Identification of TyeA residues required to interact with YopN and to regulate Yop secretion. Adv Exp Med Biol 603: 235-245.

263. Schubot FD, Jackson MW, Penrose KJ, Cherry S, Tropea JE, et al. (2005) Three-dimensional structure of a macromolecular assembly that regulates type III secretion in *Yersinia pestis*. J Mol Biol 346: 1147-1161.

264. Coombes BK, Brown NF, Valdez Y, Brumell JH, Finlay BB (2004) Expression and secretion of *Salmonella* pathogenicity island-2 virulence genes in response to acidification exhibit differential requirements of a functional type III secretion apparatus and SsaL. J Biol Chem 279: 49804-49815.

265. Van Engelenburg SB, Palmer AE Imaging type-III secretion reveals dynamics and spatial segregation of *Salmonella* effectors. Nat Methods 7: 325-330.

266. Thomas NA, Deng W, Baker N, Puente J, Finlay BB (2007) Hierarchical delivery of an essential host colonization factor in enteropathogenic *Escherichia coli*. J Biol Chem 282: 29634-29645.

267. Wulff-Strobel CR, Williams AW, Straley SC (2002) LcrQ and SycH function together at the Ysc type III secretion system in *Yersinia pestis* to impose a hierarchy of secretion. Mol Microbiol 43: 411-423.

Chapter Two – Pathogenic adaptation of intracellular bacteria by rewiring a *cis*-regulatory input function

Chapter Two – Co-authorship statement

Chapter Two consists of the following publication:

Osborne, S.E., Walters, D., Tomljenovic A.M., Mulder, D.T., Silphaduang, U., Duong, N., Lowden, M.J., Wickham, M.E., Waller, R.F., Kenney, L.J., and Coombes, B.K. (2009). Pathogenic adaptation of intracellular bacteria by rewiring a cis-regulatory input function. Proc. Natl. Acad. Sci. USA. Mar 10; 106(10): 3982-7.

The following work was conducted by authors other then myself:

1) Footprinting experiments and analysis were conducted by D.W. and L.J.K

2) ChIP – on – ChIP data outlined in Figure 2.2 was taken from the following publication: Tomljenovic-Berube, A.M., Mulder, D. T. Whiteside, M. D., Brinkman, F. S., and Coombes, B. K. (2011). Identification of the regulatory logic controlling *Salmonella* pathoadaptation by the SsrA-SsrB two-component system. PLoS Genet 6: e1000875.

3) Competitive infections were performed by SEO and BKC

4) 5’ RACE experiments were performed by U.S.

5) Fractionation experiments were performed by M.J.L., M.E.W., and R.F.W.

6) Phylogenies were constructed by B.K.C.

7) Molecular cloning was performed by S.E.O. and N.D.

8) Manuscript was written and edited by S.E.O and B.K.C.

Pathogenic adaptation of intracellular bacteria by rewiring a *cis*-regulatory input function

Suzanne E. Osborne [*], Don Walthers [†], Ana M. Tomljenovic [*], David T. Mulder [*], Uma Silphaduang [*], Nancy Duong [*], Michael J. Lowden [¶], Mark E. Wickham [§], Ross F. Waller [**], Linda J. Kenney [†] & Brian K. Coombes [*,††]

[*] *Michael G. DeGroote Institute for Infectious Disease Research, Department of Biochemistry and Biomedical Sciences, McMaster University, Hamilton, ON L8N 3Z5*

[†] *Department of Microbiology and Immunology, University of Illinois-Chicago, Chicago, IL 60612*

[¶] *Department of Chemistry, Dartmouth College, Hanover, NH 03755*

[§] *Phillips Ormonde & Fitzpatrick, 367 Collins Street, Melbourne, Vic, 3000, Australia*

[**] *School of Botany, University of Melbourne, Melbourne, Vic. Australia*

[††] *Public Health Agency of Canada, Laboratory for Foodborne Zoonoses, Guelph, ON N1G 3W4*

BIOLOGICAL SCIENCES, Microbiology (Secondary: Evolution)

Text pages: 25

Manuscript Figures: 1-5

Supplementary Figures: S1-S5

Correspondence should be addressed to B.K.C. (coombes@mcmaster.ca)

Abstract

The acquisition of DNA by horizontal gene transfer (HGT) enables bacteria to adapt to previously unexploited ecological niches. Although HGT and mutation of protein-coding sequences are well-recognized forms of pathogen evolution, the evolutionary significance of *cis*-regulatory mutations in creating phenotypic diversity through altered transcriptional outputs is not known. We show the significance of regulatory mutation for pathogen evolution by mapping and then rewiring a *cis*-regulatory module controlling a gene required for murine typhoid. Acquisition of a binding site for the *Salmonella* pathogenicity island-2 regulator, SsrB, enabled the *srfN* gene, ancestral to the *Salmonella* genus, to play a role in pathoadaptation of *S*. typhimurium to a host animal. We identified the evolved *cis*-regulatory module and quantified the fitness gain that this regulatory output accrues for the bacterium using competitive infections of host animals. Our findings highlight a mechanism of pathogen evolution involving regulatory mutation that is selected due to the fitness advantage the new regulatory output provides the incipient clones.

Introduction

A common source of genetic diversity among bacterial pathogens is horizontal acquisition of mobile genetic elements, which can harbour virulence genes required during various stages of host infection (1). In the *S. enterica* species, two major genetic acquisitions were the *Salmonella* pathogenicity islands-1 and -2, each coding for a type III secretion system (T3SS) that translocates protein effectors into host cells during infection. The SPI-1 T3SS is common to the genus *Salmonella* and injects effectors for invasion of non-phagocytic cells. Serovars within the *S. enterica* species additionally possess SPI-2, which is absent from *S. bongori*, the other recognized species of *Salmonella*. The SPI-2 T3SS injects proteins required for intracellular survival and infection of mammals (2, 3) and represented a second phase in the evolution of *Salmonella* virulence. Of particular interest is a horizontally acquired two-component regulatory system, SsrA-SsrB, that facilitated niche expansion from the environment into mammalian hosts due to regulation of the co-inherited T3SS in SPI-2. This regulatory system includes a sensor kinase, SsrA, and response regulator, SsrB, that integrates expression of the SPI-2 T3SS with other horizontally acquired effectors by binding to *cis*-regulatory elements upstream of promoters within and outside of SPI-2 (4, 5).

Virulence is a quantitative trait resulting from the interaction between bacterial and host gene products (6). Accordingly, the intracellular virulence phenotype is regulated by multiple transcription factors that integrate signals from the bacterial cell surface to coordinate expression of niche-specific genes (7). Modularity of virulence gene promoter architecture is evident in SPI-2, where combinatorial input from PhoP (8),

OmpR (9, 10) and SlyA (4, 11) on some promoters is required to launch an integrated virulence program in the host. Combinatorial control of virulence gene regulation by modular regulatory units provides plasticity in the amplitude of transcriptional outputs depending on the environment, for example in response to a more resistant host genotype (12), or in response to metabolic demands as shown in the Boolean gate logic architecture of the *lac* operon in *E. coli* (13).

Evolution of regulatory DNA, or *cis* regulatory elements (CRE), has been invoked to explain the bulk of higher organismal diversity in the context of developmental evolution ('evo-devo') (14-16) with an expanding volume of examples. However, little is known about the evolutionary significance of *cis*-regulatory mutations that may underlie bacterial pathogenesis and adaptation to various ecological niches. In the present work, we validate this evolutionary principle in a prokaryotic system by establishing that mutation of the *cis*-regulatory input for an ancestral bacterial gene (*srfN*) contributes to pathoadaptive fitness during enteric and typhoid disease in animals. Our results demonstrate that *cis*-regulatory mutation between closely related species contributes to pathoadaptive trait gain with functional consequences for the host-pathogen interaction.

Results

Identification and regulation of *srfN*. Given the importance in virulence of the SsrB response regulator encoded in the SPI-2 pathogenicity island, we sought to identify other genes in the SsrB regulon for their role in pathogenesis. Analysis of SsrB co-regulated

genes using transcriptional arrays (for methods, see (17)) identified a gene whose expression under SPI-2-inducing conditions was strongly SsrB-dependent. STM0082 mRNA was reduced ~8-fold in Δ*ssrB* cells compared to wild type, which was similar in magnitude to that of SsrB-regulated T3SS effectors *sseF* (8.6-fold) and *sspH2* (7.1-fold). STM0082 is found in pathogenic enterobacteriaceae and other γ-proteobacteria including *S. bongori*, *S.enterica*, *Yersiniae*, and the human and coral pathogen, *Serratia marcescens*, and is part of a larger family of uncharacterized bacterial 'y' genes (pfam07338) (18) (Figure 2.S1). The gene synteny around STM0082 is identical between *S.* typhimurium and *S. bongori* suggesting it was ancestral to the *Salmonella* genus prior to the divergence of lineages giving rise to *S. bongori* and *S. enterica*, which would predate the acquisition of SsrB by the *S. enterica* lineage. We named STM0082 *srfN* (SsrB-regulated factor N) and determined that SrfN localizes to the inner bacterial membrane and is not secreted or translocated by the co-expressed type III secretion system (Figure 2.S2).

SsrB controls *srfN* directly. *S.* typhimurium and *S. bongori* both contain *srfN* yet the expression of this gene in *S.* typhimurium is driven by SsrB. The absence in *S. bongori* of SPI-2 and thus the SsrA-SsrB two-component regulatory system suggested adaptive evolution of the *srfN cis*-regulatory element in *S.* typhimurium, allowing SsrB to expropriate control of *srfN* during intracellular infection. Deletion analysis of the *srfN cis*-regulatory region identified a putative CRE between 600 and 1000 base pairs upstream of the translational start site that was absolutely required for *srfN* expression (Figure 2.1A).

We used primer extension to map the location of the *srfN* promoter and transcription start site in *S.* typhimurium. RNA isolated from an *hns* mutant (5) and an isogenic *ssrB* mutant revealed a single *srfN*-specific transcript ending 654 nucleotides upstream of the translation start site (Figure 2.1B). *srfN* mRNA was significantly reduced in the absence of SsrB, consistent with protein levels. To determine whether gene expression by SsrB was a consequence of direct binding to the *srfN* regulatory region, we used purified SsrBc in footprinting protection experiments (4). SsrBc protected approximately 20 base pairs of DNA flanked by multiple DNase I hypersensitive sites between 85-65 base pairs upstream of the transcription start site (Figure 2.1C), consistent with a direct role of SsrB in transcriptional activation of *srfN*. The location of protection validates the long 5' untranslated leader sequence identified by primer extension and the extent of protection is consistent with binding by a single SsrB dimer (Liao et al., submitted), and is similar to that of another response regulator family member, NarL (19). We further verified SsrB binding to this DNA region *in vivo* using chromatin immunoprecipitation followed by PCR (Figure 2.2A) and microarray analysis (ChIP-on-chip) with a strain carrying a chromosomal *ssrB*-FLAG allele. Thirty-two ChIP-chip probes located near *srfN*, verified that SsrB was loaded onto intergenic chromosomal DNA at the precise location mapped by SsrB footprinting, but not at sites flanking this region (Figure 2.2B), or at another chromosomal location (>5000 bp in length) not regulated by SsrB (Figure 2.2C). Sequence alignment of the *srfN* regulatory region from serovars of *S. enterica* and *S. bongori* for which sequence data was available revealed a DNA signature unique to 11 of 13 serovars of *S. enterica* that mapped to the chromosomal location protected by SsrB.

This region was divergent in *S. bongori* with only 11/21 bases conserved with the *S. enterica* species (Figure 2.1D). Interestingly, one *S. enterica* serovar that showed divergence in the SsrB footprint region (Diarizonae) belongs to the IIIb subspecies that are symbionts of reptiles but rarely associated with human infection. Although subspecies IIIb contains SsrB, it forms a distinct phylogenetic branch that diverged from the class I subspecies (responsible for 99% of mammalian infections) between 20-25 Myr ago (20). We performed analyses of relative genetic distances of the *srfN cis*-regulatory region, the entire upstream DNA sequence, and the *srfN* open reading frame between *S. enterica* serovars and *S. bongori*. In neighbor joining phylogenies of all regions (Figure 2.S3), *S. enterica* subspecies I (Enterica) forms a distinct clade from subspecies IIIb (Diarizonae) and *S. bongori*, as is also seen for housekeeping genes and invasion genes (21). The region adapted to SsrB regulation (from the SsrB footprint to the start of transcription) shows less overall divergence within subspecies class I compared to the rest of the 5' untranslated region (UTR), or even the *srfN* open reading frame (Figure 2.S3), consistent with selection imposed on this regulatory region. These data identified a conserved CRE involved in regulatory evolution of *srfN* in *Salmonella* subspecies infecting warm-blooded mammals.

SrfN is a fitness factor during systemic typhoid. The identification of a gene in *S.* typhimurium appropriated by a horizontally acquired response regulator required for infection of mammals led us to hypothesize that SrfN contributes to within-host fitness. To test this, we constructed a non-polar, in-frame deletion of *srfN* in *S.* typhimurium and

tested the fitness of the mutant in competitive infections with the isogenic parent strain. Mice were infected orally and competitive indices (17) were calculated for the cecum, liver and spleen three days after infection of C57BL/6 mice. After a single round of infection, the geometric mean competitive index for the Δ*srfN* strain in the liver and spleen was 0.227 (95% CI 0.081-0.639) and 0.296 (95% CI 0.091-0.562), respectively (Figure 2.3A), showing that bacteria lacking SrfN were significantly out competed by wild type bacteria during systemic infection. Mutant cells were also out competed by wild type cells in the cecum during enteric stages of colonization with a similar magnitude of attenuation (data not shown). The *srfN* mutant was not defective for competitive (Figure 2.3B) or non-competitive growth (Figure 2.S5) *in vitro* in minimal or rich media, indicating that the phenotype of the *srfN* mutant was specific to within animal hosts.

Promoter swapping experiments with *S. bongori*. The regulatory data for *srfN* indicated an evolved dependence on the horizontally-acquired virulence regulator SsrB. We first verified that *srfN* was under SsrB control by cloning the regulatory region upstream of *srfN* in front of a *srfN*-HA allele and inducing expression in wild type *Salmonella* and Δ*ssrB* cells. SrfN-HA protein was abundant in wild type cells but highly reduced in the *ssrB* mutant (Figure 2.4A). Next, we cloned *srfN* and its 5'UTR from *S.* typhimurium into a low-copy plasmid and transformed this construct into *S. bongori* (which evolved distinctly from *S.* typhimurium in the absence of SsrB). We asked whether *S. bongori* could recognize this typhimurium-adapted promoter for gene expression, which it could not. Although SrfN-HA was expressed in *S.* typhimurium, the

protein was barely detectable in wild type *S. bongori* (Figure 2.4A), unless the pathogenicity island containing SsrAB was also co-transferred on a bacterial artificial chromosome (pSPI2). Introducing SsrAB/SPI-2 into *S. bongori* resulted in an immediate accumulation of SrfN protein (Figure 2.4A), as well as the type III secretion needle component, SseB, whose gene is expressed in an SsrB-dependent manner in SPI-2. This result raised the question whether the ancestral transcriptional machinery required for expressing *srfN* was present in *S*. typhimurium. To examine this, we first mapped the transcriptional start site for the *srfN* orthologue in *S. bongori*, which showed a transcriptional start site at position -115 bp relative to the start of translation and near-consensus -10 and -35 hexamer regions (Figure 2.S4). Next, we precisely swapped the *S. bongori* 5'UTR regulatory sequence plus 680 bp of upstream DNA (to include the divergent regulatory region) into *S*. typhimurium and asked whether this regulatory input could drive *srfN* expression. Expression of *srfN* from the *S. bongori* 5'UTR was SsrB-independent, as indicated by similar protein levels in *ssrB* null bacteria and wild type cells (Figure 2.4B) and in the absence and presence of SPI-2 in *S. bongori* (Figure 2.4C). These data suggested a conservation of the ancestral transcription factor(s) governing control of *srfN*, prompting us to investigate the regulation of the *srfN* orthologue in *S. bongori*. We deleted transcriptional regulators in *S*. typhimurium that are common to both *S*. typhimurium and *S. bongori* and tested whether these strains could express *srfN* from the *S. bongori* 5'UTR. These experiments revealed the requirement for PhoP input on the *S. bongori* CRE (Figure 2.4D), which we verified by deleting *phoP* in *S. bongori* and testing expression in low-magnesium minimal medium (Figure 2.4E). That the *srfN* CRE

from *S.* typhimurium is not well recognized in PhoP-containing *S. bongori* cells in the absence of SsrB suggest a contemporaneous loss of direct input from the ancestral PhoP response regulator. However, a direct or indirect role for PhoP cannot be ruled out, since SsrB is epistatic to PhoP in *S.* typhimurium (22). Together with the phylogenetic analysis, these data suggest that the 5'UTR controlling *srfN* in *S.* typhimurium evolved under selection due to the beneficial fitness this new regulatory input afforded incipient clones within the host.

Pathogenic adaptation via *cis*-regulatory mutation. To test the evolutionary significance of *cis*-regulatory mutation driving bacterial pathogenesis, we complemented the *S.* typhimurium *srfN* mutant with a wild type copy of *srfN* driven by the promoter evolved in either *S. bongori* or *S.* typhimurium and competed the complemented strains against wild type *S.* typhimurium cells in mixed infections of mice. Complementation of Δ*srfN* with *srfN* expressed from the promoter evolved in *S.* typhimurium (P_{St}-5'UTR) restored in-host fitness of the mutant to wild type levels as evidenced by a competitive index of 0.98 (95% CI 0.55-1.79, Figure 2.5A). In mouse experiments designed to test whether rewiring *srfN* to the 5'UTR evolved in *S. bongori* (P_{Sb}-5'UTR) could restore in-host fitness to this strain, we determined that it could not. These cells were still out-competed by wild type cells in mixed infections in animals with a relative fitness of 0.19 (95% CI 0.10-0.26) (Figure 2.5A), which was indistinguishable from the Δ*srfN* strain (0.22, 95% CI 0.08-0.63) (Figure 2.3A). This was despite the fact that *srfN* was expressed in a PhoP-dependent manner in this strain. Finally, to verify the precise requirement of

the mapped SsrB CRE for *in vivo* fitness, we deleted the chromosomal SsrB CRE identified by footprinting and replaced it with the analogous region from *S. bongori* defined in the alignment from Figure 2.1D. This strain (SsrB CRE replacement) was out competed by wild type cells in mouse infections similar to that seen with the re-wired trans complementation constructs (CI_{spleen} 0.16, 95% CI 0.09-0.23; CI_{liver} 0.13, 95% CI 0.08-0.17) (Figure 2.5B). Thus, a single adaptive *cis*-regulatory mutation enhances within-host fitness, emphasizing a new source of regulatory evolution in bacterial pathogenesis.

Discussion

Genotypic variation between *S. enterica* and *S. bongori* includes the presence in *S. enterica* of a large horizontally-acquired pathogenicity island, SPI-2. This genetic island provided the incumbent species with the machinery to access a new ecological niche in warm-blooded hosts and to replicate within immune cells. The acquisition of SPI-2 also introduced a new two-component regulatory system to the *Salmonella* genome, SsrA-SsrB, which ostensibly contributed to immediate and gradual phenotypic variation among SPI-2-containing subspecies (see Figure 2.5C). Evidence exists to suggest that SPI-2 was acquired by *S. enterica* following the branching of *S. enterica* and *S. bongori*. Arguments against the presence of SPI-2 in the last common ancestor and eventual loss in *S. bongori* include the inability to find any remnants of SPI2 in extant *S. bongori* strains. However,

in the absence of a third distinct species on which to adjudicate, maximum parsimony arguments could account for either scenario.

Other forces apart from unique gene content contribute to phenotypic variation among closely related species, such as stochastic differences in gene regulation (23) and evolution of enhancer sequences (24) and of orthologous regulators (25). In bacterial pathogens, the regulatory interactions orchestrating virulence and fitness genes collectively shape the ecology of the host-pathogen interaction. The requirement of *srfN* for intra-host fitness highlights the selective advantage achieved by fine-tuning gene expression by regulatory evolution and suggests that SrfN may have evolved unique functions in *S. enterica* for use within the animal host. That *srfN* (STM0082) was found to be required for long-term chronic infection of mice supports this view (26). Although the exact function of SrfN is not yet known, we have excluded function in motility, resistance to reactive oxygen or serum, and in chemical-genetic interactions with 60 known bioactive molecules. The unusually long 5'UTR that is generated by regulatory input from SsrB may be maintained due to the presence of a small predicted ORF on the opposite DNA strand between the mapped SsrB CRE and *srfN*. In addition, the length of the 5'UTR may imply additional functionality of this region such as post-transcriptional regulation, although this has yet to be studied experimentally.

The evolution of bacterial pathogenesis has been considered in two complementary forms; 'quantum leaps' (27) with the acquisition of genomic islands providing genes *en masse* that could contribute immediately to niche expansion and to overcoming host restriction. The acquisition of the multi-gene pathogenicity islands SPI-1

and SPI-2 represents this model of evolution, providing the incumbent clones with novel cellular machinery to interface with their host environment. Another mechanism of evolution involves gene loss or gene modification to remove (or alter) genes whose products influence fitness in a given environment (28, 29). The loss of the lysine decarboxylase gene, *cadA*, from multiple strains of *Shigella* and enteroinvasive *E. coli* is an example of this type of structural mutation that prevents host cadaverine-mediated attenuation of virulence following decarboxylation of lysine (30). Yet structural mutations can give rise to antagonistic pleiotropy and functional trade-offs as organisms move from one niche to another where selective pressures are different and the lost or modified gene product may be needed to greater or lesser extents. Instead, evolution by mutation of *cis*-regulatory input functions with concomitant changes in gene expression is well suited to quantitative trait loci involved in pathogenic adaptation. This type of adaptive divergence is well studied in eukaryotic evolutionary biology where it has been shown to reduce pleiotropy, minimize functional trade-offs and resolve adaptive conflicts (31, 32). Although the relative contributions of *cis*-regulatory mutations versus structural mutations driving quantitative traits have been debated (33, 34), empirical evidence supports the view that both regulatory (31, 33, 35-37) and structural mutations (38, 39) can shape adaptive evolution in higher organisms. Our work highlights how evolution of gene regulation via *cis*-regulatory mutation influences pathogenic adaptation with functional consequences for the host-pathogen interaction. Especially for zoonotic pathogens that are commensal, mutualist or pathogenic associates depending on the host, regulatory evolution offers a mechanism to resolve adaptive conflicts that arise from

having alleles under negative selection in one environment but positive selection in others.

Further studies to identify variation between closely related bacterial species in the cis-regulatory region of homologous genes will provide clues to the selective forces driving pathogen evolution in the host environment, a topic for which very little empirical data exists (40). Understanding how horizontally acquired transcription factors influence promoter evolution and plasticity of regulatory circuits controlling bacterial virulence and fitness is in the formative stage and the work herein exemplifies a seminal case. Our efforts here reveal a connection between virulence gene regulators and co-regulation of ancillary factors critical for pathoadaptation. Rewiring regulatory DNA to commandeer virulence-associated transcription factors is a mechanism of regulatory evolution (35, 41) to be considered to fully understand the evolutionary potential of bacterial pathogens.

Materials and Methods

Bacterial strains and growth conditions. *Salmonella enterica* serovar Typhimurium (abbreviated *S.* typhimurium here) was strain SL1344 and mutants were isogenic derivatives. *S. bongori* (serovar 66:z) was purchased from the *Salmonella* Genetic Stock Centre (Calgary, AB) and *S. bongori* SARC12 containing a bacterial artificial chromosome encoding the SPI-2 genomic island has been described elsewhere (42, 43). An acidic minimal medium low in phosphate and magnesium (LPM) used for the

induction of SPI-2 has been described previously (44). SL1344 *ushA*::cat was used for competitive infections of animals and has been described elsewhere (17).

Cloning and mutant construction. Detailed information on cloning and mutant construction is found in Supplementary information.

Type III secretion assays. Assays for type III secretion were conducted as described previously (44), with details in Supplementary information.

Promoter mapping and footprinting. The *srfN* transcription start site was identified by primer extension performed as described previously (5) using the *srfN*-specific primer CTG TTA CTG ATA GTG TTT CTT TCG. The *srfN* regulatory region was amplified by PCR with primers CGC CGG ATA ACA TAC CGC CT and GAA TGA AGC AAC CGT TGC C and cloned into pCR2.1. The resulting plasmid, pDW106, was used as a template for generation of DNA sequencing ladders. To map the SsrB input module on the *srfN* promoter, DNase I protection footprinting was performed as described previously using the purified DNA binding domain of SsrB protein (SsrBc) (5). Primers CTG TTA CTG ATA GTG TTT CTT TCG and CAT TTA TTA CTG TAC GAG GAA GC and plasmid pDW106 were used to generate footprinting templates and DNA sequencing ladders. Footprinting reactions on similarly constructed templates from sequence more proximal to the *srfN* coding sequence did not reveal SsrBc binding sites.

Competitive infection of animals. Animal protocols were approved by the Animal Ethics Committee, McMaster University. Female C57BL/6 mice (Charles River) were used throughout and infected orally with ~10^6 cfu of *S*. typhimurium in 0.1 M HEPES (pH 8.0), 0.9% NaCl. For competitive infections, mice were infected orally with a mixed inoculum containing wild-type *S*. typhimurium and an unmarked mutant strain under investigation. At 72 h after infection, bacterial load in the cecum, spleen and liver were enumerated from organ homogenates. Detailed methods for enumeration of bacteria in vivo are found in Supplementary information. The competitive index (CI) was calculated on log-transformed cfu as: (mutant/wild type) $_{output}$ / (mutant /wild type) $_{input}$. Log-transformed competitive infection data were analyzed using a one-sample t test.

Genetic analyses. Detailed references to genome sequences and genomic analyses are found in Supplementary information. Nucleotide alignments of the *srfN* coding sequence and the upstream non-coding sequence were generated with ClustalX. With the exclusion of indels, phylogenetic distance analyses were performed on the coding sequence (291 nucleotides), upstream 770 nucleotides, and the 92-nucleotide *cis*-regulatory region (LT2 nucleotides -741 to -651). Distances were calculated by TREE-PUZZLE 5.2 (45) using the Hasegawa model of substitution and a uniform rate of heterogeneity. Bootstraps were calculated using puzzleboot (shell script by A. Roger and M. Holder, http:/www.tree-puzzle.de) with 8 rate categories and invariable sites estimated from the data. Trees were inferred using WEIGHBOR 1.0.1a (46).

Acknowledgements

This work was funded by grants to BKC from the Canadian Institutes of Health Research (CIHR; MOP-82704) and the Public Health Agency of Canada. BKC is the recipient of a New Investigator Award from the CIHR, a Young Investigator Award from the American Society of Microbiology, and an Early Researcher Award from the Ontario Ministry of Research and Innovation. SO is the recipient of an Ontario Graduate Scholarship. LJK and DW were supported by grant GM-58746 from the National Institutes of Health and MCB-0613014 from the National Science Foundation.

Author contributions

SEO, DW, LJK, BKC conceived and designed experiments; SEO, DW, ND, MJL, AMT, US, BKC performed experiments; SEO, DW, DTM, LJK, RFW, MEW, BKC analysed data; SEO, DW, LJK, BKC wrote the paper.

Author statement

The authors declare that no competing interests exist.

References

1. Dobrindt U, Hochhut B, Hentschel U, & Hacker J (2004) Genomic islands in pathogenic and environmental microorganisms. *Nat. Rev. Microbiol*. 2(5):414-424.
2. Ochman H, Soncini FC, Solomon F, & Groisman EA (1996) Identification of a pathogenicity island required for *Salmonella* survival in host cells. *Proc. Natl. Acad. Sci. U.S.A.* 93:7800-7804.
3. Shea JE, Hensel M, Gleeson C, & Holden DW (1996) Identification of a virulence locus encoding a second type III secretion system in *Salmonella* typhimurium. *Proc. Natl. Acad. Sci. U. S. A.* 93(6):2593-2597.
4. Feng X, Walthers D, Oropeza R, & Kenney LJ (2004) The response regulator SsrB activates transcription and binds to a region overlapping OmpR binding sites at *Salmonella* pathogenicity island 2. *Mol. Microbiol*. 54(3):823-835.
5. Walthers D, et al. (2007) The response regulator SsrB activates expression of diverse *Salmonella* pathogenicity island 2 promoters and counters silencing by the nucleoid-associated protein H-NS. *Mol. Microbiol*. 65(2):477-493.
6. Barton NH & Keightley PD (2002) Understanding quantitative genetic variation. *Nat Rev Genet* 3(1):11-21.
7. Groisman EA & Mouslim C (2006) Sensing by bacterial regulatory systems in host and non-host environments. *Nat. Rev. Microbiol*. 4(9):705-709.

8. Bijlsma JJE & Groisman EA (2005) The PhoP/PhoQ system controls the intramacrophage type three secretion system of *Salmonella enterica. Mol. Microbiol*. 54(1):85-96.

9. Lee AK, Detweiler CS, & Falkow S (2000) OmpR regulates the two-component system SsrA- SsrB in *Salmonella* pathogenicity island 2. *J. Bacteriol*. 182(3):771-781.

10. Feng X, Oropeza R, & Kenney LJ (2003) Dual regulation by phospho-OmpR of *ssrA/B* gene expression in *Salmonella* pathogenicity island 2. *Mol. Microbiol*. 48(4):1131-1143.

11. Navarre WW, et al. (2005) Co-regulation of *Salmonella enterica* genes required for virulence and resistance to antimicrobial peptides by SlyA and PhoP/PhoQ. *Mol. Microbiol*. 56(2):492-508.

12. Zaharik ML, Vallance BA, Puente JL, Gros P, & Finlay BB (2002) Host-pathogen interactions: Host resistance factor Nramp1 up-regulates the expression of *Salmonella* pathogenicity island-2 virulence genes. *Proc. Natl. Acad. Sci. U.S.A.* 99(24):15705-15710.

13. Mayo AE, Setty Y, Shavit S, Zaslaver A, & Alon U (2006) Plasticity of the *cis*-regulatory input function of a gene. *PLoS Biol* 4(4):e45.

14. Levine M & Tjian R (2003) Transcription regulation and animal diversity. *Nature* 424(6945):147-151.

15. Carroll SB (2005) Evolution at two levels: on genes and form. *PLoS Biol* 3(7):e245.

16. Carroll SB (2000) Endless forms: the evolution of gene regulation and morphological diversity. *Cell* 101(6):577-580.

17. Coombes BK, Wickham ME, Lowden MJ, Brown NF, & Finlay BB (2005) Negative regulation of *Salmonella* pathogenicity island 2 is required for contextual control of virulence during typhoid. *Proc. Natl. Acad. Sci. U.S.A.* 102(48):17460-17465.

18. Rudd KE, Humphery-Smith I, Wasinger VC, & Bairoch A (1998) Low molecular weight proteins: a challenge for post-genomic research. *Electrophoresis* 19(4):536-544.

19. Maris AE, et al. (2002) Dimerization allows DNA target site recognition by the NarL response regulator. *Nat Struct Biol* 9(10):771-778.

20. Baumler AJ (1997) The record of horizontal gene transfer in *Salmonella*. *Trends Microbiol*. 5(8):318-322.

21. Li J, et al. (1995) Relationship between evolutionary rate and cellular location among the Inv/Spa invasion proteins of *Salmonella enterica. Proc. Natl. Acad. Sci. U.S.A.* 92(16):7252-7256.

22. Bijlsma JJ & Groisman EA (2005) The PhoP/PhoQ system controls the intramacrophage type three secretion system of *Salmonella enterica. Mol. Microbiol*. 57(1):85-96.

23. Kaern M, Elston TC, Blake WJ, & Collins JJ (2005) Stochasticity in gene expression: from theories to phenotypes. *Nat Rev Genet* 6(6):451-464.

24. MacArthur S & Brookfield JF (2004) Expected rates and modes of evolution of enhancer sequences. *Mol. Biol. Evol*. 21(6):1064-1073.

25. Winfield MD & Groisman EA (2004) Phenotypic differences between *Salmonella* and *Escherichia coli* resulting from the disparate regulation of homologous genes. *Proc. Natl. Acad. Sci. U.S.A.* 101(49):17162-17167.

26. Lawley TD, et al. (2006) Genome-wide screen for *Salmonella* genes required for long-term systemic infection of the mouse. *PLoS Pathog* 2(2):e11.

27. Ochman H, Lawrence JG, & Groisman EA (2000) Lateral gene transfer and the nature of bacterial innovation. *Nature* 405(6784):299-304.

28. Lawrence JG (2005) Common themes in the genome strategies of pathogens. *Curr Opin Genet Dev* 15(6):584-588.

29. Ma W, Dong FF, Stavrinides J, & Guttman DS (2006) Type III effector diversification via both pathoadaptation and horizontal transfer in response to a coevolutionary arms race. *PLoS Genet* 2(12):e209.

30. Maurelli AT, Fernandez RE, Bloch CA, Rode CK, & Fasano A (1998) "Black holes" and bacterial pathogenicity: a large genomic deletion that enhances the virulence of *Shigella* spp. and enteroinvasive *Escherichia coli. Proc. Natl. Acad. Sci. USA* 95:3943-3948.

31. Jeong S, et al. (2008) The evolution of gene regulation underlies a morphological difference between two *Drosophila* sister species. *Cell* 132(5):783-793.

32. Hittinger CT & Carroll SB (2007) Gene duplication and the adaptive evolution of a classic genetic switch. *Nature* 449(7163):677-681.

33. Wray GA (2007) The evolutionary significance of *cis*-regulatory mutations. *Nat Rev Genet* 8(3):206-216.

34. Hoekstra HE & Coyne JA (2007) The locus of evolution: evo devo and the genetics of adaptation. *Evolution Int J Org Evolution* 61(5):995-1016.

35. Prud'homme B, Gompel N, & Carroll SB (2007) Emerging principles of regulatory evolution. *Proc. Natl. Acad. Sci. U.S.A.* 104 Suppl 1:8605-8612.

36. Haygood R, Fedrigo O, Hanson B, Yokoyama KD, & Wray GA (2007) Promoter regions of many neural- and nutrition-related genes have experienced positive selection during human evolution. *Nat. Genet.* 39(9):1140-1144.

37. Cretekos CJ, et al. (2008) Regulatory divergence modifies limb length between mammals. *Genes Dev*. 22(2):141-151.

38. Hoballah ME, et al. (2007) Single gene-mediated shift in pollinator attraction in *Petunia*. *Plant Cell* 19(3):779-790.

39. Gojobori J, Tang H, Akey JM, & Wu CI (2007) Adaptive evolution in humans revealed by the negative correlation between the polymorphism and fixation phases of evolution. *Proc. Natl. Acad. Sci. U.S.A.* 104(10):3907-3912.

40. Brown NF, Wickham ME, Coombes BK, & Finlay BB (2006) Crossing the line: selection and evolution of virulence traits. *PLoS Pathog* 2(5):e42.

41. Prud'homme B, et al. (2006) Repeated morphological evolution through *cis*-regulatory changes in a pleiotropic gene. *Nature* 440(7087):1050-1053.

42. Duong N, et al. (2007) Thermosensing coordinates a *cis*-regulatory module for transcriptional activation of the intracellular virulence system in *Salmonella enterica* serovar Typhimurium. *J. Biol. Chem*. 282(47):34077-34084.

43. Hansen-Wester I, Chakravortty D, & Hensel M (2004) Functional transfer of *Salmonella* pathogenicity island 2 *to Salmonella bongori* and *Escherichia coli*. *Infect. Immun*. 72(5):2879-2888.

44. Coombes BK, Brown NF, Valdez Y, Brumell JH, & Finlay BB (2004) Expression and secretion of *Salmonella* pathogenicity island-2 virulence genes in response to acidification exhibit differential requirements of a functional type III secretion apparatus and SsaL. *J. Biol. Chem*. 279(48):49804-49815.

45. Strimmer K & von Haeseler A (1996) Quartet Puzzling: A Quartet Maximum-Likelihood Method for Reconstructing Tree Topologies. *Mol. Biol. Evol*. 13:964-969.

46. Bruno WJ, Socci ND, & Halpern AL (2000) Weighted neighbor joining: a likelihood-based approach to distance-based phylogeny reconstruction. *Mol. Biol. Evol.* 17(1):189-197.

Figure 2.1. Mapping the *cis*-regulatory input for *srfN*. (A) Production of SrfN requires regulatory DNA between -600 to -1000 base pairs from the translation start site. Different lengths of DNA upstream of *srfN* were tested for their ability to promote *srfN* expression. Data are western blots of SrfN and DnaK from whole cell lysates following growth of cells in inducing medium. (B) Primer extension reveals an SsrB-specific transcription start site -654 nt from the *srfN* translation start site. Boxed adenine indicates the start of the transcript. From left to right, the lanes in each panel contain G, A, T or C sequencing ladders and reactions performed on RNA isolated from an *hns/rpoS* background (+) or an isogenic *ssrB* mutant (-). (C) SsrBc binds to *srfN* promoter DNA. The purified C-terminal DNA binding domain of SsrB (SsrBc) protects from DNaseI a 20-bp site between -85 to -65 from the transcription start site. Black bar and coordinates indicate location of SsrBc binding site relative to transcriptional start site. Arrows indicate DNaseI hypersensitive sites. (D) Alignment of the *srfN* cis-regulatory region from *S. enterica* serovars and *S. bongori*. Numbers to the left and right of the alignment correspond base pair distances from the *srfN* translational start site from the respective species. The region of SsrB binding is indicated with a solid red line and the probable -35 and -10 hexamers are shown.

Figure 2.1

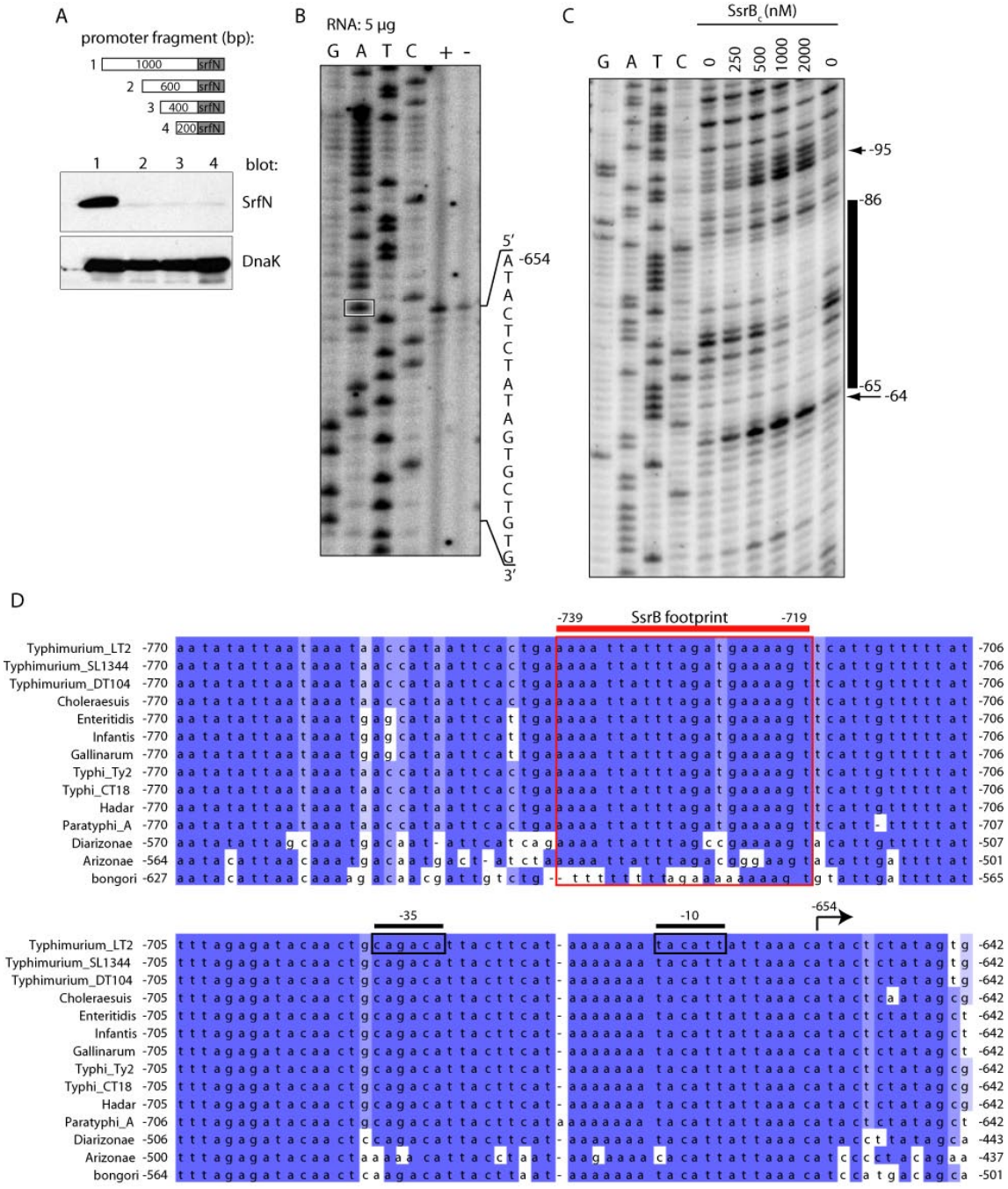
A
promoter fragment (bp):
1 1000 srfN
2 600 srfN
3 400 srfN
4 200 srfN
1 2 3 4 blot:
SrfN
DnaK
B
RNA: 5 µg
G A T C + -
5′ A T A C T C T A T A G T G C T G T G 3′
-654
C
SsrB$_c$ (nM)
G A T C 0 250 500 1000 2000 0
-95
-86
-65
-64
D
-739 SsrB footprint -719
Typhimurium_LT2 -770 aatatattaataaataaccataattcactgaaaattatttagatgaaaagttcattgttttat -706
Typhimurium_SL1344 -770 aatatattaataaataaccataattcactgaaaattatttagatgaaaagttcattgttttat -706
Typhimurium_DT104 -770 aatatattaataaataaccataattcactgaaaattatttagatgaaaagttcattgttttat -706
Choleraesuis -770 aatatattaataaataaccataattcactgaaaattatttagatgaaaagttcattgttttat -706
Enteritidis -770 aatatattaataaatgagcataattcattgaaaattatttagatgaaaagttcattgttttat -706
Infantis -770 aatatattaataaatgagcataattcattgaaaattatttagatgaaaagttcattgttttat -706
Gallinarum -770 aatatattaataaatgagcataattcattgaaaattatttagatgaaaagttcattgttttat -706
Typhi_Ty2 -770 aatatattaataaataaccataattcactgaaaattatttagatgaaaagttcattgttttat -706
Typhi_CT18 -770 aatatattaataaataaccataattcactgaaaattatttagatgaaaagttcattgttttat -706
Hadar -770 aatatattaataaataaccataattcactgaaaattatttagatgaaaagttcattgttttat -706
Paratyphi_A -770 aatatattaataaataaccataattcactgaaaattatttagatgaaaagttcatt-ttttat -707
Diarizonae -570 aatattagcaaatgacaat-attcatcagaaaattatttagccgaaaagtacattgttttat -507
Arizonae -564 aatacttaacaaatgacaatgact-atctaaaaattatttagacgggaagtacattgatttat -501
bongori -627 aatacattaacaaaagacaacgattgtctg-ttttttttagaaaaaaaagtgtattgatttat -565
-35
-10
-654
Typhimurium_LT2 -705 tttagagatacaactgcagacattacttcat-aaaaaaatacattattaaacatactctatagtg -642
Typhimurium_SL1344 -705 tttagagatacaactgcagacattacttcat-aaaaaaatacattattaaacatactctatagtg -642
Typhimurium_DT104 -705 tttagagatacaactgcagacattacttcat-aaaaaaatacattattaaacatactctatagtg -642
Choleraesuis -705 tttagagatacaactgcagacattacttcat-aaaaaaatacattattaaacatactcaatagcg -642
Enteritidis -705 tttagagatacaactgcagacattacttcat-aaaaaaatacattattaaacatactctatagct -642
Infantis -705 tttagagatacaactgcagacattacttcat-aaaaaaatacattattaaacatactctatagct -642
Gallinarum -705 tttagagatacaactgcagacattacttcat-aaaaaaatacattattaaacatactctatagct -642
Typhi_Ty2 -705 tttagagatacaactgcagacattacttcat-aaaaaaatacattattaaacatactctatagcg -642
Typhi_CT18 -705 tttagagatacaactgcagacattacttcat-aaaaaaatacattattaaacatactctatagcg -642
Hadar -705 tttagagatacaactgcagacattacttcat-aaaaaaatacattattaaacatactctatagcg -642
Paratyphi_A -706 tttagagatacaactgcagacattacttcataaaaaaatacattattaaacatactctatagct -642
Diarizonae -506 tttagagatacaactccagacattacttcat-aaaaaaatacattattaaacatacttatagca -443
Arizonae -500 tttagagatacaactaaaaacattacctaat-aagaaaaacacattattaaacatcccctacagaa -437
bongori -564 tttagagatacaactcaagacattacttaat-aaaaaaatacattattaaacatccatgacagca -501

Figure 2.2. SsrB binds to the *srfN cis*-regulatory element *in vivo*. (A) Location of ChIP-PCR primers and experimentally mapped SsrB binding site (red) with respect to *srfN* open reading frame. Bacterial cells were grown in SsrB-inducing LPM medium and sonicated DNA fragments bound to SsrB-FLAG *in vivo* were isolated by chromatin immunoprecipitation (i.p.), along with similarly processed DNA fragments from wild type cells containing untagged-SsrB. The ability of SsrB-FLAG to selectively bind to the *srfN cis*-regulatory element was determined by PCR, along with samples of pre-IP DNA (cont.). (B) ChIP-on-chip analysis of the genomic region surrounding *srfN*. SsrB binding to thirty-two syntenic probes located near *srfN* plotted against probe location. Each data point is a unique probe with averaged data from three biological replicates. Direction of transcription is shown. The location of the SsrB footprint (red circle) and the transcription start site (green circle) with respect to probe location is shown. IGR, intergenic region. (C) SsrB binding profile for a chromosomal region not regulated by SsrB. The genomic region (5887 bp) is represented by 54 unique probes. Each data point represents averaged data from three biological replicates.

Figure 2.2

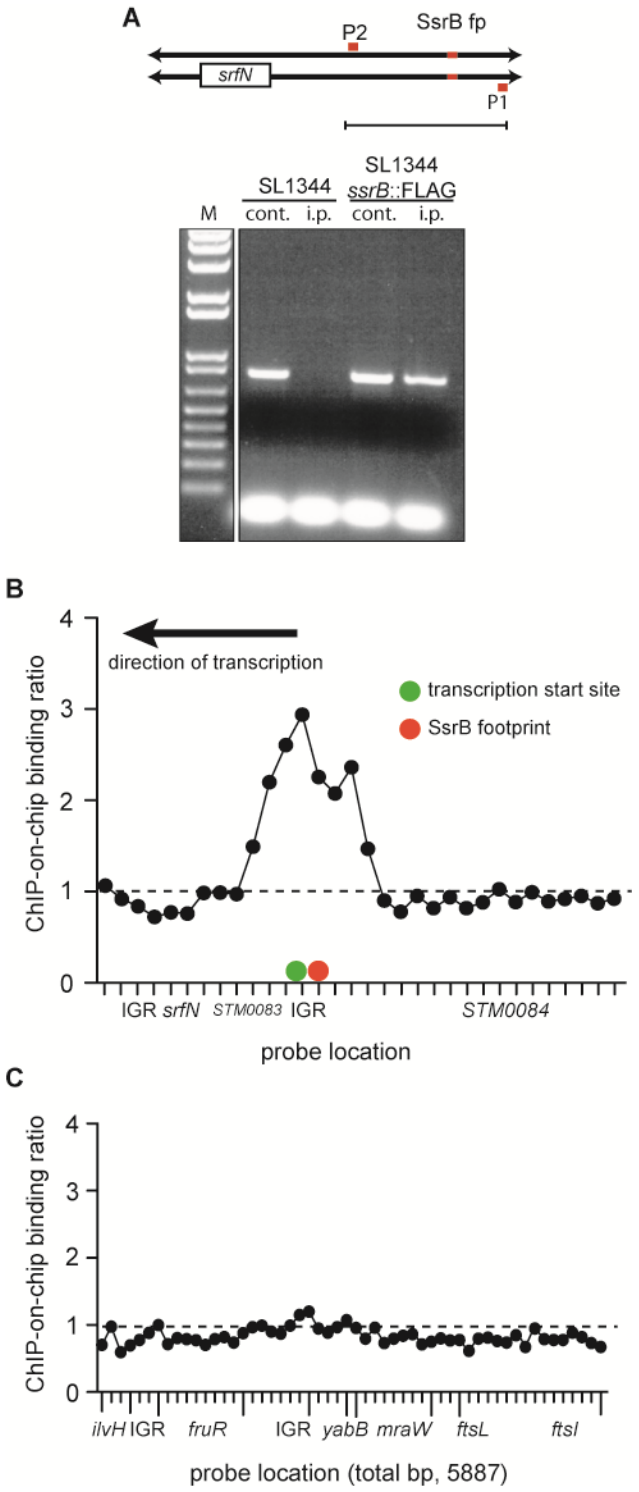
A
P2
SsrB fp
srfN
P1
SL1344
SL1344 ssrB::FLAG
M
cont.
i.p.
cont.
i.p.
B
direction of transcription
transcription start site
SsrB footprint
ChIP-on-chip binding ratio
0
1
2
3
4
IGR srfN
STM0083
IGR
STM0084
probe location
C
ChIP-on-chip binding ratio
0
1
2
3
4
ilvH IGR
fruR
IGR
yabB
mraW
ftsL
ftsI
probe location (total bp, 5887)

Figure 2.3. SrfN increases in-host fitness. (A) Δ*srfN* and wild type cells were competed in mixed infections of mice for 3 days. Competitive indices (CI) for the mutant were determined in the spleen and liver following oral infection. Each data point represents one animal and horizontal bars indicate geometric means. Data are from two experiments performed independently. *P*=0.038 (spleen), 0.006 (liver). (B) Relative *in vitro* fitness of Δ*srfN* was assessed by growth competitions with wild type cells in LPM. Relative fitness of the mutant was determined and plotted over time, where each data point represents an independent competitive culture.

Figure 2.3

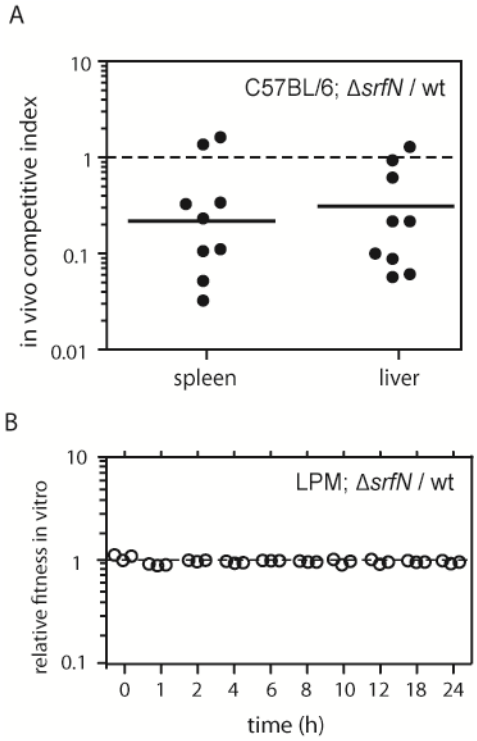
A
C57BL/6; ΔsrfN / wt
in vivo competitive index
10
1
0.1
0.01
spleen
liver
B
LPM; ΔsrfN / wt
relative fitness in vitro
10
1
0.1
0 1 2 4 6 8 10 12 18 24
time (h)

Figure 2.4. The *cis*-regulatory input for *srfN* requires SsrB. Promoter swap constructs were made that express *srfN* from the *cis*-regulatory input evolved in *S.* typhimurium (P_{STM}) or *S. bongori* (P_{Sb}). Constructs were transformed into *S.* typhimurium and *S. bongori* along with a bacterial artificial chromosome (BAC) containing the SPI-2 pathogenicity island (pSPI2) or an empty BAC (pEV). The ability of *S.* typhimurium and *S. bongori* to express *srfN* from (A) the *S. enterica* promoter (P_{STM}) or (B and C) the regulatory input evolved in *S. bongori*, is shown by western blot. P_{Sb} is recognized as a promoter in *S.* typhimurium leading to *srfN* expression, but in an SsrB-independent manner similar to that seen in *S. bongori*. Lysates were probed using antibodies against HA to detect expression of the SrfN fusion protein, and antibodies to SseB (SsrB-dependent) and DnaK (SsrB-independent) as controls. (D and E) The regulatory input driving *srfN* expression in *S. bongori* requires the PhoP response regulator. Transcription factor mutants in *S.* typhimurium and *S. bongori* were tested for their ability to recognize the *srfN* promoter from *S. bongori*, shown in immunoblots for SrfN-HA, following growth in rich (LB) or minimal medium (LPM).

Figure 2.4

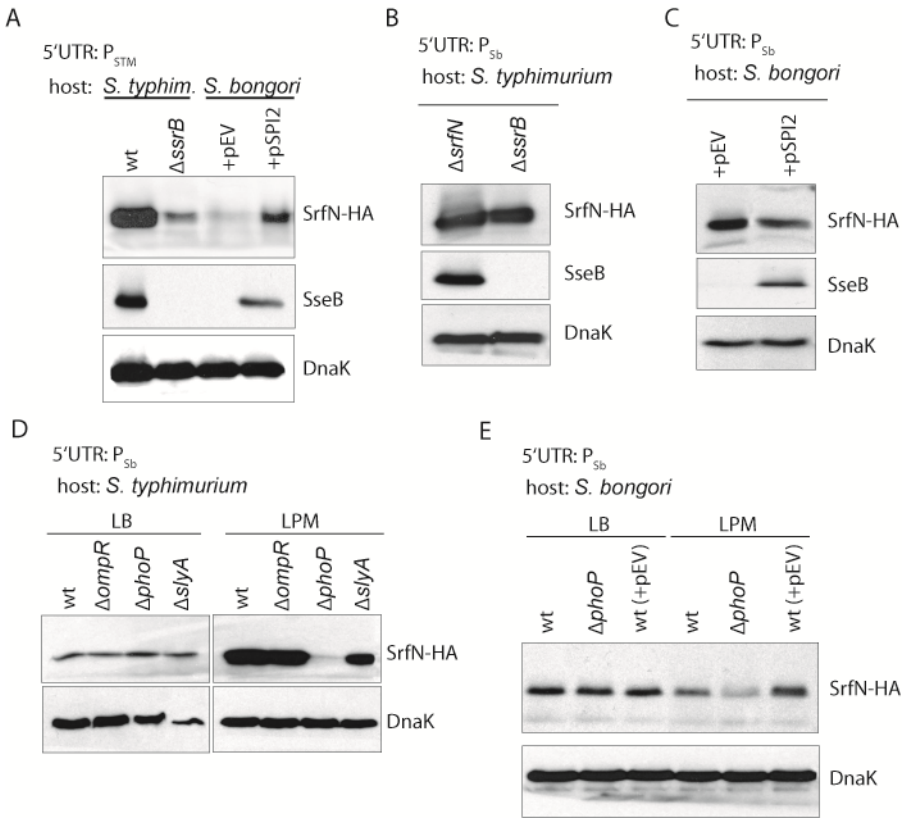
A
5'UTR: P STM
host: S. typhim. S. bongori
wt
ΔssrB
+pEV
+pSPI2
SrfN-HA
SseB
DnaK
B
5'UTR: P Sb
host: S. typhimurium
ΔsrfN
ΔssrB
SrfN-HA
SseB
DnaK
C
5'UTR: P Sb
host: S. bongori
+pEV
+pSPI2
SrfN-HA
SseB
DnaK
D
5'UTR: P Sb
host: S. typhimurium
LB
LPM
wt
ΔompR
ΔphoP
ΔslyA
SrfN-HA
DnaK
E
5'UTR: P Sb
host: S. bongori
LB
LPM
wt
ΔphoP
wt (+pEV)
SrfN-HA
DnaK

Figure 2.5. The in-host fitness benefit associated with SrfN is regulatory. Effects on in-host fitness was tested following, (A) trans complementation of Δ*srfN* with *srfN* driven by either the *S.* typhimurium 5'UTR or *S. bongori* 5'UTR, or (B) in competitive infection experiments *in vivo* against a strain where the chromosomal SsrB CRE was replaced with the analogous region from *S. bongori* (SsrB CRE replacement). Competitive indices were determined 3 days post infection in the spleen and liver. Data points represent individual animals from at least three experiments and horizontal lines are geometric means. (C) Simplified regulatory diagram showing that phosphorylated SsrB acts as a transcription factor on genes within SPI-2, along with input from additional positive (OmpR, SlyA, PhoP) and negative regulators (H-NS, Hha, YdgT). Activated SsrB also influences phenotypic variation by acting on unlinked regulatory DNA driving expression of T3SS effector genes, unlinked integrated virulence genes (such as *srfN*) and possibly other regulatory nodes.

Figure 2.5

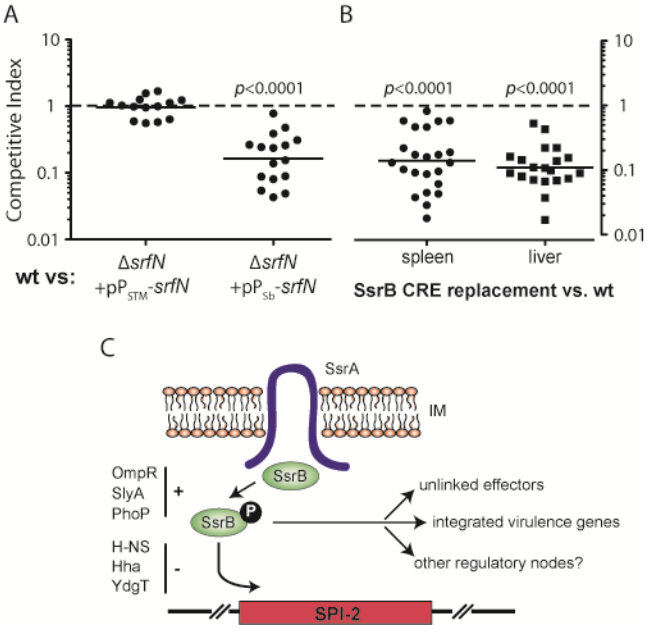
A
B
Competitive Index
10
1
0.1
0.01
p<0.0001
p<0.0001
p<0.0001
wt vs:
ΔsrfN +pP_STM-srfN
ΔsrfN +pP_Sb-srfN
spleen
liver
SsrB CRE replacement vs. wt
C
SsrA
IM
SsrB
SsrB
P
OmpR
SlyA
PhoP
+
H-NS
Hha
YdgT
-
unlinked effectors
integrated virulence genes
other regulatory nodes?
SPI-2

Supplementary Figure Legends

Figure 2.S1. SrfN is part of a protein family of unknown function. (A) Amino acid alignment of SrfN with members of pfam07338. Sequences were aligned using MAFFT v. 6 and assembled with JALVIEW v. 2.3. Organisms and gene designations are given to the left of the alignment; K-12, *Escherichia coli* strain K12; O157:H7, enterohemorrhagic *E. coli* serotype O157:H7; St, *Salmonella enterica* serovar Typhimurium. (B) Prediction of signal peptide for SrfN at position 22 of the amino acid sequence using SIGNALP v. 3.0 trained on Gram-negative input sequences. Top, neural networks model; bottom, hidden Markov model.

Figure 2.S1

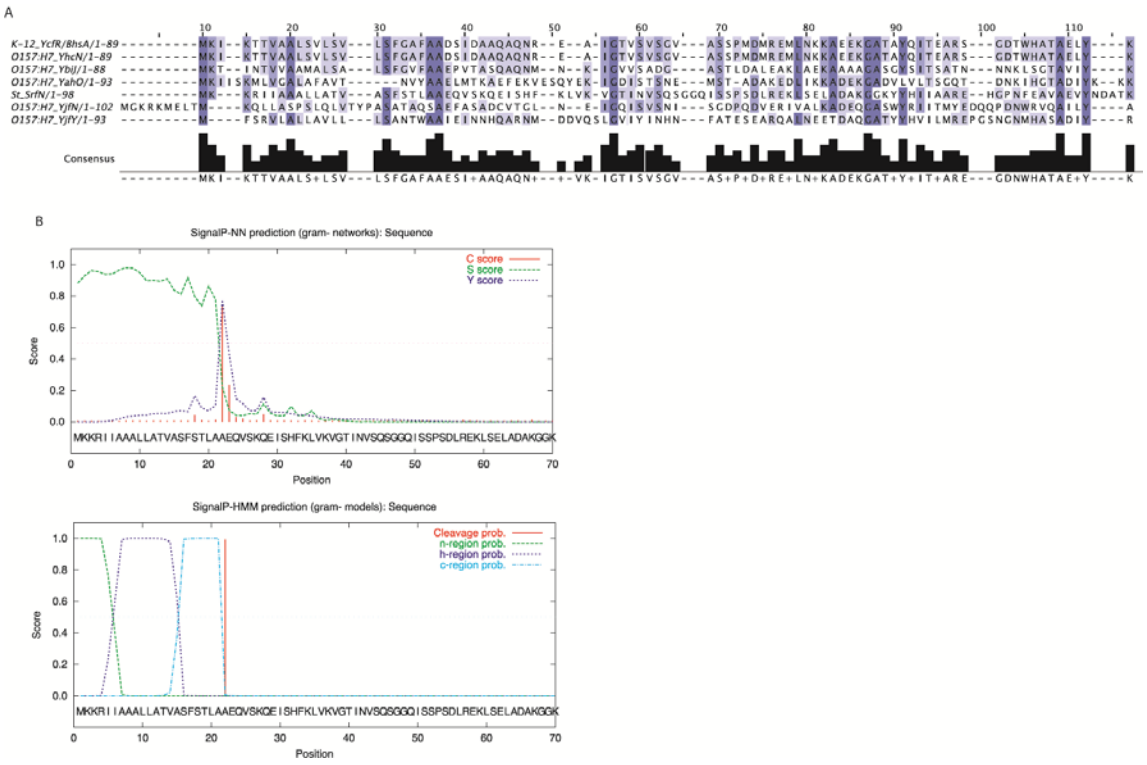
A
K-12_YcfR/BhsA/1-89
O157:H7_YhcN/1-89
O157:H7_YbjJ/1-88
O157:H7_YahO/1-93
St_SrfN/1-98
O157:H7_YjfN/1-102
O157:H7_YjfY/1-93
Consensus
B
SignalP-NN prediction (gram- networks): Sequence
C score
S score
Y score
Score
Position
MKKRIIAALLATVASFSTLAAEQVSKQEISHFKLVKVGTINVSQSGGQISSPSDLREKLSELADAKGGK
SignalP-HMM prediction (gram- models): Sequence
Cleavage prob.
n-region prob.
h-region prob.
c-region prob.

Figure 2.S2. SrfN localizes to the inner membrane during infection and is not a type III effector. (A) Western blot analysis of bacterial cell lysates (pellet) and secreted proteins from wild type, Δ*ssaR* and Δ*ssaL* mutants grown in LPM medium. Protein fractions were probed for DnaK, SrfN-HA and SseB. The positions of molecular mass standards are indicated to the left of the panel. (B) SrfN is not translocated into host cells during infection. HeLa cells were infected with either wild type *S*. Typhimurium or a strain defective in SPI-2-mediated type III secretion (Δ*ssaR*), each expressing SrfN-HA. Following infection, host cells were fractionated into pellet, membrane and cytosol fractions and probed using antibodies against HA, DnaK (bacterial cytosolic protein), tubulin (host cell cytosolic protein) and calnexin (a host cell membrane protein). (C) SrfN is targeted to the bacterial inner membrane following SsrB-dependent expression. Wild type cells expressing SrfN-HA were fractionated into periplasm (P), cytoplasm (C), inner membrane (IM) and outer membrane (OM) fractions. Protein fractions from each sample were probed using antibodies to HA, FliH (a component of the flagellar secretion apparatus that localizes to the inner membrane), MBP (a bacterial protein contained in the periplasm), DnaK (a soluble cytosolic protein) and LPS (contained in the outer membrane).

Figure 2.S2

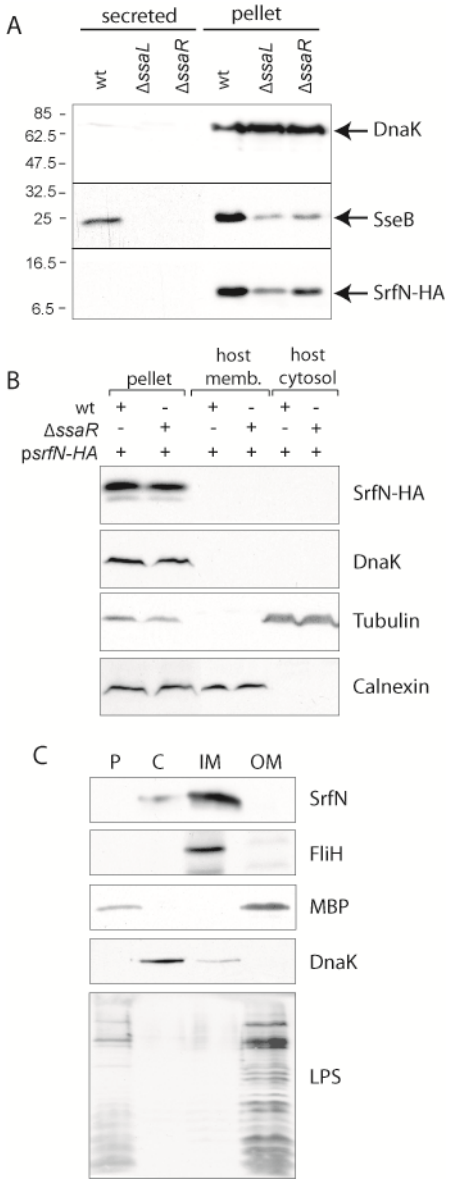
A
secreted
pellet
wt
ΔssaL
ΔssaR
wt
ΔssaL
ΔssaR
85
62.5
47.5
32.5
25
16.5
6.5
DnaK
SseB
SrfN-HA
B
pellet
host memb.
host cytosol
wt
ΔssaR
psrfN-HA
SrfN-HA
DnaK
Tubulin
Calnexin
C
P
C
IM
OM
SrfN
FliH
MBP
DnaK
LPS

Figure 2.S3. Phylogenetic trees for *srfN* and 5'UTR. Relative genetic divergence of (A) the *srfN* 5' UTR, (B) *srfN* CRE (including SsrB binding domain to the transcriptional start site identified experimentally) and (C) the *srfN* open reading frame across the six subspecies classes of *S. enterica* and *S. bongori*. Divergence is represented as distance phylogenies. Bootstrap values above 60 on major nodes indicate support for the topologies. Scale bars equal mutations per nucleotide.

Figure 2.S3

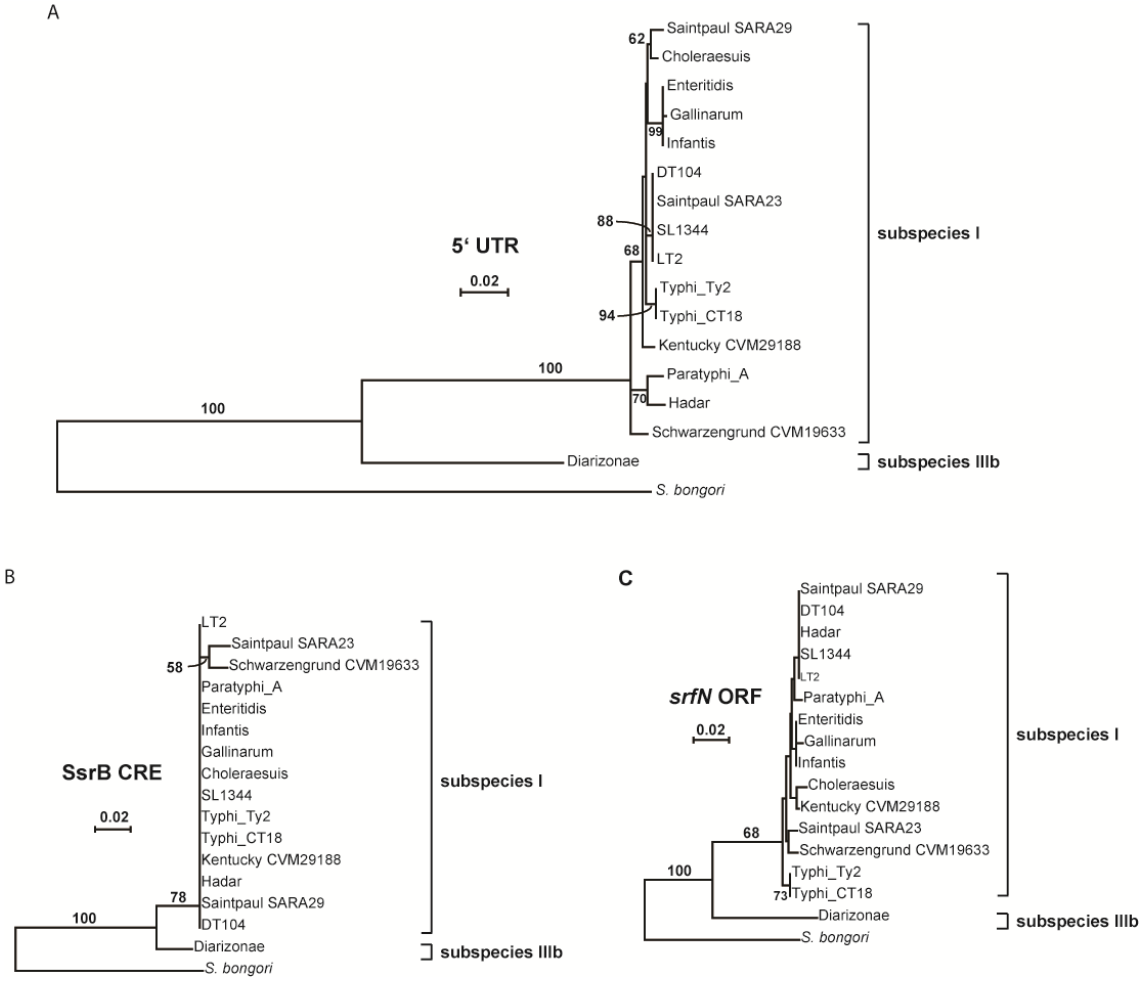
A
5' UTR
0.02
Saintpaul SARA29
Choleraesuis
Enteritidis
Gallinarum
Infantis
DT104
Saintpaul SARA23
SL1344
LT2
Typhi_Ty2
Typhi_CT18
Kentucky CVM29188
Paratyphi_A
Hadar
Schwarzengrund CVM19633
Diarizonae
S. bongori
62
99
88
68
94
100
70
100
subspecies I
subspecies IIIb
B
SsrB CRE
0.02
LT2
Saintpaul SARA23
Schwarzengrund CVM19633
Paratyphi_A
Enteritidis
Infantis
Gallinarum
Choleraesuis
SL1344
Typhi_Ty2
Typhi_CT18
Kentucky CVM29188
Hadar
Saintpaul SARA29
DT104
Diarizonae
S. bongori
58
78
100
subspecies I
subspecies IIIb
C
srfN ORF
0.02
Saintpaul SARA29
DT104
Hadar
SL1344
LT2
Paratyphi_A
Enteritidis
Gallinarum
Infantis
Choleraesuis
Kentucky CVM29188
Saintpaul SARA23
Schwarzengrund CVM19633
Typhi_Ty2
Typhi_CT18
Diarizonae
S. bongori
68
100
73
subspecies I
subspecies IIIb

Figure 2.S4. 5'RACE analysis of the *srfN* orthologue from *S. bongori*. The transcriptional start site of the *srfN* orthologue from *S. bongori* was mapped using 5' RACE. The location of the transcriptional start site is -115 nucleotides upstream of the translational start site. Transcription start site is indicated with a black dot and labelled. The presumed -10 and -35 hexamer sites are underlined with a black line and labelled as such.

Figure 2.S4

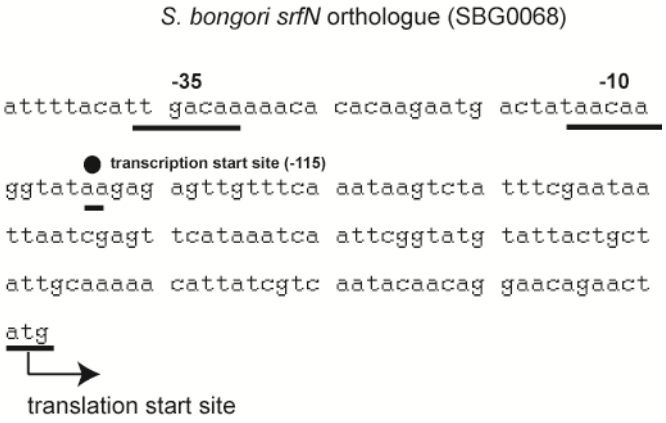
S. bongori srfN orthologue (SBG0068)
-35
-10
attttacatt gacaaaaaca cacaagaatg actataacaa
transcription start site (-115)
ggtataagag agttgtttca aataagtcta tttcgaataa
ttaatcgagt tcataaatca attcggtatg tattactgct
attgcaaaaa cattatcgtc aatacaacag gaacagaact
atg
translation start site

Figure 2.S5. Δ*srfN* has no fitness defect *in vitro*. Bacterial cells were grown in (A) minimal medium (LPM), or (B) rich medium (LB). OD_{600} of the bacterial cultures were measured every 15 minutes for 24 hours. Shown is the data for one representative experiment performed twice.

Figure 2.S5

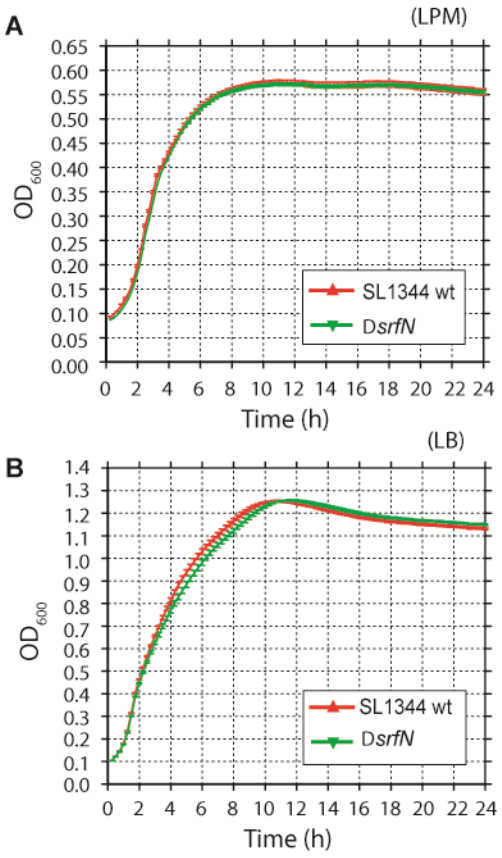
A
(LPM)
OD600
Time (h)
SL1344 wt
DsrfN
B
(LB)
OD600
Time (h)
SL1344 wt
DsrfN

Supplementary Materials and Methods

Cloning and mutant construction. Homologous recombination from a suicide plasmid was used to create unmarked, in-frame gene deletions. A DNA fragment encoding the entire *srfN* open reading frame plus ~ 0.9 kb of flanking genomic DNA was amplified by PCR, cloned into pBLUESCRIPT KS+ and then used as a template for inverse PCR, the product of which was self-ligated to delete codons 8-92. The deletion allele was sub-cloned into the suicide plasmid pRE112 (1) and transformed into *E. coli* SM10 λ*pir* to generate a donor strain for conjugation. SL1344 merodiploids were selected on streptomycin and chloramphenicol, grown in LB broth without antibiotic selection and counter selected on 5% (w/v) sucrose at 25°C. Mutants resistant to sucrose were confirmed by sequencing. For construction of an HA-tagged allele of *srfN*, chromosomal DNA from *S.* typhimurium was used as template for PCR with primers ACG CGT CGA CCG CCG GAT AAC ATA CCG and GGA AGA TCT TTT CGT CGC ATC GTT ATA AAC TTC. The resulting PCR product was cloned into pWSK129-2HA (2) as a SalI/BglII fragment and then subcloned into the 6-copy plasmid pWSK29 (3) as a SalI/XbalI fragment for expression studies. Construction of the HA-tagged orthologue from *S. bongori* was accomplished using a similar strategy to the method for *S.* typhimurium using *S. bongori* chromosomal DNA template and primers ACG CGT CGA CAG ATC CGT CTC TTC TGT AGA CAG TT and GGA AGA TCT TTT CGC TGC ATC TTT ATA AAC TTC.

For *in vivo* competition experiments, the 5' regulatory region from *S. bongori* was fused precisely to the *S*. typhimurium *srfN* open reading frame by the gene splicing by overlap extension (SOE) technique (4). Two separate PCR reactions were carried out using primer set A_B (A: ACGCGTCGAC AGA TCC GTC TCT TCT GTA GAC AGT) (B: ggc aat aat gcg ttt ttt cat AGT TCT GTT CCT GTT GTA TTG), which amplified 795 bases upstream of the translational start site from *S. bongori*, and primer set C_D (C: caa tac aac agg aac aga act ATG AAA AAA CGC ATT ATT GCC) (D: GGAAGATCT TTA TTT CGT CGC ATC GTT ATA AAC TTC), which amplified the *srfN* ORF from *S.* typhimurium. Underlined bases are the introduced restriction enzyme sites and bases in lowercase are sites of precise strand overlap in the second round PCR. PCR products were purified and 50 ng of each were used in a second PCR with primers A_D to generate the fused product, which was sequenced and cloned as a SalI-BglII fragment into pWSK129. For complementation experiments with *S*. typhimurium 5'UTR and wild type *srfN*, primer E (ACGCGTCGAC CGC CGG ATA ACA TAC CGC CTG) was used with primer D for DNA amplification.

For replacement of the 5' CRE in *S*. typhimurium, a single-step strategy was designed to delete the wild type 5' CRE and replace it with the corresponding region from *S. bongori* determined from sequence alignments. A mutagenesis template that included the *srfN* ORF and 0.9 kb of flanking DNA on either side was generated by PCR using *S.* typhimurium chromosomal DNA and primers GCT CTA GAT ATC AAT GCC TTC CGG GTA AGA and CCG AGC TCC TGT CCG CTT ACA TGA GGT TAC A. This DNA was cloned into pBLUESCRIPT KS+ and used as a template for inverse PCR using

the primers TTT TTT TTC ATC ATT GTT TTT ATT TTA GAG ATA C and GAT TTT TTT TGT CAG TGA ATT ATG GTT ATT TAT T. Inverse PCR product was purified, phosphorylated *in vitro* with T4 polynucleotide kinase, and self-ligated to generate the 5' CRE replacement. This construct was cloned into the pRE122 suicide plasmid and conjugated into *S.* typhimurium from *E. coli* SM10 *λpir*. CRE replacement mutants were selected on sucrose and sequenced to verify the 5'CRE replacement.

5' RACE. Rapid amplification of cDNA ends (RACE) was used to map the transcriptional start site of the *srfN* orthologue in *S. bongori*. RNA from *S. bongori* grown to an OD of ~0.6 was purified using the High Pure RNA isolation kit (Roche Applied Sciences). cDNA synthesis was performed using the 5'RACE System for Rapid Amplification of cDNA ends (Invitrogen) using the gene-specific primer GCG CAG CAA TAA TAT GG. *srfN* cDNA was verified by PCR using primers GGT GCC GAC CTT AAC CAG TTT GAA GTG G and AAA ACT CAT CAT CGC CAC TGC GTT ACT G, followed by homopolymeric tailing and PCR with an abridged universal anchor primer (GGCCACGCGTGCACTAGCAC) and primer GGT GCC GAC CTT AAC CAG TTT GAA GTG G. PCR products containing 5' cDNA ends were sequenced to identify the transcription start site.

Type III secretion assays. Overnight cultures of *Salmonella* were washed in LPM and sub-cultured into LPM at 37°C with shaking to an optical density of ~0.6 at 600 nm as described (5). Culture supernatants were filtered (0.22 mm HT Tuffryn membrane, Pall

Life Sciences) and mixed to a final concentration of 10% trichloroacetic acid (TCA). Precipitated proteins were washed in cold acetone and solubilized in SDS-PAGE sample buffer (100 mM Tris-HCl (pH 6.8), 20% (v/v) glycerol, 4% (w/v) SDS, 0.002% (w/v) bromophenol blue and 200 mM DTT). Whole bacterial cells were solubilized in SDS sample buffer and proteins were analysed by SDS-PAGE and immunoblotting. Antibodies used were: mouse anti-HA (1:1000), mouse anti-DnaK (1:5000), rabbit anti-SseB. Secondary antibodies were conjugated to horseradish peroxidase (HRP) and detected using chemiluminescence.

Biochemical fractionation of host cells and translocation assay. HeLa cells were infected for 8 h with *Salmonella* strains expressing HA epitope-tagged SrfN. Infected cells were scraped into cold PBS, centrifuged, and mechanically lysed through a 22-guage needle in a buffer containing 250 mM sucrose, 3 mM imidazole (pH 7.4), and 0.5 mM EDTA. Lysates were centrifuged at 3000 g to collect unbroken host cells, nuclei, cytoskeleton and bacteria and at 41000 g to collect the host cell membrane fraction (pellet) and the host cell cytosol fraction (supernatant). Each fraction was analyzed by SDS-PAGE and immunoblotting using the following antibodies: mouse anti-HA (1:1000), mouse anti-DnaK (1:5000), mouse anti-b tubulin (1:5000, clone E7, Developmental Studies Hybridoma Bank, University of Iowa), rabbit anti-calnexin (1:5000, Stressgen).

Bacterial fractionation. Mechanical fractionation of bacterial cells into cytoplasm, periplasm, inner membrane and outer membrane fractions was carried out as previously described (6) with the following modifications. Bacteria were grown overnight in LB with shaking and then sub-cultured at 1:500 into LPM pH 5.8 and grown for 16 hours at 37°C with shaking. Protease inhibitors (Complete-EDTA Free, Roche Applied Science) were used in all solutions. Protein fractions were analyzed by Western blot using rabbit anti-MBP (1:1000, New England Biolabs), rabbit anti-FliH (1:1000; a kind gift from Dr. Colin Hughes), rabbit anti-LPS (1:1000, Difco) and mouse anti-HA (1:1000).

Competitive infection of animals. Animal protocols were in accordance with the Canadian Council on the Use of Laboratory Animals and approved by the Animal Ethics Committee, McMaster University. For single infections, female C57BL/6 mice (Charles River) were infected orally with ~10^6 cfu of *S*. Typhimurium in 0.1 M HEPES (pH 8.0), 0.9% NaCl. For competitive infection experiments, two mouse strains were used that are susceptible (C57BL/6) or resistant (129S1/SvImJ) to *Salmonella* infection. C57BL/6 mice have a non-functional Nramp1s (Slc11a1) allele and have defects in controlling intracellular *Salmonella* replication, whereas 129S1/SvImJ mice are homozygous for the Nrampr allele and are able to limit intracellular replication of *Salmonella*. Mice were infected orally (~1x10^6 cfu for C57BL/6 or ~1x10^8 for 129S1/SvImJ) with a mixed inoculum containing wild-type *Salmonella* resistant to chloramphenicol and an unmarked mutant strain under investigation. At 72 h after infection the cecum, spleen and liver were homogenized (Mixer Mill, Retsch, Germany) in PBS, diluted and plated on solid LB

medium containing streptomycin for determination of total *Salmonella* cfu. Colonies were replica printed onto chloramphenicol-containing plates for enumeration of SL1344 *ushA*::cat. The competitive index (CI) was calculated on log-transformed cfu as: (mutant/wild type) $_{output}$ / (mutant /wild type) *input*. Log-transformed competitive infection data were analyzed using a one-sample t test.

Genetic analyses. Genome sequences for *S. enterica* serovar Typhimurium and serovar Typhi were obtained from GenBank. The genome sequence of *S. bongori* 12419 was obtained from the Wellcome Trust Sanger Institute (http://www.sanger.ac.uk) Pathogen Sequencing Unit as an assembled flat file. Sequence data for the following organisms were produced by the *Salmonella* Sequencing Group at the Sanger Institute and can be obtained from ftp://ftp.sanger.ac.uk/pub/pathogens/Salmonella (*S. bongori* 12419, ATCC 43975; *S. enterica* Enteritidis PT4, NCTC 13349; *S. enterica* Gallinarum 287/91, NCTC 13346; *S. enterica* Hadar; *S. enterica* Infantis; *S. enterica* Typhimurium DT104, NCTC 13348; *S*. enterica Typhimurium SL1344, NCTC 13347; *S. enterica* Typhi Ty2; *S. enterica* Typhi CT18; S. enterica Paratyphi A strain AKU_12601). Sequence data for *S. enterica* Diarizonae, 61:1,v:1,5,(7) strain CDC 01-0005, ATCC BAA-639 was produced by the Genome Sequencing Center at Washington University School of Medicine in St. Louis. The genome sequence for *S. enterica* Choleraesuis strain SC-B67 (7), *S. enterica* Typhi CT18 (8), and *S. enterica* Typhimurium LT2 (9) have been published. Gene synteny plots and genome comparisons were performed using BLAST (http://www.ncbi.nlm.nih.gov/BLAST/), ARTEMIS

(http://www.sanger.ac.uk/Software/Artemis/), and MAUVE (version 2.0, build 12) (10). Sequence alignments were constructed using MAFFT v.6 (http://align.bmr.kyushu-u.ac.jp/mafft/online/server/) and assembled using JALVIEW v.2.3. Primary amino acid sequence for SrfN was used as a query string in SIGNALP v.3.0 to examine signal peptide probability by neural network and hidden Markov models trained on Gram-negative bacteria (http://www.cbs.dtu.dk/services/SignalP).

Chromatin immunoprecipitation. For chromatin immunoprecipitation experiments, the wild type *ssrB* gene was replaced on the chromosome with an *ssrB*::FLAG allele as published previously (11). Bacterial cultures were grown in either LB or LPM (pH 5.8) to OD_{600} ~0.6. Formaldehyde was added (final concentration of 1%) and incubated at room temperature for 5 min on an orbital shaker set at 35 rpm. Cross-linking was quenched by the addition of glycine to 125 mM followed by incubation for 5 min, swirling briefly every minute. Cells were harvested by centrifugation, washed twice with cold phosphate-buffered saline (pH 7.4), and resuspended in a 1:1 mix of ChIP lysis buffer consisting of 10 mM Tris (pH 8.0), 50 mM NaCl, 10 mM EDTA (pH 8.0), 20% sucrose, 10 mg/mL lysozyme and 2X RIPA solution containing 100 mM Tris (pH 8.0), 300 mM NaCl, 20% Tergitol (type NP-40), 10% sodium deoxycholate, 10% SDS, 1X EDTA-free protease inhibitor cocktail (Roche), in a volume 1/10 the original culture volume. The cell suspension was incubated at 37^{o}C for 30 min to lyse bacteria. 0.5 ml of cell lysate was sonicated (5 x 15 second pulses) using a Fisher 500 Dismembrator (Fisher Scientific) set at 20% intensity. DNA was verified for proper shearing within 200-1000 bp by running

the input DNA on an agarose gel after RNase treatment. Cell debris was removed by centrifugation, and the supernatant was retained for use as the input sample in immunoprecipitation experiments. For immunoprecipitation of SsrB-FLAG cross-linked DNA, 800 μL of input DNA was incubated with 50 μL pre-washed α-FLAG-M2 agarose resin (Sigma) at 4^{o}C overnight on a rolling shaker. After overnight incubation, IP resin was washed twice with cold 1X RIPA solution, twice with LiCl wash buffer (10 mM Tris [pH 8.0], 250 mM LiCl, 1 mM EDTA [pH 8.0], 0.5% Tergitol [type NP-40], 0.5% sodium deoxycholate), and once with TE buffer (10 mM Tris [pH 8.0], 1 mM EDTA [pH 8.0]). Fifty microliters of input DNA was reserved as input control. Resin-bound IP DNA and input DNA were treated with RNase A (20 μg/mL) for 30 min at 37^{o}C to remove RNA. IP resin was washed once more with TE buffer and resuspended in 200 μL ChIP elution buffer (50 mM Tris [pH 8.0], 10 mM EDTA [pH 8.0], 1% SDS). 150 μL of ChIP elution buffer was also added to input DNA for a final volume of 200 μL. Samples were incubated for 10 min at 65^{o}C, followed by the addition of Proteinase K (final concentration 0.8 mg/mL) and samples were incubated for 2 h at 42^{o}C, following with overnight incubation at 65^{o}C. The eluted IP DNA and input DNA were purified using phenol/chloroform extraction, precipitated with ethanol, and resuspended in nuclease-free water (Invitrogen). Following purification, PCR and microarray analysis (ChIP-chip) was used to analyze immunoprecipitated DNA. For PCR, input DNA was diluted to 1/10 concentration of IP DNA, and 0.5 μL of DNA samples were used as template for PCR in 25 μL reactions using Platinum Taq polymerase (Invitrogen) as directed by the manufacturer. PCR was allowed to proceed for 30 cycles and products were analyzed by

electrophoresis on a 1% agarose gel. For ChIP-chip analysis, DNA was sonicated from three biological replicates of SL1344 grown under SsrB-activating conditions (LPM) or non-inducing conditions (LB) and immunoprecipitated with anti-FLAG antibody as described above. DNA was labelled and hybridized to a *Salmonella enterica* serovar Typhimurium strain SL1344 tiled micrarray (Oxford Gene Technologies, Cat. No. 040021) in a two-colour format using genomic DNA as control. All raw data and probe mapping and was processed using source code written in-house.

References

1. Edwards RA, Keller LH, & Schifferli DM (1998) Improved allelic exchange vectors and their use to analyze 987P fimbria gene expression. *Gene* 207(2):149-157.
2. Coombes BK, et al. (2007) SseL is a *Salmonella*-specific translocated effector integrated into the SsrB-controlled *Salmonella* pathogenicity island 2 type III secretion system. *Infect. Immun.* 75(2):574-580.
3. Wang RF & Kushner SR (1991) Construction of versatile low-copy-number vectors for cloning, sequencing and gene expression in *Escherichia coli. Gene* 100:195-199.
4. Heckman KL & Pease LR (2007) Gene splicing and mutagenesis by PCR-driven overlap extension. *Nat Protoc* 2(4):924-932.
5. Coombes BK, Brown NF, Valdez Y, Brumell JH, & Finlay BB (2004) Expression and secretion of *Salmonella* pathogenicity island-2 virulence genes in response to acidification exhibit differential requirements of a functional type III secretion apparatus and SsaL. *J. Biol. Chem.* 279(48):49804-49815.
6. Gauthier A, Puente JL, & Finlay BB (2003) Secretin of the enteropathogenic *Escherichia coli* type III secretion system requires components of the type III apparatus for assembly and localization. *Infect. Immun.* 71(6):3310-3319.

7. Chiu CH, et al. (2005) The genome sequence of *Salmonella enterica* serovar Choleraesuis, a highly invasive and resistant zoonotic pathogen. *Nucleic Acids Res* 33(5):1690-1698.

8. Parkhill J, et al. (2001) Complete genome sequence of a multiple drug resistant *Salmonella enterica* serovar Typhi CT18. *Nature* 413(6858):848-852.

9. McClelland M, et al. (2001) Complete genome sequence of *Salmonella enterica* serovar Typhimurium LT2. *Nature* 413(6858):852-856.

10. Darling AC, Mau B, Blattner FR, & Perna NT (2004) Mauve: multiple alignment of conserved genomic sequence with rearrangements. *Genome Res* 14(7):1394-1403.

11. Duong N, et al. (2007) Thermosensing coordinates a *cis*-regulatory module for transcriptional activation of the intracellular virulence system in *Salmonella enterica* serovar Typhimurium. *J. Biol. Chem*. 282(47):34077-34084.

Chapter Three – Characterization of DalS, an ATP-binding Cassette Transporter for D-alanine, and its role in pathogenesis in *Salmonella enterica*

Chapter Three – Co-authorship statement

Chapter three consists of the following publication:

Osborne, S.E., Tuinema, B.R., Mok, M.C.Y., Lau, P.S., Bui, N.K., Tomljenovic-Berube, A.M., Vollmer, W., Zhang, K., Junop, M., and Coombes, B.K. (2012). Characterization of DalS, an ATP-binding Cassette Transporter for D-alanine, and its role in pathogenesis in *Salmonella enterica*. Journal of Biological Chemistry, [In Press].

The following work was conducted by authors other then myself:

1) Peptidoglycan purification was performed by S.E.O. and muropeptide profiling was conducted by N.K.B. and W.V.
2) Purification of DalS and fluorescence thermal shift assays were conducted by B.R.T. with significant intellectual contribution towards experimental design and analysis of results by S.E.O.
3) Transport assays were designed by S.E.O. and performed by P.S.L. and S.E.O.
4) Crystallization and structural analysis of DalS performed by K.Z., M.C.Y.M and J.M with intellectual contribution by S.E.O. and B.K.C
5) Purification of SsrBc and EMSAs performed by A.M.T.B. with DNA reagents supplied by S.E.O.
6) Manuscript written by S.E.O. and B.K.C.

Characterization of DalS, an ATP-binding Cassette Transporter for D-alanine, and its role in pathogenesis in *Salmonella enterica*

Suzanne E. Osborne[1,2], Brian R. Tuinema[1,2], Mac C.Y. Mok[2], Pui Sai Lau[2], Nhat Khai Bui[3], Ana M. Tomljenovic-Berube[1,2], Waldemar Vollmer[3], Kun Zhang[2], Murray Junop[1,2], and Brian K. Coombes[1,2*]

[1]Michael G. DeGroote Institute for Infectious Disease Research, Hamilton, Ontario, Canada, L8N 3Z5

[2]Department of Biochemistry and Biomedical Sciences, McMaster University, Hamilton, Ontario. L8N 3Z5.

[3]Centre for Bacterial Cell Biology, Institute for Cell and Molecular Biosciences, Newcastle University, Newcastle upon Tyne, United Kingdom

Running title: D-alanine ABC transporter required for *Salmonella* virulence

To whom correspondence should be addressed: Brian K. Coombes, Department of Biochemistry and Biomedical Sciences, and the Michael G. DeGroote Institute for Infectious Disease Research, McMaster University, 1280 Main St. West, Hamilton, Ontario, Canada. L8S 4K1, Tel.: (905) 525-9140; E-mail: coombes@mcmaster.ca

KEY WORDS: SsrB, ABC transporter, D-alanine

Background: Bacterial pathogens acquire nutrients for survival during host infection.

Result: DalSTUV is an ABC transporter for D-alanine and contributes to virulence *in vivo*.

Conclusion: Nutrient exchange during the host-pathogen interaction can direct disease outcome.

Significance: This is the first report of an ABC transporter for D-alanine.

SUMMARY

Expansion into new host niches requires bacterial pathogens to adapt to changes in nutrient availability and to evade an arsenal of host defences. Horizontal acquisition of *Salmonella* Pathogenicity Island (SPI) - 2 permitted the expansion of *Salmonella enterica* serovar Typhimurium into the intracellular environment of host cells by allowing it to deliver bacterial effector proteins across the phagosome membrane. This is facilitated by the SsrA-SsrB two-component regulatory system and a type III secretion system encoded within SPI-2. SPI-2 acquisition was followed by evolution of existing regulatory DNA, creating an expanded SsrB regulon involved in intracellular fitness and host infection. Here, we identified an SsrB-regulated operon comprising an ABC transporter in *Salmonella*. Biochemical and structural studies determined that the periplasmic solute-binding component, STM1633/DalS, transports D-alanine and that DalS is required for intracellular survival of the bacteria and for fitness in an animal host. This work exemplifies the role of nutrient exchange at the host-pathogen interface as a critical determinant of disease outcome.

INTRODUCTION

Horizontal gene transfer (HGT) is a major driver of bacterial evolution, allowing rapid gains in function through acquisition of virulence machinery and other fitness factors. Evolution of *Salmonella enterica* as a mammalian pathogen was driven by two major HGT events. Acquisition of *Salmonella* pathogenicity island (SPI)-1 conferred the ability to invade intestinal epithelial cells and SPI-2 allowed for intracellular proliferation and systemic dissemination. SPI-2 encodes a type III secretion system that delivers virulence proteins called effectors into the host cell where they modify host cell biology. Common targets include the host cell cytoskeleton, endosome trafficking and immune signalling cascades including NF-κB (1-3). Expression of SPI-2 is driven by the two-component regulatory system SsrA-SsrB (4) with additional inputs from the ancestral regulatory networks of OmpR (5), SlyA (6), PhoP (7) and H-NS (8) to fine-tune virulence gene expression in response to environmental cues.

Host cells detect and respond to microbial infection through recognition of pathogen associated molecular patterns (PAMPs) including lipopolysaccharide, flagellin and peptidoglycan. Peptidoglycan, a critical and ubiquitous component of bacterial cell walls, is composed of glycan chains of alternating N-acetylglucosamine and N-acetylmuramic acid residues linked by short peptides (9). Newly made peptides typically contain L-alanine, D-glutamic acid, *meso*-diaminopimelic acid and two terminal D-alanine residues and these peptides are cross-linked and trimmed during peptidoglycan synthesis and maturation.

During infection of host cells *Salmonella* resides in an intracellular vacuole called the *Salmonella*-containing vacuole (SCV). Nutrient and small molecule exchange across the SCV provides an opportunity for host-pathogen interaction however very little is known about this. Bacteria commonly employ ATP-Binding Cassette (ABC) transporters for nutrient exchange with the environment. ABC importers consist of four components; a periplasmic binding protein that binds ligand with high affinity, two transmembrane proteins that span the inner membrane through which the ligand is shuttled, and a cytoplasmic ATPase dimer that energizes the transport process (10). ABC importers vary in their specificity and can bind a wide variety of ligands, including cations, amino acids, polysaccharides and polypeptides.

Here we have structurally and biochemically characterized the periplasmic binding protein component of a novel D-alanine ABC transporter encoded within the *STM1633-STM1636* operon in *Salmonella enterica* serovar Typhimurium. The solute-binding component (STM1633) was named DalS (**D-al**anine transporter in ***S****almonella*) to reflect its binding specificity, with the other linked components of the system named according to standard nomenclature for ABC transport systems. We found that *dalS* was co-regulated with the SPI-2 virulence locus through direct activation by SsrB, suggesting a role for this system during intracellular infection. Accordingly, we demonstrate that a *dalS* deletion mutant has a fitness defect *in vivo*. We identified D-alanine as the ligand for DalS and verified this specificity by determining the crystal structure to 1.9 Å in complex with D-alanine. This work provides the first example of an ABC transporter for D-alanine and highlights the importance of this amino acid for *Salmonella* fitness during infection.

EXPERIMENTAL PROCEDURES

Bacterial Strains and Growth Conditions - All strains are isogenic derivatives of *Salmonella enterica* serovar Typhimurium SL1344 (*S.* Typhimurium). Unless otherwise indicated, bacteria were grown in LB at 37°C, 225 rpm. For expression of SsrB-regulated genes, a low phosphate, low magnesium minimal medium with an acidic pH (LPM pH 5.8) was used as described (11). For nutrient drop-out studies, casamino acids were replaced with individual amino acids added separately at the same concentration as that found in casamino acids. The marked SL1344 *ushA*::Cm strain has been described previously and was used for competitive infections of animals (12). An in-frame, unmarked deletion of *ssrB* (Δ*ssrB*) was used as described previously (4).

Cloning and Mutant Construction. An in-frame, unmarked deletion of *dalS* (Δ*dalS*) was constructed using homologous recombination from a suicide plasmid. The entire *dalS* open reading frame plus 700 bp flanking either side of the gene was amplified by PCR using primers SEO068 and SEO069. PCR product was cloned into pBLUESCRIPT as a KpnI/SacI fragment. Primers SEO070 and SEO071 were used for inverse PCR of pBLUESCRIPT (*dalS*). Product was then self ligated to generate the deletion allele of *dalS* which was subsequently sub-cloned into the mobilizable plasmid pRE112 and transformed into DH5α λpir. Transformants were conjugated with wild type *S.* Typhimurium and merodiploids selected based on resistance to both streptomycin and chloramphenicol. Merodiploids were grown for 6 h without antibiotics and then counter

selected on agar plates containing 5% (w/v) sucrose. Clones having lost chloramphenicol resistance were PCR screened for deletion of *dalS* using primers SEO068 and SEO069.

For construction of the *dalS* chromosomal β-galactosidase transcriptional reporter, 1 kb of DNA immediately upstream of *dalS* was PCR amplified using primers SEO007 and SEO008 and cloned into pIVET5n as an XhoI/MfeI fragment and confirmed by sequencing. pP_{dalS}-*lacZ* was transformed into DH5α λpir and conjugated into wild type and Δ*ssrB S.* Typhimurium. Merodiploids were selected based on resistance to both streptomycin and ampicillin.

To generate *dalS* containing a C-terminal 2-HA tag, the entire open reading frame for *dalS* including 1 kb of the upstream promoter region was PCR amplified from *S.* Typhimurium genomic DNA using primers SEO027 and SEO037. The resulting PCR fragment was cloned into pWSK29 as a SalI/XbaI fragment and verified by sequencing.

The expression construct for purification of DalS-6HIS was generated by PCR amplification with primers SEO172 and SEO173. Point mutants were constructed using splicing by overlapping extension (SOE) PCR (13). Initial fragments were amplified from *S.* Typhimurium chromosomal DNA using primer pairs; SEO172, BRT36 and BRT37, SEO173 for the M146T mutant and SEO172, BRT38 and BRT39, SEO173 for the M146A mutant. Products were purified, combined and a second PCR was performed using primers SEO172 and SEO173. PCR products were cloned into pET3a as NdeI/BamHI fragments and confirmed by sequencing. Constructs were transformed into *E. coli* BL21 (DE3). The C-terminal DNA binding domain plus linker region of SsrB (SsrBc) (bases 420-644) was cloned in pET3a using primers SsrBc-HISF and SsrBc-

HISR as an NdeI/BamHI fragment to generate C-terminal 6x His tag (SsrBc-6HIS). Constructs were confirmed by sequencing and transformed into *E. coli* BL21 (DE3).

Protein Purification - *E. coli* BL21 (DE3) carrying pDalS-6HIS, pDalSM146A-6HIS or pDalSM146T-6HIS was grown in LB at 37°C to an OD_{600nm} ~ 0.55 and then induced with 0.5 mM IPTG (Bioshop) and grown at 22°C for an additional 3 hours. Cells were centrifuged at 4000 g for 13 min at 4°C, washed in PBS and then resuspended in 20 mL cold lysis buffer containing 20 mM Tris pH 7.5, 0.5 M NaCl. Cells were lysed by sonication (Misonix Sonicator, Ultrasonic Processor S-400) at 40% amplitude with 3 pulses of 30 seconds in 1 min intervals. Whole cell lysates were centrifuged at 10,000 g for 20 min at 4°C. The supernatant was added to Ni-NTA beads (Qiagen) following equilibration with TBS (40 mM Tris pH 7.5, 0.5 M NaCl). The column was washed with 50 mL TBS containing increasing concentrations of imidazole (10 mM, 20 mM, 40 mM) and then protein was eluted in TBS containing 80 mM imidazole and run on SDS-PAGE for purity determination. Pure protein aliquots were pooled and concentrated using 3K Amicon Ultra Centrifugal filters (Millipore, UFC800324) and stored at -80°C.

E. coli BL21 (DE3) carrying (p*ssrBc*-6HIS) was inoculated 1:50 into LB and grown at 37°C with aeration to OD_{600nm} ~0.8. Cultures were induced with 1 mM IPTG and grown at 16°C for 24 h. Pellets collected by centrifugation at 4000 rpm, 4°C for 10 min and washed with PBS. Pellets were resuspended in Nickel Buffer A (20 mM Tris pH 8.5, 500 mM KCl, 10% glycerol, 0.1% LDAD, 10 mM imidazole with protease inhibitors). Bacteria were lysed by three passages through a French Press (French Press

Cell Disruptor, Thermo) and clarified by centrifugation at 20,000 rpm, 4°C for 40 min. Supernatant was filter sterilized and applied to a nickel column (Amersham Hi-Trap Ni^{2+}-NTA) pre-equilibrated with Nickel Buffer A. Protein was washed with 10 mL Nickel Buffer A, then 10 mL each of 5%, 10%, and 15% Nickel Buffer B (20 Mm Tris pH 8.5, 500 mM KCl, 10% glycerol, 0.1% LDAO, 300 mM imidazole). Protein was eluted with 10 mL 100% Nickel Buffer B into 5 mL of Nickel Buffer B to limit precipitation. Purified protein was then dialyzed overnight with storage buffer (20 mM Tris pH 8.5, 150 mM NaCl), then centrifuged to isolate soluble protein. Glycerol was added to 20%, and protein was stored at -80°C.

Genetic Analysis - Genome sequences for *S.* Typhimurium LT2, SL1344, DT104, *S. enterica* Enteritidis PT4, *S. enterica* Gallinarum 287/91, *S. enterica* Hadar, *S. enterica* Infantis, *S. enterica* Typhi Ty2 and CT18, *S. enterica* Paratyphi A and *S. enterica* Choleraesuis were obtained from the Wellcome Trust Sanger Institute (http://www.sanger.ac.uk) Pathogen Sequencing Unit. Promoter regions were aligned using MAFFT (v6.707b) (http://mafft.cbrc.jp/alignment/server/index.html). Identification of the SsrB regulatory motif was determined previously (4).

β-galactosidase Assays - Wild type and Δ*ssrB Salmonella* containing chromosomally encoded P_{dalS}-*lacZ* were inoculated 1:100 into LPM pH 5.8 and grown at 37°C with aeration. At the indicated time points the OD_{600nm} was determined and 200 µL of culture was collected for transcriptional reporter activity as described previously (14). Relative

light units (RLU) of β-galactosidase activity was quantified using 96-well black microtitre plates (Corning) using a top-reading plate luminometer (Envision, 2102 Multilabel Reader). For each time point, RLU was normalized to the OD_{600nm}.

Immunoblotting - Bacteria were sub-cultured 1:100 into LB or LPM pH 5.8 and grown to OD_{600nm} ~0.6. Cells were centrifuged and pellets resuspended in SDS-PAGE sample buffer [100 mM Tris-HCl (pH 6.8), 20% (v/v) glycerol, 4% (w/v) SDS, 0.002% (w/v) bromophenol blue and 200 mM DTT] in a volume adjusted to the optical density of the parent culture as described previously (11). Five µL from each sample was run on 12% SDS-PAGE and analyzed by immunoblotting using the following antibodies: mouse anti-HA (1:2000, Covance), mouse anti-DnaK (1:5000, Stressgen), rabbit anti-SseB (1:2000, (11), rabbit anti-SseC (1:5000, gift from Michael Hensel), rabbit anti-YidC (1:2000, gift from Eric Brown), mouse anti-MBP (1:2000, New England Biolabs), rabbit anti-RssB (1:2000, gift from Susan Gottesman) and rabbit anti-RpoS (1:2000, gift from Susan Gottesman), goat anti-mouse HRP (1:5000, Sigma) and goat anti-rabbit HRP (1:5000, Sigma). Conjugated HRP was detected using chemiluminescence (Western Lightning Plus-ECL, PerkinElmer).

Electrophoretic Mobility Shift Assays - The *dalS* promoter region from position -252 to -91 relative to the translational start site was PCR amplified using primers SEO161 and SEO162 to generate a 5’ biotin tagged fragment and SEO163 and SEO162 to generate the identical fragment lacking the biotin tag. PCR products were purified from native PAGE

using Qiagen Gel Extraction Kit. 50 mM Tris-HCl pH 7.5, 50 ng/µL poly dI:dC (Sigma, P4929) and 0.5 nM of 5' biotin DNA were mixed and purified SsrBc-6HIS was added to each reaction mixture and sample incubated at 37°C for 20 min. Controls contained a 100-fold excess of unlabelled DNA or biotin labelled non-specific *rrsH* amplified using primers rrsHF and rrsHR. Samples were run on 8% native PAGE and transferred to a Biodyne B positive nylon membrane (Pierce, 77016). Membranes were dried and DNA crosslinked for 15 min using a transilluminator. Membranes developed using a chemiluminescence based kit (Chemiluminescence Nucleic Acid Detection Module, Pierce) according to the manufacturer's directions.

Cell Culture - RAW264.7 cell culture lines were grown at 37°C, 5% CO_2 in DMEM/10%FBS (Gibco) unless otherwise indicated. Overnight cultures of wild type, Δ*ssrB*, Δ*dalS* and Δ*dalS* (p*dalS*-2HA) were opsonised in DMEM/20% human serum at 37°C for 30 min. Bacteria were diluted in DMEM/10% FBS and added to ~ 5 x 10^5 RAW 264.7 macrophages at multiplicity of infection of 1000 in tissue culture plate wells. Infected cells were centrifuged at 500 g for 5 min and then incubated for 30 min to allow for uptake. Infected cells were washed 3 times with PBS and 100 µg/mL gentamicin (Bioshop) was added to each well and incubated for 1.5 h. Cells were washed as before and either lysed or cultured for an additional 18 h in medium containing 10 µg/mL gentamicin. At the indicated times macrophages were lysed in 250 µL lysis buffer [1% Triton X100, 0.1% SDS]. Lysates were serial diluted and plated for CFU determination.

Fold replication was determined as CFU (20 h)/CFU (2 h). Data were normalized to fold replication of wild type for each experiment.

Competitive Infection of Animals - All animal protocols were performed in accordance with the Canadian Council on the Use of Laboratory Animals and approved by the McMaster University Animal Ethics Committee. Female C57BL/6 mice (Charles River) were orally infected with ~1 x 10^6 *Salmonella* in 0.1 M Hepes pH 8.0, 0.9% NaCl containing an equal number of chloramphenicol-resistant wild type bacteria and an unmarked mutant under study. At 3 days post mice were sacrificed by cervical dislocation and spleen, liver and cecum were harvested. Tissues were homogenized in a Mixer Mill (5min, 30 Hz) (Retsch), serial diluted and plated on LB agar containing streptomycin to determine total CFU counts. Colonies were replica plated onto LB agar containing both streptomycin and chloramphenicol (10 µg/mL) to determine the ratio of chloramphenicol resistant to sensitive colonies. Competitive index was calculated as (mutant/wild type)$_{output}$/(mutant/wild type) $_{input}$. Statistical analysis was performed using a one sample t test. For survival studies, female C57BL/6 mice were orally infected with ~1 x 10^6 CFU of either wild type or Δ*dalS S.* Typhimurium and endpoints were determined based on body condition scoring and loss of > 20% body weight.

Fluorescence Thermal Shift Assay - The fluorescence thermal shift assay was performed essentially as described previously (15). Amino acids were purchased from Sigma unless otherwise indicated. The assay was performed with a 480 Lightcycler

(Roche) (498 nm excitation, 610 nm emission). Each reaction contained 10 µM protein, 5x concentration of SyPro Orange (Invitrogen) and 1 mM of the indicated amino acid dissolved in 100 mM HEPES, 150 mM NaCl, pH 7.5 in a 96 well plate (Roche). Samples were initially equilibrated at 25°C for 10 min and a melting curve program was run on the LightCycler with a 1°C temperature increase every 30 seconds up to 99°C. Software calculated the first derivative values (-d/dt) from raw fluorescence data to determine T_m. A ΔT_m of > 2°C upon addition of amino acid was considered positive binding as described (15).

Protein Crystalization - Selenomethionine derivatized DalS was expressed in B834 (DE3) cells using M9 SeMET high-yield growth media Kit (Medicilon). The protein was purified using nickel affinity chromatography and buffer exchanged into 20 mM Tris pH 7.5 and 100 mM NaCl. Protein crystals were grown using the hanging drop vapour diffusion method. Purified DalS-6HIS (concentrated to 4 mg/mL) was mixed at a 2:1 ratio with a precipitant of 10% (w/v) PEG-3000, Na/K phosphate pH 6.2. The mixture was equilibrated against 800 µL of 1.65 M $(NH_4)_2SO_4$ and crystals formed after two days at 4˚C. To form a complex with glycine, purified DalS was mixed at a 2:1 ratio with a precipitant containing 10% (w/v) PEG-3000 and CHES pH 9.5. Glycine was added to the drop to a final concentration of 5 mM and the drop was equilibrated over 800 µL of 1.5 M $(NH_4)_2SO_4$. Crystals formed overnight at 4°C. Crystals of sufficient size were flash frozen with liquid nitrogen. Anomalous data was collected under cryogenic conditions (100K) at beam line X29 at the National Synchrotron Light Source at Brookhaven National Labs

and processed using HKL2000 (16). Phenix-AutoSol (17) was used to locate 7 heavy atom sites and also for phasing and density modification. Iterative rounds of model building and refinement were carried out using Coot (18) and Phenix-Refine (17). The final R_{work} and R_{free} values for crystals grown in the presence of glycine were 19% and 20.3% respectively. The final R_{work} and R_{free} values for crystals grown in the absence of glycine were 19% and 21.6% respectively. All final models were analyzed using PROCHECK which indicated 93.5% residues lie in favourable regions, 5.9% lie in allowed regions and 0.5% lie in generously allowed regions. Residues 1-24 were not included in any of the final models due to disorder. Structural images were generated using PyMol (The PyMOL Molecular Graphics System, Version 1.2, Schrödinger, LLC).

Transport Assay - Wild type and Δ*dalS* were grown in 5 mL of LPM pH 5.8 for 3 hours at 37°C with shaking. Cells were centrifuged and resuspended in PBS and grown at 37°C for 30 minutes. 5 µL of [^{3}H]-D-alanine (60 Ci/mmol, 1 mCi/ml; ART 0179; American Radiolabeled Chemicals Inc., Missouri, USA) or [^{3}H]-glycine (60Ci/mmol, 1mCi/mL, Perkin Elmer) were added to the cultures. Every 30 seconds 200 µL aliquots were spotted onto 0.2 µm nitrocellulose filters under vacuum. Filters were washed with 4 mL ice cold PBS and added to a Fast Turn Cap Mini Poly-Q scintillation vial (Beckman Coulter) containing 4 mL EcoScint A scintillation fluid (LS-273, National Diagnostics). Filter samples were left to saturate in the vials for 30 min, before reading on the Beckman Coulter LS 6500 scintillation counter.

RESULTS

Co-regulation of dalS with SPI-2 -The *dalSTUV* operon (Figure 3.1A), which is conserved across all *Salmonella* lineages, was co-regulated with the SPI-2 virulence machinery in *S*. Typhimurium in transcriptional profiling experiments, where *dalS* showed an ~ 10-fold decrease in mRNA levels in an *ssrB* deletion mutant (4). In accord with these data, another group showed that *dalS/STM1633* clustered into an SsrB-controlled regulatory network enriched in virulence genes including genes in SPI-2 and with *srfN* (19), the latter of which we previously showed was required for *in vivo* fitness (20). To confirm the microarray results, we constructed a chromosomally encoded *lacZ* transcriptional reporter (P_{dalS}-*lacZ*) in both wild type (wt) and Δ*ssrB* backgrounds and measured β-galactosidase activity over time in SPI-2 inducing minimal media (LPM pH 5.8) (11). In agreement with the microarray data, the activity of the *dalS* promoter increased over time and this expression was diminished in Δ*ssrB* (Figure 3.1B). DalS protein analyzed by western blot in wt and Δ*ssrB* cells showed that DalS levels were increased in minimal medium compared to LB and that SsrB was required for full expression of DalS in minimal medium (Figure 3.1C).

The *dalS* promoter region was bound by SsrB in chromatin immunoprecipitation (ChIP)-on-chip experiments (4). To confirm that SsrB directly binds to the *dalS* promoter, an electrophoretic mobility shift assay was performed using a purified DNA fragment spanning nucleotide position -252 to -92 that incorporated the SsrB binding peak. Incubation of this DNA fragment with increasing concentrations of purified SsrBc (5)

resulted in a retardation of band migration (Figure 3.1D) that was inhibited in the presence of unlabeled competitor DNA confirming that SsrB binds to the *dalS* promoter. Consistent with this finding, an SsrB binding motif was identified at position -185 to -168 relative to the *dalS* translational start site (Figure 3.1E). Together these results indicate that SsrB has direct transcriptional input into the expression of *dalS*.

DalS is a Virulence Factor Required for Intracellular Survival - Given the well documented role of SsrB in *S. enterica* pathogenesis we hypothesized that DalSTUV was required for full intracellular virulence. We constructed an unmarked, in-frame deletion of *dalS* (Δ*dalS*), which had no effect on growth of the bacteria under any *in vitro* condition examined (Figure 3.S1A). C57BL/6 mice orally infected with wt *S.* Typhimurium had a mean survival time of 5 days (Figure 3.2A) whereas mice infected with Δ*dalS* had a mean survival time that was delayed by one day (6 days; $p = 0.03$). To determine whether the *dalS* mutant had a reduced ability to replicate in peripheral tissues we performed a competitive infection of C57BL/6 mice with a mixed inoculum of wt and Δ*dalS*. After 3 days of infection, the bacterial load in the spleen, liver and cecum was determined and expressed as a competitive index (21). The *dalS* mutant was consistently recovered in lower amounts compared to wt, with competitive index values of 0.72 (spleen), 0.66 (liver) and 0.76 (cecum) (Figure 3.2B).

To examine whether Δ*dalS* was deficient for intracellular replication, macrophage-like RAW264.7 cells were infected with wt or Δ*dalS* and the ability of the bacteria to survive and replicate over 20 hours was determined by standard gentamicin

protection assays. Although Δ*dalS* was able to replicate in macrophages, it did not reach the same level of replication as wt, a defect that was recovered by complementation (Figure 3.2C). In mice, complementation of the *dalS* deletion also restored the replication defect seen in earlier competitive infections (data not shown). These results indicate that DalS contributes to intracellular survival and to the competitive fitness of *Salmonella* during animal infections.

DalS is an ABC Importer for D-Alanine - Each protein encoded in the *dalSTUV* operon has strong similarity to components of ATP-binding cassette (ABC) transporters (Figure 3.S2). DalS was identified as the periplasmic binding protein, DalT and DalV are homologous to the membrane spanning transport channel and DalU was identified as the cytoplasmic ATPase. Specifically, the *dalSTUV* operon was related to a family of polar amino acid (PAA) importers. Alignments for DalU showed particularly strong conservation of the Walker A, Walker B boxes and the ABC signature motif (Figure 3.S2D). The membrane spanning permeases DalT and DalV were predicted to have 4 to 5 membrane spanning domains (Figure 3.S3C). Consistent with the prediction that DalS is the periplasmic component of this ABC transporter, cellular fractionation experiments showed localization of DalS-2HA exclusively to the periplasmic fraction (Figure 3.S2B).

To identify the substrate(s) of DalS, we purified DalS and used this protein in a fluorescence thermal shift (FTS) assay previously developed to identify the amino acid specificity of solute-binding proteins in the bacterial ABC transport family (15). Amino acids were added to DalS-6HIS in the presence of SyPro Orange and fluorescence

measurements were acquired during thermal shift. In the FTS assay we identified glycine and D-alanine as specific ligands for DalS, whereas the glycine derivative betaine, L-alanine, or other amino acids did not register as positive in this screen (Figure 3.3A).

To confirm that DalSTUV functions to transport the ligands identified by FTS, we studied the accumulation of [^{3}H]-glycine and [^{3}H]-D-alanine by wild type and Δ*dalS* cells. Cells were grown in minimal medium to exponential phase then transferred to PBS for a 30 minute starvation period prior to addition of ligand. Cells were collected at 30 sec time intervals following ligand addition and intracellular radioactivity was measured. In these experiments, cells lacking *dalS* consistently had lower levels of intracellular [^{3}H]-D-alanine compared to wild type cells (Figure 3.3B), whereas the uptake of [^{3}H]-glycine was unaffected by DalS (Figure 3.3C). These data suggested that D-alanine was the biological substrate, which we set out to verify using structural information.

To structurally characterize this D-alanine periplasmic binding protein, we crystallized DalS and solved the structure to 1.9Å resolution (Table 3.S2). DalS crystallized bound to its ligand D-alanine despite extensive dialysis even in the presence of molar excess glycine, suggesting high affinity for the D-alanine ligand. Similar to previously characterized periplasmic binding proteins, DalS had a bi-lobe structure with each lobe consisting of a core of β-sheets surrounded by α helices (Figure 3.4A). Lobe I ($\beta_1\beta_2\beta_3\alpha_1\beta_4\alpha_2\beta_5$ and $\alpha_6\alpha_7$) and lobe II ($\beta_7\alpha_3\beta_8\alpha_4\beta_9\alpha_5\beta_{10}$) were separated by segments composed of β_6 and β_{11}. β_{11} contained the conserved hinge domain (DQLGIA) common to periplasmic binding proteins (Figure 3.4A and 3.4B). DalS crystallized with a monomer in the asymmetric unit and behaved as a monomer in solution during size

exclusion chromatography (data not shown). Based on the structure, charged side chains Arg102 and Glu191, and a hydroxyl belonging to Ser97 stabilize the ammonium and carboxylate groups of D-alanine (Figure 3.4B). The ligand is further stabilized by several main chain peptide bonds (Gly95, Ala147 and Ser97). Trp77 and Tyr148 additionally confer hydrophobic interactions. Although Met146 does not directly interact with D-alanine, it likely contributes to ligand specificity due to steric hindrance (Figure 3.4D). To test this hypothesis we made point mutants with similar (M146T) and smaller side chains (M146A). M146T was found to additionally accommodate methionine as a binding ligand (Figure 3.4E) whereas the DalS variant with the M146A mutation was highly promiscuous and allowed for the accommodation of seven new binding ligands (Figure 3.4E). Although the binding profile for glycine was altered in both mutants, the binding of D-alanine was unaffected. This finding highlights M146 as a critical residue in conferring ligand specificity. DalS demonstrated significant structural similarity despite sharing only moderate sequence similarity (14% identity, 57% similarity) to the previously characterized histidine-binding periplasmic binding protein, HisJ (22) and to the lysine-arginine-ornithine-binding protein LAO from *Salmonella* (23) with RMSD values within the binding pocket of 0.429 and 0.470 Å, respectively. Interestingly, the amino acids responsible for direct ligand binding are conserved as well (Figure 3.4C and 3.4D). In addition to orthologs in the *Salmonella* genus, similarity searches identified a putative periplasmic binding protein and extracellular binding protein from *Dickeya dadantii* and *D. zeae* respectively, in which all ligand-binding interacting residues were conserved (data not shown). These data provide strong evidence that DalSTUV comprise

the components of an ABC importer for D-alanine, which to our knowledge is the first report of a transporter of this specificity.

DalS is not involved in peptidoglycan structure - The identification of DalSTUV as an importer for D-alanine led us to examine its potential role in peptidoglycan structure. Peptidoglycan, a critical component of the cell wall present in most bacteria, contains D-alanine in its stem peptides and its fine structure often changes with species and growth condition. Digestion of peptidoglycan with a muramidase yields a complex mixture of fragments called muropeptides which differ in the length of the stem peptide, the number of connected peptides and the presence or not of secondary modifications (24). High-pressure liquid chromatography analysis of muropeptides purified from wild type and DalS-deficient cells identified no significant difference in the peptidoglycan composition (Figure 3.S3). These data suggest that DalSTUV is not involved in establishing the core structure of peptidoglycan, a result that is consistent with the lack of *in vitro* growth phenotype for *dalS* mutant cells.

DISCUSSION

In this work we identified and characterized the first example of an ABC transporter for D-alanine. We found that DalS was co-regulated with the SPI-2 encoded virulence machinery through direct SsrB-dependent activation, allowing its expression to be modified during intracellular infection. Accordingly, cell culture and animal infections

demonstrated that DalS contributed to a quantifiable fitness gain for *S*. Typhimurium only during host infection whereas its presence for growth *in vitro* was completely dispensable. Biochemical and structural characterization identified DalSTUV as an ABC importer for D-alanine where DalS is localized to the periplasm to serve as the periplasmic binding component in this system.

Peptidoglycan is a key pathogen-associated molecular pattern (PAMP) recognized by the host innate immune system. Given its substrate binding profile, we thought that DalS might play a role in peptidoglycan structure but this was found not to be the case. D-alanine is the terminal subunit of the peptidoglycan stem pentapeptide and is released during the processes of peptide cross-linking by transpeptidases and trimming of tetrapeptides to tripeptides by DD-carboxypeptidases. It is possible that DalSTUV contributes to the recycling of D-alanine released during peptidoglycan synthesis and remodeling within the host cell, which might become more important in this particular environmental niche compared to bacteria grown in a liquid culture. Indeed, peptidoglycan remodeling takes place in intracellular *Salmonella* typhimurium (25) and the deficiency of another peptidoglycan recycling pathway, the AmpD-AmpG system, has been shown to influence virulence in *Salmonella*. For example, loss of AmpD, a peptidoglycan recycling protein in *Salmonella* attenuates intracellular survival and augments the host innate immune response to mutant cells due to accumulation of cytosolic muropeptide (26). However some evidence suggests that the major role of the DalS transport system is not for D-alanine recycling from the periplasm. For example, mutants that are defective for cell wall recycling are sensitized to cell wall-active

antibiotics (27). Thus we predicted that if DalS had a major role in D-alanine re-uptake then DalS-mutant cells would be sensitized to wall-active drugs, which they were not (data not shown). In addition, recycling of murein cell wall in *Salmonella* occurs by re-uptake of two major intact cell wall peptides (L-Ala-D -Gly-D-*meso*-diaminopimelic acid, and L-Ala-D -Gly-D-*meso*-diaminopimelic acid-D -Ala) by the oligopeptide permease, Opp, as opposed to periplasmic hydrolysis followed by reutilization of the constituent amino acids (28). Importantly, Opp mutants were growth-defective, showing a clear physiological role for peptide recycling, whereas the *dalS* mutant was not affected in growth in any *in vitro* media tested. Alternatively, given the limited distribution of DalS to the *Salmonella* genus, it is possible that DalSTUV plays a unique role in the intracellular lifestyle of this organism during infection, possibly through modulation of the host innate immune system, production of a secondary metabolite, or satisfying a within-host nutritional requirement that will require further work to address.

The high conservation of amino acids within the DalS binding pocket in comparison with HisJ and LAO, which we confirmed with our structural analysis, led us to initial predictions that DalS was involved in transporting polar amino acids. However data from our ligand screen did not support this hypothesis but rather showed an interaction with D-alanine and glycine. A second crystal structure of STM1633 deposited in the protein data bank (PBD 3R39) contains two monomers within the asymmetric unit, one bound to D-alanine and the other to glycine. However, despite extensive dialysis even in a large excess of glycine, DalS was reproducibly purified in the presence of bound D-alanine, making determinations of binding affinity difficult (data not shown). These data

suggested that glycine might be a weaker or non-biological ligand. Future work will determine the physiological relevance of the apparent dual ligand specificity of DalS.

As an intracellular pathogen, *Salmonella* must rapidly adapt to changing conditions as it transitions between environmental and host lifestyles. Up-regulation of existing nutrient importers through regulatory evolution, which is the case for DalS through its incorporation into the SsrB regulon, confers a fitness advantage to the bacteria that promotes infection of a host. This work highlights the importance of nutrient exchange across the host-pathogen interface as a critical determinant of disease outcome.

REFERENCES

1. Ochman, H., Soncini, F. C., Solomon, F., and Groisman, E. A. (1996) *Proc Natl Acad Sci U S A* **93**, 7800-7804
2. Shea, J. E., Hensel, M., Gleeson, C., and Holden, D. W. (1996) *Proc Natl Acad Sci U S A* **93**, 2593-2597
3. Haraga, A., Ohlson, M. B., and Miller, S. I. (2008) *Nat Rev Microbiol* **6**, 53-66
4. Tomljenovic-Berube, A. M., Mulder, D. T., Whiteside, M. D., Brinkman, F. S., and Coombes, B. K. *PLoS Genet* **6**, e1000875
5. Feng, X., Walthers, D., Oropeza, R., and Kenney, L. J. (2004) *Mol Microbiol* **54**, 823-835
6. Linehan, S. A., Rytkonen, A., Yu, X. J., Liu, M., and Holden, D. W. (2005) *Infect Immun* **73**, 4354-4362
7. Bijlsma, J. J., and Groisman, E. A. (2005) *Mol Microbiol* **57**, 85-96
8. Walthers, D., Carroll, R. K., Navarre, W. W., Libby, S. J., Fang, F. C., and Kenney, L. J. (2007) *Microbiol* **65**, 477-493
9. Vollmer, W., Blanot, D., and de Pedro, M. A. (2008) *FEMS Microbiol Rev* **32**, 149-167
10. Davidson, A. L., Dassa, E., Orelle, C., and Chen, J. (2008) *Microbiol Mol Biol Rev* **72**, 317-364
11. Coombes, B. K., Brown, N. F., Valdez, Y., Brumell, J. H., and Finlay, B. B. (2004) *J Biol Chem* **279**, 49804-49815

12. Coombes, B. K., Wickham, M. E., Lowden, M. J., Brown, N. F., and Finlay, B. B. (2005) *Proc Natl Acad Sci U S A* **102**, 17460-17465

13. Heckman, K. L., and Pease, L. R. (2007) *Nat Protoc* **2**, 924-932

14. Silphaduang, U., Mascarenhas, M., Karmali, M., and Coombes, B. K. (2007) *J Bacteriol* **189**, 3669-3673

15. Giuliani, S. E., Frank, A. M., and Collart, F. R. (2008) *Biochemistry* **47**, 13974-13984

16. Otwinowski, Z., Minor, W. (1997) Processing of X-ray diffraction data collected in oscillation mode, Academic Press, New York

17. Adams, P. D., Afonine, P. V., Bunkoczi, G., Chen, V. B., Davis, I. W., Echols, N., Headd, J. J., Hung, L. W., Kapral, G. J., Grosse-Kunstleve, R. W., McCoy, A. J., Moriarty, N. W., Oeffner, R., Read, R. J., Richardson, D. C., Richardson, J. S., Terwilliger, T. C., and Zwart, P. H. Acta Crystallogr D. *Biol Crystallogr* **66**, 213-221

18. Emsley, P., and Cowtan, K. (2004) Acta Crystallogr D Biol Crystallogr 60, 2126-2132

19. Yoon, H., McDermott, J. E., Porwollik, S., McClelland, M., and Heffron, F. (2009) *PLoS Pathog* **5**, e1000306

20. Osborne, S. E., Walthers, D., Tomljenovic, A. M., Mulder, D. T., Silphaduang, U., Duong, N., Lowden, M. J., Wickham, M. E., Waller, R. F., Kenney, L. J., and Coombes, B. K. (2009) *Proc Natl Acad Sci U S A* **106**, 3982-3987

21. Beuzon, C. R., and Holden, D. W. (2001) *Microbes Infect* **3**, 1345-1352

22. Yao, N., Trakhanov, S., and Quiocho, F. A. (1994) *Biochemistry* **33**, 4769-4779

23. Oh, B. H., Pandit, J., Kang, C. H., Nikaido, K., Gokcen, S., Ames, G. F., and Kim, S. H. (1993) *J Biol Chem* **268**, 11348-11355

24. Glauner, B. (1988) *Anal Biochem* **172**, 451-464

25. Quintela, J. C., de Pedro, M. A., Zollner, P., Allmaier, G., and Garcia-del Portillo, F. (1997) *Mol Microbiol* **23**, 693-704

26. Folkesson, A., Eriksson, S., Andersson, M., Park, J. T., and Normark, S. (2005) *Cell Microbiol* **7**, 147-155

27. Votsch, W., and Templin, M. F. (2000) *J Biol Chem* **275**, 39032-39038

28. Goodell, E. W., and Higgins, C. F. (1987) *J Bacteriol* **169**, 3861-3865

Acknowledgements - We thank members of the Coombes laboratory for critical reading of the manuscript. We also thank the laboratory of Dr. Yingfu Lee for use of their radioactivity facilities.

FOOTNOTES

*This work was supported by Canadian Institutes of Health Research grant MOP-82704 to BKC, the Canada Research Chairs program to BKC, and Infrastructure Investment from the Canada Foundation for Innovation to BKC.

[1]To whom correspondence may be addressed: Department of Biochemistry and Biomedical Sciences, McMaster University, 1280 Main Street West., Health Sciences Centre Room 4H17, Hamilton, Ontario, Canada. L8S 4K1.

[2]SEO is the recipient of the CIHR-Vanier Canada Graduate Scholarship.

[3]BRT and AMTB are recipients of an Ontario Graduate Scholarship.

[4]BKC is a CIHR New Investigator and the Canada Research Chair in Infectious Disease Pathogenesis.

FIGURE LEGENDS

Figure 3.1. DalS is Regulated by SsrB. (A) Diagram of the genetic region surrounding the *dalS* operon. Black genes indicate horizontal acquisitions in *S. enterica* that are absent from *S. bongori*. (B) Wild type (WT) and Δ*ssrB* containing chromosomal *lacZ* transcriptional reporters for the *dalS* promoter were grown in LPM pH 5.8 and β-galactosidase activity was quantified by chemiluminescence. Relative light units (RLU) were normalized at each time point (n = 3). (C) Levels of DalS-2HA protein in wt and Δ*ssrB* cells were determined using western analysis. DalS-2HA was detected using an antibody directed against the HA tag. DnaK was used as a loading control. SseB was used as a positive control as a gene product whose expression is dependent on SsrB. Figures are representative of three experiments with identical results. (D) Electrophoretic mobility shift assay using purified SsrBc-6HIS incubated with a 5' biotin labelled *dalS* promoter fragment spanning positions -252 to -91 and detected using a streptavidin-HRP based chemiluminescence. Data is representative of three experiments with identical results. (E) Alignment of the *dalS* promoter across several *Salmonella* strains. Positions relative to the translational start site are indicated. Red box indicates the location of the SsrB binding motif determined previously (4).

Figure 3.1

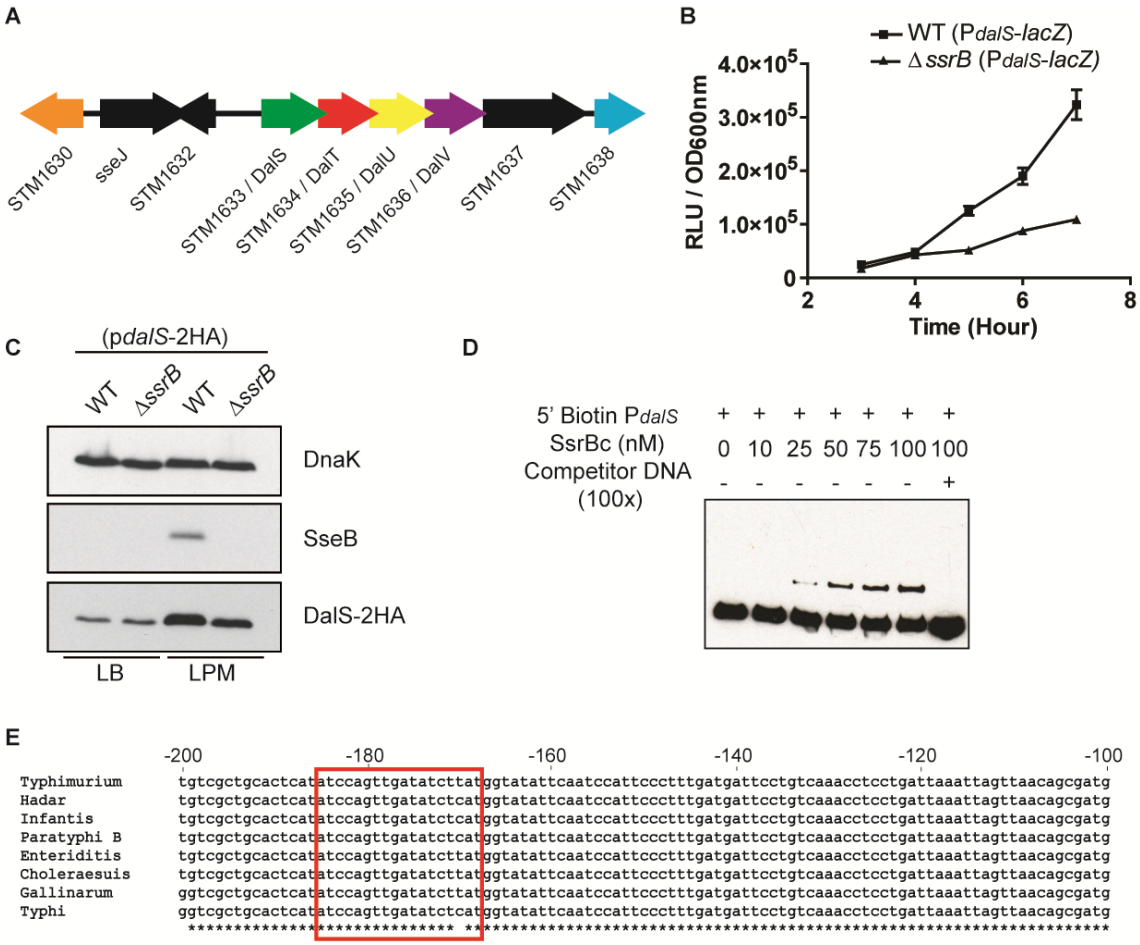
A
STM1630
sseJ
STM1632
STM1633 / DalS
STM1634 / DalT
STM1635 / DalU
STM1636 / DalV
STM1637
STM1638
B
WT (PdalS-lacZ)
ΔssrB (PdalS-lacZ)
RLU / OD600nm
4.0×10^5
3.0×10^5
2.0×10^5
1.0×10^5
0
2
4
6
8
Time (Hour)
C
(pdalS-2HA)
WT
ΔssrB
WT
ΔssrB
DnaK
SseB
DalS-2HA
LB
LPM
D
5' Biotin PdalS
SsrBc (nM)
Competitor DNA (100x)
+ + + + + + +
0 10 25 50 75 100 100
- - - - - - +
E
-200
-180
-160
-140
-120
-100
Typhimurium tgtcgctgcactcatatccagttgatatcttatggtatattcaatccattccctttgatgattcctgtcaaacctcctgattaaattagttaacagcgatg
Hadar tgtcgctgcactcatatccagttgatatctcatggtatattcaatccattccctttgatgattcctgtcaaacctcctgattaaattagttaacagcgatg
Infantis tgtcgctgcactcatatccagttgatatctcatggtatattcaatccattccctttgatgattcctgtcaaacctcctgattaaattagttaacagcgatg
Paratyphi B tgtcgctgcactcatatccagttgatatctcatggtatattcaatccattccctttgatgattcctgtcaaacctcctgattaaattagttaacagcgatg
Enteriditis tgtcgctgcactcatatccagttgatatcttatggtatattcaatccattccctttgatgattcctgtcaaacctcctgattaaattagttaacagcgatg
Choleraesuis tgtcgctgcactcatatccagttgatatcttatggtatattcaatccattccctttgatgattcctgtcaaacctcctgattaaattagttaacagcgatg
Gallinarum ggtcgctgcactcatatccagttgatatcttatggtatattcaatccattccctttgatgattcctgtcaaacctcctgattaaattagttaacagcgatg
Typhi ggtcgctgcactcatatccagttgatatctcatggtatattcaatccattccctttgatgattcctgtcaaacctcctgattaaattagttaacagcgatg

Figure 3.2. Deletion of *dalS* attenuates *S*. Typhimurium virulence *in vivo*. (A) Survival of C57BL/6 mice orally infected with wt or Δ*dalS* (n = 8). (B) C57BL/6 mice orally infected with a mixed inoculum of wt and Δ*dalS*. Competitive index values were determined after 3 days of infection. Each data point represents an individual animal and horizontal bars are the geometric means. (C) The contribution of DalS to *Salmonella* intracellular replication in macrophages was assessed by gentamicin protection assays in RAW264.7 cells. Macrophages were infected with the indicated strains and the change in intracellular bacteria numbers was determined between 2 and 20 h post-infection and normalized to wt. Δ*ssrB* was used as a negative control. (n = 5). (*, $p < 0.05$; ***, $p < 0.001$).

Figure 3.2

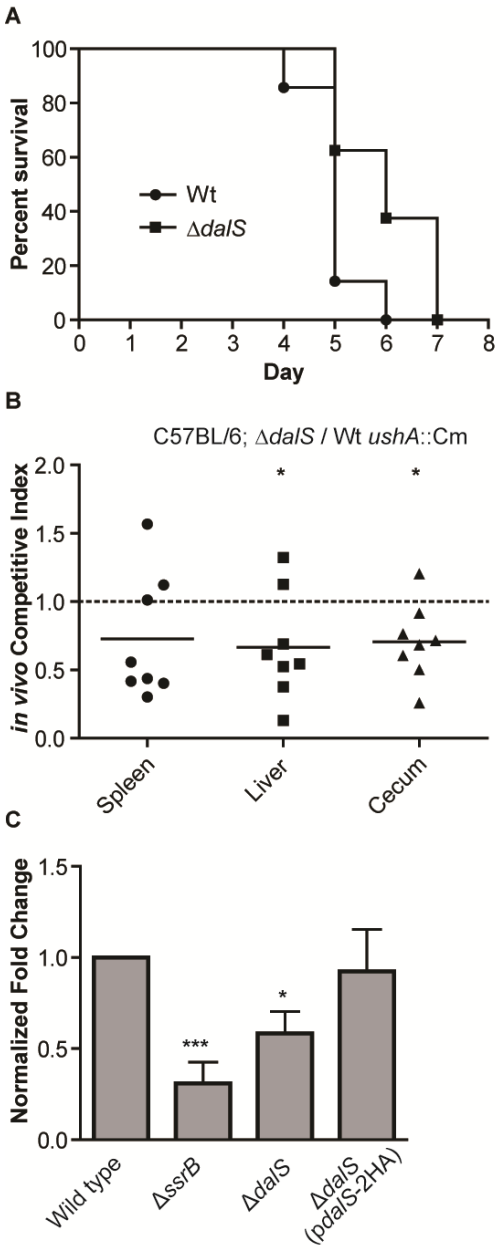
A
Percent survival
100
80
60
40
20
0
Wt
ΔdalS
0 1 2 3 4 5 6 7 8
Day
B
C57BL/6; ΔdalS / Wt ushA::Cm
in vivo Competitive Index
2.0
1.5
1.0
0.5
0.0
*
*
Spleen
Liver
Cecum
C
Normalized Fold Change
1.5
1.0
0.5
0.0
***
*
Wild type
ΔssrB
ΔdalS
ΔdalS (pdalS-2HA)

Figure 3.3. DalS is a Transporter for D-Alanine. (A) Fluorescence thermal shift assay to determine the DalS binding substrate. Purified DalS-6HIS was incubated with amino acids as indicated by their single-letter code (B = betaine; D-ala = D-alanine). Changes in melting temperature (ΔT_m) relative to controls lacking ligand were monitored based on fluorescence of the indicator dye SyPro Orange. Dashed line indicates the 2°C cut off for positivity; (n = 5). Transport assay for (B) [^{3}H]-D-alanine and (C) [^{3}H]-glycine incorporation. Wild type and Δ*dalS* cells were grown in LPM pH 5.8 to exponential phase then transferred to PBS for a 30 minute starvation. Amino acids were added to the cultures and cell-associated radioactivity was measured by scintillation counting. The experiment was repeated three times each with triplicate experimental replicates.

Figure 3.3

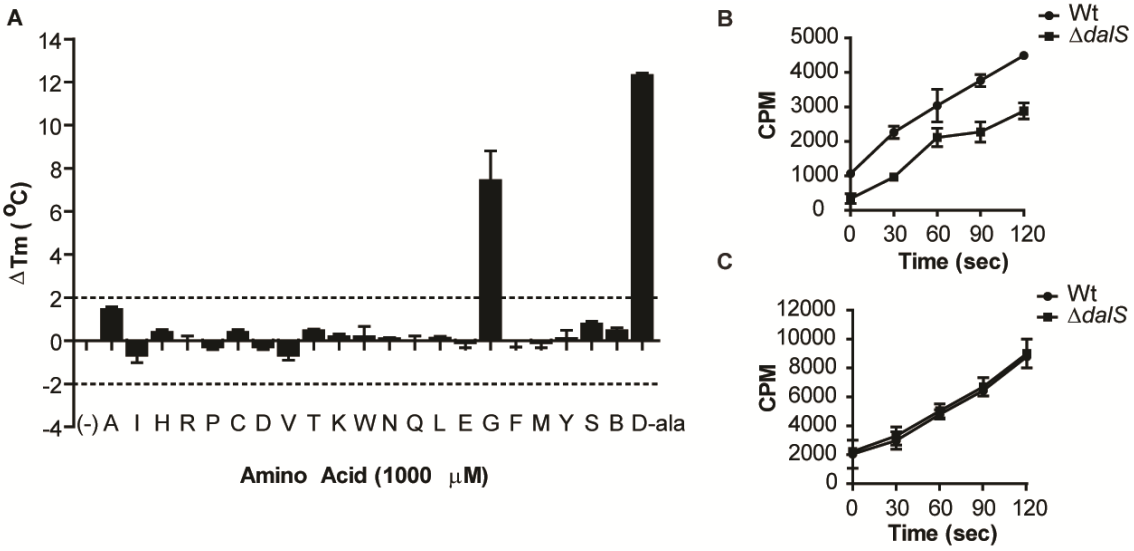
A
ΔTm (°C)
14
12
10
8
6
4
2
0
-2
-4
(-) A I H R P C D V T K W N Q L E G F M Y S B D-ala
Amino Acid (1000 μM)
B
Wt
ΔdalS
CPM
5000
4000
3000
2000
1000
0
0 30 60 90 120
Time (sec)
C
Wt
ΔdalS
CPM
12000
10000
8000
6000
4000
2000
0
0 30 60 90 120
Time (sec)

Figure 3.4. DalS is a Periplasmic binding protein with high specificity for D-alanine. (A) Ribbon diagram of DalS in complex with its ligand D-alanine. Secondary structure elements are labelled. D-alanine is drawn in stick model with the carbon (green), oxygen (red) and nitrogen (blue) atoms. (B) Stereo image of the DalS (purple) binding pocket. Binding residues and D-alanine are drawn as stick models with oxygen (red) and nitrogen (blue) atoms indicated. A single ordered water molecule interacting with D -alanine is shown as a red sphere. Black dashed lines indicate hydrogen bonding interactions. Pictorial 2-D representation of DalS with D -alanine binding interactions. Residues and ligand are shown as ball and stick figures with each atom labelled. Dash lines represent hydrogen bonds with distances labelled in angstroms. Semi-circles with linear protrusions indicate amino acids mediating hydrophobic contacts. (C) ClustalW alignment of DalS and the *S. bongori* homologue SBG1467. Residues important in ligand interaction (green) and the conserved hinge domain (blue) are indicated. (D) Binding pocket of DalS (gold) overlaid with the crystal structures of HisJ (purple) and LAO (gray). Residues important for interaction with the ligands D -alanine, histidine and arginine are indicated. (E) Fluorescence thermal shift assay for DalS-6HIS carrying the point mutants M146T and M146A was carried out as described above ($n = 3$) (*; $p < 0.05$, **: $p < 0.01$, ***; $p < 0.001$).

Figure 3.4

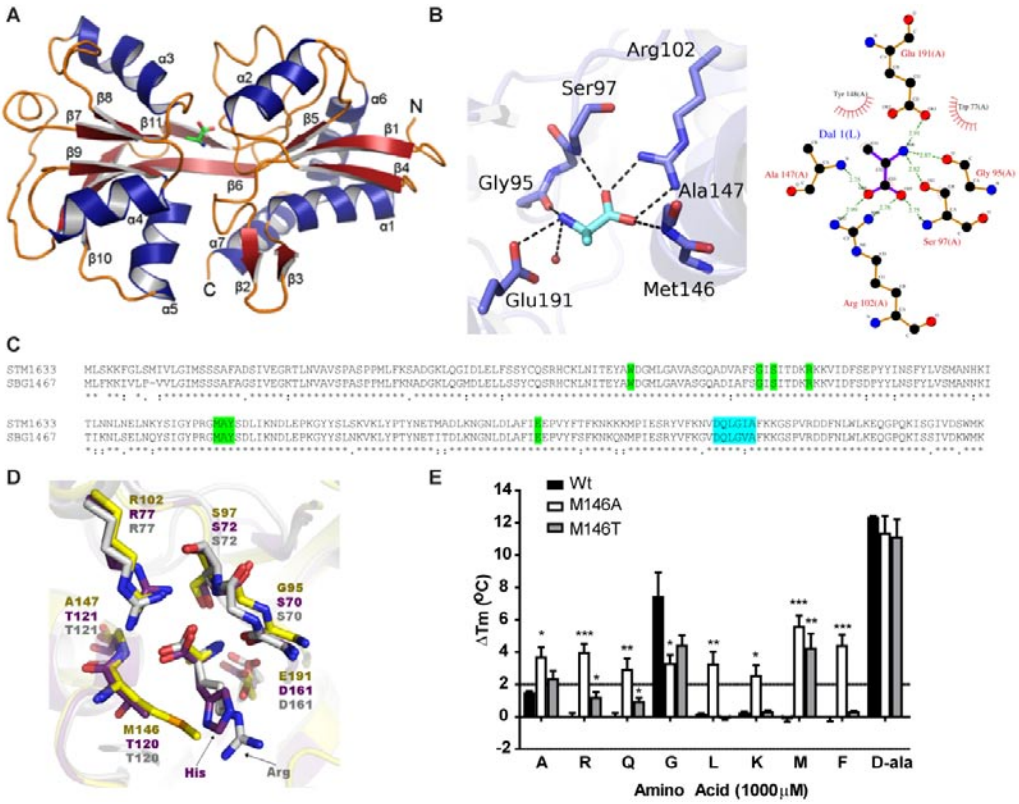
A
B
C
D
E
Arg102
Ser97
Gly95
Ala147
Glu191
Met146
R102
R77
S97
S72
G95
S70
A147
T121
E191
D161
M146
T120
His
Arg
Wt
M146A
M146T
ΔTm (°C)
A R Q G L K M F D-ala
Amino Acid (1000μM)

SUPPLEMENTARY EXPERIMENTAL PROCEDURES

Bacterial Strains and Growth Conditions. For growth in amino acid limiting conditions, LPM pH 5.8 was made as described previously lacking casamino acids and with the addition of 0.052 mM histidine (Sigma) and 0.19 mM glycine (Sigma) or 0.25 mM D-alanine (Sigma).

Genetic Analysis. BLAST (http://blast.ncbi.nlm.nih.gov/Blast.cgi) was performed using the open reading frames of DalS, DalT, DalU, and DalV. Alignments of top BLAST hits were performed using MAFFT. DalS was aligned to the Lysine/Arginine/Ornithine (LAO) binding protein (23) and the Histidine binding protein (HisJ) (22) from *S.* Typhimurium. DalU was aligned with ABC transporter ATPases HisP and GlnQ from *Geobacillus kaustophilus* HTA426 (27). The membrane spanning permeases DalT, DalU, and their *S. bongori* homologues SBG1468 and SBG1469.5 were aligned as above and transmembrane domains predicted using TMpred (http://www.ch.embnet.org/software/TMPRED_form.html). BLAST analysis was performed on DalS excluding *Salmonella*. Aligned residues were visually scanned for complete conservation of binding residues identified in DalS. DalS was aligned using ClustalW to the resulting putative PBP (gi|251788814) from *Dickeya zeae* Ech1591 and the extracellular solute binding protein (gi|307132037) from *D. dadantii* 3937.

Growth Assays. Wild type and Δ*dalS* were inoculated 1:100 into both LB and LPM pH 5.8 and 400 µL was grown in triplicate for 24 hours at 37°C with aeration. OD_{600nm} was monitored every 15 min using a Bioscreen C or a Synergy HT Multi-Mode Microplate Reader (BioTek). Stationary phase cultures were serial diluted in PBS and plated on LB agar plates overnight at 37°C to quantify colony forming units.

Osmotic Shock. *S*. Typhimurium (p*dalS*-2HA) was sub-cultured 1:100 into 200 mL LB and grown at 30°C to OD_{600nm} ~0.6. Bacteria were washed in cold PBS and resuspended in cold 20 mM Tris-HCl (Bioshop), 20% sucrose (Bioshop) pH 8.0 with Complete EDTA-free protease inhibitor cocktail tablets (Roche). 5 mM EDTA (Bioshop) and 75 µg/mL lysozyme (Bioshop) were then added. The suspension was incubated at 4°C for 45 min with gentle shaking. Ten mM $MgCl_2$ was added and the sample was centrifuged at 25,000 rpm, 4°C, 1 hour (Beckman, Ultima MAX-E Ultracentrifuge, MLA80 rotor). Supernatant containing periplasm was concentrated (Amicon Ultra Ultracel – 10k, Millipore) and the pellet was saved for fractionation. Five µg of protein was analyzed by Western Blot as described for bacterial fractionation.

Bacterial Fractionation. Pellets from osmotic shock were washed once in cold PBS (Bioshop). Bacteria resuspended in 20 mM Tris-HCl pH 7.5 (Bioshop), 5mM EDTA (Bioshop) with Complete EDTA-free protease inhibitor cocktail tablets (Roche). Bacteria lysed by 2 passages through French Press (French Press Cell Disruptor, Thermo). Lysate centrifuged at 30,000 rpm, 4°C, 40 min (Beckman, Optima MAX-E Ultracentrifuge,

MLA80 rotor). The supernatant was removed from cytoplasmic pellet and centrifuged as above at 80,000 rpm. The supernatant was removed from membrane pellet and discared. Cytoplasmic and membrane pellets were sequentially resuspended 1 mL PBS using 18, 21 and 25 gauge needle tips. Five µg of protein from each fraction was analyzed by western analysis.

Purification of peptidoglycan and muropeptides. The preparation of peptidoglycan and muropeptides was performed as described previously (24). Five hundred-mL of cells was grown in LB to mid-exponential phase (OD_{600nm} ~ 0.6). Cells were washed by centrifugation in wash buffer (50 mM Na_3PO_4, pH 7.0) and the pellet was resuspended in 10 mL wash buffer. Cells were added drop-wise to an equal volume of boiling SDS (50 mM Na_3PO_4, pH 7.0, 8% SDS) and boiled for 30 min. Once cooled, peptidoglycan was collected by ultracentrifugation at 60,000 rpm for 45 min (Beckman, Optima MAX-E Ultracentrifuge, MLA80 rotor). The pellet was washed by repeated ultracentrifugation as above in wash buffer until traces of SDS was removed. The final pellet was resuspended in 10 mM Tris pH 7.0, 10 mM NaCl. Peptidoglycan was sonicated (Sonicator 3000, Misonix) for 3 minutes with 20 second pulses to solubilise the peptidoglycan. Peptidoglycan was then incubated for 2 h at 37°C with Amylase (100 µg/L), DNase (10 µg/mL), RNase (50 µg/mL), $MgSO_4$ (20 mM) and imidazole (0.32 M final concentration), followed by proteinase (200 µg/mL) for 1 h at 60°C. SDS reflux was repeated as above to isolate peptidoglycan. Peptidoglycan was collected as washed by ultracentrifugation as above. Final peptidoglycan pellet was resuspended in 1mL sterile

ddH_2O. To digest peptidoglycan, the sample was sonicated as described above and incubated overnight at 37°C with shaking with mutanolysin (50 µg/mL, Sigma). Samples were boiled for 10 min to inactivate the enzyme then centrifuged at 16,000 g for 30 min at room temperature and the supernatant was collected. The concentration of peptidoglycan was determined at 206 nm in a quartz 96-well plate.

Muropeptide Analysis. *Salmonella* muropeptides were reduced with sodium borohydride and separated by high-pressure liquid chromatography as described for those from *E. coli* (24). Muropeptide were assigned in Fig. 3.S3 by comparing their retention time to that of known *E. coli* muropeptides. The muropeptides of Gram-negative bacteria including *Salmonella* have identical structures and muropeptides profiles of different species vary mainly due to differences in the relative amount of each muropeptide (25,28).

SUPPLEMENTARY FIGURE LEGENDS

Figure 3.S1. Loss of *dalS* does not impair growth *in vitro*. Wt and Δ*dalS* were inoculated into either LB (A) or LPM pH 5.8 containing 52 µM histidine (B) or 0.25 mM D-alanine and the optical density was monitored every 15 min for 24 h.

Figure 3.S1

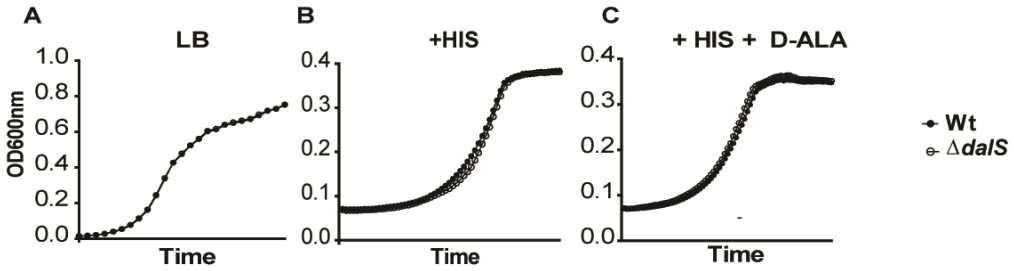
A
LB
B
+HIS
C
+ HIS + D-ALA
OD600nm
1.0
0.8
0.6
0.4
0.2
0.0
0.4
0.3
0.2
0.1
0.0
Time
Wt
ΔdalS

Figure 3.S2. DalS is a periplasmic binding protein. (A) Alignment of DalS with known periplasmic binding proteins from polar amino acid ABC transporters HisJ and LAO from *S.* Typhimurium. (B) To determine the localization of DalS in cells, wt (p*dalS*-2HA) was osmotically shocked and fractionated into periplasmic, cytoplasmic and membrane fractions. Equal amounts of protein from each fraction were analyzed by western blot. DnaK was used as a loading control, YidC as a membrane fraction control, MBP as a periplasmic control and both RssB and RpoS were used as cytoplasmic controls. Data is representative of 3 experiments with identical results. (C) Alignment of the membrane spanning permeases from both *S. enterica* and *S. bongori*. Predicted membrane spanning regions indicated (green). (D) Alignment of ATPase DalU(STM1635) with known ABC transporter ATPases HisP and GlnQ. Conserved domains indicated (blue) including the Walker A and B domains, the Q, D and H loops and the ABC signature motif.

Figure 3.S2

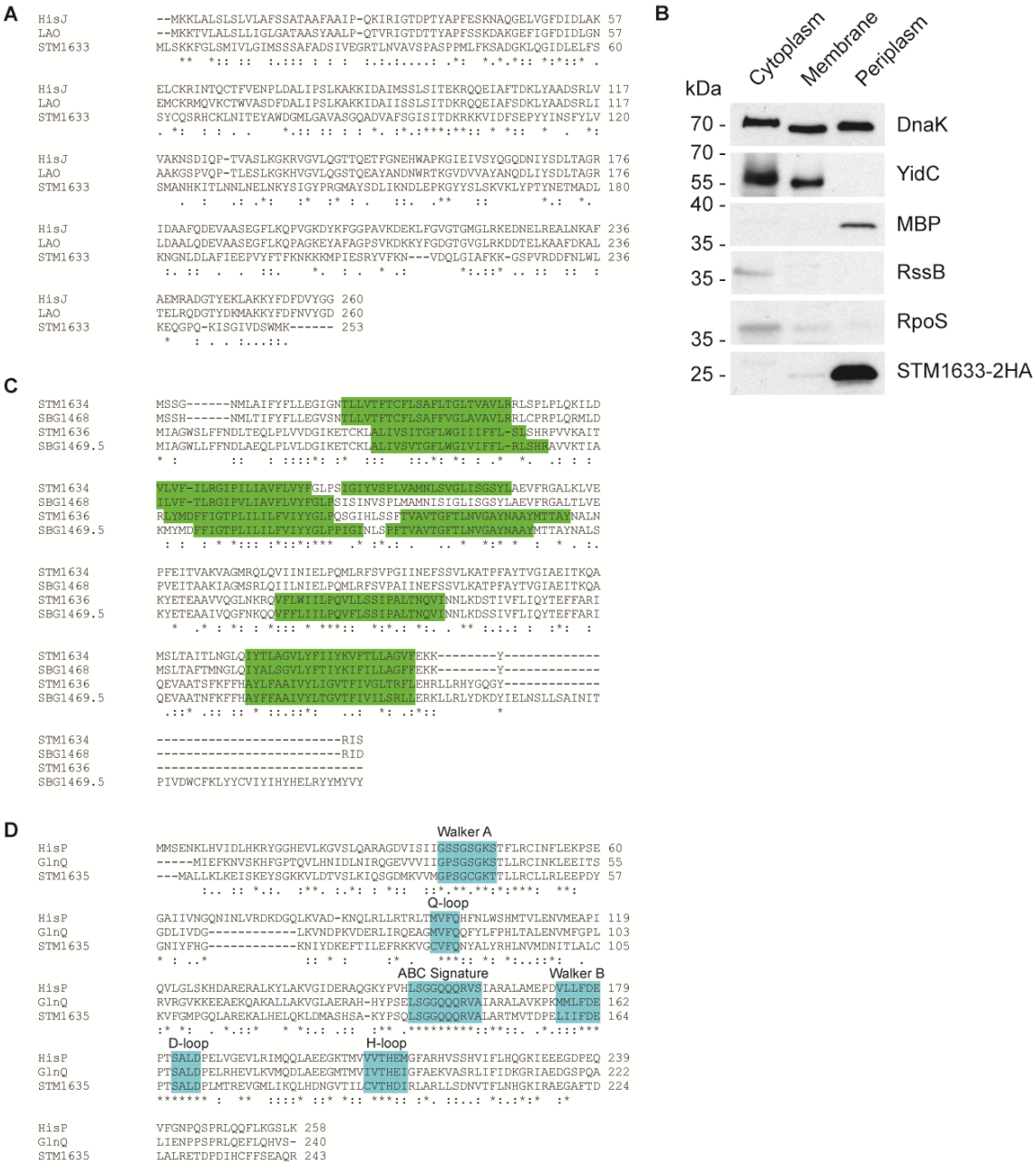
A
HisJ --MKKLALSLSLVLAFSSATAAFAAIP-QKIRIGTDPTYAPFESKNAQGELVGFDIDLAK 57
LAO --MKKTVLALSLLIGLGATAASYAALP-QTVRIGTDTTYAPFSSKDAKGEFIGFDIDLGN 57
STM1633 MLSKKFGLSMIVLGIMSSSAFADSIVEGRTLNVAVSPASPPMLFKSADGKLQGIDLELFS 60
HisJ ELCKRINTQCTFVENPLDALIPSLKAKKIDAIMSSLSITEKRQQEIAFTDKLYAADSRLV 117
LAO EMCKRMQVKCTWVASDFDALIPSLKAKKIDAIISSLSITDKRQQEIAFSDKLYAADSRLI 117
STM1633 SYCQSRHCKLNITEYAWDGMLGAVASGQADVAFSGISITDKRKKVIDFSEPYYINSFYLV 120
HisJ VAKNSDIQP-TVASLKGKRVGVLQGTTQETFGNEHWAPKGIEIVSYQGQDNIYSDLTAGR 176
LAO AAKGSPVQP-TLESLKGKHVGVLQGSTQEAYANDNWRTKGVDVVAYANQDLIYSDLTAGR 176
STM1633 SMANHKITLNNLNELNKYSIGYPRGMAYSDLIKNDLEPKGYYSLSKVKLYPTYNETMADL 180
HisJ IDAAFQDEVAASEGFLKQPVGKDYKFGGPAVKDEKLFGVGTGMGLRKEDNELREALNKAF 236
LAO LDAALQDEVAASEGFLKQPAGKEYAFAGPSVKDKKYFGDGTGVGLRKDDTELKAAFDKAL 236
STM1633 KNGNLDLAFIEEPVYFTFKNKKKMPIESRYVFKN---VDQLGIAFKK-GSPVRDDFNLWL 236
HisJ AEMRADGTYEKLAKKYFDFDVYGG 260
LAO TELRQDGTYDKMAKKYFDFNVYGD 260
STM1633 KEQGPQ-KISGIVDSWMK------ 253
B
kDa
Cytoplasm
Membrane
Periplasm
70 -
70 -
55 -
40 -
35 -
35 -
35 -
25 -
DnaK
YidC
MBP
RssB
RpoS
STM1633-2HA
C
STM1634 MSSG------NMLAIFYFLLEGIGNTLLVTFTCFLSAFLTGLTVAVLRRLSPLPLQKILD
SBG1468 MSSH------NMLTIFYFLLEGVSNTLLVTFTCFLSAFFVGLAVAVLRRLCPRPLQRMLD
STM1636 MIAGWSLFFNDLTEQLPLVVDGIKETCKLALIVSITGFLWGIIIFFL-SISHRPVVKAIT
SBG1469.5 MIAGWLLFFNDLAEQLPLVLDGIKETCKLALIVSVTGFLWGIVIFFL-RLSHRAVVKTIA
STM1634 VLVF-ILRGIPILIAVFLVYFGLPSIGIYVSPLVAMNLSVGLISGSYLAEVFRGALKLVE
SBG1468 ILVF-TLRGIPVLIAVFLVYFGLPSISINVSPLMAMNISIGLISGSYLAEVFRGALTLVE
STM1636 RLYMDFFIGTPLILILFVIYYGLPQSGIHLSSFTVAVTGFTLNVGAYNAAYMTTAYNALN
SBG1469.5 KMYMDFFIGTPLILILFVIYYGLPPIGINLSPFTVAVTGFTLNVGAYNAAYMTTAYNALS
STM1634 PFEITVAKVAGMRQLQVIINIELPQMLRFSVPGIINEFSSVLKATPFAYTVGIAEITKQA
SBG1468 PVEITAAKIAGMSRLQIILNIELPQMLRFSVPAIINEFSSVLKATPFAYTVGIAEITKQA
STM1636 KYETEAAVVQGLNKRQVFLWIILPQVLLSSIPALTNQVINNLKDSTIVFLIQYTEFFARI
SBG1469.5 KYETEAAIVQGFNKQQVFFLIILPQVFLSSIPALTNQVINNLKDSSIVFLIQYTEFFARI
STM1634 MSLTAITLNGLQIYTLAGVLYFTIYKVFTLLAGVFEKK--------Y------------
SBG1468 MSLTAFTMNGLQIYALSGVLYFTIYKIFILLAGFFEKK--------Y------------
STM1636 QEVAATSFKFFHAYLFAAIVYLIGVTFIVGLTRFLEHRLLRHYGQGY------------
SBG1469.5 QEVAATNFKFFHAYFFAAIVYLTGVTFIVILSRLLERKLLRLYDKDYIELNSLLSAINIT
STM1634 -------------------------RIS
SBG1468 -------------------------RID
STM1636 ----------
SBG1469.5 PIVDWCFKLYYCVIYIHYHELRYYMYVY
D
Walker A
HisP MMSENKLHVIDLHKRYGGHEVLKGVSLQARAGDVISIIGSSGSGKSTFLRCINFLEKPSE 60
GlnQ -----MIEFKNVSKHFGPTQVLHNIDLNIRQGEVVVIIGPSGSGKSTLLRCINKLEEITS 55
STM1635 ---MALLKLKEISKEYSGKKVLDTVSLKIQSGDMKVVMGPSGCGKTTLLRCLLRLEEPDY 57
Q-loop
HisP GAIIVNGQNINLVRDKDGQLKVAD-KNQLRLLRTRLTMVFQHFNLWSHMTVLENVMEAPI 119
GlnQ GDLIVDG------------LKVNDPKVDERLIRQEAGMVFQQFYLFPHLTALENVMFGPL 103
STM1635 GNIYFHG------------KNIYDKEFTILEFRKKVGCVFQNYALYRHLNVMDNITLALC 105
ABC Signature
Walker B
HisP QVLGLSKHDARERALKYLAKVGIDERAQGKYPVHLSGGQQQRVSIARALAMEPDVLLFDE 179
GlnQ RVRGVKKEEAEKQAKALLAKVGLAERAH-HYPSELSGGQQQRVAIARALAVKPKMMLFDE 162
STM1635 KVFGMPGQLARERKALHELQKLDMASHSA-KYPSQLSGGQQQRVALARTMVTDPELIIFDE 164
D-loop
H-loop
HisP PTSALDPELVGEVLRIMQQLAEEGKTMVVVTHEMGFARHVSSHVIFLHQGKIEEEGDPEQ 239
GlnQ PTSALDPELRHEVLKVMQDLAEEGMTMVIVTHEIGFAEKVASRLIFIDKGRIAEDGSPQA 222
STM1635 PTSALDPLMTREVGMLIKQLHDNGVTILCVTHDIRLARLLSDNVTFLNHGKIRAEGAFTD 224
HisP VFGNPQSPRLQQFLKGSLK 258
GlnQ LIENPPSPRLQEFLQHVS- 240
STM1635 LALRETDPDIHCFFSEAQR 243

Figure 3.S3. DalS does not influence peptidoglycan structure. Muropeptide profile for digested peptidoglycan isolated from wt and Δ*dalS*. Major peaks are indicated. Data is representative of two biological replicates. Tri. disaccharide-tripeptide monomer; Tetra, disaccharide-tetrapeptide monomer; Tetra-tetra, dimer of two tetra monomers cross-linked at the tetrapeptide side chains; Penta, disaccharide-pentapeptide monomer; A_2pm, meso-diaminopimelic acid.

Figure 3.S3

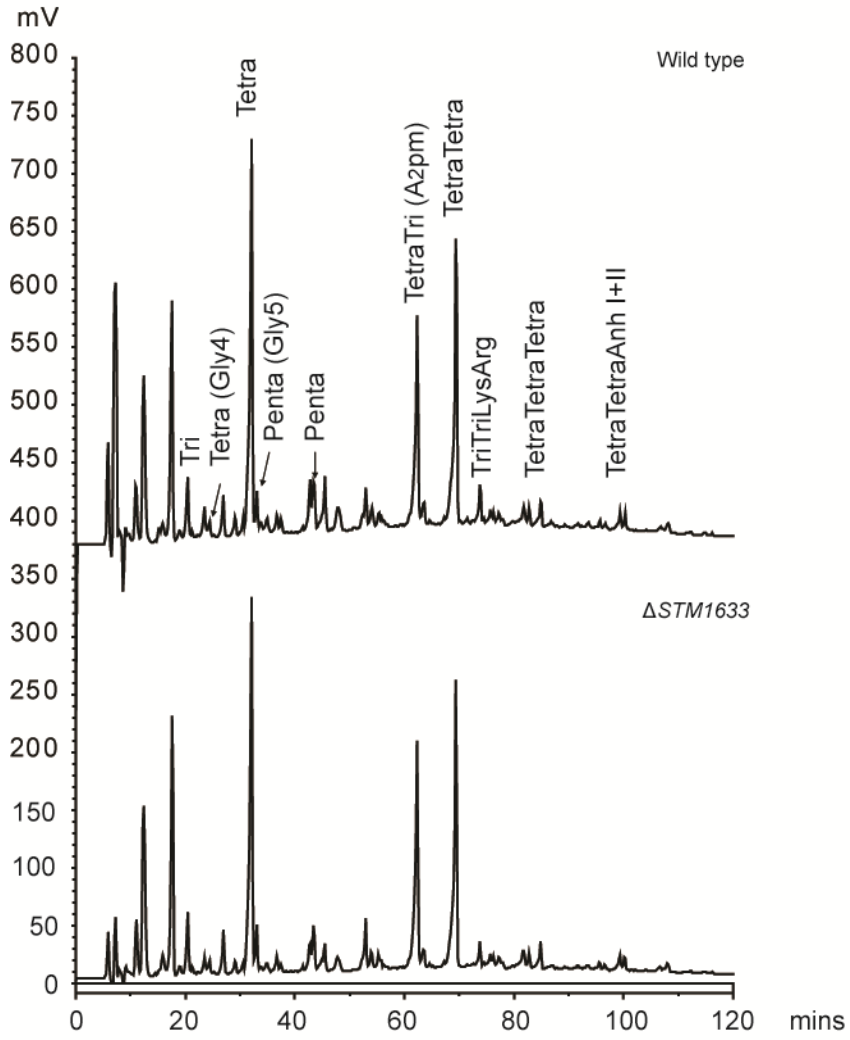
mV
800
750
700
650
600
550
500
450
400
350
300
250
200
150
100
50
0
Wild type
Tetra
Tri
Tetra (Gly4)
Penta (Gly5)
Penta
TetraTri (A2pm)
TetraTetra
TriTriLysArg
TetraTetraTetra
TetraTetraAnh I+II
ΔSTM1633
0
20
40
60
80
100
120
mins

Table 3.S1: Primers Used in Experimental Procedures

Primer Name	Sequence
SEO001	GCAAGCTAATTATAAGGAGATGAAATTGGAATCGCCACTAGTGTAGGCTGGAGCTGCTTCG
SEO002	GGCCACACGTATGCCCCTGCACCTCAATCGTGAGAGTGCAACATATGAATATCCTCCTTA
SEO007	CCGCTCGAGTGTAAAAATGCTTCCGACCG
SEO008	CACCAATTGTTACATCGATAAGCCAAATTTT
SEO013	GTTGCGAACCTTTGGGAGTACAGACAATGCAAGAGAATTATAAGGTGTAGGCTGGAGCTGCTTCG
SEO014	CTTCGCGGTGAGAGGCGCATTCGCCTCATGCTTTAGAACCGTCCATATGAATATCCTCCTTA
SEO027	ACGCGTCGACCACATTGGCGAGCAGGAA
SEO037	GCTCTAGATTACTACGCATAATCCGGCACATCATACGGATACGCATAATCCGGCACATCATACGGATAAAATTTCATCCAGCTATCGACAATGCCAG
SEO068	GGGGTACCCCGTTGCCAGGATAACTTAA
SEO069	CGAGCTCAAAGCCATGAGTATCACCTC
SEO070	ACGCGTCGACGCTATCTATTTCCTGTAGTAAG
SEO071	ACGCGTCGACTAGTAAGCTATGTCATCAGG
SEO161	7TATGTCCAGTATACTAATGTC
SEO162	TATGTCCAGTATACTAATGTC
SEO163	ATGTATTCCATCGCTGTTAAC
SEO172	GGAATTCCATATGTTATCCAAAAAATTTGGCTTATC
SEO173	AAGGATCCCTAGTGGTGGTGGTGGTGGTGTTTCATCCAGCTATCGACAATGCC
BTR36	AGTAAGCCGTTCCTCGAGGGTATCCAATAGAATATTTATT
BRT37	CCCTCGAGGAACGGCTTACTCCGACCTTATCAAAAACGAT
BRT38	AGTAAGCCGCTCCTCGAGGGTATCCAATAGAATATTTATT
BRT39	CCCTCGAGGAGCGGCTTACTCCGACCTTATCAAAAACGAT
SsrBc-HISF	GGAATTCCATATGGAATTAAACGCTGACACGACC
SsrBc-HISR	CGCGGATCCTTATTAGTGATGGTGATGGTGATGATACTCTATTAACCTCATTCTTCGGGC
rrshF	7AATACCGCATAACGTCGCAA
rrshR	TGCAATATTCCCCACTGCTG

* 7; biotin

Table 3.S2: Data Collection for STM1633 Crystal Structure Refinement

Data Collection	STM1633 + 5mM L-gly	STM1633 (apo)
Wavelength (Å)	0.9792	0.9792
Space group	$P6_122$	$P6_122$
Cell parameters		
a, b, c	81.08, 81.08, 187.9	79.83, 79.83, 188.63
α, β, γ	90, 90, 120	90, 90, 120
No. Copies in cell	12	12
Resolution range (Å)	50.0-1.9 (1.93-1.90)	50.0-2.0 (2.03-2.00)
Data Redundancy	21.0 (21)	21.0 (20.9)
Completeness (%)	97.5	97.5
I/σ(I)	25 (4.7)	37 (6.1)
R_{merge} (%)	9.4 (83.9)	8.3 (70.1)
Wilson *B* factor	28.7	26.4

Model and refinement	Model with D-Ala	Model with L-Gly	Model with L-Gly
Resolution range (Å)	50.0-1.9	50.0-1.9	50.0-2.0
R_{work} (%)	19	19	18.4
R_{free} (%)	20.3	20.3	21.6
Refl. Observed	28934	28934	24299
Refl. Test set	2000	2000	1998
No. of protein atoms	1811	1811	1815
No. of ligand atoms	6	5	5
No. of waters	168	168	124
rmsd bond lengths (Å)	0.012	0.012	0.006
rmsd bond angles (Å)	0.95	0.95	0.99
Average *B* factor ($Å^2$)	35.54	35.4	33.2

Chapter Four – Transcriptional priming of *Salmonella* Pathogenicity Island-2 precedes cellular invasion

Chapter Four – Co-authorship statement

Chapter four consists of the following publication:

Osborne, S.E. and Coombes, B.K. (2011). Transcriptional priming of *Salmonella* Pathogenicity Island-2 precedes cellular invasion. PLoS One; 6(6):e21648.

1) Design of experiments and writing of the manuscript done by S.E.O. and B.K.C.

2) All experiments performed by S.E.O.

Transcriptional priming of *Salmonella* Pathogenicity Island-2 precedes cellular invasion

Suzanne E. Osborne [1] and Brian K. Coombes [1*]

[1] Michael G. DeGroote Institute for Infectious Disease Research, Department of Biochemistry and Biomedical Sciences, McMaster University, Hamilton, ON. L8N 3Z5. Canada.

Key Words: *Salmonella*, SsrB, SPI-2, *in vivo* imaging

[*] Corresponding author:

Brian Coombes, PhD.,

Department of Biochemistry and Biomedical Sciences

HSC-4H17, McMaster University

Phone: 905-525-9140 ext 22159

Fax: 905-522-9033

e-mail: coombes@mcmaster.ca

Abstract

Invasive salmonellosis caused by *Salmonella enterica* involves an enteric stage of infection where the bacteria colonize mucosal epithelial cells, followed by systemic infection with intracellular replication in immune cells. The type III secretion system encoded in *Salmonella* Pathogenicity Island (SPI)-2 is essential for intracellular replication and the regulators governing high-level expression of SPI-2 genes within the macrophage phagosome and in inducing media thought to mimic this environment have been well characterized. However, low-level expression of SPI-2 genes is detectable in media thought to mimic the extracellular environment suggesting that additional regulatory pathways are involved in SPI-2 gene expression prior to cellular invasion. The regulators involved in this activity are not known and the extracellular transcriptional activity of the entire SPI-2 island *in vivo* has not been studied. We show that low-level, SsrB-independent promoter activity for the *ssrA-ssrB* two-component regulatory system and the *ssaG* structural operon encoded in SPI-2 is dependent on transcriptional input by OmpR and Fis under non-inducing conditions. Monitoring the activity of all SPI-2 promoters in real-time following oral infection of mice revealed invasion-independent transcriptional activity of the SPI2 T3SS in the lumen of the gut, which we suggest is a priming activity with functional relevance for the subsequent intracellular host-pathogen interaction.

Introduction

Salmonella enterica causes a range of foodborne diseases from self-limiting gastroenteritis to fatal systemic infections. The virulence capabilities of *Salmonella* is mediated by two type III secretion systems (T3SSs) which function to deliver bacterial proteins (called effectors) into host cells that can reprogram various aspects of host biology [1,2]. The two T3SS in *Salmonella* are encoded by separate horizontally acquired pathogenicity islands termed *Salmonella* Pathogenicity Island (SPI)-1 and SPI-2. The T3SS-1 allows *Salmonella* to invade into host epithelial cells and is needed to establish infection in the gastrointestinal tract [3]. Following passage across the host epithelial barrier the bacteria are engulfed by resident immune cells, chiefly macrophages [4,5], and induce the expression of the T3SS-2 [6,7]. Effectors translocated by the T3SS-2 play a critical role in protection against an arsenal of host defences including recruitment of reactive oxygen (ROS) and reactive nitrogen (RNS) species to the *Salmonella* containing vacuole (SCV) [8,9].

The T3SS in SPI-2 is organized into four major operons; a regulatory operon, a structural-1 operon, an effector/chaperone operon and a structural-2 operon. Genes in these operons are controlled by promoters in front of *ssrA*, *ssaB*, *sseA* and *ssaG* respectively [10,11]. We recently identified two additional promoters (*ssaM* and *ssaR*) in the structural-2 operon [11]. The major regulator of SPI-2 gene expression is a two-component regulatory system encoded by the genes *ssrA* and *ssrB* in the linked regulatory

operon. In response to an unidentified environmental cue, the SsrA sensor kinase autophosphoryates and activates the SsrB response regulator that can bind to an evolved palindrome sequence to induce gene expression from the SPI-2 promoters and at several promoters outside of SPI-2 [11,12]. Expression of *ssrA* and *ssrB* is autoregulated and also dependent on several ancestral transcription factors including the two-component systems PhoP-PhoQ, OmpR-EnvZ, as well as SlyA and Fis. SPI-2 is negatively regulated by H-NS, Hha and YdgT [13,14,15,16,17,18,19].

It is well established that transcriptional activity in SPI-2 is highly induced following intracellular invasion into cells as well as in *in vitro* conditions thought to mimic the intracellular environment [20,21,22]. However, we and others have reported low-level SPI-2 gene expression in non-inducing media that does not simulate the intracellular environment [22,23,24]. Of particular importance is that the expression under non-inducing conditions is independent of SsrB, suggesting another transcriptional input pathway for SPI-2 gene expression that may precede cellular invasion. In addition to its role in systemic dissemination of bacteria, accumulating evidence indicates that the SPI-2 T3SS contributes to bacterial colonization of the gut and to intestinal inflammation [25,26,27]. It was also shown using recombinase-based *in vivo* expression that three promoters in SPI-2 (*sseA, ssaG* and *spiC*/*ssaB*) are activated within 15 min after entering mouse ileal loops [28]. These data suggest that a transcriptional regulatory circuit operates to induce low-level gene expression in SPI-2 prior to *Salmonella*'s invasion into host cells.

We analyzed the activity of all six promoters in SPI-2 in both inducing and non-inducing media in a variety of *Salmonella* mutants lacking the regulators involved in SPI-2 gene expression. Inducing media resulted in high simultaneous activity of each SPI-2 promoter that was dependent on SsrB. In contrast, SPI-2 promoters had low-level activity in non-inducing media that was independent of SsrB but instead dependent on OmpR or Fis. We further analyzed SPI-2 promoter activity during animal infection in real time and found that SPI-2 promoters were activated immediately following entry into the small intestine that was independent of invasion. Using cultured epithelial cells we demonstrate that SPI-2 has two distinct activation events; an immediate invasion- and host cell-independent up-regulation and the classical intracellular activity.

Results

Regulation of SPI-2 under non-inducing conditions

To compare the activity of SPI-2 promoters in both inducing and non-inducing conditions *in vitro* we constructed bacterial luciferase transcriptional reporters for each of the six promoters in SPI-2 (*ssrA*, *ssaB*, *sseA*, *ssaG*, *ssaM* and *ssaR*) [10,11]. To simulate inducing conditions we used an acidic minimal medium low in phosphate and magnesium (LPM pH 5.8) that is well established to activate robust SPI-2 gene expression [22]. M9-CAA medium containing millimolar concentrations of divalent cations and a neutral pH

was used as a non-inducing media [29]. Wild type *S.* Typhimurium containing transcriptional reporters were grown in M9-CAA until mid-log phase at which point they were sub-cultured into either inducing or non-inducing media followed by continuous luminescence measurements. Following transfer to LPM each SPI-2 promoter was induced with the same kinetics but the magnitude of this activity varied with each reporter (Figure 4.1A). Promoter activity peaked at early to mid-exponential phase and then declined and remained constant at ~20-30% of maximum activity (Table 4.S1 and 4.S2 for complete dataset). We consistently observed an early, low-level reporter activity primarily from the regulatory and structural-1 promoters (*ssrA* and *ssaG*) under non-inducing conditions (Figure 4.1B), followed by delayed activity from the remaining structural-2 and effector promoters (Figure 4.1C). These results suggested that SPI-2 promoters had unique transcriptional inputs under inducing and non-inducing conditions that gave rise to differential timing and magnitude of gene expression.

SPI-2 expression in non-inducing conditions has distinct regulatory inputs

In order to understand the regulatory input contributing to the activity of SPI-2 promoters in non-inducing conditions, we measured promoter activity in eight different mutants each lacking a major regulator known to be involved in virulence gene expression in *Salmonella* [11,18,19,30,31,32], including *ssrB*, *ompR*, *slyA*, *phoP*, *fis*, *ydgT*, *hha* and *hns*. Loss of the known activators SsrB, OmpR, SlyA, PhoP or Fis caused a marked decrease in the promoter activity observed in LPM for each SPI-2 promoter (Table 4.1; Figures 4.S1-4.S2, Tables 4.S1-4.S2 for full dataset). Interestingly, loss of

PhoP altered the temporal dynamics of all promoters with the exception of the *ssrA* promoter (Figure 4.S1). Deletion of the known SPI-2 repressors YdgT, Hha or expression of dominant negative H-NS (HNSQ92am) [33] increased SPI-2 promoter activity in most cases although loss of YdgT and Hha caused a decrease in *ssaG* and *ssaR* promoter activity (Figure 4.S2). The *ssrA* and *ssaG* promoter activity in M9-CAA was independent of SsrB. Instead, the *ssrA* promoter activity in M9-CAA was dependent on OmpR and partially dependent on Fis, and *ssaG* promoter activity was dependent only on Fis. These results confirmed that the low-level SPI-2 promoter activity under non-inducing conditions had distinct regulatory inputs to that needed for high-level expression under inducing conditions thought to mimic the intracellular environment.

SPI-2 promoters are induced in the lumen of the gut following oral infection

The observation that SPI-2 promoters are modestly active under non-inducing conditions suggested that extracellular priming of SPI-2 gene expression may occur. Previous work using recombinase-based *in vivo* expression had established that three promoters, (*sseA*, *ssaG*, and *ssaB*/*spiC*), were active in the lumen of the murine gut following direct injection of bacteria into ileal loops [28]. However, the *in vivo* activity of the entire complement of SPI-2 promoters following oral infection has not been tested. Mice infected by oral gavage with individual *Salmonella* strains that report the activity of each SPI-2 promoter were subjected to *in vivo* luminescence imaging immediately following infection (Figure 4.2). Each SPI-2 promoter was simultaneously and immediately activated with luciferase signal being localized exclusively to the small

intestine in the first 35 min following infection, as determined by *ex vivo* imaging of individual organs at the terminal time point (Figure 4.3). When we compared the normalized light flux from each promoter, we found no significant difference in relative promoter activity, nor differences in the number of bacteria of each reporter strain recovered from each organ (data not shown). To assess promoter activity in animals over a longer time period, mice were imaged every day for three days following oral infection. These data showed that *sseA* promoter activity remained active over three days in bacteria localized in the gut (Figure 4.S3). Using *ex vivo* imaging at necropsy we also detected luminescence signal originating from systemic tissues as expected since *S.* Typhimurium gives rise to an invasive infection in mice (Figure 4.S3).

The rapid increase in SPI-2 promoter activity observed following bacterial entry into the small intestine suggested that this transcriptional activity was originating in the gut lumen prior to bacterial invasion of the epithelium. To investigate this, we constructed the P_{sseA}-*lux* reporter in an *invA* mutant that is defective for cellular invasion [34] and quantified luminescence following oral infection. Promoter activity from the invasion-deficient strain showed a rapid increase after infection, similar in tempo and magnitude to that from wild type cells (Figure 4.4). As expected, luminescence was localized exclusively to the small intestine, suggesting that immune cell sampling of luminal bacteria was not responsible for this activity. These data are consistent with results using direct injection into murine ileal loops of recombinase-based reporter strains [28]. These

results demonstrate that following entry of *S.* Typhimurium in to the intestinal lumen, all SPI-2 promoters undergo a rapid increase in activity that precedes cellular invasion.

SPI-2 transcriptional priming is in-dependent of host cell contact

Our finding that SPI-2 promoters are rapidly induced following entry into the lumen but prior to invasion promoted us to question whether this activity was dependent on host cell contact. P_{sseA}-*lux* reporter bacteria were pre-grown in either M9-CAA or LB then subcultured into DMEM/10%FBS and luminescence activity was recorded in 96-well plates in the presence or absence of HeLa epithelial cells. Plates were centrifuged to synchronize host cell contact. Regardless of the pre-growth media, P_{sseA}-*lux* activity was found to have an immediate burst of transcriptional activity within the first 15 minutes that was independent of both invasion and the presence of HeLa cells (Figure 4.5). A second spike in transcriptional activity was observed at 1 hour post-infection which reflects arrival in the intracellular niche owing to the dependence on both HeLa cells and invasion. This data supports the model that SPI-2 undergoes two distinct transcriptional activation events; an early priming activation and a transcriptional up-regulation specific to the intracellular niche.

Discussion

Since the discovery of the T3SS-2 [6,7], extensive work has elucidated its essential role for intracellular survival of *S.* Typhimurium. The regulation of this system

has been well characterized for conditions thought to mimic the intracellular environment encountered by the bacteria following cellular invasion. However little is known about the regulation of the SPI-2 T3SS preceding cellular invasion, although we think such a regulatory input would have relevance. *Salmonella* survival in macrophages and other cell types requires deployment of bacterial effectors by the SPI-2 T3SS that are known to block phagosome maturation and to counteract host defensive mechanisms such as reactive oxygen and nitrogen species [8,9,35,36]. These processes are invoked essentially immediately following phagocytosis, which would require a coincident functional response from the T3SS.

Although all SPI-2 promoters had simultaneous and high activity upon transfer to a synthetic inducing media, most – particularly the *ssaG* and *ssrA* promoters – had significant albeit lesser activity in non-inducing media. Surprisingly, the SPI-2 response regulator SsrB accounted for less than 5% of this activity and instead the transcriptional input was dominated by OmpR and Fis. Indeed, Fis binding sites have been identified upstream of *ssaG* [37] and OmpR and SsrB binding sites overlap at the *ssrA* promoter [14], which is entirely consistent with the transcriptional inputs we measured. Expression of SPI-2 immediately following entry of the bacteria into the small intestine is also consistent with a growing body of evidence indicating that the SPI-2 T3SS contributes to intestinal colonization. Using a recombinase-based reporter system and mouse ileal loops it was shown that the *sseA* promoter was activated within 15 min of entry into the ileum [28] when bacterial cells are associated with the apical surface of the host epithelium.

This activity was also dependent on OmpR, suggesting that this regulatory input may be a key source of transcriptional priming *in vivo* prior to cellular invasion. Bovine and mouse infections have shown that the SPI-2 T3SS is necessary for enteric infection and triggers colitis in a MyD88-dependent manner [25,26,27,38]. Our data in conjunction with these findings provides strong evidence for the expression of the SPI-2 T3SS in the intestine. It also implies that alternative extracellular signals are involved in SPI-2 regulation within the intestinal lumen, with possible candidates being mammalian body temperature [33], the acidity encountered during transit through the stomach, or other signals that are presently unknown.

The exact role of SPI-2 promoter activity in the intestinal lumen is presently unclear. Although SPI-2 is needed for enteric infection, this phenotype does not manifest until several days after infection, suggesting that the early transcriptional activity we measured is unrelated to this functionality. Instead, we propose that rapid activation of SPI-2 following entry into the lumen of the host gut reflects a need for transcriptional priming for survival within the intracellular environment. Consistent with the notion of transcriptional priming, in mice in which disease is dominated by a systemic infection of the reticuloendothelial system, we found each promoter in SPI-2 to be active within five minutes following oral infection. This activity was sustained even in bacteria with a genetic lesion in the invasion machinery, indicating that SPI-2 transcriptional priming precedes cellular invasion. The T3SS-2 is needed for *Salmonella* to evade host antibacterial mechanisms such as reactive oxygen and nitrogen delivery to the nascent

phagosome [8,9] and SPI-2 mutant bacteria have a marked defect in preventing NADPH oxidase recruitment to the phagosome [39]. However, reactive oxygen generation inside nascent phagosomes by the host NADPH oxidase complex is detectable within 1-min following phagocytosis of reactive oxygen-sensitive beads [40] or yeast cells [41], which argues strongly for transcription priming of this bacterial defence system before the invasion event. Further research will be needed to quantify the intracellular fitness benefit immediately succeeding invasion that is conferred by this early SPI-2 gene expression.

Methods and Materials

Ethics Statement. All animal work was approved by the Animal Review Ethics Board at McMaster University under Animal Use Protocol #09-07-26, and conducted according to guidelines set by the Canadian Council on Animal Care.

Bacterial Strains and Growth Conditions. *Salmonella enterica* serovar Typhimurium strain SL1344 was used for all experiments and all mutants are derivatives thereof. Bacteria were grown at 37°C with aeration in the presence of selective antibiotics where appropriate as follows: ampicillin (100 µg/mL), kanamycin (50 µg/mL), chloramphenicol (34 µg/mL), tetracycline (12 µg/mL) and streptomycin (50 µg/mL). For transcriptional reporter experiments, bacteria were cultured overnight in M9-CAA minimal media (5 mM $Na_2HPO_4•7H_2O$, 22 mM KH_2PO_4, 8.6 mM NaCl, 18.6 mM NH_4Cl, 11.1 mM glucose, 2 mM $MgSO_4$, 100 µM $CaCl_2$, 0.1% casamino acids). Low phosphate, low

magnesium medium (LPM) [22] pH 5.8 was used as a highly-inducing medium for SPI-2 gene expression (5 mM KCl, 7.5 mM $(NH_4)_2SO_4$, 80 mM MES, 38 mM glycerol, 0.1% casamino acids, 24 µM $MgCl_2$, 337 µM PO_4^{3-}).

Cloning and Mutant Construction. Unmarked, in-frame deletions of *slyA* and *ompR* as well as a marked in-frame deletion of *fis* (*fis*::Kan) were constructed using Lambda red recombination [42]. Transcriptional reporters with *luxCDABE* were constructed in pGEN-*luxCDABE* [43] for all six of the promoters identified in SPI-2 [11] including *ssrA, ssaB, sseA, ssaG, ssaM,* and *ssaR*. All primers used for mutant construction and cloning of transcriptional reporters are listed in Table S2.

Transcriptional Reporter Assays. Bacteria were grown overnight in M9 CAA at 37°C with shaking and then sub-cultured 1:100 into M9 CAA in 96-well plates (Costar). Bacteria were grown at 37°C (150 rpm) and optical density at 600 nm (OD_{600}) and luminescence were measured every 15 min using an Envison 2104 Multiwell plate reader (PerkinElmer). Luminescence data was normalized to OD_{600nm} for each time point and adjusted to the luminescence at time zero.

***In vivo* Bioluminescence Imaging**. Three days prior to infection, abdominal fur was removed from the mice using a depilatory cream. *Salmonella* with luciferase reporters were grown overnight in M9 CAA with selective antibiotics at 37°C. Bacteria were

washed twice and resuspended in 0.1 M HEPES (pH 8.0), 0.9% NaCl. Female C57BL/6 mice (Jackson Laboratories) were infected by oral gavage with ~10^8 live bacteria. Animals were immediately anaesthetized with 2% isofluorane carried in 2% oxygen and imaged dorsally in an IVIS Spectrum (Caliper Life Sciences). Greyscale and luminescence images were captured at 5 min intervals for 35 min and processed using Living Image Software. After the imaging session, mice were sacrificed and individual organs were imaged *ex vivo* and then processed for bacterial load determination by homogenization in a Mixer Mill (Retsch; Haan, Germany) and selective plating on solid media. Total flux was normalized to the initial flux recorded at time zero.

HeLa Cell Culture. HeLa cells were seeded in 96-well plates with clear bottoms at 2 x 10^5 cells/mL 24 hours prior to infection. Overnight cultures of wild type or invasion-deficient Δ*invA* carrying (pP_{sseA}-*lux*) were pregrown in with LB or M9-CAA for 3 hours then subcultured 1:100 into DMEM (Gibco) with 10% fetal bovine serum (FBS). 50µL was added to the 96-well plates and centrifuged at 500 x g for 5 minutes. Bioluminescence was recorded as described above. Cells were grown at 37°C in 5% CO_2.

Financial Disclosure

This research was funded through an operating grant from the Canadian Institutes of Health Research (CIHR; MOP-82704) and an infrastructure grant from Canada

Foundation for Innovation Leaders Opportunity Fund. The funders had no role in study design, data collection and analysis, decision to publish, or preparation of the manuscript.

Acknowledgements

SEO is the recipient of the CIHR-Vanier Canada Graduate Scholarship. BKC is a CIHR New Investigator and the Boehringer Ingelheim Young Investigator in the Biological Sciences.

Figure Legends

Figure 4.1. SPI-2 expression in inducing and non-inducing conditions *in vitro*. *S.* Typhimurium with luciferase transcriptional reporters for each SPI-2 promoter were sub-cultured from actively growing cultures in M9-CAA into either (A) inducing (LPM pH 5.8) or (B) non-inducing (M9-CAA) media. Luminescence was quantified continuously and normalized to OD_{600nm} at each time point (n = 12). Heat maps represent the percent activity relative to each individual promoter's maximal expression level.

Figure 4.1

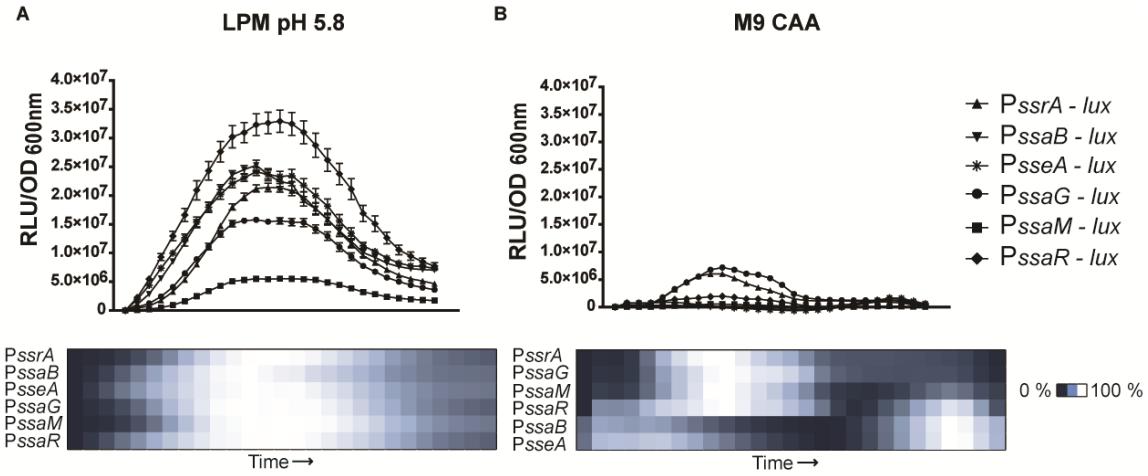
A
LPM pH 5.8
B
M9 CAA
RLU/OD 600nm
4.0×10^7
3.5×10^7
3.0×10^7
2.5×10^7
2.0×10^7
1.5×10^7
1.0×10^7
5.0×10^6
0
PssrA - lux
PssaB - lux
PsseA - lux
PssaG - lux
PssaM - lux
PssaR - lux
PssrA
PssaB
PsseA
PssaG
PssaM
PssaR
Time ⟶
0 %
100 %

Figure 4.2. SPI-2 promoter activity increases immediately following entry into the small intestine. Mice were infected by oral gavage with *S.* Typhimurium strains carrying the luciferase transcriptional reporters. Animals were anesthetised and luminescence was measured as described in Methods. Colour bars for each reporter time course are indicated. Data is representative of four biological replicates each showing similar results.

Figure 4.2

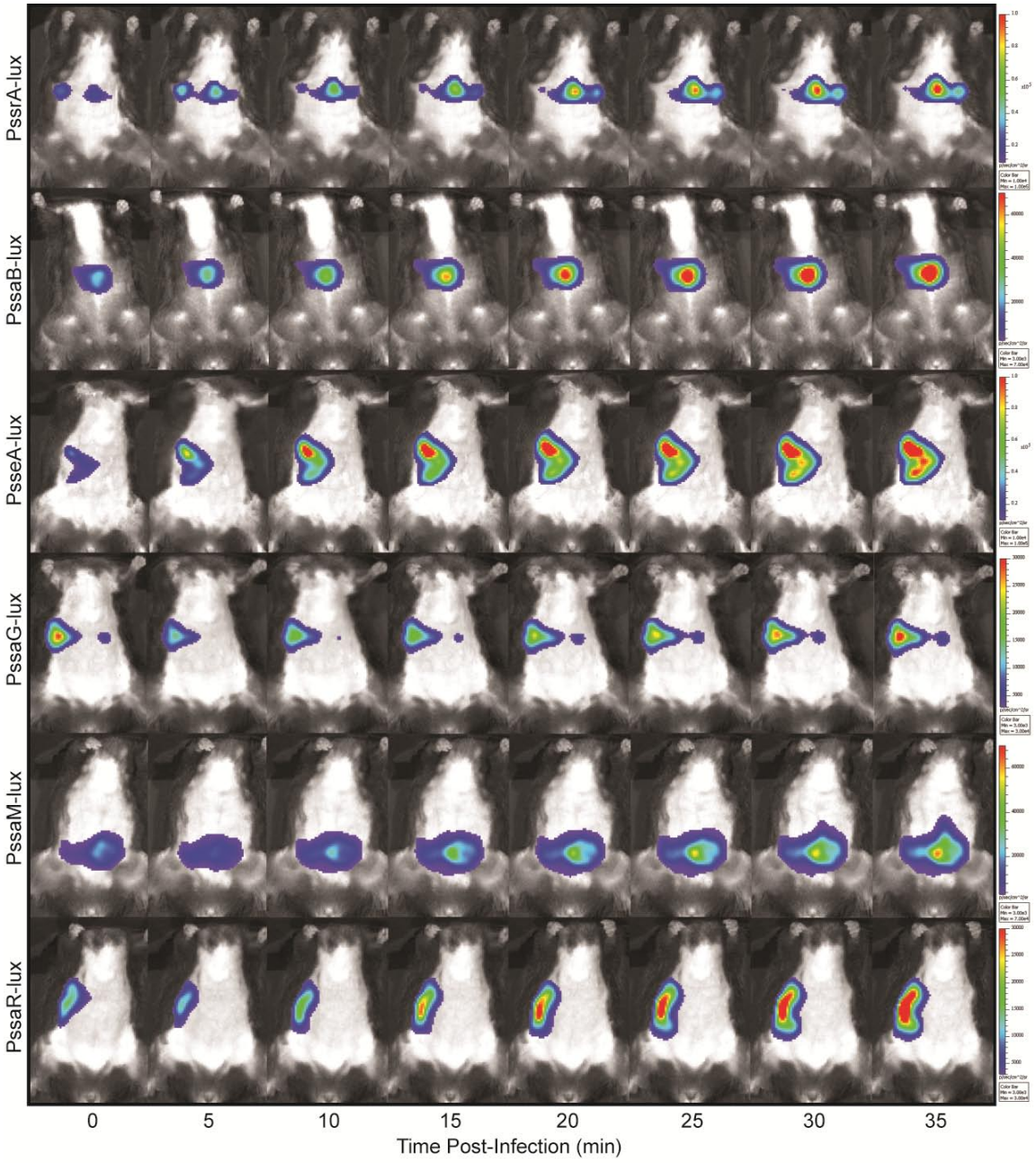
PssrA-lux
PssaB-lux
PsseA-lux
PssaG-lux
PssaM-lux
PssaR-lux
0
5
10
15
20
25
30
35
Time Post-Infection (min)

Figure 4.3. Quantification and *ex vivo* imaging of luminescence. (A) Quantification of luminescence (total flux) is shown as the mean with standard deviation for each time point (n = 4). (B) Individual organs (S, spleen and L, liver, left panels; SI, small intestine; LI, large intestine and C, cecum, right panels) were imaged *ex vivo* at necropsy. (C) Light flux from individual organs was normalized to bacterial load. Data are the means with standard deviation from four organs for each reporter strain at the termination of the 35 min imaging session.

Figure 4.3

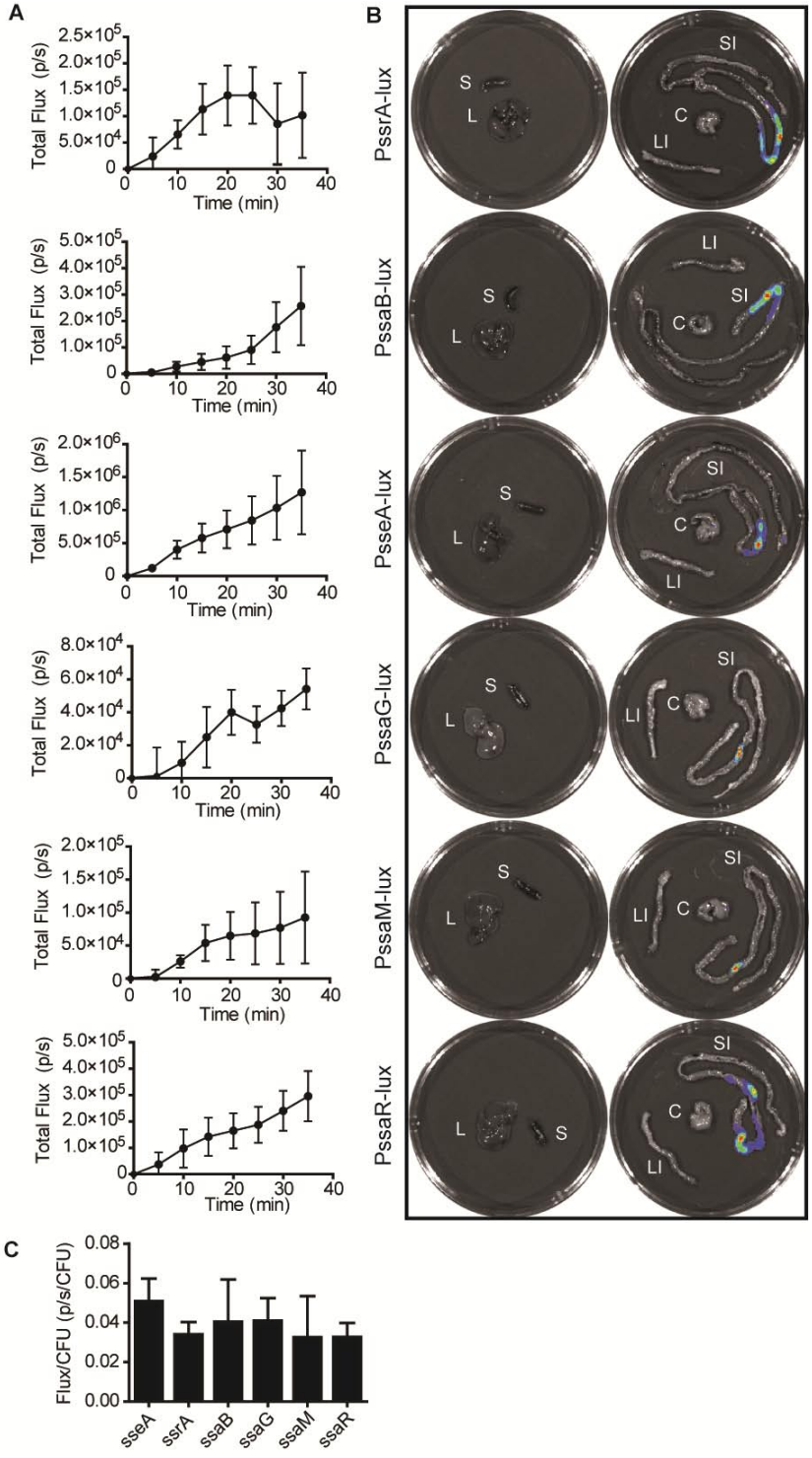
A
Total Flux (p/s)
Time (min)
B
PssrA-lux
PssaB-lux
PsseA-lux
PssaG-lux
PssaM-lux
PssaR-lux
S
L
C
LI
SI
C
Flux/CFU (p/s/CFU)
sseA
ssrA
ssaB
ssaG
ssaM
ssaR

Figure 4.4. SPI-2 promoter activity in the small intestine does not require T3SS-1-mediated invasion. Mice were infected with an invasion-deficient mutant (*invA*::Kan) carrying an *sseA* promoter fusion to *luxCDABE*. Immediately after infection, anesthetised mice were imaged as described. (A) Whole-body luminescence from infected mice. Images are representative of three individual animals. (B) Quantification of luminescence (total flux) is shown as the mean with standard deviation for each time point (n = 3). (C) Individual organs (spleen and liver, left panel; small intestine, colon and cecum, right panel) were imaged *ex vivo* at necropsy.

Figure 4.4

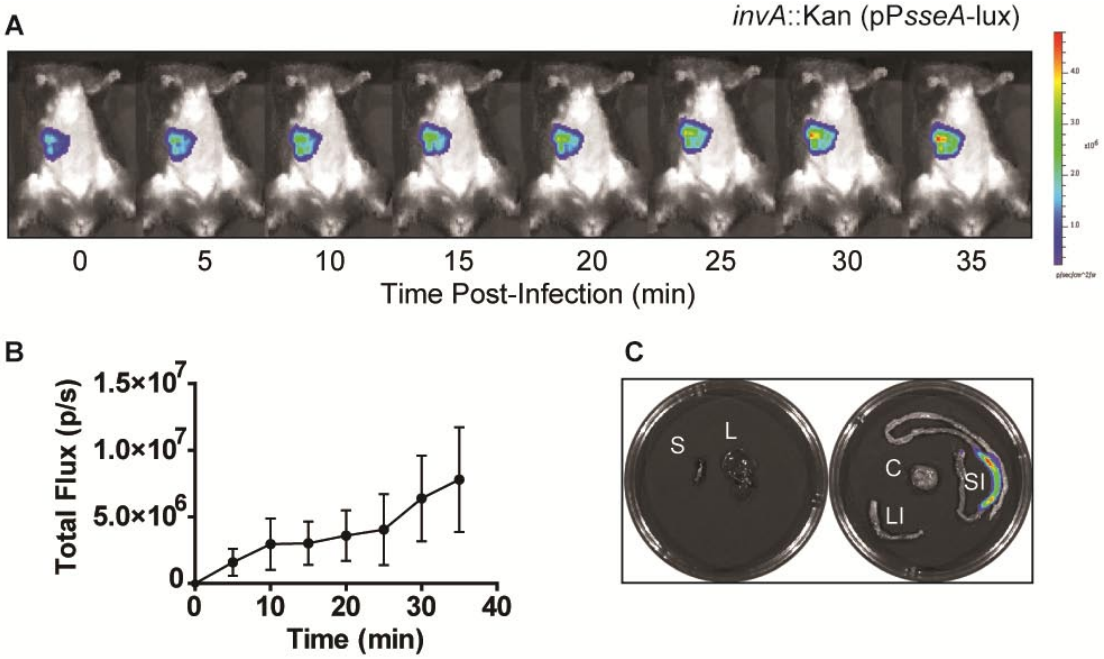
A
invA::Kan (pPsseA-lux)
0
5
10
15
20
25
30
35
Time Post-Infection (min)
B
Total Flux (p/s)
1.5×10^7
1.0×10^7
5.0×10^6
0
0
10
20
30
40
Time (min)
C
S
L
C
SI
LI

Figure 4.5. SPI-2 undergoes two stages of transcriptional up-regulation. Wt or invasion deficient (Δ*invA*) *Salmonella* carrying *sseA* bioluminescence promoter fusions were pre-grown in M9-CAA or LB then subcultured into DMEM/10%FBS. Bioluminescence activity was then monitored in the presence or absence of HeLa cells.

Figure 4.5

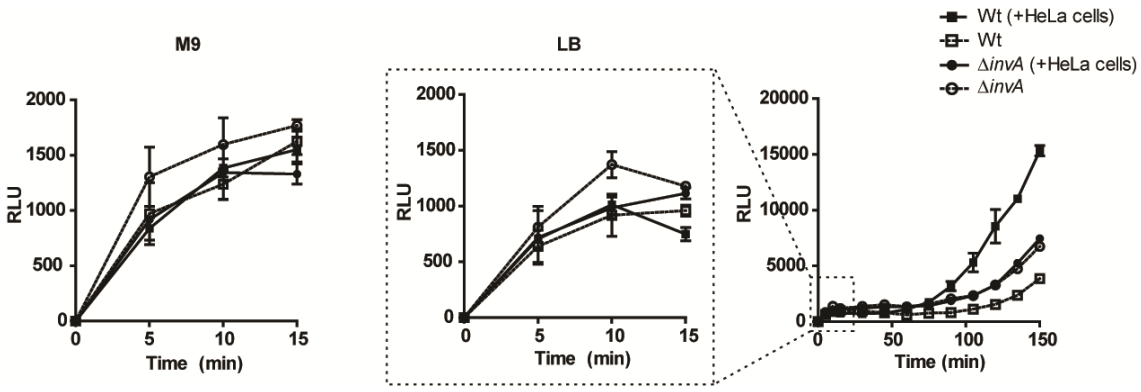
M9
LB
Wt (+HeLa cells)
Wt
ΔinvA (+HeLa cells)
ΔinvA
RLU
Time (min)
2000
1500
1000
500
0
5
10
15
20000
15000
10000
5000
50
100
150

Table 4.1. Transcriptional reporter activity relative to wild type

	Mutant background						
LPM pH 5.8	Δ*ssrB*	Δ*ompR*	Δ*slyA*	*phoP* ::Cm	*fis* ::Cm	Δ*hha* Δ*ydgT*	*hns* Q92am
P_{ssrA}	67 ± 6.4	0.1 ± 0.0	59 ± 4.9	72 ± 12	75 ± 10	250 ± 67	390 ± 14
P_{ssaB}	0.0 ± 0.0	0.1 ± 0.1	0.9 ± 0.2	20 ± 5.8	4.6 ± 4.9	263 ± 52	270 ± 20
P_{sseA}	0.2 ± 0.0	0.8 ± 0.1	1.2 ± 0.3	37 ± 9.4	12 ± 8.3	296 ± 37	247 ± 25
P_{ssaG}	15 ± 1.5	12 ± 2	11 ± 1.2	36 ± 4.8	10 ± 4.3	26 ± 10	173 ± 14
P_{ssaM}	2.9 ± 0.2	3.1 ± 0.5	3.4 ± 0.2	24 ± 5.8	9.9 ± 3.0	1050 ± 41	413 ± 72
P_{ssaR}	3.6 ± 0.5	3.6 ± 0.7	4.2 ± 0.5	33 ± 6.4	12 ± 1.9	26 ± 1.2	96 ± 3.3
M9-CAA							
P_{ssrA}	95 ± 3.9	0.4 ± 0.0	105 ± 12	106 ± 3.0	50 ± 3.1	599 ± 208	176 ± 18
P_{ssaG}	100 ± 6.7	114 ± 3.6	96 ± 1.3	96 ± 6.4	18 ± 0.7	240 ± 50	117 ± 8.8

Supporting Figure Legends

Figure 4.S1. SPI-2 expression in inducing versus non-inducing conditions has distinct regulatory inputs. Graphs represent the entire dataset collected for the experiments involving transcriptional activators summarized in Table 1. Wild type *S.* Typhimurium carrying luciferase transcriptional reporters for each SPI-2 promoter were sub-cultured from actively growing cultures in M9-CAA into either inducing (LPM pH 5.8) or non-inducing (M9-CAA) media. Luminescence was measured continuously and normalized to OD_{600nm} at each time point (n = 12). Data are the means with standard deviation.

Figure 4.S1

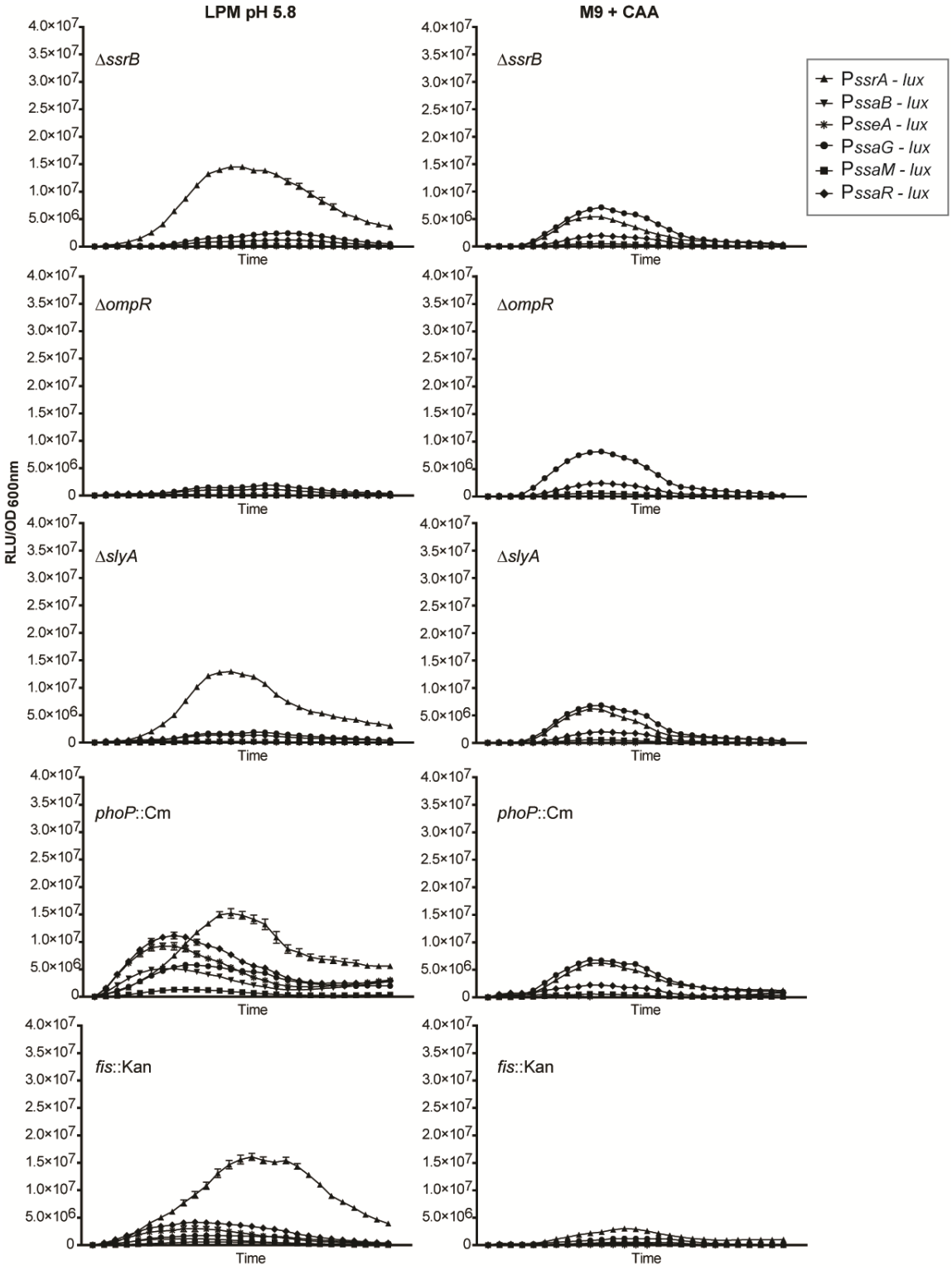
LPM pH 5.8
M9 + CAA
ΔssrB
ΔompR
ΔslyA
phoP::Cm
fis::Kan
RLU/OD 600nm
Time
PssrA - lux
PssaB - lux
PsseA - lux
PssaG - lux
PssaM - lux
PssaR - lux

Figure 4.S2. SPI-2 expression in inducing versus non-inducing conditions for transcriptional repressor mutants. Graphs represent the entire dataset collected for the experiments involving transcriptional repressors summarized in Table 1. Wild type *S.* Typhimurium carrying luciferase transcriptional reporters for each SPI-2 promoter were sub-cultured from actively growing cultures in M9-CAA into either inducing (LPM pH 5.8) or non-inducing (M9-CAA) media. Luminescence was measured continuously and normalized to OD_{600nm} at each time point (n = 12). Data are the means with standard deviation.

Figure 4.S2

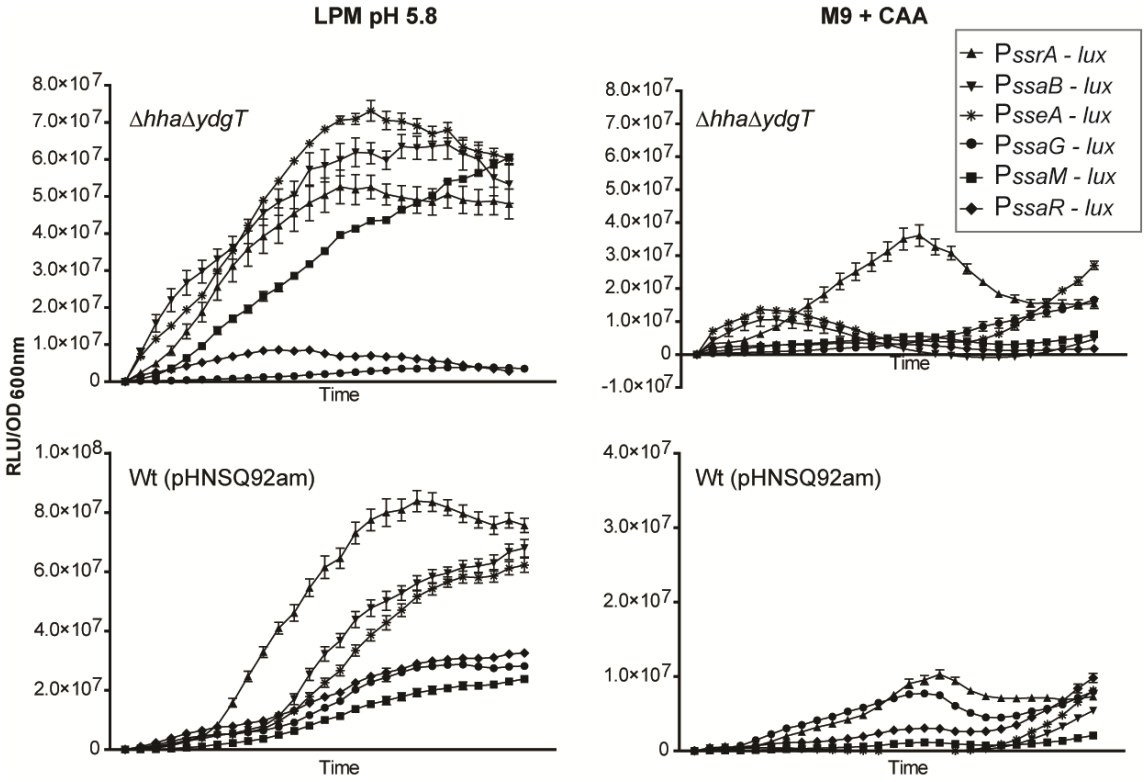
LPM pH 5.8
M9 + CAA
PssrA - lux
PssaB - lux
PsseA - lux
PssaG - lux
PssaM - lux
PssaR - lux
ΔhhaΔydgT
Wt (pHNSQ92am)
RLU/OD 600nm
Time

Figure 4.S3. The *sseA* promoter remains active from 1 to 3 days post infection. Mice were infected with wild type *Salmonella* containing the *sseA* transcriptional reporter. (A) Luminescence images were acquired every 24 h and are representative of three individuals animals. (B) Total flux from whole-animal imaging was quantified and is shown as the mean with standard deviation (n = 3). (C) At 3 days post-infection organs from infected mice from (A) were imaged *ex vivo* (S, spleen; L, liver; C, cecum; SI, small intestine; LI, large intestine).

Figure 4.S3

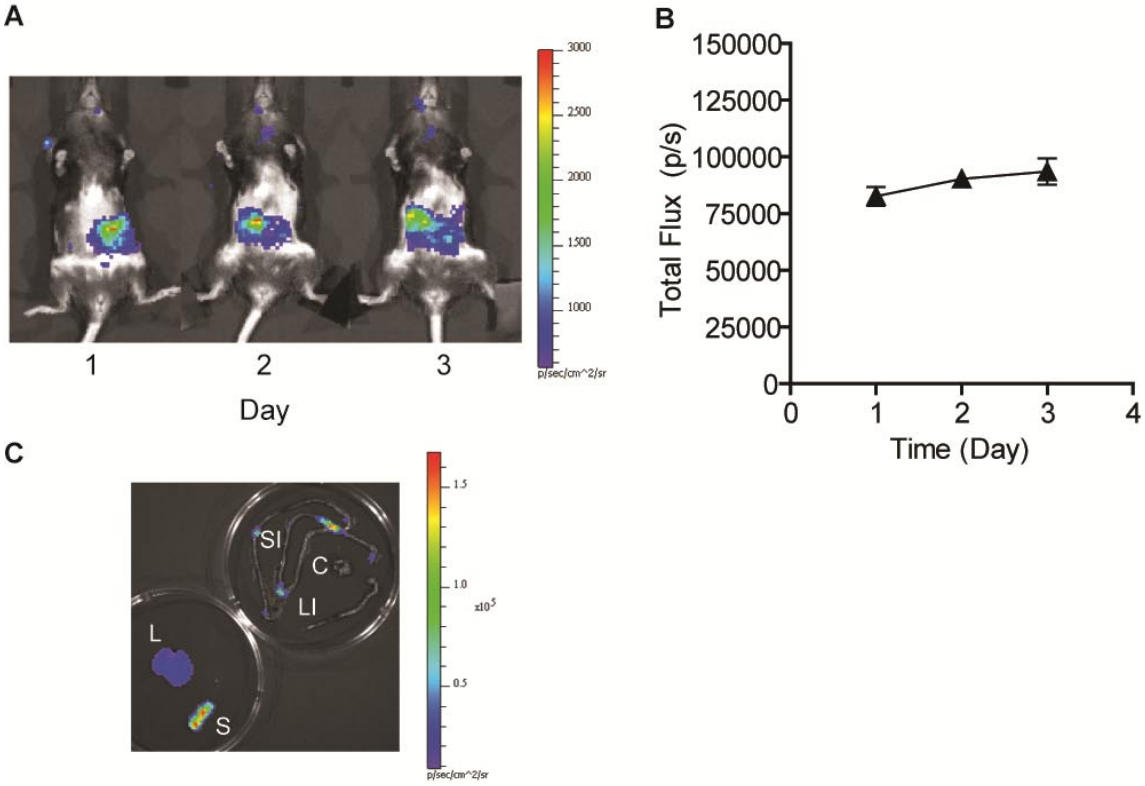
A
3000
2500
2000
1500
1000
p/sec/cm^2/sr
1
2
3
Day
B
150000
125000
100000
75000
50000
25000
0
Total Flux (p/s)
0
1
2
3
4
Time (Day)
C
SI
C
LI
L
S
1.5
1.0
x10^5
0.5
p/sec/cm^2/sr

Table 4.S1 – Quantification of Luminescence Activity Dynamics

Wild type

Promoter LPM pH 5.8	Rate of Luminescence Increase (RLU/min)	Max. Instantaneous Rate of Luminescence Increase (RLU/min)	Time of Max. Instantaneous Increase Rate (min)	Max. Luminescence (RLU/OD600nm)	Time of Max. Luminescence (min)	Steady State % of Max.
ssrA	$1.9 \times 10^5 \pm 1.6 \times 10^4$	$2.5 \times 10^5 \pm 2.3 \times 10^4$	115 ± 9	$2.2 \times 10^7 \pm 2.4 \times 10^6$	180 ± 15	24 ± 4
ssaB	$2.0 \times 10^5 \pm 2.0 \times 10^4$	$2.4 \times 10^5 \pm 2.3 \times 10^4$	115 ± 22	$2.5 \times 10^7 \pm 3.1 \times 10^6$	165 ± 30	29 ± 2
sseA	$1.8 \times 10^5 \pm 3.8 \times 10^4$	$2.0 \times 10^5 \pm 3.6 \times 10^4$	85 ± 38	$2.5 \times 10^7 \pm 1.5 \times 10^6$	170 ± 38	33 ± 4
ssaG	$1.4 \times 10^5 \pm 2.4 \times 10^4$	$1.8 \times 10^5 \pm 3. \times 10^4$	95 ± 23	$1.7 \times 10^7 \pm 4.3 \times 10^5$	185 ± 46	25 ± 5
ssaM	$5.7 \times 10^4 \pm 1.1 \times 10^4$	$6.7 \times 10^4 \pm 1.2 \times 10^4$	110 ± 17	$5.8 \times 10^6 \pm 6.1 \times 10^5$	190 ± 48	33 ± 1
ssaR	$2.3 \times 10^5 \pm 6.4 \times 10^4$	$3.2 \times 10^5 \pm 1.1 \times 10^5$	100 ± 17	$3.4 \times 10^7 \pm 3.3 \times 10^6$	180 ± 40	25 ± 3
Promoter M9						
ssrA	$8.8 \times 10^4 \pm 6.2 \times 10^3$	$1.0 \times 10^5 \pm 1.2 \times 10^4$	70 ± 9 **	$6.1 \times 10^6 \pm 3.5 \times 10^5$	130 ± 9	N/A
ssaG	$8.1 \times 10^4 \pm 3.5 \times 10^3$	$1.0 \times 10^5 \pm 1.2 \times 10^4$	70 ± 9	$7.2 \times 10^6 \pm 4.7 \times 10^5$	135 ± 0	N/A

Δ*ssrB*

Promoter LPM pH 5.8	Rate of Luminescence Increase (RLU/min)	Max. Instantaneous Rate of Luminescence Increase (RLU/min)	Time of Max. Instantaneous Increase Rate (min)	Max. Luminescence (RLU/OD600nm)	Time of Max. Luminescence (min)	Steady State % of Max.
ssrA	$1.6 \times 10^5 \pm 2.3 \times 10^4$	$1.8 \times 10^5 \pm 1.6 \times 10^4$	115 ± 17	$1.5 \times 10^7 \pm 1.4 \times 10^6$	185 ± 9	26 ± 1
ssaB	$2.6 \times 10^1 \pm 1.3 \times 10^1$	$1.9 \times 10^2 \pm 4.4 \times 10^1$	140 ± 17	$5.1 \times 10^3 \pm 1.9 \times 10^3$	200 ± 17	0
sseA	$3.0 \times 10^2 \pm 1.1 \times 10^2$	$9.1 \times 10^2 \pm 2.7 \times 10^2$	90 ± 65	$5.4 \times 10^4 \pm 6.2 \times 10^3$	225 ± 15	11 ± 3
ssaG	$1.4 \times 10^4 \pm 1.6 \times 10^3$	$2.8 \times 10^2 \pm 5.3 \times 10^3$	160 ± 46	$2.5 \times 10^6 \pm 2.5 \times 10^5$	245 ± 17	22 ± 6
ssaM	$2.0 \times 10^3 \pm 4.3 \times 10^2$	$2.5 \times 10^3 \pm 7.1 \times 10^2$	135 ± 15	$1.7 \times 10^5 \pm 8.7 \times 10^3$	215 ± 23	17 ± 9
ssaR	$9.7 \times 10^3 \pm 4.8 \times 10^3$	$1.7 \times 10^4 \pm 3.6 \times 10^3$	130 ± 9	$1.2 \times 10^6 \pm 1.6 \times 10^5$	250 ± 17	19 ± 8
Promoter M9						
ssrA	$7.8 \times 10^4 \pm 9.1 \times 10^3$	$9.3 \times 10^4 \pm 1.4 \times 10^4$	105 ± 0	$5.8 \times 10^6 \pm 2.4 \times 10^5$	140 ± 17	N/A
ssaG	$8.0 \times 10^4 \pm 1.6 \times 10^4$	$9.8 \times 10^4 \pm 2.0 \times 10^4$	95 ± 17	$7.2 \times 10^6 \pm 4.8 \times 10^5$	145 ± 9	N/A

Δ*ompR*

Promoter LPM pH 5.8	Rate of Luminescence Increase (RLU/min)	Max. Instantaneous Rate of Luminescence Increase (RLU/min)	Time of Max. Instantaneous Increase Rate (min)	Max. Luminescence (RLU/OD600nm)	Time of Max. Luminescence (min)	Steady State % of Max.
ssrA	$6.0 \times 10^1 \pm 1.1 \times 10^1$	$3.8 \times 10^2 \pm 1.1 \times 10^2$	120 ± 15	$1.4 \times 10^4 \pm 2.3 \times 10^3$	195 ± 54	0.3 ± 0.1
ssaB	$5.0 \times 10^2 \pm 1.4 \times 10^1$	$8.3 \times 10^2 \pm 1.5 \times 10^2$	45 ± 15	$3.2 \times 10^4 \pm 2.0 \times 10^4$	145 ± 83	0.0 ± 0.0
sseA	$2.5 \times 10^3 \pm 4.5 \times 10^2$	$3.5 \times 10^3 \pm 4.3 \times 10^2$	50 ± 9	$2.1 \times 10^5 \pm 3.2 \times 10^4$	105 ± 0	0.0 ± 0.0
ssaG	$1.2 \times 10^4 \pm 1.7 \times 10^3$	$2.6 \times 10^4 \pm 1.2 \times 10^3$	125 ± 9	$2.0 \times 10^6 \pm 3.0 \times 10^5$	230 ± 9	0.2 ± 0.0
ssaM	$2.0 \times 10^3 \pm 2.8 \times 10^2$	$3.1 \times 10^3 \pm 3.1 \times 10^2$	130 ± 9	$1.8 \times 10^5 \pm 2.7 \times 10^4$	145 ± 9	0.2 ± 0.0
ssaR	$6.5 \times 10^3 \pm 1.2 \times 10^3$	$1.4 \times 10^4 \pm 1.3 \times 10^3$	90 ± 65	$1.2 \times 10^6 \pm 2.4 \times 10^5$	225 ± 15	0.2 ± 0.0
Promoter M9						
ssrA	$2.8 \times 10^2 \pm 5.9 \times 10^1$	$4.2 \times 10^2 \pm 5.3 \times 10^1$	90 ± 26	$2.3 \times 10^4 \pm 1.2 \times 10^3$	120 ± 26	N/A
ssaG	$9.7 \times 10^4 \pm 8.7 \times 10^3$	$1.2 \times 10^5 \pm 1.2 \times 10^4$	80 ± 9	$8.2 \times 10^6 \pm 2.6 \times 10^5$	150 ± 0	N/A

Δ*slyA*

Promoter LPM pH 5.8	Rate of Luminescence Increase (RLU/min)	Max. Instantaneous Rate of Luminescence Increase (RLU/min)	Time of Max. Instantaneous Increase Rate (min)	Max. Luminescence (RLU/OD600nm)	Time of Max. Luminescence (min)	Steady State % of Max.
ssrA	$1.4 \times 10^5 \pm 1.1 \times 10^4$	$1.8 \times 10^5 \pm 4.1 \times 10^3$	125 ± 9	$1.3 \times 10^7 \pm 1.1 \times 10^6$	180 ± 0	26 ± 4
ssaB	$3.4 \times 10^3 \pm 8.1 \times 10^2$	$4.8 \times 10^3 \pm 1.2 \times 10^3$	50 ± 9	$2.3 \times 10^5 \pm 6.0 \times 10^4$	105 ± 15	26 ± 2
sseA	$4.2 \times 10^3 \pm 1.2 \times 10^3$	$5.6 \times 10^3 \pm 1.4 \times 10^3$	40 ± 9	$3.1 \times 10^5 \pm 7.7 \times 10^4$	85 ± 9	20 ± 3
ssaG	$1.8 \times 10^4 \pm 5.1 \times 10^3$	$2.7 \times 10^4 \pm 6.7 \times 10^3$	120 ± 0	$1.9 \times 10^6 \pm 2.0 \times 10^5$	215 ± 9	26 ± 13
ssaM	$2.4 \times 10^3 \pm 3.5 \times 10^2$	$3.2 \times 10^3 \pm 9.8 \times 10^2$	120 ± 0	$2.0 \times 10^5 \pm 1.2 \times 10^4$	160 ± 9	19 ± 4
ssaR	$1.0 \times 10^4 \pm 2.9 \times 10^3$	$1.9 \times 10^4 \pm 2.4 \times 10^3$	85 ± 61	$1.4 \times 10^6 \pm 1.7 \times 10^5$	195 ± 40	30 ± 8
Promoter M9						
ssrA	$8.1 \times 10^4 \pm 4.6 \times 10^3$	$1.1 \times 10^5 \pm 8.0 \times 10^3$	90 ± 0	$6.4 \times 10^6 \pm 7.2 \times 10^5$	140 ± 9	N/A
ssaG	$8.8 \times 10^4 \pm 1.1 \times 10^4$	$1.1 \times 10^5 \pm 1.8 \times 10^4$	90 ± 0	$6.9 \times 10^6 \pm 9.1 \times 10^4$	145 ± 9	N/A

***phoP*::Cm**

Promoter LPM pH 5.8	Rate of Luminescence Increase (RLU/min)	Max. Instantaneous Rate of Luminescence Increase (RLU/min)	Instantaneous Increase Rate (min)	Max. Luminescence (RLU/OD600nm)	Time of Max. Luminescence (min)	Steady State % of Max.
ssrA	$1.3 \times 10^5 \pm 2.0 \times 10^4$	$1.7 \times 10^5 \pm 2.4 \times 10^4$	125 ± 23	$1.6 \times 10^7 \pm 2.3 \times 10^6$	175 ± 9	35 ± 5
ssaB	$7.3 \times 10^4 \pm 2.3 \times 10^4$	$8.7 \times 10^4 \pm 2.5 \times 10^4$	35 ± 9	$5.2 \times 10^6 \pm 1.5 \times 10^6$	95 ± 9	58 ± 33
sseA	$1.3 \times 10^5 \pm 3.8 \times 10^4$	$1.7 \times 10^5 \pm 4.0 \times 10^4$	30 ± 0	$9.4 \times 10^6 \pm 2.4 \times 10^6$	95 ± 9	34 ± 21
ssaG	$5.5 \times 10^4 \pm 9.2 \times 10^3$	$7.2 \times 10^4 \pm 6.6 \times 10^3$	70 ± 9	$6.0 \times 10^6 \pm 8.1 \times 10^5$	130 ± 17	36 ± 19
ssaM	$1.6 \times 10^4 \pm 3.8 \times 10^3$	$2.0 \times 10^4 \pm 6.0 \times 10^3$	75 ± 15	$1.4 \times 10^6 \pm 3.4 \times 10^5$	115 ± 9	28 ± 17
ssaR	$1.4 \times 10^5 \pm 2.3 \times 10^4$	$1.7 \times 10^5 \pm 2.7 \times 10^4$	30 ± 0	$1.1 \times 10^7 \pm 2.2 \times 10^6$	100 ± 9	26 ± 15
Promoter M9						
ssrA	$7.6 \times 10^4 \pm 5.5 \times 10^3$	$8.9 \times 10^4 \pm 9.8 \times 10^3$	95 ± 9	$6.4 \times 10^6 \pm 1.8 \times 10^5$	145 ± 9	N/A
ssaG	$8.0 \times 10^4 \pm 3.0 \times 10^3$	$1.0 \times 10^5 \pm 3.1 \times 10^3$	85 ± 9	$6.9 \times 10^6 \pm 4.6 \times 10^5$	140 ± 9	N/A

***fis*::Kan**

Promoter LPM pH 5.8	Rate of Luminescence Increase (RLU/min)	Max. Instantaneous Rate of Luminescence Increase (RLU/min)	Time of Max. Instantaneous Increase Rate (min)	Max. Luminescence (RLU/OD600nm)	Time of Max. Luminescence (min)	Steady State % of Max.
ssrA	$1.0 \times 10^5 \pm 1.6 \times 10^4$	$1.5 \times 10^5 \pm 2.6 \times 10^4$	165 ± 0	$1.6 \times 10^7 \pm 2.3 \times 10^6$	215 ± 23	26 ± 2
ssaB	$1.6 \times 10^4 \pm 1.6 \times 10^4$	$1.7 \times 10^4 \pm 1.8 \times 10^4$	55 ± 9	$1.2 \times 10^6 \pm 1.3 \times 10^6$	105 ± 15	16 ± 8
sseA	$3.5 \times 10^4 \pm 2.7 \times 10^4$	$4.3 \times 10^4 \pm 3.0 \times 10^4$	50 ± 9	$3.0 \times 10^6 \pm 2.1 \times 10^6$	135 ± 0	9 ± 2
ssaG	$1.8 \times 10^4 \pm 1.1 \times 10^4$	$2.5 \times 10^4 \pm 1.1 \times 10^4$	65 ± 9	$1.8 \times 10^6 \pm 7.3 \times 10^5$	150 ± 15	18 ± 1
ssaM	$5.2 \times 10^3 \pm 1.7 \times 10^3$	$7.1 \times 10^3 \pm 2.7 \times 10^3$	85 ± 17	$5.7 \times 10^5 \pm 1.7 \times 10^5$	155 ± 17	10 ± 1
ssaR	$4.5 \times 10^4 \pm 1.1 \times 10^4$	$5.7 \times 10^4 \pm 1.6 \times 10^4$	65 ± 9	$4.2 \times 10^6 \pm 6.4 \times 10^5$	140 ± 9	10 ± 0
Promoter M9						
ssrA	$2.3 \times 10^4 \pm 1.1 \times 10^3$	$3.3 \times 10^4 \pm 4.0 \times 10^3$	105 ± 15	$3.0 \times 10^6 \pm 1.9 \times 10^5$	180 ± 0	N/A
ssaG	$8.5 \times 10^3 \pm 6.7 \times 10^2$	$1.3 \times 10^4 \pm 2.3 \times 10^2$	135 ± 52	$1.3 \times 10^6 \pm 5.3 \times 10^4$	195 ± 26	N/A

Δ*hha* Δ*ydgT*

Promoter LPM pH 5.8	Rate of Luminescence Increase (RLU/min)	Max. Instantaneous Rate of Luminescence Increase (RLU/min)	Time of Max. Instantaneous Increase Rate (min)	Max. Luminescence (RLU/OD600nm)	Time of Max. Luminescence (min)	Steady State % of Max.
ssrA	$3.9 \times 10^5 \pm 1.9 \times 10^5$	$4.9 \times 10^5 \pm 1.9 \times 10^5$	140 ± 87	$5.5 \times 10^7 \pm 1.5 \times 10^7$	225 ± 26	88 ± 6
ssaB	$4.5 \times 10^5 \pm 2.3 \times 10^5$	$6.2 \times 10^5 \pm 2.2 \times 10^5$	150 ± 108	$6.7 \times 10^7 \pm 1.3 \times 10^7$	270 ± 45	80 ± 15
sseA	$3.7 \times 10^5 \pm 2.5 \times 10^4$	$5.3 \times 10^5 \pm 5.8 \times 10^4$	175 ± 61	$7.5 \times 10^7 \pm 9.2 \times 10^6$	225 ± 15	82 ± 4
ssaG	$1.6 \times 10^4 \pm 6.2 \times 10^3$	$3.4 \times 10^4 \pm 1.8 \times 10^4$	270 ± 0	$4.3 \times 10^6 \pm 1.7 \times 10^6$	340 ± 61	N/A
ssaM	$1.9 \times 10^5 \pm 2.3 \times 10^4$	$3.6 \times 10^5 \pm 2.7 \times 10^4$	170 ± 69	$6.1 \times 10^7 \pm 2.3 \times 10^6$	375 ± 0	N/A
ssaR	$5.5 \times 10^4 \pm 1.7 \times 10^3$	$1.2 \times 10^5 \pm 2.4 \times 10^4$	15 ± 0	$8.9 \times 10^6 \pm 4.1 \times 10^5$	200 ± 62	35 ± 20
Promoter M9						
ssrA	$2.1 \times 10^5 \pm 7.8 \times 10^4$	$3.0 \times 10^5 \pm 8.3 \times 10^4$	125 ± 17	$3.6 \times 10^7 \pm 1.3 \times 10^7$	220 ± 17	N/A
ssaG	$1.2 \times 10^5 \pm 2.5 \times 10^4$	$1.7 \times 10^5 \pm 2.7 \times 10^3$	340 ± 61	$1.7 \times 10^7 \pm 3.5 \times 10^6$	360 ± 26	N/A

Wild type (pHNSQ92am)

Promoter LPM pH 5.8	Rate of Luminescence Increase (RLU/min)	Max. Instantaneous Rate of Luminescence Increase (RLU/min)	Time of Max. Instantaneous Increase Rate (min)	Max. Luminescence (RLU/OD600nm)	Time of Max. Luminescence (min)	Steady State % of Max.
ssrA	$4.9 \times 10^5 \pm 6.4 \times 10^4$	$7.1 \times 10^5 \pm 1.2 \times 10^5$	230 ± 38	$8.5 \times 10^7 \pm 3.0 \times 10^6$	285 ± 30	N/A
ssaB	$3.5 \times 10^5 \pm 1.7 \times 10^5$	$6.2 \times 10^5 \pm 9.0 \times 10^5$	200 ± 23	$6.8 \times 10^7 \pm 5.0 \times 10^6$	385 ± 9	N/A
sseA	$3.0 \times 10^5 \pm 8.6 \times 10^4$	$5.3 \times 10^5 \pm 9.9 \times 10^4$	250 ± 23	$6.3 \times 10^7 \pm 6.2 \times 10^6$	385 ± 9	N/A
ssaG	$1.6 \times 10^5 \pm 3.6 \times 10^4$	$2.9 \times 10^5 \pm 6.1 \times 10^4$	230 ± 38	$2.9 \times 10^7 \pm 2.4 \times 10^6$	330 ± 15	N/A
ssaM	$1.2 \times 10^5 \pm 1.2 \times 10^4$	$1.8 \times 10^5 \pm 1.4 \times 10^4$	230 ± 38	$2.4 \times 10^7 \pm 4.2 \times 10^6$	390 ± 0	N/A
ssaR	$1.5 \times 10^5 \pm 1.1 \times 10^4$	$2.6 \times 10^5 \pm 6.2 \times 10^4$	230 ± 38	$3.3 \times 10^7 \pm 1.1 \times 10^6$	385 ± 9	N/A
Promoter M9						
ssrA	$7.4 \times 10^4 \pm 1.3 \times 10^4$	$1.3 \times 10^5 \pm 3.1 \times 10^4$	210 ± 15	$1.1 \times 10^7 \pm 1.1 \times 10^6$	245 ± 9	N/A
ssaG	$4.6 \times 10^4 \pm 3.8 \times 10^3$	$7.5 \times 10^4 \pm 2.1 \times 10^4$	265 ± 95	$8.4 \times 10^6 \pm 6.3 \times 10^5$	275 ± 100	N/A

Table 4.S2. Primers Used in Study

Construct	Primer Name	Sequence
Δ*slyA*	SEO001	gcaagctaattataaggagatgaaattggaatcgccactagtgtaggctggagctgcttcg
	SEO002	ggccacacgtatgcccctgcacctcaatcgtgagagtgcaacatatgaatatcctcctta
Δ*ompR*	SEO013	gttgcgaacctttgggagtacagacaatgcaagagaattataaggtgtaggctggagctgcttcg
	SEO014	cttcgcggtgagaagcgcattcgcctcatgctttagaaccgtccatatgaatatcctcctta
fis ::Kan	SEO147	agaaataaagagctgacagaactatgttcgaacaacgcgtagtgtaggctggagctgcttcg
	SEO148	aacaagcagttagctaatcgaaattagttcatgccgtatttcatatgaatatcctcctta
pP_{ssrA}-*luxCDABE*	SEO135	cgatacgtattacagccaaataattattgttgt
	SEO136	cgggatcctctggcataaagggtgaagt
pP_{ssaB}-*luxCDABE*	SEO123	cgggatccgtgccatcctttgccgttt
	SEO124	cgatacgtattacatgaatccctcctcagacat
pP_{sseA}-*luxCDABE*	SEO129	ggggtaccgcaaggttcaaccattacttg
	SEO130	cgatacgtattacgcagccttttttctttatca
pP_{ssaG}-*luxCDABE*	SEO121	cgggatccatatggagagtggtagaatag
	SEO122	cgatacgtattataattgtgcaatatccataa
pP_{ssaM}-*luxCDABE*	SEO119	cgggatccaatcaggttttattctgatacctgg
	SEO120	cgatacgtattaaatgagatcccaatccatcct
pP_{ssaR}-*luxCDABE*	SEO137	cgggatccccacaacaggtgctctttga
	SEO138	cgatacgtattatcgataaggcgctaatgctt

References

1. Galan JE, Wolf-Watz H (2006) Protein delivery into eukaryotic cells by type III secretion machines. Nature 444: 567-573.
2. Cornelis GR (2006) The type III secretion injectisome. Nat Rev Microbiol 4: 811-825.
3. Jones BD, Ghori N, Falkow S (1994) *Salmonella* typhimurium initiates murine infection by penetrating and destroying the specialized epithelial M cells of the Peyer's patches. J Exp Med 180: 15-23.
4. Richter-Dahlfors A, Buchan AM, Finlay BB (1997) Murine salmonellosis studied by confocal microscopy: *Salmonella* typhimurium resides intracellularly inside macrophages and exerts a cytotoxic effect on phagocytes in vivo. J Exp Med 186: 569-580.
5. Salcedo SP, Noursadeghi M, Cohen J, Holden DW (2001) Intracellular replication of *Salmonella* typhimurium strains in specific subsets of splenic macrophages *in vivo*. Cell Microbiol 3: 587-597.
6. Shea JE, Hensel M, Gleeson C, Holden DW (1996) Identification of a virulence locus encoding a second type III secretion system in *Salmonella* typhimurium. Proc Natl Acad Sci U S A 93: 2593-2597.
7. Ochman H, Soncini FC, Solomon F, Groisman EA (1996) Identification of a pathogenicity island required for *Salmonella* survival in host cells. Proc Natl Acad Sci U S A 93: 7800-7804.

8. Vazquez-Torres A, Xu Y, Jones-Carson J, Holden DW, Lucia SM, et al. (2000) *Salmonella* pathogenicity island 2-dependent evasion of the phagocyte NADPH oxidase. Science 287: 1655-1658.

9. Chakravortty D, Hansen-Wester I, Hensel M (2002) *Salmonella* pathogenicity island 2 mediates protection of intracellular *Salmonella* from reactive nitrogen intermediates. J Exp Med 195: 1155-1166.

10. Walthers D, Carroll RK, Navarre WW, Libby SJ, Fang FC, et al. (2007) The response regulator SsrB activates expression of diverse *Salmonella* pathogenicity island 2 promoters and counters silencing by the nucleoid-associated protein H-NS. Mol Microbiol 65: 477-493.

11. Tomljenovic-Berube AM, Mulder DT, Whiteside MD, Brinkman FS, Coombes BK Identification of the regulatory logic controlling *Salmonella* pathoadaptation by the SsrA-SsrB two-component system. PLoS Genet 6: e1000875.

12. Xu X, Hensel M Systematic analysis of the SsrAB virulon of *Salmonella enterica*. Infect Immun 78: 49-58.

13. Bijlsma JJ, Groisman EA (2005) The PhoP/PhoQ system controls the intramacrophage type three secretion system of *Salmonella enterica*. Mol Microbiol 57: 85-96.

14. Feng X, Walthers D, Oropeza R, Kenney LJ (2004) The response regulator SsrB activates transcription and binds to a region overlapping OmpR binding sites at *Salmonella* pathogenicity island 2. Mol Microbiol 54: 823-835.

15. Stapleton MR, Norte VA, Read RC, Green J (2002) Interaction of the *Salmonella* typhimurium transcription and virulence factor SlyA with target DNA and identification of members of the SlyA regulon. J Biol Chem 277: 17630-17637.

16. O Croinin T, Carroll RK, Kelly A, Dorman CJ (2006) Roles for DNA supercoiling and the Fis protein in modulating expression of virulence genes during intracellular growth of *Salmonella enterica* serovar Typhimurium. Mol Microbiol 62: 869-882.

17. Navarre WW, Porwollik S, Wang Y, McClelland M, Rosen H, et al. (2006) Selective silencing of foreign DNA with low GC content by the H-NS protein in *Salmonella*. Science 313: 236-238.

18. Coombes BK, Wickham ME, Lowden MJ, Brown NF, Finlay BB (2005) Negative regulation of *Salmonella* pathogenicity island 2 is required for contextual control of virulence during typhoid. Proc Natl Acad Sci U S A 102: 17460-17465.

19. Silphaduang U, Mascarenhas M, Karmali M, Coombes BK (2007) Repression of intracellular virulence factors in *Salmonella* by the Hha and YdgT nucleoid-associated proteins. J Bacteriol 189: 3669-3673.

20. Cirillo DM, Valdivia RH, Monack DM, Falkow S (1998) Macrophage-dependent induction of the *Salmonella* pathogenicity island 2 type III secretion system and its role in intracellular survival. Mol Microbiol 30: 175-188.

21. Deiwick J, Nikolaus T, Erdogan S, Hensel M (1999) Environmental regulation of *Salmonella* pathogenicity island 2 gene expression. Mol Microbiol 31: 1759-1773.

22. Coombes BK, Brown NF, Valdez Y, Brumell JH, Finlay BB (2004) Expression and secretion of *Salmonella* pathogenicity island-2 virulence genes in response to acidification exhibit differential requirements of a functional type III secretion apparatus and SsaL. J Biol Chem 279: 49804-49815.

23. Bustamante VH, Martinez LC, Santana FJ, Knodler LA, Steele-Mortimer O, et al. (2008) HilD-mediated transcriptional cross-talk between SPI-1 and SPI-2. Proc Natl Acad Sci U S A 105: 14591-14596.

24. Miao EA, Freeman JA, Miller SI (2002) Transcription of the SsrAB regulon is repressed by alkaline pH and is independent of PhoPQ and magnesium concentration. J Bacteriol 184: 1493-1497.

25. Coombes BK, Coburn BA, Potter AA, Gomis S, Mirakhur K, et al. (2005) Analysis of the contribution of *Salmonella* pathogenicity islands 1 and 2 to enteric disease progression using a novel bovine ileal loop model and a murine model of infectious enterocolitis. Infect Immun 73: 7161-7169.

26. Coburn B, Li Y, Owen D, Vallance BA, Finlay BB (2005) *Salmonella enterica* serovar Typhimurium pathogenicity island 2 is necessary for complete virulence in a mouse model of infectious enterocolitis. Infect Immun 73: 3219-3227.

27. Bispham J, Tripathi BN, Watson PR, Wallis TS (2001) *Salmonella* pathogenicity island 2 influences both systemic salmonellosis and *Salmonella*-induced enteritis in calves. Infect Immun 69: 367-377.

28. Brown NF, Vallance BA, Coombes BK, Valdez Y, Coburn BA, et al. (2005) *Salmonella* pathogenicity island 2 is expressed prior to penetrating the intestine. PLoS Pathog 1: e32.

29. Deiwick J, Nikolaus T, Erdogan S, Hensel M (1999) Environmental regulation of *Salmonella* pathogenicity island 2 gene expression. Mol Microbiol 31: 1759-1773.

30. Yoon H, McDermott JE, Porwollik S, McClelland M, Heffron F (2009) Coordinated regulation of virulence during systemic infection of *Salmonella enterica* serovar Typhimurium. PLoS Pathog 5: e1000306.

31. Vivero A, Banos RC, Mariscotti JF, Oliveros JC, Garcia-del Portillo F, et al. (2008) Modulation of horizontally acquired genes by the Hha-YdgT proteins in *Salmonella enterica* serovar Typhimurium. J Bacteriol 190: 1152-1156.

32. Navarre WW, Halsey TA, Walthers D, Frye J, McClelland M, et al. (2005) Co-regulation of *Salmonella enterica* genes required for virulence and resistance to antimicrobial peptides by SlyA and PhoP/PhoQ. Mol Microbiol 56: 492-508.

33. Duong N, Osborne S, Bustamante VH, Tomljenovic AM, Puente JL, et al. (2007) Thermosensing coordinates a cis-regulatory module for transcriptional activation of the intracellular virulence system in *Salmonella enterica* serovar Typhimurium. J Biol Chem 282: 34077-34084.

34. Galan JE, Curtiss R, 3rd (1991) Distribution of the *invA, -B, -C,* and *-D* genes of *Salmonella* typhimurium among other *Salmonella* serovars: *invA* mutants of *Salmonella* typhi are deficient for entry into mammalian cells. Infect Immun 59: 2901-2908.

35. Waterman SR, Holden DW (2003) Functions and effectors of the *Salmonella* pathogenicity island 2 type III secretion system. Cell Microbiol 5: 501-511.

36. Abrahams GL, Hensel M (2006) Manipulating cellular transport and immune responses: dynamic interactions between intracellular Salmonella enterica and its host cells. Cell Microbiol 8: 728-737.

37. Lim S, Kim B, Choi HS, Lee Y, Ryu S (2006) Fis is required for proper regulation of *ssaG* expression in *Salmonella enterica* serovar Typhimurium. Microb Pathog 41: 33-42.

38. Hapfelmeier S, Stecher B, Barthel M, Kremer M, Muller AJ, et al. (2005) The *Salmonella* pathogenicity island (SPI)-2 and SPI-1 type III secretion systems allow *Salmonella* serovar typhimurium to trigger colitis via MyD88-dependent and MyD88-independent mechanisms. J Immunol 174: 1675-1685.

39. Gallois A, Klein JR, Allen LA, Jones BD, Nauseef WM (2001) *Salmonella* pathogenicity island 2-encoded type III secretion system mediates exclusion of NADPH oxidase assembly from the phagosomal membrane. J Immunol 166: 5741-5748.

40. VanderVen BC, Yates RM, Russell DG (2009) Intraphagosomal measurement of the magnitude and duration of the oxidative burst. Traffic 10: 372-378.

41. Tlili A, Dupre-Crochet S, Erard M, Nusse O (2011) Kinetic analysis of phagosomal production of reactive oxygen species. Free Radical Biology and Medicine 50: 438-447.

42. Datsenko KA, Wanner BL (2000) One-step inactivation of chromosomal genes in Escherichia coli K-12 using PCR products. Proc Natl Acad Sci U S A 97: 6640-6645.

43. Lane MC, Alteri CJ, Smith SN, Mobley HL (2007) Expression of flagella is coincident with uropathogenic *Escherichia coli* ascension to the upper urinary tract. Proc Natl Acad Sci U S A 104: 16669-16674.

44. Coombes BK, Lowden MJ, Bishop JL, Wickham ME, Brown NF, et al. (2007) SseL is a *Salmonella*-specific translocated effector integrated into the SsrB-controlled *Salmonella* pathogenicity island 2 type III secretion system. Infect Immun 75: 574-580.

Appendix A – Supplementary Data Pertaining to Chapter 3

APPENDIX A – Supplementary Data Pertaining to Chapter 3

Appendix A is composed of additional results which were excluded from the publication presented in Chapter 3 but which links this publication to the overall theme of *cis*-regulatory evolution. Methods and materials not previously described in Chapter 3 are presented in Appendix B.

The following work was conducted by persons other then me:

1) Original identification of the SsrB binding motif highlighted in Figure A.1 was presented in the following publication: Tomljenovic-Berube, A.M., Mulder, D. T. Whiteside, M. D., Brinkman, F. S., and Coombes, B. K. (2011). Identification of the regulatory logic controlling *Salmonella* pathoadaptation by the SsrA-SsrB two-component system. PLoS Genet 6: e1000875.

2) Cloning, protein purification and fluorescence thermal shift assays were performed by an undergraduate summer student Brian R. Tuinema working under my supervision. I maintained a significant intellectual contribution to the design, implementation and analysis of these experiments.

Figure A.1 – The DalS homologue in *S. bongori* (SBG1467) lacks the SsrB binding motif within its promoter. Alignment of the *dalS* promoter across several *S. enterica* strains and the *S. bongori* homologue (SBG1467) reveals absence of the SsrB binding site in *S. bongori*. Segment absent from *S. bongori* corresponds to the exact DNA fragment utilized for electrophoretic mobility shift assays in Chapter 3 (Figure 3.1d). The red box indicates the location of the SsrB binding site. The translational start site is indicated by the green box. (*, Indicates conservation across all alignments).

Figure A.1

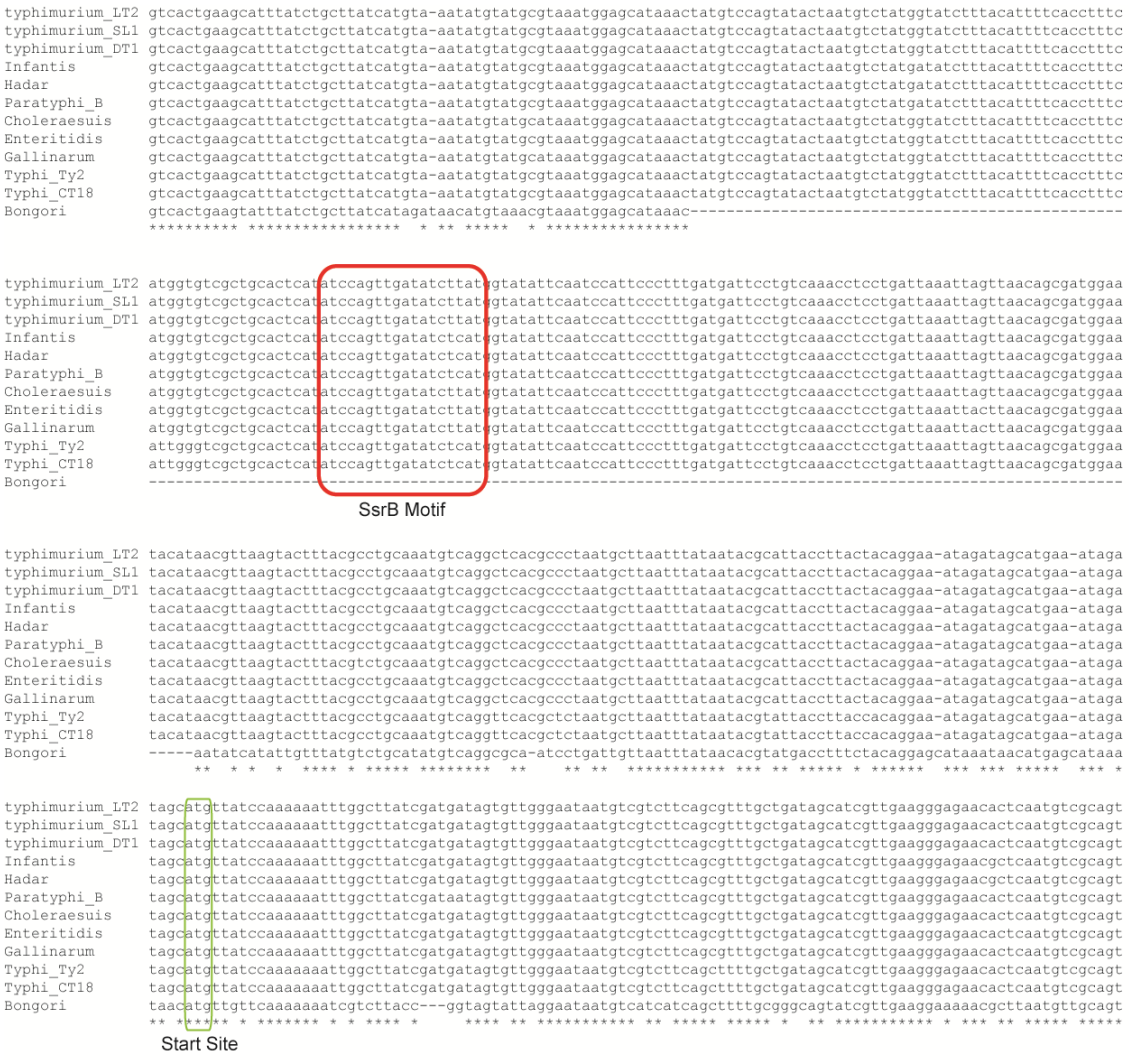

Figure A.2 – The *S. bongori* DalS homologue (SBG1467) is SsrB-independent. *S. enterica* wild type (WT) and Δ*ssrB* carrying pSBG1467-2HA under the control of the *S. bongori* promoter, were grown in LB and LPM pH 5.8 for 6 hours. Lysates were analyzed by immunoblotting. DnaK was used as a loading control. SseB was used as a positive control for SsrB-dependent regulation. Image is representative of 3 biological replicates.

Figure A.2

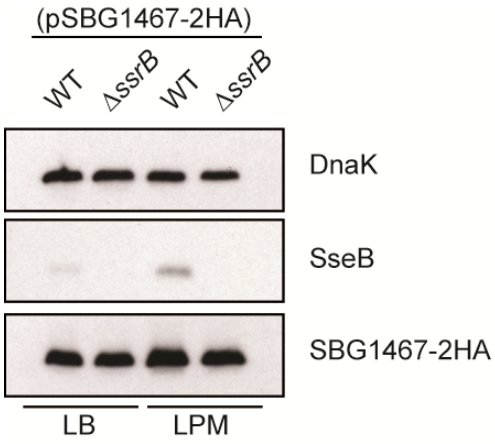

Figure A.3 – SBG1467 cannot fully complement Δ*dalS in vivo*. (A) Extension of Figure 3.2 c. RAW264.7 cells were infected with Δ*dalS* carrying pSBG1467-2HA (*S. bongori* DalS homologue) under control of the *S. bongori* promoter. Fold increase in intracellular bacteria between 2 and 20 hours was assessed using a gentamicin protection assay and normalized to wild type. ($n = 5$). (*, $p < 0.05$). **(B)** Ability of DalS-2HA and SBG1467-2HA to complement Δ*dalS* was assessed by competitive infection of C57BL/6 mice with a mixed innoculum of Wt *ushA*::Cm (pWSK29) and Δ*dalS* carrying either p*dalS*-2HA or pSBG1467-2HA. (*, $p < 0.05$; **, $p < 0.01$; ***, $p < 0.001$).

Figure A.3

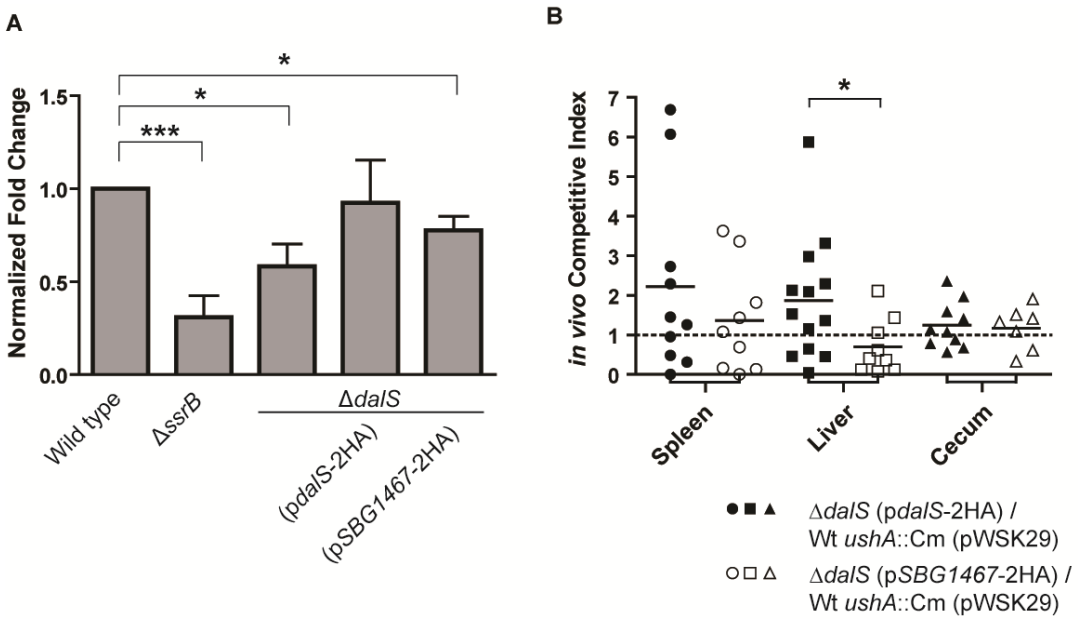
A
Normalized Fold Change
1.5
1.0
0.5
0.0
***
*
*
Wild type
ΔssrB
ΔdalS
(pdalS-2HA)
(pSBG1467-2HA)
B
in vivo Competitive Index
7
6
5
4
3
2
1
0
*
Spleen
Liver
Cecum
ΔdalS (pdalS-2HA) /
Wt ushA::Cm (pWSK29)
ΔdalS (pSBG1467-2HA) /
Wt ushA::Cm (pWSK29)

Figure A.4 – Ancestral regulators contribute to expression of *dalS* and *SBG1467*. (A) To determine the contributions of several transcription factors to expression of *dalS*, chromosomally encoded *lacZ* transcriptional fusions to the *dalS* promoter in Wt, Δ*ompR*, Δ*slyA* and *phoP*::Cm genetic backgrounds were grown in LPM pH 5.8 for 5 hours. Lysates were analyzed for β-galactosidase activity using chemiluminescence. RLU was normalized to OD_{600nm}. Promoter activity for each mutant represented as a percent of the activity seen in Wt (n = 3). **(B)** Wt, Δ*ompR*, Δ*slyA* and *phoP*::Cm containing pSBG1467-2HA were grown in LPM pH 5.8 to an OD_{600nm} ~ 0.6. Lysates were analyzed by immunoblotting. DnaK used as a loading control. Data is representative of three biological replicates with identical results.

Figure A.4

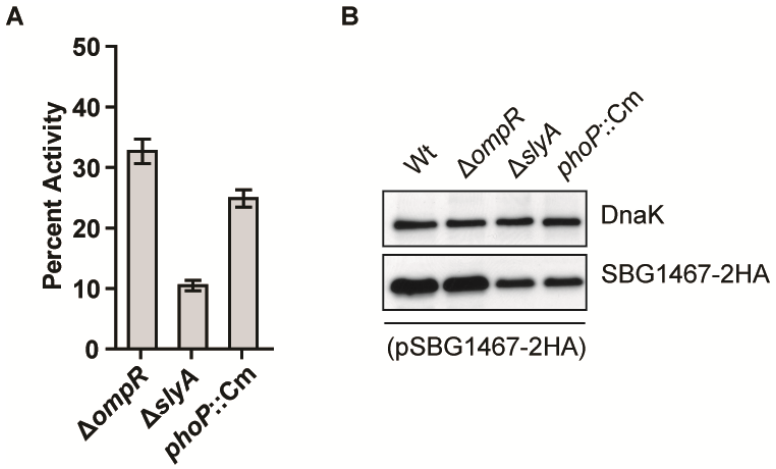
A
Percent Activity
50
40
30
20
10
0
ΔompR
ΔslyA
phoP::Cm
B
Wt
ΔompR
ΔslyA
phoP::Cm
DnaK
SBG1467-2HA
(pSBG1467-2HA)

Figure A.5 – SBG1467 binds Glycine and D-alanine. Fluorescence thermal shift assay to determine if SBG1467 binds to same amino acids as DalS. Purified SBG1467-6HIS was incubated with the indicated amino acid (B = betaine, D-ala = D-alanine) and the change melting temperature relative to controls lacking ligand were monitored ($n > 5$). A change of greater then 2^{o}C was used as significance cut off.

Figure A.5

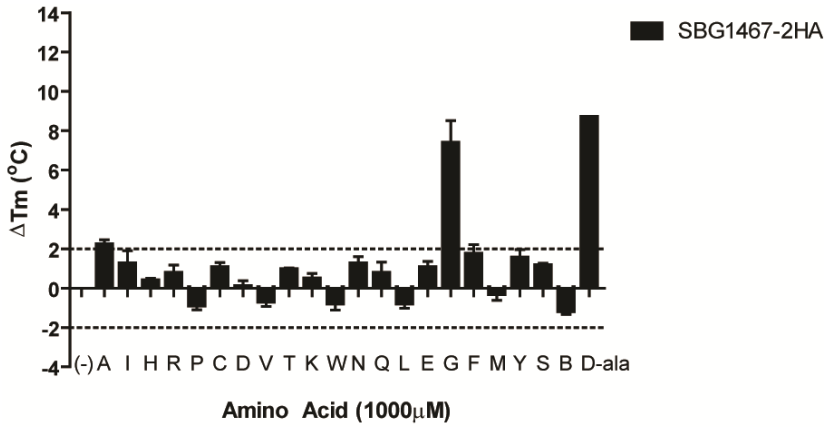
SBG1467-2HA
ΔTm (°C)
14
12
10
8
6
4
2
0
-2
-4
(-) A I H R P C D V T K W N Q L E G F M Y S B D-ala
Amino Acid (1000μM)

Figure A.6 - DalS influences β-lactam susceptibility and cell morphology. (A) Disk diffusion assays for wild type (Wt) and Δ*dalS*. Ampicillin (1 mg), D-cycloserine (0.1 mg) and kanamycin (0.5 mg) was added to filter disks and placed on lawn of $6.5x10^5$ cells. Diameter of zone of clearance was quantified ($n = 3$). Wt and Δ*dalS* cells grown to exponential phase in LB were negatively stained using 2% phosphotungstic acid and visualized by scanning transmission electron microscopy. **(B)** Dimensions of cells were quantified and population grouped based on ratio of length to width. **(C)** Representative images reflective of over 100 images across two biological replicates.

Figure A.6

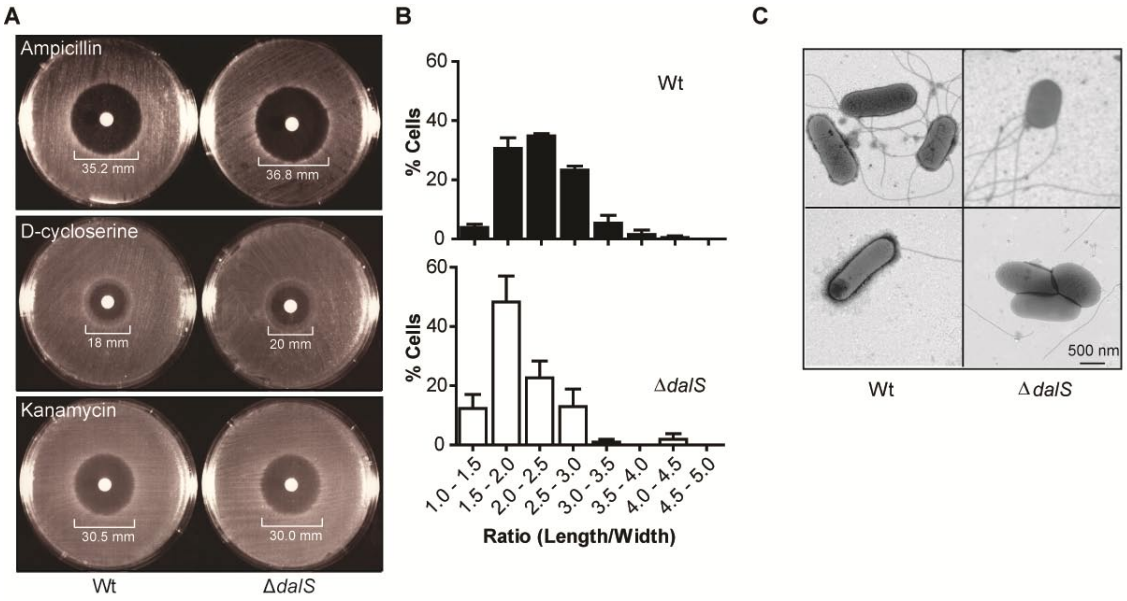
A
Ampicillin
35.2 mm
36.8 mm
D-cycloserine
18 mm
20 mm
Kanamycin
30.5 mm
30.0 mm
Wt
ΔdalS
B
Wt
% Cells
60
40
20
0
ΔdalS
1.0 - 1.5
1.5 - 2.0
2.0 - 2.5
2.5 - 3.0
3.0 - 3.5
3.5 - 4.0
4.0 - 4.5
4.5 - 5.0
Ratio (Length/Width)
C
500 nm
Wt
ΔdalS

Figure A.7 - DalS modulates NO production in macrophages. (A) To determine macrophage activation levels, RAW264.7 cells were infected with Wt or Δ*dalS* and 72 hours post infection supernatents were collected and analyzed for NO production using Griess reagent and macrophage protein levels. NO was normalized to protein concentration ($n = 3$) (**, $p < 0.01$). **(B)** $NOS2^{-/-}$ (B6.129P2-$nos2^{tm1Lau}$/J) mice were orally infected with a mixed innoculum of Wt *ushA*::Cm and Δ*dalS*. At 3 days post-infection competitive indices were determined for the spleen, liver and cecum. Each data point represents an individual animal and horizontal bars are the mean.

Figure A.7

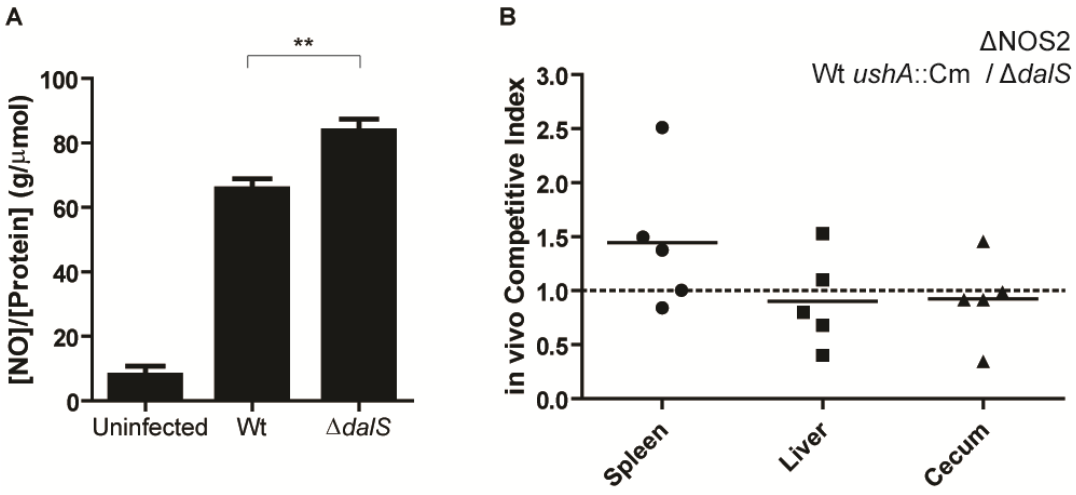
A
**
[NO]/[Protein] (g/μmol)
100
80
60
40
20
0
Uninfected
Wt
ΔdalS
B
ΔNOS2
Wt ushA::Cm / ΔdalS
in vivo Competitive Index
3.0
2.5
2.0
1.5
1.0
0.5
0.0
Spleen
Liver
Cecum

Appendix B – Supplementary Methods and Materials

Appendix B – Supplementary Methods and Materials

Appendix B contains additional experimental procedures corresponding to the supplementary data presented in Appendix A. For experiments similar to those presented in Chapter 3, refer to methods and materials contained within that chapter.

EXPERIMENTAL PROCEDURES

Genetic Analysis. Genome sequences for *S. enterica* strains were obtained as described in Chapter 3 Experimental Procedures. *S. bongori* 12419 was obtained from the Wellcome Trust Sanger Institute (http://www.sanger.ac.uk) Pathogen Sequencing Unit. Promoter regions were aligned with MAFFT (v6.707b) (http://mafft.cbrc.jp/alignment/server/index.html).

Cloning and Mutant Construction. A C-terminally 2HA tagged *SBG1467* was constructed by PCR amplifying *SBG1467* including 1000 bp of the promoter region from *S. bongori* genomic DNA using primers SEO117 (ACGCGTCGACCCCTCTCTATGAATCCATGAGGATA) and SEO118 (GGAAGATCTTTTCATCCATTTATCAACGATGC) and cloned as a SalI/BglII fragment into pWSK29-2HA.

Construction of the C-terminally 6HIS tagged SBG1467 was achieved through PCR amplification with primers SEO174 (GGAATTCCATATGTTGTTCAAAAAAATCGTCTTACC) and SEO175 (AAGGATCCCTAGTGGTGGTGGTGGTGTTTCATCCATTTATCAACGATGCT) and cloned into pET3a as NdeI/BamHI fragments and confirmed by sequencing. Constructs were transformed into *E. coli* BL21 (DE3).

Deletions of *ssrB* (Δ*ssrB*), *ompR* (Δ*ompR*), *slyA* (Δ*slyA*) and *phoP* (*phoP*::Cm) were described previously [1].

Protein Purification. SBG1467-6HIS was purified from *E. coli* BL21 (DE3) as described for DalS-6HIS in Chapter 3.

β-galactosidase Assays. Relative light units were quantified as described in Chapter 3 using Δ*slyA*, Δ*ompR* and *phoP*::Cm merodiploids carrying chromosomally encoded P_{dalS}-*lacZ* at an ~ OD_{600nm} of 0.6.

Immunoblotting. Wild type, Δ*ssrB*, Δ*ompR*, Δ*slyA* and *phoP*::Cm *S.* Typhimurium carrying pSBG1467-2HA were grown in LB and LPM pH 5.8 and analyzed by immnoblotting as described in Chapter 3.

Cell Culture. RAW264.7 cells were infected with Δ*dalS* (pSBG1467-2HA) and a gentamicin protection assay was performed exactly as described in Chapter 3.

Competitive Infection of Animals. Mixed infections with wild type *ushA*::Cm and Δ*dalS* were performed using female B6.129P2-nos2^{tm1Lau}/J (Jax Laboratories) mice and the competitive index was determined as described in Chapter 3. Competitive infections were also performed in female C57BL/6 mice (Jackson Laboratories) using mixed inoculums of wild type *ushA*::Cm (pWSK29) and either Δ*dalS* (p*dalS*-2HA) or Δ*dalS* (p*SBG1467*-2HA).

Fluorescence Thermal Shift Assays. Assay performed as described in Chapter 3 using purified SBG1467-6HIS.

Disk Diffusion Assays. Wild type and Δ*dalS* were grown overnight in LB. Cells were diluted to ~6x10^6 CFU/mL in 0.85% NaCl. 100µL was then plated on LB agar plates. Sterile disks were added to the center of the plates. 10µL of ampicillin (100 mg/mL, Bioshop), D-cycloserine (10 mg/mL, Sigma) and kanamycin (50 mg/mL, Bioshop) were added to the disk. Plates were incubated overnight at 37^{o}C. Zone of clearance was manually quantified.

Transmission Electron Microscopy. Overnight cultures were floated on a carbon-stabilized Formvar support on 200-mesh copper TEM grids for 1 minute. Grids were washed three times in ddH_2O and then stained with 2% phosphotungstic acid. A JEOL-

1200EX transmission electron microscope (McMaster University Electron Microscopy Facility) was used to capture images. For each of two biological replicates over 50 images were acquired and quantified.

Nitric Oxide Production Assay. RAW264.7 cells were plated at 5 x 10^5 cells in DMEM/10% FBS in a 96-well plate, and cells were infected with *S.* Typhimurium as described above. Culture supernatants were collected at 72hrs post-infection, and assayed for nitrite levels by the Griess method [2]. NO levels were normalized to protein concentration, measured using a DC Protein Assay (BioRad) to control for number of macrophage cells.

REFERENCES

1. Osborne SE, Coombes BK Transcriptional priming of *Salmonella* Pathogenicity Island-2 precedes cellular invasion. PLoS One 6: e21648.

2. Green LC, Wagner, D.A., Glogowski, J., Skipper, P.L., Wishnok, J.S., and Tannenbaum, S.R. (1982) Analysis of nitrate, nitrite and [^{15}N] nitrate in biological fluids. Anal Biochem 126: 131-138.

Chapter Five - Discussion

Chapter Five - Discussion

Purpose and Major Findings

The *S. enterica* lineage diverged from *S. bongori* following an evolutionary quantum leap; the horizontal acquisition of SPI-2. Integration of SPI-2 and its regulatory system SsrAB into the ancestral genome was critical for survival in the SCV. The purpose of this study was to explore the contribution of *cis*-regulatory evolution following the procurement of SPI-2 to the emergence of *S. enterica* as an intracellular pathogen.

The first aim of this project was to ascertain whether ancestral genes had been incorporated into the SsrB regulon and to assess the corresponding fitness gain. We established that *srfN* and *dalS*, which are ancestral to *Salmonella*, are directly regulated by SsrB (Figures 2.1, 2.2, 3.1 and A.2). An SsrB recognition motif in the CREs of *srfN* and *dalS* appeared through single nucleotide substitutions and an insertion respectively (Figure 2.1D and A.1). Congruent with protein-coding adaptations, modes of *cis*-regulatory evolution include substitutions, insertions, deletions and rearrangements [1]. Both *srfN* and *dalS* contributed to a fitness gain when expressed from their SsrB-dependent promoters in animal infections (Figures 2.3, 2.4, 2.5, 3.2, A.3 and A.5). Although we were unable to establish a function for SrfN, DalS was classified as the periplasmic binding protein of an ABC transporter for D-alanine. This was the first example of a transport system for this particular substrate.

The second aim of this project was to investigate the role of ancestral regulatory networks in moderating the temporal-spatial dynamics of SPI-2 gene expression. Consistent with published literature, we found that OmpR, SlyA, PhoP, Fis, H-NS, Hha and YdgT moderated SPI-2 through governance of *ssrAB* expression. Unlike the flagellar and SPI-1 T3SSs, an expression hierarchy for SPI-2 was not observed in synthetic inducing media (Figure 4.1). In contrast, a prioritized expression profile was observed in non-inducing media and was driven by differential regulatory inputs: OmpR at the *ssrA* promoter and Fis at the *ssaG* promoter. SPI-2 reporter dynamics *in vivo* indicated that SPI-2 was expressed in the intestinal lumen prior to invasion of epithelial cells. These results indicated that ancestral regulatory inputs aid in establishing transcriptional hierarchy for SPI-2.

SrfN: Remaining Questions

Future work should aim to elucidate the function of SrfN. Such studies would be additionally beneficial in defining the family of unknown proteins to which SrfN belongs. In contrast to our findings (Figure 2.S2), a subsequent publication detected very modest, T3SS-independent translocation of SrfN into the host [2]. The authors suggest that SrfN uptake into host cells occurs through outer membrane vesicles (OMVs); spherical structures that are pinched off bacterial outer membranes [3,4,5]. OMVs allow delivery of unstable effectors at higher concentrations [6]. Identification of host or bacterial proteins which interact with SrfN would be the first step in elucidating its function. Monitoring

common cellular targets of SPI-2 effectors including cytoskeleton dynamics or inflammatory signalling cascades following microinjection of SrfN would serve as a secondary strategy for functional characterization.

DalS: Remaining Questions

DalSTUV is a D-alanine ABC transporter required for full virulence. The mechanism by which D-alanine uptake contributes to survival within the SCV should be the focus of future research. DalS may be important in sequestering D-alanine away from the host D-amino acid oxidase (DAO). DAO was shown to have antibacterial activity against *Staphylococcus aureus* through D-amino acid-dependent generation of the reactive oxygen species (ROS) H_2O_2 [7]. A connection between the SsrB regulon and prevention of ROS-mediated killing has already been established. SPI-2 prevented recruitment of the NADPH oxidase, a ROS generator, to the SCV [8]. Macrophages isolated from NADPH oxidase deficient (*phox* $^{-/-}$) mice were unable to reduce the bacterial burden following *S. enterica* infection [9]. It is possible that DalS reduces ROS-mediated killing by sequestering D-alanine away from DAO. This hypothesis is consistent with the lack of a growth defect for Δ*dalS* in the absence of host cells. In contrast to this prediction, elevated levels of D-alanine in culture media increased intracellular replication (data not shown). Future studies should aim to examine the susceptibility of Δ*dalS* to DAO *in vitro* and examine whether the virulence defect is recovered in DAO $^{-/-}$ mice.

It is possible that DalS recycles the terminal D-alanine residue of the peptidoglycan peptide chain. Peptidoglycan turnover defects are associated with virulence attenuation consistent with our finding that deletion of *dalS* reduces intracellular replication (Figure 3.2). Δ*dalS* displayed an, albeit modest, increased susceptibility to peptidoglycan-targeting antibiotics (Figure A.6a) and an altered gross morphology (Figure A.6b) consistent with peptidoglycan being a critical constituent of the bacterial cell envelope. As the host receptors Nod1 and Nod2 recognize peptidoglycan fragments containing specific peptide chain components including *m*-diaminopimelic acid, differential induction of an innate immune response may explain the elevated reactive nitrogen species response observed during infection with Δ*dalS* relative to wild type (Figure A.7) [10]. A more thorough determination of the minimum inhibitory concentration of peptidoglycan-targeting antimicrobials would clarify the modest susceptibility of Δ*dalS* to these compounds. [^{3}H]- D-alanine should be used to monitor peptidoglycan turnover in Δ*dalS* compared to wild type. Measuring activation of signalling cascades such as NF-κB would establish whether Δ*dalS* specifically elevates the nitric oxide response or if this simply reflects a generally increased pro-inflammatory response.

Understanding the mechanism by which D-alanine uptake improves intracellular replication would provide insight into the importance of nutrient exchange across the SCV. Given that availability of metabolites can be influenced by host diet, such studies may reveal novel therapeutic strategies.

SPI-2 Hierarchy: Remaining Questions

The regulatory *ssrA* promoter and the structural *ssaG* promoter were primed in non-inducing media by OmpR and Fis respectively. Other studies have shown that the OmpR/Fis and SsrB binding sites overlap at these promoters [11,12]. It was recently shown that preferential binding of OmpR occurred when DNA was relaxed [13]. Although Fis occupancy of the *ssrA* promoter deceased during DNA relaxation, it would be informative to conduct similar experiments at the *ssaG* promoter. DNA is less supercoiled in oxygenated environments suggesting that OmpR-dependent priming of the *ssrA* promoter may occur when bacteria migrate from the oxygen depleted lumen and become juxtaposed to epithelial cells as this site has elevated oxygen availability [14]. EMSAs should be performed at both promoters to determine if OmpR/Fis and SsrB compete for binding and examine *in vitro* conditions that influence competitive promoter occupancy. Uncoupling these regulatory inputs would allow assessment of their contribution to intracellular replication as a similar transcriptional surge at the *phoP* promoter was required for virulence [15]. Uncoupling studies may prove difficult owing to the lack of defined recognition motifs for OmpR and Fis.

A more rigorous analysis of transcription using *in vivo* imaging may provide novel insight into SPI-2 gene expression. Such studies are currently limited by animal-to-animal variability in absolute signal which makes it impossible to discern subtle difference in gene expression. Compatible reporter systems simultaneously utilized in a single animal would be required to tease apart *in vivo* transcriptional regulation.

Prioritized transcriptional activation of the flagellar and SPI-1 T3SSs is established through divergent regulatory inputs at effector promoters. InvF in complex with its chaperone SicA specifically drives SPI-1 effector expression [16,17,18]. In *Shigella*, effector expression is controlled by MxiE [19,20]. BsaN in complex with its chaperone BicA similarly controls effector expression in *B. pseudomallei* [21]. This raises the question whether SPI-2 has any yet unidentified effector-specific regulatory inputs. Our laboratory recently demonstrated that deletion of the translocon *sseC* caused a significant increase in transcription from an effector promoter (Cooper, C.A. unpublished data). Loss of the SseC chaperone SscA also modified SPI-2 gene expression. Future work should aim to systematically examine the contribution of the SseC-SscA complex to transcriptional regulation of each SPI-2 promoter followed by identification of any interacting auxiliary proteins.

It is not yet possible to discern whether SPI-2 was acquired with its existing CREs or whether they are the result of *cis*-regulatory evolution. SPI-2 is similar in content and gene synteny to the locus for enterocyte effacement (LEE) encoded in EPEC and the *Sodalis* symbiosis region (SSR)-3 encoded in the tsetse symbiont *Sodalis glossinidius* [22]. Alignment of SSR-3 with SPI-2 revealed conservation of the T3SS apparatus genes. In contrast, substantial drift has occurred in the CREs which only maintain a degree of conservation at the SsrB binding site [23]. Considering that OmpR and Fis binding overlaps at the SsrB motif in SPI-2 and that *S. glossinidius* encodes EnvZ/OmpR and PhoP/PhoQ it is possible that these regulatory inputs are maintained. Subsequent work

could compare regulatory inputs using SSR-3 transcriptional reporters expressed in an *S. enterica* background

Defining Virulence Factors

Comparative genomic analysis allows for straightforward identification of genes present in pathogenic organisms that are absent from their non-pathogenic counterparts. Unfortunately such strategies bias research efforts towards characterization of horizontally acquired genes. A comprehensive model of host-pathogen interactions requires knowledge of both acquired and ancestral genes as exemplified by *srfN* and *dalS*.

There exists a plethora of studies examining networks of SPI-2 co-regulated genes in addition to mutational screens in a variety of infection models. A close examination of this literatures reveals continued identification of genes involved in amino acid, nucleotide, carbohydrate, lipid and ion metabolism or transport as potential virulence factors, yet they are not traditionally considered agents of pathogenesis [23,24,25,26]. Nutrient uptake, as seen with DalS, may confer fitness advantages within nutrient limiting host environments. The nutritional composition of the SCV remains an uncharted avenue of research potential and future studies should endeavour to fill this knowledge gap.

Cis-Regulatory Evolution

From a theoretical perspective, CRE mutations should have a higher probability of being adaptive since they circumvent potentially deleterious consequences of protein modification. Having discovered that DalS is a transporter allows theoretical predictions to be made regarding the relative tradeoffs associated with both forms of evolution. The fitness advantage associated with increased intracellular D-alanine uptake could have driven selection for up-regulation of DalS expression or through coding sequence mutations which increased the affinity of DalS for D-alanine. Despite conservation of residues mediating substrate binding, comparison of the fluorescence thermal shift data for DalS and the *S. bongori* homologue (Figure 3.4 and A.5) reveals that the ΔT_m profiles following addition of D-alanine were not identical. Although not a true measure of binding affinity, the FTS data suggests a divergent protein-substrate interaction indicative of coding sequence mutations. Enhanced binding affinity, as achieved through selection of beneficial protein coding perturbations, could not continue indefinitely as DalS would have to retain the ability to release D-alanine to the DalTUV transporter. Structural evolution may have occurred for DalS but it remains logical that *cis*-regulatory modification to increase expression of the transporter would have been less evolutionarily constrained. A recent study mutagenized *Saccharomyces cerevisiae* carrying a P_{TDH3}-YFP (yellow fluorescent protein) chromosomal reporter and systematically characterized mutations affecting fluorescence. They found that increased levels of YFP was never associated with a modified coding sequence but was observed in 50% of *cis*-regulatory

mutations [27]. Genome wide studies in eukaryotes have shown a strong correlation between *cis*-regulatory adaptation and transcriptional up-regulation [28,29]. These results suggest that *cis*-regulatory modification may be the preferential mode of evolution when increased expression is beneficial.

Mutations in the CREs of SPI-2 likely produce fewer plieotropic consequences than structural modifications. Deletion or mutation of structural components of the SPI-2 T3SS typically abolishes virulence. In contrast, due to the degenerate nature of DNA recognition motifs, deletion of entire segments of the SsrB binding motif upstream of SPI-2 promoters was not sufficient to prevent expression [23] (unpublished observations). This supports the argument that CRE mutations are less deleterious.

In the debate surrounding *cis*-regulatory evolution, a distinction is often made between anatomical versus physiological traits as arguments for the evolutionary benefit of CREs have been based almost exclusively on anatomical features. Opponents are quick to point out that anatomy cannot be the sole providence of *cis*-regulatory evolution. Our identification of a bacterial nutrient uptake system as having undergone *cis*-regulatory evolution clearly demonstrates that physiological traits are similarly influenced by CRE modification.

Regulatory evolution studies to date often fail to empirically demonstrate that the CRE modifications directly correspond to a fitness gain. Here we have demonstrated that *cis*-regulatory evolution of *srfN* and *dalS* have directly contributed to fitness *in vivo*. The rapid generation time, genome availability, ease of genetic manipulation and availability

of host infection models may allow pathogenic bacteria to be a fruitful source of discovery for additional examples of *cis*-regulatory evolution.

Cis-Regulatory Evolution: Future Directions

With thousands of complete bacterial genome sequences, the potential to identify examples of *cis*-regulatory polymorphisms by comparative genomics is enormous. Only genome-wide studies on regulatory versus coding divergence will reveal which contributes more strongly to evolution. Whole genome studies examining potential *cis*-regulatory evolution in eukaryotes have recently been conducted. In *Mus musculus* and *S. cerevisiae* researchers have examined pathway-level gene expression evolution between closely related species and have identified hundreds of genes belonging to diverse networks as showing evidence of regulatory selection [28,29]. Future studies on *cis*-regulatory evolution in pathogenic bacteria will require genomic information from both pathogenic and non-pathogenic isolates as well as knowledge of a transcription factor's global regulon. An alternative would be to conduct microarray analysis in related organisms and examine pathway-level selective changes in gene expression.

There have now been several studies which have followed the evolutionary fate of bacteria grown in selective *in vitro* conditions. The most famous was a 20,000 generation adaptation of *E. coli* to glucose-limited media in which researchers found multiple examples of parallel phenotypic changes indicative of adaptive evolution [See [30] for full review]. *In vitro* synthetic evolution experiments should report on CRE changes since

these studies, in occurrences where the genetic determinants of adaptation were identified, have traditionally been biased towards examining mutations in coding sequence despite these changes often being insufficient to account for the observed fitness gains [31].

The first study to examine bacterial evolution using animal models as selective environments assessed adaptation of mutator bacteria to the mouse intestine [32]. Although the authors observed increased *in vivo* fitness they did not map the genetic mutations. Synthetic evolution experiments which adapted *S.* Typhimurium to growth in BALB/c mice and *E. coli* in germ-free mice demonstrated morphological changes and increased fitness yet failed to determine the genetic constituents responsible for the adaptation [33,34]. *In vivo* evolution experiments followed by genome sequencing of evolved isolates could begin to address whether mutations in the coding or regulatory sequence are more important contributors to phenotypic change.

Concluding Remarks

The results presented here support our hypothesis that *cis*-regulatory modifications following horizontal acquisition of SPI-2 have contributed to the evolution of *S. enterica* as an intracellular pathogen. Mounting evidence from developmental biology combined with this work demands inclusion of regulatory evolution in the Modern Synthesis. The study of *cis*-regulatory adaptation not only aids our understanding of the emergence of infectious disease, it provides insight into how profitable variations

arise, explains phenotypic divergence between closely related organisms, illuminates the importance of non-coding DNA and guides our appreciation of the universal process of evolution.

References

1. Wittkopp PJaK, G. (2012) Cis-regulatory elements: molecular mechanisms and evolutionary processes underlying divergence. Nature Reviews Genetics 13: 59-69.

2. Yoon H, Ansong C, McDermott JE, Gritsenko M, Smith RD, et al. (2011) Systems analysis of multiple regulator perturbations allows discovery of virulence factors in *Salmonella*. BMC Syst Biol 5: 100.

3. Bomberger JM, Maceachran DP, Coutermarsh BA, Ye S, O'Toole GA, et al. (2009) Long-distance delivery of bacterial virulence factors by *Pseudomonas aeruginosa* outer membrane vesicles. PLoS Pathog 5: e1000382.

4. Kesty NC, Mason KM, Reedy M, Miller SE, Kuehn MJ (2004) Enterotoxigenic *Escherichia coli* vesicles target toxin delivery into mammalian cells. EMBO J 23: 4538-4549.

5. Wai SN, Lindmark B, Soderblom T, Takade A, Westermark M, et al. (2003) Vesicle-mediated export and assembly of pore-forming oligomers of the enterobacterial ClyA cytotoxin. Cell 115: 25-35.

6. Kulp A, Kuehn MJ (2010) Biological functions and biogenesis of secreted bacterial outer membrane vesicles. Annu Rev Microbiol 64: 163-184.

7. Nakamura H, Fang J, Maeda H (2012) Protective Role of D-Amino Acid Oxidase against *Staphylococcus aureus* Infection. Infect Immun 80: 1546-1553.

8. Vazquez-Torres A, Xu Y, Jones-Carson J, Holden DW, Lucia SM, et al. (2000) *Salmonella* pathogenicity island 2-dependent evasion of the phagocyte NADPH oxidase. Science 287: 1655-1658.

9. Vazquez-Torres A, Jones-Carson J, Mastroeni P, Ischiropoulos H, Fang FC (2000) Antimicrobial actions of the NADPH phagocyte oxidase and inducible nitric oxide synthase in experimental salmonellosis. I. Effects on microbial killing by activated peritoneal macrophages in vitro. J Exp Med 192: 227-236.

10. Girardin SE, Boneca IG, Carneiro LA, Antignac A, Jehanno M, et al. (2003) Nod1 detects a unique muropeptide from gram-negative bacterial peptidoglycan. Science 300: 1584-1587.

11. Feng X, Walthers D, Oropeza R, Kenney LJ (2004) The response regulator SsrB activates transcription and binds to a region overlapping OmpR binding sites at *Salmonella* pathogenicity island 2. Mol Microbiol 54: 823-835.

12. Lim S, Kim B, Choi HS, Lee Y, Ryu S (2006) Fis is required for proper regulation of *ssaG* expression in *Salmonella enterica* serovar Typhimurium. Microb Pathog 41: 33-42.

13. Cameron AD, Dorman CJ (2012) A Fundamental Regulatory Mechanism Operating through OmpR and DNA Topology Controls Expression of *Salmonella* Pathogenicity Islands SPI-1 and SPI-2. PLoS Genet 8: e1002615.

14. Marteyn B, West NP, Browning DF, Cole JA, Shaw JG, et al. (2010) Modulation of *Shigella* virulence in response to available oxygen in vivo. Nature 465: 355-358.

15. Shin D, Lee EJ, Huang H, Groisman EA (2006) A positive feedback loop promotes transcription surge that jump-starts *Salmonella* virulence circuit. Science 314: 1607-1609.

16. Darwin KH, Miller VL (2000) The putative invasion protein chaperone SicA acts together with InvF to activate the expression of *Salmonella* typhimurium virulence genes. Mol Microbiol 35: 949-960.

17. Darwin KH, Miller VL (1999) InvF is required for expression of genes encoding proteins secreted by the SPI1 type III secretion apparatus in *Salmonella* typhimurium. J Bacteriol 181: 4949-4954.

18. Eichelberg K, Galan JE (1999) Differential regulation of *Salmonella* typhimurium type III secreted proteins by pathogenicity island 1 (SPI-1)-encoded transcriptional activators InvF and *hilA*. Infect Immun 67: 4099-4105.

19. Mavris M, Page AL, Tournebize R, Demers B, Sansonetti P, et al. (2002) Regulation of transcription by the activity of the *Shigella flexneri* type III secretion apparatus. Mol Microbiol 43: 1543-1553.

20. Demers B, Sansonetti PJ, Parsot C (1998) Induction of type III secretion in *Shigella flexneri* is associated with differential control of transcription of genes encoding secreted proteins. EMBO J 17: 2894-2903.

21. Sun GW, Chen Y, Liu Y, Tan GY, Ong C, et al. Identification of a regulatory cascade controlling Type III Secretion System 3 gene expression in *Burkholderia pseudomallei*. Mol Microbiol 76: 677-689.

22. Toh H, Weiss BL, Perkin SA, Yamashita A, Oshima K, et al. (2006) Massive genome erosion and functional adaptations provide insights into the symbiotic lifestyle of *Sodalis glossinidius* in the tsetse host. Genome Res 16: 149-156.

23. Tomljenovic-Berube AM, Mulder DT, Whiteside MD, Brinkman FS, Coombes BK Identification of the regulatory logic controlling *Salmonella* pathoadaptation by the SsrA-SsrB two-component system. PLoS Genet 6: e1000875.

24. Lawley TD, Chan K, Thompson LJ, Kim CC, Govoni GR, et al. (2006) Genome-wide screen for *Salmonella* genes required for long-term systemic infection of the mouse. PLoS Pathog 2: e11.

25. Chaudhuri RR, Peters SE, Pleasance SJ, Northen H, Willers C, et al. (2009) Comprehensive identification of *Salmonella enterica* serovar typhimurium genes required for infection of BALB/c mice. PLoS Pathog 5: e1000529.

26. Yoon H, McDermott JE, Porwollik S, McClelland M, Heffron F (2009) Coordinated regulation of virulence during systemic infection of *Salmonella enterica* serovar Typhimurium. PLoS Pathog 5: e1000306.

27. Gruber JD, Vogel K, Kalay G, Wittkopp PJ (2012) Contrasting properties of gene-specific regulatory, coding, and copy number mutations in *Saccharomyces cerevisiae*: frequency, effects, and dominance. PLoS Genet 8: e1002497.

28. Fraser HB, Babak T, Tsang J, Zhou Y, Zhang B, et al. (2011) Systematic detection of polygenic cis-regulatory evolution. PLoS Genet 7: e1002023.

29. Fraser HB, Moses AM, Schadt EE (2010) Evidence for widespread adaptive evolution of gene expression in budding yeast. Proc Natl Acad Sci U S A 107: 2977-2982.

30. Philippe N, Crozat E, Lenski RE, Schneider D (2007) Evolution of global regulatory networks during a long-term experiment with *Escherichia coli*. Bioessays 29: 846-860.

31. Cooper TF, Rozen DE, Lenski RE (2003) Parallel changes in gene expression after 20,000 generations of evolution in *Escherichia coli*. Proc Natl Acad Sci U S A 100: 1072-1077.

32. Giraud A, Matic I, Tenaillon O, Clara A, Radman M, et al. (2001) Costs and benefits of high mutation rates: adaptive evolution of bacteria in the mouse gut. Science 291: 2606-2608.

33. Lee SM, Wyse A, Lesher A, Everett ML, Lou L, et al. (2010) Adaptation in a mouse colony monoassociated with *Escherichia coli* K-12 for more than 1,000 days. Appl Environ Microbiol 76: 4655-4663.

34. Nilsson AI, Kugelberg E, Berg OG, Andersson DI (2004) Experimental adaptation of *Salmonella* typhimurium to mice. Genetics 168: 1119-1130.